ANTIBODY CHARACTERISATION OF DISC1, A GENE IDENTIFIED AT A CHROMOSOMAL TRANSLOCATION ASSOCIATED WITH PSYCHIATRIC ILLNESS

Rachel James

PhD

University of Edinburgh

2003

I declare this thesis has been composed by myself, and the work presented within is my own, unless otherwise stated.

Rachel James
May 2003

Acknowledgements

First of all I would like to thank my supervisors, Kirsty Millar and David Porteous for their help, guidance and support during the course of my PhD. In particular, Kirsty for always being available for advice and reassuring chats, and David for being able to see the bigger picture. Secondly I would like to thank the other members of the t(1;11) group, both past and present, but in particular Sheila Christie and Jude Fantes. Sheila has always been a cheery face to have around, and Jude was of great help in microscope use and image analysis.

Thanks also to everyone in the Medical Genetics Section as I don't think there is a single person who hasn't provided help or reagents at one time or another during my PhD, but in particular Ben Pickard for use of his microscope, Pat Malloy (& Jude again) for FISH analysis, Varrie Ogilvie for cell staining protocols and Xinsheng Nan for tips on protein expression. Outside of the section, I would like to thank Akira Sawa for providing his DISC1 antibody.

The rest of the PhD students provided much needed distracting chat, sympathetic ears and overall entertainment. Though there have been many over the years, of the current crop thanks to Jean, Sarah, Helen, Simon, and Stephane, but also to Katie for Monday night yoga and beer (an unlikely combination but one that works).

Finally, the biggest thanks goes to my family, Maxie, Laura and Gaggie, for their support and encouragement over the years. Last but by no means least, Ben has been my rock throughout my PhD, and has contributed more than his fair share to the completion of this thesis. I am gratefully appreciative of their commitment to me.

Abstract

DISC1 (Disrupted in Schizophrenia) was identified at the breakpoint of a chromosomal translocation associated with schizophrenia and other psychiatric illnesses in a large Scottish family. Recent linkage studies have also identified the DISC1 locus as a susceptibility factor for schizophrenia in Finnish families and *DISC1* is emerging as a candidate gene for psychiatric illness. At the time of identification *DISC1* was novel and the function of the DISC1 protein was completely unknown. To characterise the function of DISC1, antibodies were raised against the DISC1 protein using both a peptide and bacterially expressed recombinant protein as the antigen. The resulting antibodies were characterised thoroughly to ensure their specificity for DISC1. Multiple transcripts of *DISC1* had been identified and the initial aim was to determine which of the transcripts were translated into functional proteins. Multiple DISC1-related proteins were found to exist in human but only a single isoform was identified in mouse and rat. In addition the protein expression levels of DISC1 were examined in lymphoblastoid cell lines derived from members of the original translocation family. No evidence for a truncated protein resulting from the translocated chromosome was found but preliminary results suggest that levels of DISC1 are significantly reduced in translocation carriers. The subcellular localisation of DISC1 was studied in human neuroblastoma and glioblastoma cell lines. DISC1 was found to colocalise with mitochondria in a cytoskeletal associated pattern, and in differentiated neuroblastoma cells DISC1 localised to the tips of developing neurites suggesting a possible role in neurite outgrowth. Further characterisation of the function of DISC1 should now focus on its relationship with the mitochondria to ascertain the significance of this association to both the function and subsequent dysfunction of the nervous system.

Contents

Chapter 5

DISC1-related proteins in human

Chapter 6

DISC1 protein expression levels in lymphoblastoid cell lines derived from t(1;11) family members

Chapter 7

DISC1-related proteins in mouse and rat

Chapter 8

Subcellular localisation of DISC1

Chapter 9

DISC1 localisation during differentiation of neuroblastoma cell lines

Chapter 10

Concluding Remarks & Future Work

List of figures

List of tables

Abbreviations

α	alpha
α-^{32}P	α-phosphorus-32
aa	amino acid
alt	alternative
AMPA	α-amino-3-hydroxy-5-methyl-4-isoxasole-4-propionic acid
ATCC	American Type Culture Collection
β	beta
BAC	bacterial artificial chromosome
BDNF	brain derived neurotrophic factor
BLAST	basic local alignment search tool
bp	base pair
BSA	bovine serum albumin
°C	degrees centigrade
cDNA	complementary DNA
CNS	central nervous system
COX6c	cytochrome oxidase subunit VIc
CRC	Cancer Research Campaign
CT	computed tomography
d	day(s)
DAB	diamino-benzidine
Dabco	triethylenediamine
DALY	Disability Adjusted Life Year
DAPI	4',6-diamidino-2phenylindole dihydrochloride
dCTP	deoxycytidine triphosphate
DEPC	diethyl polycarbonate
dH_2O	distilled water
DISC1	Disrupted-in-Schizophrenia 1
DISC2	Disrupted-in-Schizophrenia 2
DMEM	Dulbecco's MOD Eagle Medium
DMSO	dimethyl sulfoxide
DNA	deoxyribonucleic acid
dNTP	deoxynucleotide triphosphate
DTT	dithiothreitol
DZ	dizygotic
ECACC	European Collection of Cell Cultures
E.coli	*Escherichia coli*
EDTA	ethylenediaminetetraacetic acid
Eef1a2	Eukaryotic elongation factor 1a2
ELISA	Enzyme-Linked ImmunoSorbent Assay
ER	endoplasmic reticulum
ERP	event related potential
Es	extremely short transcript / isoform
EST	expressed sequence tag
FBS	foetal bovine serum

FISH	fluorescent *in situ* hybridization
fMRI	functional MRI
γ	gamma
g	grams
GABA	gamma-aminobutyric acid
GAPDH	glyceraldehyde-phosphate-dehydrogenase
GFAP	glial fibrillary acidic protein
GFP	green fluorescent protein
GST	glutathione-S-transferase
HGMP-RC	Human Genome Mapping Project Resource Centre
his	histidine
HRP	horseradish peroxidase
5-HT	serotonin
IgG	immunoglobin G
IPTG	isopropylthio-β-D-galactoside
kb	kilobase
kDa	kilodaltons
KLH	keyhole limphet hemocyanin
L	long transcript / isoform
LB	Luria-Bertani
LD	linkage disequilibrium
LMP	low melting point
LOD	logarithm of odds
LSD	lysergic acid diethylamide
Lv	long variant transcript / isoform
µCi	microcuries
µF	microfaraday
µg	micrograms
µl	microlitre
µM	microns
M	molar
MAP	microtubule associated protein
Mb	megabase
MeOH	methanol
mg	milligrams
$MgCl_2$	magnesium chloride
mGluR5	metabotropic glutamate receptor subtype 5
ml	millilitres
mM	millimolar
MMC	Molecular Medicine Centre
MP	melting point
MRC	Medical Research Council
MRI	magnetic resonance imaging
mRNA	messenger RNA
ms	millisecond
MZ	monozygotic
NAALADase	N-acetyl- alpha-linked acidic dipeptidase
$NaHCO_3$	sodium bicarbonate

NaCl	sodium chloride
NaH_2PO_4	disodium hydrogen phosphate
NaOH	sodium hydroxide
NEAA	non-essential amino acids
NF	neurofilament
ng	nanograms
Ni-NTA	nickel-nitrilotriacetic acid
NLS	nuclear localisation signal
nm	nanometers
NMDA	*N*-Methyl-D-aspartate
NP-40	nonylphenylpolyethylene glycol
Ω	ohm
OD	optical density
PBS	phosphate buffered saline
PBS-T	PBS with Tween-20
PCP	phencyclidine
PCR	polymerase chain reaction
PET	positron emission tomography
PFA	paraformaldehyde
PVDF	polyvinylidene difluoride
RA	retinoic acid
RNA	ribonucleic acid
RNAi	RNA interference
rpm	revolutions per minute of rotor
RT	reverse transcriptase
RT-PCR	reverse transcriptase PCR
SAPU	Scottish Antibody Production Unit
S1	short transcript / isoform 1
S2	short transcript / isoform 2
SDS	sodium dodecyl sulphate
SDS-PAGE	SDS-polyacrylamide gel electrophoresis
SSC	standard saline citrate
TAE	Tris-acetate
Taq	*Thermus aquaticus*
TE	Tris-EDTA
TPA	12-O-tetradecanoyl-13-phorbol-acetate
TRAX	Translin-associated factor X
Tween 20	polyethylene glycol sorbitan monolaurate
U	units
UTR	untranslated region
UV	ultraviolet
V	volts
w	week(s)
xg	measure of relative centrifugal force

CHAPTER 1

INTRODUCTION

1. Introduction

1.1 Preface

My thesis was performed within a research group, investigating the genetic cause of psychiatric illness. The family our research has been based upon (section 1.6.1), present with a number of different psychiatric disturbances, of which schizophrenia and recurrent major depression are the most common. The appearance of depression and other psychiatric illnesses is often found in the relatives of schizophrenics, therefore schizophrenia is believed to be the predominant phenotype within the family. Thus the aim of this introduction is to provide an overview of the current knowledge and understanding of schizophrenia research. There is extensive literature on all aspects of schizophrenia, yet the key findings appear consistently in many review papers. Consequently in this introduction, original papers for many of the "facts" about schizophrenia have not been referenced, and in general appropriate review papers are provided.

1.2 Schizophrenia

Schizophrenia was first described in the late 19th century, by the psychiatrist Emil Kraeplin, who named it dementia praecox to reflect both the cognitive and behavioural impairment (dementia) associated with the early age of onset (praecox) of the disease. The disorder was renamed schizophrenia in the early 20th century by Eugen Bleuler, deriving its name from the Greek words for split (schiz) and mind (phrenia) (Andreasen, 1995). The choice of words was to highlight the severe fragmentation of the mind, but has led to the general misconception that schizophrenics have a split personality, which is by no means characteristic of schizophrenia.

Schizophrenia affects 1% of the population worldwide, and its frequency of occurrence is fairly consistent across countries, cultures and genders (Lewis and Lieberman, 2000). The typical age of onset is between 15 and 25 year for males

while for females the onset is usually about 5 years later (Lewis, 2000). In addition to the earlier age of onset, some data suggest males also show a poorer response to treatment and more marked neuropathological abnormalities (Lewis and Lieberman, 2000), implying a more severe manifestation of the disorder.

The impact schizophrenia has on both a social and economic level cannot be underestimated. In the UK alone there are 185400 people receiving medical treatment for schizophrenia, and the annual cost of schizophrenia is estimated at more than £1.7 billion. Although the effect on the individual is difficult to quantify, a measure called the Disability Adjusted Life Year (DALY) was implemented by the World Health Organisation, World Bank and Harvard School of Public Health, to attempt to calculate the relationship between disease and its economic and social impact. The DALY is equivalent to healthy years of life lost to premature mortality or disability, and for schizophrenia, it is estimated 4.7% of an individual's life will be lost to the disabling effect of illness (Hyman, 2000). Furthermore eight of the ten leading causes of disability in the United States are neuropsychiatric disorders, highlighting the importance for an increased understanding into the development of these disorders.

1.2.1 Symptoms

Schizophrenia is a heterogenous disorder characterised by a large number of symptoms. The presentation and severity of these symptoms varies from person to person, and it is probable that schizophrenia is an umbrella term for several different disorders (Heyman and Murray, 1992). Psychiatric diagnoses included within the spectrum of schizophrenia include schizoaffective disorder, atypical psychosis, delusional disorder and personality disorders (schizotypical, schizoid and paranoid) (Prescott and Gottesman, 1993).

The diagnosis of schizophrenia is currently based on two diagnostic systems: the fourth edition of the American Psychiatric Association's Diagnostic and Statistical

Manual (DSM-IV), and the tenth International Classification of Disease (ICD-10) (Andreasen, 1995). Based on these diagnostic criteria, the core symptoms are divided into two categories based on the perceived exaggeration (positive) or loss (negative) of normal brain function. Positive symptoms include hallucinations, delusions and disorganized thought, while the negative symptoms refer to the loss of motivation and emotional vibrancy. The negative symptoms of schizophrenia have been largely neglected to date (Brown and Pluck, 2000), yet these are the most disabling, showing considerable resistance to current drug therapies (section 1.2.2).

In addition to deficits in emotional and perceptual processes, schizophrenia involves cognitive, motor and social disturbances (Lewis and Lieberman, 2000), suggesting the involvement of multiple brain regions. This is in contrast to most other psychiatric illnesses where a specific brain function or system is affected, for example, mood in depression and appetite drive in anorexia nervosa. Some of the symptoms of schizophrenia represent premorbid features of the illness, and although not diagnostically informative, are present well before the ascertainment of schizophrenia. These include reduced IQ, antisocial behaviour and subtle motor abnormalities (Frith, 1995; Chua and Murray, 1996; Lewis and Lieberman, 2000).

1.2.1.1 Overlap with bipolar disorder

No single symptom is unique to schizophrenia and there is considerable diagnostic overlap with bipolar disorder. Bipolar disorder, or manic depression, is characterised by cyclic episodes of mania and depression, which can be related to the positive and negative symptoms of schizophrenia, respectively. The frequency of occurrence, disease prognosis and familial clustering are also similar between the two disorders. Furthermore recent findings from linkage studies suggest there are common chromosomal loci for schizophrenia and bipolar disorder susceptibility genes on 22q11-13, 18p11.2, 13q32 and 10p14 (Berrettini, 2000). This suggests that though there are pathological features unique to either schizophrenia or bipolar disorder (Baumann and Bogerts, 1999; Knable, 1999; Knable *et al.*, 2001), there may be a common aetiological origin for the disorders, with the exact phenotype being dependent on interacting genetic and environmental factors.

1.2.1.2 Endophenotypes

The heterogeneity of schizophrenia has hampered attempts to identify susceptibility genes. In an attempt to simplify the schizophrenic phenotype, endophenotypes have been examined. Endophenotypes are heritable traits that can be correlated with the disease, and must be quantifiable but can be biological (anatomical, electrophysiological, biochemical) or cognitive (neuropsychological) (Leboyer *et al.*, 1998). Event related potentials (ERPs) are an example of a physiological endophenotype for schizophrenia. ERP's represent externally measured electrical signals of the brain, induced in response to a specific auditory, visual or somatosensory stimulus. In schizophrenics the most consistent ERP differences are a decrease in amplitude of signals and an increased time between stimulus and signal peaks. The most pronounced differences have been observed with the P300 ERP that typically occurs approximately 300ms following auditory or visual stimulus (Ford, 1999; Blackwood, 2000).

Endophenotypes have begun to show success in refining diagnostic categories for linkage studies (Freedman *et al.*, 1997). Additional applications of endophenotypes include determining the suitability of animal models for schizophrenia and identifying candidate genes (section 1.5.2) (Pulver, 2000).

1.2.2 Treatment

Treatment for schizophrenia is at present not wholly efficacious. In general, the positive symptoms are responsive to drug treatment, while the negative symptoms remain largely drug resistant (Andreasen, 1995). The incomplete efficacy of the drugs reflects the current lack of knowledge regarding the underlying pathology, and there is a definite need for the development of more specific drugs.

The drugs used to treat schizophrenia are known as neuroleptics or antipsychotics, and are primarily designed to antagonise dopamine receptors (section 1.3.1.1). There are two classes of neuroleptics, typical and atypical, the classification of which is based upon the pharmacological profile of the two drug classes, and the apparent

reduction in certain unwanted side effects of the atypical neuroleptics (Rang and Dale, 1991).

1.2.2.1 Typical neuroleptics

Typical neuroleptics, such as chlorpromazine, are non-selective drugs, antagonising dopamine receptors, as well as α-adrenergic, serotonin (5-HT), muscarinic acetylcholine and histamine receptors (Stone, 1995). Typical neuroleptics are associated with unpleasant extrapyramidal side-effects due to unwanted dopamine receptor antagonism within the nigrostriatal pathway. The development of Parkinsonism-like symptoms, including muscle rigidity, loss of mobility and tremor, is closely related to the dose of drug used. Parkinsonism-like symptoms develop rapidly in a large number of patients yet are reversible. On the other hand, tardive dyskinesia is irreversible and linked to long term neuroleptic treatment. Tardive dyskinesia is a serious movement disorder, akin to Huntington's chorea, and involves involuntary movements of the face, tongue, trunk and limbs.

1.2.2.2 Atypical neuroleptics

The atypical neuroleptics show a reduction in extrapyramidal side effects, and although still dopamine receptor antagonists, are known to have increased potency at 5-HT receptors (Stone, 1995). In addition, the atypical neuroleptic, clozapine, is more effective in treating the negative symptoms of schizophrenia, particularly in patients who have shown previous drug resistance (Sawa and Snyder, 2002). Nonetheless clozapine is associated with the fatal blood disorders, leukopenia (reduction in white blood cells) and agranulocytosis (absence of neutrophils), therefore requiring regular blood monitoring.

1.2.2.3 Psychosocial treatment

Finally the use of psychosocial treatments (Kane and McGlashan, 1995) to aid the individual in returning to a normal life must not be forgotten. Treatments include social skills training, cognitive behavioural therapies and family intervention

strategies. The combined approach of drug and psychosocial treatment will no doubt be the most successful way to tackle schizophrenia.

1.3 The neurobiology of schizophrenia

Schizophrenia has largely been neglected as a neurobiological disease, nevertheless the biology of schizophrenia is beginning to take shape. Evidence of brain abnormalities in schizophrenic individuals has come from three main areas of research: the pharmacology of neurotransmitters (section 1.3.1), brain imaging (section 1.3.2) and post-mortem studies (section 1.3.3).

1.3.1 Involvement of neurotransmitters

1.3.1.1 Dopamine

Initial theories regarding the pathogenesis of schizophrenia came from the use of psychotropic drugs. LSD (lysergic acid diethylamide), mescaline and amphetamine cause schizophrenic-like symptoms in humans (Sedvall and Farde, 1995), mimicking the positive side of schizophrenia. In animals, amphetamine induces a number of schizophrenic-like effects including increased motor activity, alertness and grooming, deficits in sensorimotor function, aggressive and stereotyped behaviours (Gainetdinov *et al.*, 2001). These effects are ameliorated with neuroleptic treatment, and the amphetamine model of schizophrenia has long been the benchmark for determining the efficacy of novel neuroleptics. LSD and amphetamine are both monoamine agonists, predominantly associated with dopamine (amphetamine) and 5-HT (LSD) neurotransmission (Harrison, 1999). With the advent of chlorpromazine (section 1.2.2.1), a dopamine receptor antagonist, the dopamine hypothesis of schizophrenia came into play. The main tenet of this hypothesis is hyperactivity within the dopaminergic mesolimbic system is responsible for the positive symptoms of schizophrenia.

Ligand binding PET (positron emission tomography) enabled dopamine neurotransmission to be examined directly in schizophrenic patients, and initial

studies reported increases in dopamine D_2 receptors (Sedvall and Farde, 1995). However two factors in particular have hampered conclusive results (Harrison, 1999). Firstly, all neuroleptics are dopamine receptor antagonists and therefore have a profound effect on dopamine receptor number. Consequently it is unclear if reported increases in dopamine receptor number in schizophrenic patients are a consequence of disease or due to neuroleptic treatment. Secondly, within the brain there are five dopamine receptor subtypes, with several variants of each subtype (Sealfon and Olanow, 2000). Elucidating the involvement of a specific receptor subtype, in the absence of receptor specific drugs is a difficult task, yet one which requires further investigation. Recent molecular dissection of the function of the D_2 receptor subtypes, D_2L and D_2S, found involvement of the D_2L receptor only in the antipsychotic effect of haloperidol (Usiello *et al.*, 2000). The receptors act at different sites and are either predominantly presynaptic (D_2S) or postsynaptic (D_2L). It has been suggested (Harrison, 1999; Lewis and Lieberman, 2000) that abnormalities in presynaptic dopamine function may be the proximal cause of illness, therefore selective targeting of the D_2S receptor may be therapeutically beneficial.

The dopamine hypothesis has been the predominant influence in schizophrenia research, but it is now clear that dopamine dysfunction does not account for all the symptoms of schizophrenia. It would be unwise to exclude dopamine completely but disturbances in other neurotransmitter systems are also likely to be involved. Good candidates include 5-HT, glutamate (section 1.3.1.2) and GABA (Carlsson *et al.*, 2001). The involvement of multiple neurotransmitters seems probable given the intricate interdependence of neurotransmitter systems.

1.3.1.2 Glutamate

The suggested involvement of glutamate in schizophrenia is again based largely on the effect of psychotropic drugs. NMDA receptor antagonists, including PCP (phencyclidine) and ketamine, produce psychotomimetic effects in humans (Tamminga, 1998; Sharp *et al.*, 2001). Crucially both positive symptoms and cognitive disturbances, indicative of negative symptomology, are induced. PCP induced animal models cause behaviours similar to amphetamine (section 1.3.1.1),

for example increased motor activity, sensorimotor deficits and stereotyped behaviour, but social behaviour and cognitive functions are also affected (Gainetdinov *et al.*, 2001). These effects are reversed with neuroleptic treatment. In contrast to the hypothesis of dopamine hyperactivity, it is glutamate hypoactivity that is suggested to be of importance in the pathogenesis of schizophrenia.

The glutamate hypothesis is at an earlier stage of investigation than the dopamine hypothesis of schizophrenia. Nonetheless evidence is emerging to support the involvement of glutamate in schizophrenia. Post-mortem brain studies report alterations in expression of glutamate receptors, including AMPA and kainate receptors (Tamminga, 1998; Harrison, 1999), and abnormalities in glutamate metabolism (Tsai *et al.*, 1995). Furthermore transgenic mice with NMDA receptor subunits knocked out (Miyamoto *et al.*, 2001) or knocked down (Mohn *et al.*, 1999) show schizophrenic-like phenotypes. Of particular note, mice lacking the NR2A subunit (Miyamoto *et al.*, 2001), show increased motor activity and learning deficits, coupled to glutamate hypoactivity and dopamine and 5-HT hyperactivity.

As for the dopamine hypothesis it does not look like there will be a simple conclusion regarding the apparent glutamatergic deficit in schizophrenia. It is likely that neurotransmitter disturbances are not the primary cause of schizophrenia but reflect the consequence of an as yet unidentified pathology.

1.3.2 Macroscopic brain abnormalities

Brain imaging technologies allow direct structural (1.3.2.1) and functional (1.3.2.2) information to be gleaned about the pathology of schizophrenia. Furthermore, representative schizophrenia associated pathology would be a useful diagnostic tool, and also enable the suitability of animal models to be determined.

1.3.2.1 Structural brain imaging

The most consistent structural observation is enlargement of the lateral and third ventricles in schizophrenics. The initial study performed in 1976 using computed tomography (CT) has since been replicated many times, using both CT and the higher resolution afforded by magnetic resonance imaging (MRI) (Cannon, 1996; Chua and Murray, 1996; Harrison, 1999). With the enlargement of the cerebral ventricles, there is a concomitant reduction in brain volume. Brain volume, in particular cortical and subcortical grey matter, is reduced 5 – 10% in schizophrenic patients (Weinberger, 1995). This is reflected by an associated decrease in post-mortem brain weight (Cannon, 1996; Chua and Murray, 1996).

The most consistent reductions in grey matter volume are within the temporal lobe and associated limbic structures (hippocampus and amygdala) (McCarley *et al.*, 1999). Less consistent reductions are reported for the dorsolateral prefrontal cortex with evidence for the involvement of subcortical regions such as thalamus. These brain regions are well placed for the pathogenesis of schizophrenia: the temporal lobe is associated with auditory halluncinations (Frith, 1995), while the hippocampus and amygdala are studied for their involvement in memory and emotion respectively. The prefrontal cortex is involved in complex behaviours, including cognitive processes and emotional behaviours (Fuster, 2001), while the thalamus plays an important role in the processing of sensory information.

At present, neither the increased ventricles nor the reduction in grey matter can be used as diagnostic tools, as considerable overlap between patient and control groups is observed (Cannon, 1996; Harrison, 1999). Nonetheless the possibility remains that people at risk of developing schizophrenia can be identified: in a group of individuals at high genetic risk of developing schizophrenia, with two or more first or second degree relatives affected, the volume of the left amygdala-hippocampal complex and both thalamic nuclei were reported to be smaller (Lawrie *et al.*, 1999). Future objectives would be to provide preventive or coping measures for individuals at risk.

1.3.2.2 Functional brain imaging

Functional brain imaging offers the advantage of monitoring brain activity while a cognitive task is performed or a symptom occurs. During a learning and recall task, a reduction in blood flow within the prefrontal-thalamic-cerebellar circuitry was found in schizophrenic subjects (Andreasen *et al.*, 1996). Furthermore the functional basis of hallucinations has also been examined (Silbersweig *et al.*, 1995). PET performed while subjects were experiencing an auditory hallucination, again implicated multiple brain regions, both cortical (including limbic cortex) and subcortical (including thalamus and striatum). With the recent development of fMRI (functional MRI), offering increased temporal and spatial resolution, the possibility of identifying a diagnostic disturbance remains.

Brain regions implicated with both structural and functional abnormalities are beginning to emerge, but regions of less obvious involvement with schizophrenia are also showing evidence of dysfunction. The cerebellum has long been associated with motor functions, and indeed premorbid features of schizophrenia (section 1.2.1) include motor abnormalities, such as abnormal gait and clumsiness. Furthermore the cerebellum has also been implicated in cognitive function (Fiez, 1996), and highlights the importance of viewing schizophrenia as a systemic brain disorder.

1.3.3 Microscopic brain abnormalities

The search for defining pathological features of schizophrenia is fraught with limitations, not least because of restrictions regarding the procurement and use of human brain tissue. One of the main priorities is ruling out chronic neuroleptic treatment in any potential pathological alteration, which can partly be achieved by neuroleptic administration in animals. With the considerable phenotypic heterogeneity of schizophrenia (section 1.2.1), and overlap with other psychiatric (section 1.2.1.1) and neurological diseases (Brown and Pluck, 2000), the chances of finding a pathological feature unique to schizophrenia are slim.

1.3.3.1 Cytoarchitecture

The cytoarchitectural findings are not as reproducible as the structural abnormalities (section 1.3.2) but there is growing consensus on a number of abnormalities. Firstly schizophrenic brains show a distinct absence of gliosis (Weinberger, 1995; Harrison, 1999). Gliosis is commonly associated with neurodegenerative diseases, and not with pathological insults that occur early in development. Consequently the absence of gliosis, and other features not discussed (Heyman and Murray, 1992; Raedler *et al.*, 1998), has led to the hypothesis that schizophrenia is a neurodevelopmental disorder. Secondly cells of the dorsolateral prefrontal cortex and hippocampus show decreased neuronal cell body size (Harrison, 1999), with a reported increase in neuronal density. Finally disarray of pyramidal hippocampal neurons and disordered laminar architecture of entorhinal cortex are often quoted as being indicative of schizophrenic brains. To date the evidence for these abnormalities has not been unequivocally determined (Harrison, 1999; Weinberger, 1999).

1.3.3.2 Molecular phenotype

Post-mortem brain tissue has been used to examine a large number of molecules, at the level of mRNA or protein. Techniques adopted include immunoblotting, immunohistochemistry, RT-PCR and more recently microarrays. A vast number of changes have been reported in schizophrenic brain with dorsolateral prefrontal cortex and hippocampus again producing the most suggestive results (Harrison, 1999; Weinberger, 1999), although these regions are also likely to be the most well studied. The examination of widespread brain regions, such as cerebellum, is warranted (Katsetos *et al.*, 1997). Coupled to the massive number of molecules implicated from recent microarray studies (Mirnics *et al.*, 2000; Hakak *et al.*, 2001; Vawter *et al.*, 2001; Mimmack *et al.*, 2002), the challenge will be in validation and replication of results. In turn the need for good positional genetic targets (sections 1.4 & 1.5) is emphasised.

Although as suspected, no diagnostic pathological feature has been identified for schizophrenia, the neuropathological findings have begun to offer support to the notion that synaptic disturbances are involved. First, synaptic protein measurements

are assumed to reflect synaptic density, therefore reductions in synaptic markers reported in schizophrenia, indicate a decrease in the number of synapses. Second, neuronal cell body size is proportional to the dendritic and axonal arborizations (Harrison, 1999; Weinberger, 1999), therefore smaller cell bodies (section 1.3.3.1) indicate less complex dendritic and axonal trees. Third, cortical grey matter volume is reduced in schizophrenics (section 1.3.2.1), suggesting the increase in neuronal density (section 1.3.3.1) reflects an alteration in cell packing, in turn related to the synaptic connections between neurons (Raedler *et al.*, 1998; Selemon and Goldman-Rakic, 1999). Therefore at present one view of schizophrenia could be of reduced synaptic connectivity resulting in impaired brain function.

1.4 Evidence for a genetic component to schizophrenia

It is apparent from the familial clustering of schizophrenia that a component of the disease is inherited, reflected in the 80% heritability estimate for schizophrenia (Owen and Cardno, 1999). The lifetime risk for schizophrenia is approximately 10 times greater in siblings or children of schizophrenics than in the general population, and the risk increases with the number of relatives affected (McGuffin *et al.*, 1995). Unequivocal support for a genetic contribution to schizophrenia came from a series of classical twin and adoption studies.

1.4.1 Twin studies

Monozygotic (MZ) twins are genetically identical, while dizygotic (DZ) twins share 50% of their genes. Twins share a common environment during foetal development and consequently twin studies are very powerful methods of investigating the extent of genetic contribution to a phenotype. Twin studies are assessed in terms of concordance rates, the probability that a twin is affected given that the co-twin is affected. For any given disorder, a significantly higher concordance rate in MZ compared to DZ twins indicates a genetic aetiology. For schizophrenia, the concordance rates are 46% for MZ and 14% for DZ twins (McGuffin *et al.*, 1995; O'Donovan and Owen, 1996). This indicates genes are major aetiological factors in schizophrenia. The lack of 100% concordance for MZ twins implicates

environmental factors as well, with the contribution from nonshared environment calculated to be of primary importance (Tsuang, 2000; Tandon and McGuffin, 2002).

1.4.2 Adoption studies

Twin studies suggest that both genes and environment play a role in the development of schizophrenia. A second social paradigm has been used to further examine the relationship between genes and the environment. Adoptions studies were used to determine the occurrence of schizophrenia in adoptees born to schizophrenic parents compared with those born to nonschizophrenic parents. The conclusion was that the biological relatives of schizophrenics have an increased risk of schizophrenia and related disorders, compared to adoptive relatives or control adoptees (McGuffin *et al.*, 1995; O'Donovan and Owen, 1996). Thus adoption studies again point strongly towards a genetic contribution to schizophrenia.

1.4.3 Pattern of inheritance

Simple Mendelian diseases are caused by highly penetrant but rare functional polymorphisms in a single gene. This enables tracking of the disease gene through generations of a family. Unlike Mendelian diseases, schizophrenia shows no such genetically tractable mutation, and the pattern of inheritance within a single family is complex (Lander and Schork, 1994), suggesting that it is a susceptibility to develop psychiatric illness that is inherited.

Genetic models of schizophrenia, favour oligogenic (several genes of modest effect) or polygenic (many genes of minor effect) inheritance, with the additive effect of the genes determining the final phenotype. Alternatively, a number of independent single genes of major effect, showing either reduced penetrance or interaction with several modifier genes, could account for the complex pattern of inheritance (McGuffin *et al.*, 1995; O'Donovan and Owen, 1996). Another layer of complexity is added by the interaction between genes and the environment (Tsuang, 2000). With all models, the inheritance of increasing numbers of genetic mutations could account for the spectrum of disorders associated with schizophrenia (section 1.2.1), and

depending on the mutations inherited could explain the phenotypic similarity with bipolar disorder (section 1.2.1.1).

1.5 Genetic approaches to identify susceptibility genes for schizophrenia

To identify the genetic component of an inherited disease, a number of approaches are used. Positional cloning (section 1.5.1) and the candidate gene approach (section 1.5.2) have been the predominant methods of choice in psychiatric genetics. An alternative has been to use cytogenetic abnormalities (section 1.5.3) as a gross signpost to the underlying genetic lesion. As yet, no mutation or polymorphism has been convincingly demonstrated to contribute to the genetic basis of schizophrenia. Attempts to define the genetic aetiology are confounded in part by the unclear mode of inheritance (section 1.4.3) and phenotypic heterogeneity (section 1.2.1) of the disease.

1.5.1 Positional cloning

Positional cloning is the use of naturally occurring DNA polymorphisms to identify regions of the genome that are shared among affected relatives and tend to differ between affected and unaffected. The general strategy involves first establishing linkage between a disease and a specific chromosomal region. Linkage disequilibrium (LD) is then used to fine map the locus followed by association studies to further define the locus and identify the functional polymorphism (O'Donovan and Owen, 1996; Karayiorgou and Gogos, 1997).

Linkage assigns an approximate chromosomal location to a disease gene by looking for cosegregation between the disease and genetic markers spread evenly at appropriate intervals across the genome. Linkage has been successfully utilized in the identification of single genes of major effect, yet in order to detect genes of minor or modest effect (section 1.4.3) with sufficient power, large families with multiple affected individuals are needed (Moldin, 1997), a considerable drawback to

linkage studies in schizophrenia. Despite positive linkage reports of schizophrenia to almost every human chromosome, independent replication of positive linkage findings coupled to meta-analysis has begun to identify loci that are likely to harbour schizophrenia susceptibility genes. Promising chromosomal loci include 1q21-22, 8p21-22 and 22q11-12 (Jurewicz *et al.*, 2001; Badner and Gershon, 2002; Waterwort *et al.*, 2002). As these genomic regions are large and likely to contain many genes, the next step is to use LD to narrow down the target region.

1.5.2 Candidate genes

Candidate genes are implicated in the genetic basis of a disease due to either their location in a genomic region linked to the disease (positional candidate) or their proposed involvement in the phenotype (model based or hypothesis driven candidates) (Glatt and Freimer, 2002). The majority of candidate genes for schizophrenia have fallen into the latter category.

Candidate genes are tested using association studies, and the most frequently used method is the case-control association study which is based on the comparison of allele frequencies in a group of cases versus controls (Karayiorgou and Gogos, 1997). Association studies offer several advantages over linkage: they do not require large families with multiple affected individuals or any prior knowledge about the mode of inheritance. However an obvious limitation to association studies is that they require candidate genes as well as functional polymorphisms within the genes, and are based on the assumption that there is a common ancient mutation within the gene conferring susceptibility.

Candidate genes for schizophrenia have included NOTCH4 (Wei and Hemmings, 2000; McGinnis *et al.*, 2001; Sklar *et al.*, 2001), dopamine D_3 and 5-HT_{2a} receptors (O'Donovan and Owen, 1999). To date though there has been no replicated significant finding of association of schizophrenia with any gene.

1.5.3 Cytogenetics

The final and less common approach to identifying the genetic component of an inherited illness is to use chromosomal rearrangements as markers for positional cloning. This approach has been successfully utilized in cancer genetics, and a number of chromosomal rearrangements have been described in association with psychiatric illness (MacIntyre *et al.*, 2003).

Chromosomes have traditionally been detected by Giemsa staining to produce the "G-band" profile. FISH (fluorescent *in situ* hybridisation) is the method of choice nowadays, allowing detection of specific nuclei acid regions of the chromosome (Elseth and Baumgardner, 1995). Chromosomal rearrangements include balanced or unbalanced translocations, inversions or the formation of ring structures (Bassett, 1992). Balanced translocations result in rearrangement of the chromosome with no alteration in the total amount of chromosomal material. On the other hand unbalanced translocations involve duplication or deletion of the chromosome. A balanced translocation found to cosegregate with schizophrenia (St Clair *et al.*, 1990) will be described (section 1.6).

1.6 A translocation associated with schizophrenia

The group within which my PhD project was undertaken, has used the less orthodox genetic approach to identify susceptibility genes for schizophrenia (section 1.5.3), and work within the group has focussed on the characterisation of a translocation cosegregating with psychiatric illness.

The MRC Cytogenetics Registry (Edinburgh) contains karyotypic and clinical data on 282 pedigrees with familial autosomal anomalies. This resource was surveyed to determine if any pedigrees were associated with the presence of psychiatric illness (St Clair *et al.*, 1990). A single pedigree was identified with a balanced translocation cosegregating with schizophrenia and other related psychiatric diagnoses in a large Scottish family. The translocation occurs between the q arms of chromosomes 1 and

11 (Figure 1.1B). Recent high resolution FISH mapped the breakpoint regions to chromosome 1q42.1 and 11q14.3 (Millar *et al.*, 2001).

1.6.1 t(1;11) family

The pedigree is referred to within the group, and this thesis, as the t(1;11) family. A total of 87 family members have been karyotyped (Blackwood *et al.*, 2001). 37 members carried the translocation while 50 are noncarriers, including 18 married-in relatives (Figure 1.1A). The family shows a spectrum of psychiatric disturbances with schizophrenia and recurrent major depression as the predominant phenotypes (Table 1.1). A psychiatric evaluation has been performed for 29 carriers and 38 noncarriers. It is important to note that both the primary (St Clair *et al.*, 1990) and follow up psychiatric diagnoses (Blackwood *et al.*, 2001) were carried out by psychiatrists blind to karyotype status. Of the 29 carriers, with both karyotype and clinical data, 21 (72%) show a psychiatric diagnosis. Conversely of the 38 noncarriers, none have a major psychiatric disturbance. Indeed the major psychiatric diagnoses of schizophrenia, recurrent major depression and bipolar disorder only occur when the translocation is present. There are also family members who are t(1;11) carriers but show no psychiatric disturbance. Incomplete penetrance of the phenotype suggests modifier genes or environmental influences are involved.

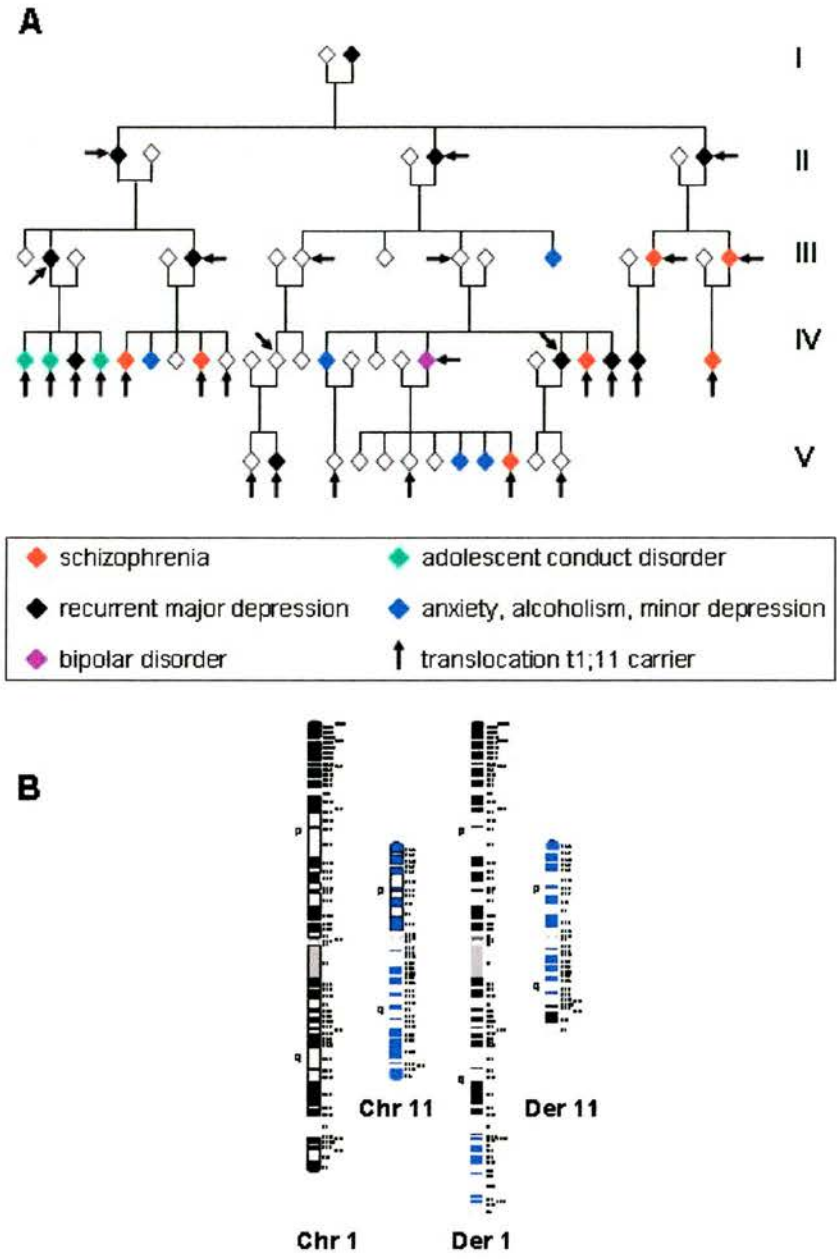

FIGURE 1.1: A translocation cosegregates with psychiatric illness in a Scottish family

A: Part of the t(1;11) family. The members shown are those for whom karyotype status is known and psychiatric evaluation has been performed.

B: The karyotype of the balanced translocation cosegregating with psychiatric illness in the t(1;11) family. Normal chromosomes 1 (black) and 11 (blue), and the derived (der) chromosomes are shown. The translocation occurs between 1q42.1 and 11q14.3.

TABLE 1.1: Psychiatric diagnoses within the t(1;11) family

DIAGNOSIS	t(1;11) CARRIER	NON CARRIER
schizophrenia	7	0
bipolar affective disorder	1	0
recurrent major depression	10	0
adolescent conduct disorder	2	1
minor depression	1	3
alcoholism	0	1
no psychiatric diagnosis	8	33
TOTAL	**29**	**38**

The psychiatric diagnoses present in the t(1;11) family (Figure 1.1) have been summarised. The individuals included represent family members for whom both karyotype and clinical data is available.

Linkage analysis determines the likelihood of a chance association between the translocation and psychiatric illness within the family. Linkage results are reported as LOD scores; LOD scores of >1.9 and >3.3 have been proposed as minimum thresholds for suggestive and significant linkage respectively (Lander and Kruglyak, 1995). Utilization of a number of different phenotypic models allows the relationship between phenotype and translocation to be determined. In the initial study (St Clair *et al.*, 1990), schizophrenia and schizoaffective disorder alone generated a maximum LOD of 2.19. Including recurrent major depression increased the maximum LOD to 3.33 while adolescent conduct and emotional disorder increased the maximum LOD to 4.34. Inclusion of minor psychiatric phenotypes (generalised anxiety, minor depressive episode and chronic alcoholism), substantially reduced the maximum LOD to 1.49. In the recent follow up study (Blackwood *et al.*, 2001), a maximum LOD score of 7.1 was obtained based on a clinical phenotype of schizophrenia, bipolar disorder and recurrent major depression. Restricting the phenotype to schizophrenia or bipolar affective disorder and recurrent major depression generated maximum LOD scores of 3.6 and 4.5 respectively. This highlights the importance of this locus for depression and bipolar disorder as well. The highly significant correlation between the t(1;11) translocation and psychiatric illness in this family has lead to the following hypothesis. A gene or genes located at or near the breakpoint on chromosome 1 or 11 is a gene(s) of major effect in

conferring susceptibility to psychiatric illness in this family. In the best case scenario, a gene would be directly disrupted by the breakpoint, while a second possibility would be that the translocation has indirect effects on a neighbouring gene.

1.6.2 Chromosome 11

The initial search for genes disrupted by the translocation began on chromosome 11, as chromosome 11q had been implicated in two other translocations associated with psychiatric illness (Muir *et al.*, 1995 & references therein). The chromosome 11 breakpoint region has been completely sequenced, and although a number of genes were identified within the vicinity of the breakpoint (Figure 1.2), no genes were found to be directly disrupted by the translocation (Semple *et al.*, 2001 & references therein). The closest gene to the breakpoint, a processed α-tubulin pseudogene, lies over 300kb from the translocation (Devon *et al.*, 1997). Of the remaining genes identified, two are involved in glutamate transmission (section 1.3.1.2), the metabotropic glutamate receptor subtype 5 (mGluR5) and NAALADase II, a peptidase involved in glutamate production.

Investigation of mGluR5 within the group, using a case-control association study, identified a significant difference in mGluR5 allele frequency between schizophrenics and controls (Devon *et al.*, 2001). Furthermore, reduced NAALADase (N-acetyl-alpha-linked acidic dipeptidase) NAALADase activity was reported in post-mortem brain (Tsai *et al.*, 1995). Thus this region does contain a number of functionally interesting genes, but as none are directly disrupted by the translocation, long-range position effects on gene expression would need to be invoked.

1.6.3 Chromosome 1

The translocation breakpoint region on chromosome 1 has also been fully sequenced (Millar *et al.*, 1998; Millar *et al.*, 2000b). Two novel genes, *DISC1* and *DISC2*

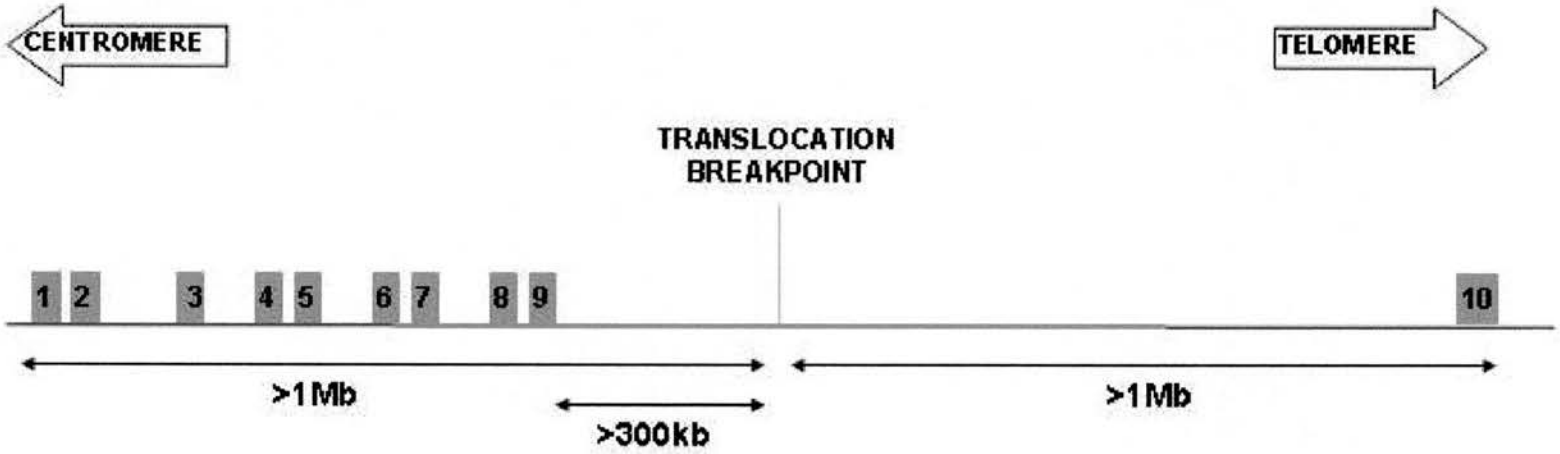

1: metabotropic glutamate receptor subtype 5 (GRM5)

2: tyrosinase

3: NADPH oxidase 4 (NOX4)

4,5,7,10: Ensembl predicted genes

6: NAALADaseII

8: chord domain-containing protein 1 (CHP1)

9: α-tubulin pseudogene

FIGURE 1.2: Genes identified within the chromosome 11 breakpoint region

No genes are directly disrupted by the translocation but 10 genes were identified within a 2Mb region surrounding the breakpoint.

(Disrupted-In-Schizophrenia 1 & 2), were found to be directly disrupted by the translocation (Figure 1.3). In addition *TRAX* (Translin-Associated Factor X), a previously described gene was identified upstream from the translocation (Millar *et al.*, 2000a). Due to their direct disruption by the translocation, *DISC1* and *DISC2*, became our best candidate genes for the development of psychiatric illness in this family. DISC1 is the focus of my PhD and will be discussed in detail (section 1.7).

1.6.3.1 DISC2

DISC2 is transcribed antisense to exon 9 of *DISC1* (Figure 1.3). The 3' end of *DISC2* is tagged by the UniGene cluster Hs.96883, yet to date the 5' end of *DISC2* has not been identified. Multiple tissue Northern blots detected *DISC2* transcripts in adult heart only, but RT-PCR indicated *DISC2* was also transcribed in foetal brain, kidney and spleen (Millar *et al.*, 2000b). No open reading frame has been identified within the incomplete 15kb *DISC2* transcript, suggesting the gene lacks protein coding potential. *DISC2* does share structural similarities to non-coding RNA's, indicating a putative role for the transcript. Non-coding RNA's are an emerging group of molecules which are reported to have roles in post-transcriptional regulation of gene expression, guiding RNA modifications and gene dosage (Kelley and Kuroda, 2000; Eddy, 2001; Lehner *et al.*, 2002). *DISC2* orthologues were detected in mouse and primate cell lines (K.Millar, personal communication), but were not detected in puffer fish (Taylor *et al.*, 2003).

1.6.3.2 TRAX

TRAX had previously been identified (Aoki *et al.*, 1997) and was mapped to chromosome 1q42.1 approximately 150 – 250kb upstream from the translocation breakpoint (Millar *et al.*, 2000a). TRAX shares homology to Translin (Aoki *et al.*, 1997) and additionally, both proteins localise to the same neuronal location (Finkenstadt *et al.*, 2000) and form a protein complex in brain (Finkenstadt *et al.*, 2002). Translin is involved in mRNA translation in dendrites (Kobayashi *et al.*, 1998), and by analogy TRAX has been suggested to have a role in similar functions. *TRAX* lies 50kb upstream from *DISC1* (K.Millar, personal communication), yet five

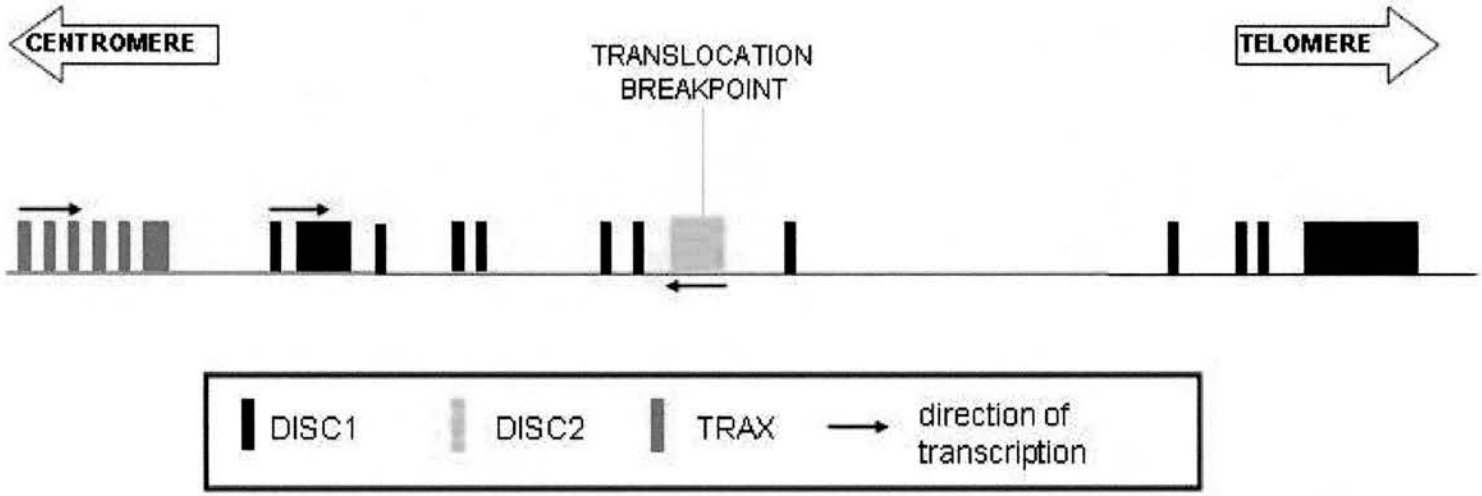

FIGURE 1.2: Genomic organisation of the chromosome 1 breakpoint region

Two novel genes, *DISC1* and *DISC2*, were found to be directly disrupted by the translocation. *DISC2* is transcribed antisense to *DISC1*. A third gene, *TRAX*, was identified 50kb upstream from the 5' end of *DISC1*.

intergenic transcripts containing *TRAX* spliced to *DISC1* were identified (Millar *et al.*, 2000a). In one of the transcripts the open reading frame was maintained, therefore it is possible that a functional TRAX-DISC1 fusion protein is produced or alternatively the intergenic transcripts may have a regulatory role.

1.7 DISC1

Full-length *DISC1* is comprised of 13 exons and covers >50kb of genomic sequence. The first ATG start codon of *DISC1* is not strongly predicted as the site of translation initiation, and it is possible that a downstream start codon is utilized (Millar *et al.*, 2000b). NIX (Nucleotide Identity X) identified two potential promoters 55 and 359bp upstream from the 5' end of *DISC1*. The translocation disrupts *DISC1* within intron 8, the effect of this on *DISC1* expression is not known (potential effects will be discussed in chapter 6).

1.7.1 DISC1 transcripts

DISC1 transcripts were detected in all foetal and adult tissues tested, suggesting *DISC1* is ubiquitously expressed (Millar *et al.*, 2000b). A major transcript of 7.5kb and a less abundant transcript of 4kb (K.Millar, personal communication) were detected on adult human multiple tissue Northern blots. In foetal tissue the transcripts were only detectable by RT-PCR indicating they are of lower abundance. The full-length or long (L) transcript utilizes all 13 exons. At the time of identification, a commonly spliced variant of full-length *DISC1* was detected. The splice variant or long variant (Lv) utilizes a proximal splice site in exon 11, thereby reducing the transcript by 66 nucleotides. Since the initial identification of *DISC1*, a number of putative alternative transcripts have been identified (Figure 1.4). The short 1 (S1) transcript utilizes an alternative terminal exon 9 (exon 9a) and 3' untranslated region (UTR), while a similar transcript short 2 (S2), splices from exon 9 into intron 9 before terminating (K.Millar, personal communication). The extremely short (Es) transcript utilizes an alternative 3'UTR after exon 3 and may

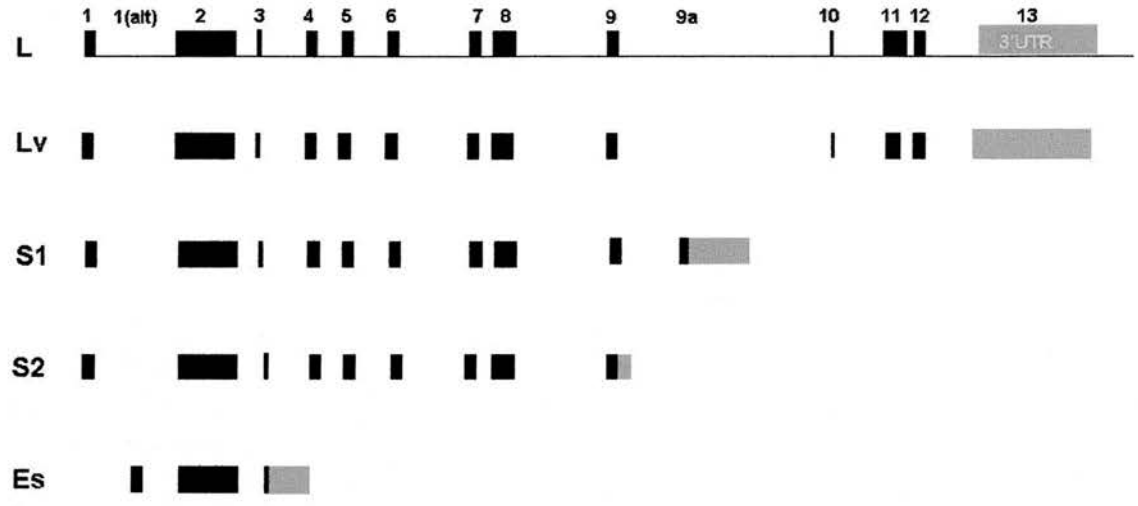

FIGURE 1.4: Alternative *DISC1* transcripts in human

The exon structure of the five putative *DISC1* transcripts, L, Lv, S1, S2 and Es, are indicated. Black and grey boxes represent exons and the 3'UTR of each transcript, respectively. The exact composition of the Es transcript remains to be determined and in the present study the Es transcript was assumed to be comprised of an alternative (alt) exon 1 in conjunction with the alternative 3'UTR as suggested from the available cDNA clone EMBL: AK025293.

also utilize an alternative exon 1 (GenBank: AK025293). UniGene clusters representing the Es (Hs.376142) and S1 (Hs.212335) transcripts provide *in-silico* support. In addition, the S1 transcript had been detected by RT-PCR in human foetal liver and adult heart (M.Taylor, personal communication) but there was no *in-vivo* support for the Es and S2 transcripts.

1.7.2 DISC1 protein

In-silico analysis was performed on the protein sequence of the L DISC1 isoform (Millar *et al.*, 2000b; Taylor *et al.*, 2003). DISC1 consists of N- and C-terminal domains. The two termini approximate to exon boundaries, with the first two exons encoding the N-terminus and the remainder of the gene encoding the C-terminus.

The two termini can also be distinguished based on secondary structure prediction and levels of conservation between species (section 1.7.3).

The N-terminus is comprised of one or more globular domains, with a weakly predicted nuclear localisation signal (NLS) (Taylor *et al.*, 2003). It shares no homologies to any known proteins. Conversely, the C-terminus consists of alpha helical and looped structures, interspersed with regions of coiled coil forming potential. Similarities exist between the C-terminus and structural proteins or proteins involved in transport and motility (Millar *et al.*, 2000b). However these are due to the coiled-coil regions and are unlikely to be functionally relevant. Due to the modular structure of the coiled-coils, these are anticipated to represent the protein interaction domains of DISC1 (Taylor *et al.*, 2003). In addition two leucine zippers are present within the C-terminus (K.Millar, personal communication) and may also have a role in mediating DISC1 protein interactions.

If the *DISC1* transcripts utilize exons 1 and 2, the consequence of alternative splicing, would be to generate proteins with the same N-terminus but slightly varied C-termini. The C-termini would differ by the absence of amino acids, presence of novel amino acids and the number of coiled-coils present (Figure 1.5). The Lv isoform is identical to the L isoform, and differs by the loss of 22 amino acids only. The S1, S2 and Es isoforms are all truncated with respect to the full-length isoforms, and contain novel residues at the C-termini: 18 (S1) or 1 (S2 and Es) amino acids. If the Es transcript utilizes the alternative exon 1, a novel 14 amino acids would be generated at the N-terminus. Furthermore if a truncated protein were generated due to the translocation event, it would be similar to the S isoforms.

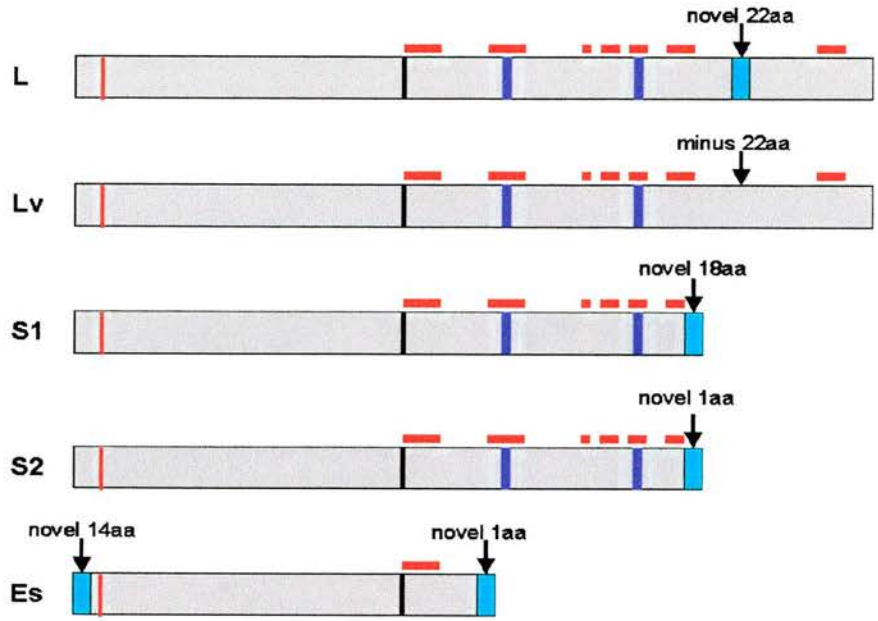

FIGURE 1.5: DISC1 protein isoforms

The predicted protein structure of the DISC1 isoforms. The boundary between the N- and C-terminus is indicated by the black line. The N-terminal NLS is indicated by the vertical red line. Horizontal red bars represent the seven coiled-coil regions within the C-terminus. C-terminal leucine zippers are indicated by purple lines. Novel or spliced amino acid residues are highlighted above the structure. Both the N- and C-terminus show regions of hydrophobicity. Furthermore putative glycosylation and phosphorylation sites were identified within both termini, while glycosaminoglycan and myristoylation sites were identified within the N-terminus. For detailed annotation of these sites see Figure 3.1 (Taylor, 2002).

1.7.3 DISC1 orthologues

Recently three papers, including one from our group, were published describing *DISC1* orthologues in mouse, rat and fish species (Ma *et al.*, 2002; Ozeki *et al.*, 2003; Taylor *et al.*, 2003). Unlike *DISC2* (section 1.6.3.1), *DISC1* is present in all species examined including chimpanzee and other primates (K.Millar, personal communication). The overall gene structure is maintained although there is evidence for alternative splicing strategies in mouse, rat (described in section 7.2) and pufferfish (Taylor *et al.*, 2003). DISC1 is poorly conserved across species with the

N-terminus being less well conserved than the C-terminus. Between human and mouse the N-terminus shows 52% identity, 63% similar and the C-terminus 61% identity, 78% similar (Taylor *et al.*, 2003). The maintenance of distinct N- and C-termini is maintained between species, as are the N-terminal NLS and C-terminal coiled coil regions, suggesting these are functionally important. An alternative exon 1 was reported for mouse (Ozeki *et al.*, 2003). The *in-silico* detection of an alternative exon 1 in both mouse and human (section 1.7.1), increases the likelihood that this exon is real.

1.7.4 Independent association of the DISC locus with schizophrenia

The use of single large families to identify susceptibility genes has one main concern: it is possible the gene identified may be rare or unique to the single family, and though still potentially informative, not relevant to the disease in the widespread population. In such cases validation of findings from independent linkage or association studies is vital.

Therefore it was with great encouragement that a Finnish group published positive linkage of schizophrenia to chromosome 1q, including the *DISC* locus (Ekelund *et al.*, 2001). A total of 558 affected and 1206 unaffected individuals from 221 families were genotyped. The strongest evidence for linkage (LOD = 3.21) was with a microsatellite marker located within intron 9 of *DISC1*. A follow-up study found strongest association for a marker within exon 13 (Ekelund, 2002). Thus encouragingly, *DISC1* is emerging as a candidate gene for schizophrenia in independent populations.

1.8 Aims of thesis

The aim of this thesis was to investigate the function of DISC1 through the development of antibodies. The focus has been on human DISC1 due to the potential for species differences.

The antibodies were generated using both recombinant protein expression and peptide selection (chapter 3). Extensive characterisation of the antibodies was performed (chapter 4), using a number of methodologies, including specificity for recombinant DISC1, possible detection of a DISC1 negative cell line, utilization of tagged proteins and independent DISC1 antibodies.

Following successful characterisation of the antibodies, the first goal was to determine the protein expression pattern of human DISC1 (chapter 5). The availability of lymphoblastoid cell lines derived from t(1;11) family members enabled an initial investigation into the effect of the translocation on DISC1 (chapter 6). Preliminary efforts were also made to examine DISC1 in mouse and rat (chapter 7).

The second goal was to examine the subcellular localisation pattern of DISC1 in cultured human cells (chapter 8). In addition the phenotype of differentiated neuroblastoma cell lines was examined (chapter 9) to allow DISC1 to be examined in a neuronal like cell.

CHAPTER 2

MATERIALS & METHODS

2. Materials & Methods

2.1 Materials

All general use chemicals were from Sigma and cell culture reagents from Invitrogen, unless otherwise stated.

2.2 Methods

2.2.1 Prokaryotic Cell Culture

2.2.1.1 Transformation of plasmid DNA into bacterial cells by heat-shock

Transformation of plasmid DNA was performed for all recombinant protein expression experiments. The *E.coli* cells used are summarised in Table 2.1. All competent cells were obtained as gifts from either David Elliott (MRC Human Genetics Unit) or Scott Bader (CRC Labs, MMC, University of Edinburgh) and were prepared as described (section 2.2.1.3). Transformations were performed using a standard heat-shock protocol as follows. An aliquot of competent cells was thawed on ice. 1µl of plasmid DNA was added to 100µl of competent cells and the cells were cooled on ice for 30 minutes. Next, the cells were heated to 42°C for 45 seconds and then cooled on ice for a further 2 minutes. For growth of the cells (and to allow expression of the antibiotic resistance of the plasmid), 900µl of LB-Broth was added and the cells were grown at 37°C for 1 hour with shaking. Typically 100µl of transformed cells were plated onto LB-agar plates with the appropriate antibiotics added. Plates were grown overnight at 37°C. Following successful growth, colonies on the plates were picked immediately. The plates were never stored, as storage of the plates was found to reduce or completely abolish protein expression from the constructs.

TABLE 2.1: *E.coli* cells used for recombinant protein expression

STRAIN	DERIVATION	GENOTYPE	KEY FEATURES	ANTIBIOTIC RESISTANCE
BL21	B834	F⁻ *ompT hsdS*$_B$ ($r_B^- m_B^-$) *gal dcm*	lacks *lon* and *ompT* proteases	none
BL21 (DE3)	B834	F⁻ *ompT hsdS*$_B$ ($r_B^- m_B^-$) *gal dcm* (DE3)	as for BL21	none
BL21(DE3)pLysS	B834	F⁻ *ompT hsdS*$_B$ ($r_B^- m_B^-$) *gal dcm* (DE3) pLysS (Cm^R)	as for BL21	chloramphenicol
BLR(DE3)	BL21	F⁻ *ompT hsdS*$_B$ ($r_B^- m_B^-$) *gal dcm* Δ(*srl-recA*)*306*::Tn*10*(Tc^R)(DE3)	BL21 *recA* mutant	tetracycline
JM109		e14-(McrA-) *rec*A1 *end*A1 *gyr*A96 *thi-1* *hsd*R17(rK- mK+) *sup*E44 *rel*A1 Δ (*lac-pro*AB) [F' *tra*D36 *pro*AB *lac*I^qZΔM15]	more commonly used for DNA preparation	none

Luria-Bertani broth (LB)	1% (w:v) Bacto-Tryptone (Difco) 0.5% (w:v)Bacto-Yeast extract (Difco) 0.1% (w:v) NaCl pH 7.0 autoclave
LB-agar	LB broth with 15 g of Bacto-Agar (Difco) per litre autoclave

2.2.1.2 Transformation of plasmid DNA into bacterial cells by electroporation

Electroporation of plasmid DNA was performed for all standard DNA procedures including subcloning and preparation of plasmid DNA. DH5α electrocompetent *E.coli* cells were obtained from Sheila Christie (Medical Genetics Section). The use of electrocompetent DH5α cells ensures high transformation efficiency. To transform the plasmid DNA into DH5α cells, an aliquot of cells was thawed on ice and 1µl of dialysed DNA (section 2.2.5.7) was added to 50µl cells. The cells were cooled on ice for 2 minutes and then transferred to an electroporation cuvette. Cells were electroporated at 2.5V, 25µF and 200Ω using a GenePulser™ apparatus (BIORAD). A time signal of approximately 4.8 seconds was obtained with successful transformations. Following electroporation of the cells, 1ml of LB-Broth was added and the cells were incubated at 37°C for 1 hour with shaking. Finally, cells were plated onto LB-agar plates with the appropriate antibiotics added. For subcloning, the whole transformation was plated (typically in batches of 100µl, 200µl and 500µl), whilst for plasmid DNA preparation usually only 100µl of cells were plated. Plates were grown overnight at 37°C and then stored at 4°C for a maximum of 1 month.

2.2.1.3 Preparation of competent E.coli cells

BL21, BL21(DE3) and BLR(DE3) competent cells were prepared using a standard calcium chloride method. For BLR(DE3) cells, all cell growth steps included tetracycline (at a final concentration of 12.5µg / ml) in the growth medium. This is

necessary to maintain the tetracycline resistance marker, which is also associated with the *recA* mutation in this strain. Cells were streaked onto LB-agar plates and grown overnight at 37°C. A single colony was picked into 5ml of LB-Broth and grown overnight at 37°C with shaking. The following day, 1ml of the overnight culture was innoculated into 200ml of LB-Broth and grown at 37°C with shaking until the OD ≅ 0.6 when read at a wavelength of 600nm. The culture was cooled on ice for 30 minutes and then centrifuged for 5 minutes at 1700xg, 4°C. The cell pellet was resuspended gently in 100ml of 50mM calcium chloride and left on ice for 1 hour. Next the cells were centrifuged for 5 minutes at 1700xg, 4°C and then resuspended in 10ml of freezing mix (50mM calcium chloride / 20% (v:v) glycerol). Finally the cells were aliquoted into 200µl samples and snap-frozen on dry-ice / ethanol, before storing at -70°C. The transformation efficiency of the cells was tested by transforming with a plasmid of known concentration.

2.2.1.4 Preparation and recovery of bacterial glycerol stocks

Glycerol stocks were prepared for long-term storage of bacterial cells. Cells were frozen in cryotubes by adding 300µl of 50% (v:v) glycerol to 700µl of bacterial culture. The tube was vortexed before snap-freezing in dry-ice / ethanol and storing at -70°C. To recover the cells, a loop was scraped across the surface and then streaked onto LB-agar plates with the appropriate antibiotics if necessary.

2.2.1.5 Antibiotics

Antibiotics were added to the growth medium at the concentrations outlined in Table 2.2. Ampicillin and carbenicillin were prepared in dH_2O while tetracycline and chloramphenicol were prepared in ethanol. Antibiotics were stored at 4°C as recommended by the manufacturers.

TABLE 2.2: Concentrations of antibiotics used for *E.coli* cell culture

ANTIBIOTIC	STOCK CONCENTRATION	FINAL CONCENTRATION
ampicillin	50mg / ml	50µg / ml
tetracycline	5mg / ml	12.5µg / ml
chloramphenicol	25mg / ml	25µg / ml
carbenicillin	50mg / ml	50µg / ml

2.2.1.6 Expression of recombinant protein in bacterial cells

Both the pET and pGEX protein expression systems are chemically inducible by the addition of IPTG. To induce recombinant protein expression from both constructs, the following protocol was adapted to ensure an optimal yield of recombinant protein. A single colony was picked from a LB-agar plate into 5ml of LB-Broth with the appropriate antibiotics added. The culture was grown overnight at 37°C with shaking and the next day 1ml of the overnight culture was innoculated into 100ml of LB-Broth with the appropriate selection. The cultures were grown at 37°C with shaking until the OD was between 0.4 - 0.6 when read at a wavelength of 600nm. 1ml of cells was removed at this stage to be used as a pre-induced sample to aid identification of the induced protein. IPTG was added to the LB-Broth, to a final concentration of 1mM and the cells were induced for between 3 – 6 hours by continued growth at 37°C with shaking. 1ml samples of cells were taken when necessary with a final sample taken at the end of the induction period. After induction, the cells were centrifuged for 20 minutes at 1700xg, 4°C. The cell pellets were stored at -20°C until expression levels of the recombinant protein had been determined by analysis of the pre-induced and induced samples. Pellets were not stored for longer than 2 weeks at -20°C as degradation of the recombinant proteins began to occur after this time period. The samples that were removed to determine the expression level of the recombinant protein, were centrifuged for 5 minutes at 16000xg, 4°C and the cell pellets resuspended in a final volume of 100µl (50µl 2x protein sample buffer / 10µl 1M DTT / 40µl dH_2O). The lysate was then boiled for 5 minutes followed by centrifugation for 5 minutes at 16000xg, 4°C. Cell lysates were stored at -20°C until SDS-PAGE analysis (section 2.2.3.1).

2.2.1.7 Purification of His-tagged recombinant proteins

The following purification protocol was adapted from the QIAGEN QIA*expressionist*™ handbook (4th edition). The cell pellet had been stored at -20°C (section 2.2.1.6). The pellet was resuspended in 1ml of lysis buffer with 1x complete™ protease inhibitors (Roche), and sonicated on ice, at a wave amplitude of approximately 10 microns for 1 – 2 minutes, to release the bacterial cell proteins. 5µl of the lysate was removed for subsequent analysis by SDS-PAGE, before separating the soluble (supernatant) and insoluble (pellet) proteins by centrifugation for 15 minutes at 30000xg, 4°C. To determine whether the fusion protein had been successfully solubilised, 5µl of the soluble fraction was removed for SDS-PAGE analysis. To purify the His tagged protein, 0.25ml of Ni-NTA Superflow was added to the soluble supernatant and the slurry was rotated for 1 hour at 4°C to allow binding of the His-tagged proteins. The beads were pelleted by centrifugation for 5 minutes at 16000xg and the flow-through removed. 5µl of the flow-through was stored for SDS-PAGE analysis, representing the unbound protein. The beads were washed 4 times in 0.5ml of wash buffer, and 5µl of each wash was removed for SDS-PAGE analysis. To elute the His-tagged proteins, the beads were resuspended in 0.5ml of elution buffer, incubated for 5 minutes at room-temperature before centrifuging the beads for 5 minutes at 16000xg. The eluted protein was removed and the procedure repeated a total of four times. 5µl of each elution was removed for SDS-PAGE analysis, whilst the rest of each elution was stored at -70°C. All 5µl samples were prepared for SDS-PAGE analysis in a final volume of 15µl (7.5µl 2x protein sample buffer / 1.5µl 1M DTT / 1µl dH_2O). The samples were boiled for 5 minutes, centrifuged for 5 minutes at 16000xg, 4°C and then analysed by SDS-PAGE (section 2.2.3.1) to determine the success of the purification.

Lysis buffer	10mM imidazole 50mM NaH_2PO_4 300mM NaCl 1% (v:v) Triton-X-100 10% (v:v) glycerol pH8.0; stored at 4°C autoclave	Wash buffer	20mM imidazole 50mM NaH_2PO_4 300mM NaCl pH8.0 autoclave
Elution buffer	250mM imidazole 50mM NaH_2PO_4 300mM NaCl pH8.0 autoclave		

2.2.1.8 Purification of GST-tagged recombinant proteins

For purification of GST-tagged proteins, the protocol outlined above for His-tagged proteins (section 2.2.1.7) was followed with a few adjustments, namely in the buffers and matrix used but also in the elution conditions. The lysis, wash and elution buffers are outlined below. The matrix used for purification was glutathione agarose (Sigma) which was prepared for use by pelleting the beads at 16000xg for 5 minutes, washing in PBS and then resuspending in PBS to give a 1:1 slurry (w:v). To elute the GST-tagged protein from the glutathione agarose, the elution step was repeated only three times.

Lysis buffer	50mM Tris-HCl (pH8.0) 400mM NaCl 1% (v:v) Triton-X-100 10% (v:v) glycerol autoclave stored at 4°C	Wash buffer	1x PBS autoclave

Elution buffer 10mM reduced glutathione
50mM Tris-HCl (pH8.0)
autoclave

2.2.2 Eukaryotic Cell Culture

2.2.2.1 Growth of cells

Manipulation of eukaryotic cells was performed in an Envair Class II Microbiological Safety Cabinet. Cells were typically grown in T.25 or T.75 tissue-culture flasks with filter caps (CellStar®; greiner bio-one). Cells were maintained in a 37°C incubator with 5% carbon dioxide and were generally fed every 3 – 4 days using the appropriate growth medium (Table 2.3).

2.2.2.2 Passage of surface-adherent cells

The growth medium was aspirated from the flask and the cells were washed once in PBS Dulbecco's. An appropriate volume of trypsin:versene (1:1) was added to the cells and the flask was incubated at 37°C until the cells had begun to dissociate from the flask. The flask was washed out using a 4-fold volume of medium to trypsin:versene and the cell suspension was centrifuged for 3 minutes at 100xg. The cell pellet was then resuspended in an appropriate volume of growth medium and the cells re-plated at a suitable density, typically 1:20 or 1:50 for the SH-SY5Y, LAN-5 and U373 MG cell lines.

2.2.2.3 Passage of suspension cells

The cells were washed from the flask in a suitable volume of medium and centrifuged for 3 minutes at 100xg. The cell pellet was resuspended in an appropriate volume of growth medium and the cells re-plated at a suitable density, typically 1:3 for all of the lymphoblastoid cell lines.

TABLE 2.3: Growth medium and origin of eukaryotic cell lines

CELL LINE [1]	TISSUE (CELL TYPE) DERIVED FROM [2]	GROWTH MEDIUM [3]
SH-SY5Y [4]	brain (neuroblastoma)	DMEM : HamF12 (1:1) / 1x NEAA
LAN-5 [5]	brain (neuroblastoma)	RPMI 1640 / 1x NEAA / 1mM sodium pyruvate
TE671 [5]	brain (cerebellar medulloblastoma)	DMEM / 4mM L-glutamine / 1mM sodium pyruvate
U373 MG [6]	brain (glioblastoma)	DMEM / 2mM L-glutamine
MOG-G-CCM [6]	brain (astrocytoma)	DMEM / 2mM L-glutamine
HepG2 [7]	liver (hepatocellular carcinoma)	DMEM
MCF7 [7]	mammary gland (adenocarcinoma)	DMEM
293 [8]	embryonic kidney	DMEM / 2mM L-glutamine
MAFLI [9]	lymphoblastoid	RPMI 1640
KK47 [9]	lymphoblastoid	RPMI 1640 / 2mM L-glutamine
ROMAR [9]	lymphoblastoid	RPMI 1640
CACO-2 [9]	colon (colorectal carcinoma)	DMEM / 2mM L-glutamine / 1x NEAA
CHO [9]	ovary	RPMI 1640

[1] all cell lines are of human origin, except the CHO cell line which is derived from Chinese hamster

[2] all cell lines are surface adherent except the three lymphoblastoid cell lines which grow as suspension cultures

[3] in addition, all cells were grown in 10% FBS with 100U / ml penicillin & 100μg / ml streptomycin

[4] initially obtained from Organon Laboratories NV but latterly from ECACC

[5] obtained from Organon Laboratories

[6] obtained from Helen Bell; Department of Clinical Neurosciences, University of Edinburgh

[7] obtained from Karen Chapman; Molecular Endocrinology Section, MMC, University of Edinburgh

[8] obtained from Ian Simpson; Genes & Development Group, University of Edinburgh

[9] available within the Medical Genetics Section

2.2.2.4 Preparation and recovery of cell stocks

For long-term storage cells were stored in liquid nitrogen. Stocks were made of all cell lines obtained. The cells were pelleted and the cell pellet resuspended in an appropriate volume of freeze-mix (90% FBS / 10% DMSO): 3ml (T.25) or 9ml (T.75) depending on the size of the flask. 1ml of cell suspension per vial was aliquoted into NUNC™ cryotubes (Nalge Nunc International) and the cells slow-frozen at -70°C before transferring to liquid nitrogen the next day. To resuscitate the cells, a cryotube was removed from liquid nitrogen into a beaker of warm (37°C) water and transferred to the safety cabinet. The cells were thawed using pre-warmed medium and plated into a T.25 flask.

2.2.2.5 Differentiation of neuroblastoma cell lines

Retinoic acid induced differentiation of the LAN-5 and SH-SY5Y cell lines was performed as described (Hill and Robertson, 1998; Guarneri *et al.*, 2000; Magni *et al.*, 2000; Tucholski *et al.*, 2001). The LAN-5 cells were plated at a density of 4 x 10^3 cells / cm^2 and SH-SY5Y cells were plated at a density of 1.3 x 10^3 cells / cm^2. Retinoic acid (Sigma) was prepared as a 1M stock solution in 100% ethanol and stored for a maximum of 2 weeks at -70°C, protected from the light. The day after plating, retinoic acid was added to the growth medium at a final concentration of 1mM. The retinoic acid-containing growth medium was changed every 2 days and the cells were typically exposed to retinoic acid for a maximum of 7 days. Control wells were set up with only ethanol added to the growth medium.

The extended BDNF-induced differentiation of the SH-SY5Y cell line was performed as described (Encinas *et al.*, 2000). Rat-tail collagen (Sigma) was used to coat the coverslips or wells. The collagen was diluted to a final concentration of 0.05 mg / ml and left to evaporate overnight. As above, cells were plated at a density of 1.3 x 10^3 cells / cm^2. The initial part of the protocol was as above for retinoic-acid differentiation. After 5 days in retinoic acid, 50ng / ml BDNF (Sigma) was added to serum-free growth medium and the cells were cultured in the presence of BDNF for

an additional 7 days. The BDNF-containing growth medium was changed every 3 days. Again control wells were set up which did not undergo differentiation.

2.2.2.6 Cytoskeletal disruption of cell lines

Microtubule disruption was performed using nocodazole (methyl-(5-[2-thienylcarbonyl]-1H-benzimidazol-2-yl)carbamate) and taxol (paclitaxel). Microfilament disruption was performed using cytochalasin B. All three drugs were obtained from Sigma. Stock concentrations were prepared in DMSO and stored according to the manufacturer's instructions.

Initial experiments were performed to determine the optimal concentration of drug to use. The concentrations tested were: 0.5, 2, 5 & 10μg / ml nocodazole; 1, 10, 50 & 100μM taxol; 10, 20, 50 & 100μM cytochalasin B. The drugs were added to fresh growth medium and the cells were incubated at 37°C for two hours. The cells were then fixed and processed as usual (section 2.2.4.10). To ensure the DMSO was having no adverse effect on the cells, control wells were incubated in the appropriate volume of DMSO alone.

2.2.2.7 Exposure of microtubules to cold

The following protocol was modified from those published by Job *et al* (Denarier *et al.*, 1998; Bosc *et al.*, 2001; Andrieux *et al.*, 2002). The cells were exposed to the cold by packing the plates in ice for 30 – 60 minutes. The cells were then fixed and processed as usual (section 2.2.4.10).

2.2.2.8 Reformation of the tubulin network

This protocol was adapted from one published by Zmuda & Rivas for location of the centrosome after microtubule depolymerization (Zmuda and Rivas, 1998). In the present study the protocol was used to examine reformation of the tubulin network. Cells were incubated in 2μg / ml nocodazole for 90 minutes and then incubated in drug-free medium for a defined time period (section 8.6). After two rinses in cytoskeletal buffer (CB), the cells were extracted for 1 minute in 0.2% (v:v) Triton-X-100 / 0.25% (v:v) gluteraldehyde / 1μM taxol in CB. Finally the cells were rinsed

once in CB buffer and fixed in methanol for processing as usual (section 2.2.4.10). Appropriate controls were set up to determine the effect of the extraction step on cells that had not been treated with nocodazole.

CB buffer
130mM HEPES
10mM EGTA
2mM $MgCl_2$
pH 6.9

2.2.3 Protein methods

2.2.3.1 SDS-PAGE electrophoresis

Discontinuous SDS-PAGE was performed using the BIORAD Mini-Protean® 3 electrophoresis cell. The separating and stacking gels were prepared as described (Harlow and Lane, 1999a). In general separating gels of 8% and 15% were used for resolution of large and small molecular weight proteins respectively, whilst a stacking gel of 4.3% was used for all gels. Protein was loaded into the wells in 1x Laemmli sample buffer with 1mM DTT added for reduction of the protein. The markers used were either the Precision Broad Range Protein Standards™ (BIORAD) or Mark12™ Wide Range Protein Standard (Invitrogen). Typically 10µl of marker was loaded per marker lane for a gel that was to be Coomassie stained (section 2.2.3.2), while 15µl of marker was loaded per marker lane for a gel that was to be Western blotted (section 2.2.4.7). The gel was submerged in 1x Laemmli running buffer and a constant voltage (approximately 100V) passed through the buffer to allow migration of the protein through the gel.

Laemmli Protein Sample Buffer (2x)
4% (v:v) SDS
20% (v:v) glycerol
120mM Tris pH 6.8
0.01% (w:v) bromophenol blue

Laemmli Running Buffer (10x)
250mM Tris
1.92M glycine
1% (v:v) SDS
pH 8.3
autoclave

2.2.3.2 Coomassie staining of SDS-PAGE gels

After SDS-PAGE (section 2.2.3.1) protein bands were visualised by staining the gel in Coomassie for 20 – 60 minutes with gentle agitation. The gel was destained until the protein bands were clearly visible with a low blue background; usually the gel was destained overnight. Next, the gel was vacuum-dried to provide a permanent record. To prevent cracking of the gel whilst drying, the gel was submerged in dH_2O for one hour with agitation. The gel was then sandwiched between a piece of cellophane membrane (BIORAD) and filter paper, and dried for 90 minutes at 80°C using a Model 583 gel dryer (BIORAD).

Coomassie stain	40% (v:v) methanol
	10% (v:v) glacial acetic acid
	0.1% (w:v) Brilliant Blue R250
	filter
Destain	20% (v:v) isopropanol
	7.5% (v:v) glacial acetic acid

2.2.3.3 Preparation of protein lysates from cell lines

Cells were grown in an appropriate size of flask. The cells were pelleted and the cell pellet resuspended in RIPA buffer with 1x complete™ protease inhibitors (Roche) added: for a T.75 flask, 0.5ml RIPA buffer was used. The cell lysate was sonicated on ice to reduce the viscosity of the lysate and then incubated at 100°C for 5 minutes. Finally the lysate was cleared by centrifugation for 5 minutes at 16000xg and the supernatant was aliquoted and stored at -70°C. The quality of each lysate was determined by SDS-PAGE analysis (section 2.2.3.1).

RIPA buffer 50mM Tris-HCl (pH 7.5)
150mM NaCl
1% (v:v) NP 40
0.5% (w:v) sodium deoxycholate
0.1% (v:v) SDS
autoclave
stored at 4°C

2.2.3.4 Preparation of protein lysates from human tissue

The tissue was weighed and finely ground under liquid nitrogen using a pestle and mortar. The tissue was transferred to a bijou tube on dry-ice and a volume of human tissue lysis buffer with complete™ protease inhibitors (Roche) was added: 10µl lysis buffer per mg of tissue was used. Next the sample was homogenized and incubated on ice for 15 minutes with RNase A (200µg / ml). The lysate was then sonicated on ice and cleared by centrifugation for 5 minutes at 16000xg. The supernatant was aliquoted and stored at -70°C. The quality of each lysate was determined by SDS-PAGE analysis (section 2.2.3.1).

Human tissue lysis buffer 2x PBS
0.1% (v:v) SDS
1% (v:v) NP 40
0.5% (w:v) deoxycholic acid
1mM EDTA
autoclave
stored at 4°C

2.2.3.5 Preparation of protein lysates from mouse & rat tissue

The tissue was weighed and homogenized in ice-cold 0.32M sucrose with 1x complete™ protease inhibitors (Roche) added: 10µl sucrose solution per mg of tissue was used. Following homogenization the samples were aliquoted and stored at -70°C. Tissue lysates were only subjected to centrifugation if the lysates contained

lots of tissue debris. The quality of each lysate was determined by SDS-PAGE analysis (section 2.2.3.1).

2.2.3.6 Quantification of protein by UV detection

The following equation is from Using Antibodies (Harlow and Lane, 1999b). The protein concentration of purified antibodies was determined by measuring the OD_{280} and then calculating the antibody concentration using the approximation below:

$$OD_{280} \text{ of IgG at } 1mg / ml = 1.35$$

2.2.3.7 Quantification of protein by use of the BIORAD DC Protein Assay

The concentration of protein lysates was determined by using the BIORAD DC Protein Assay. This assay is similar to the Lowry assay and measures the protein concentration of the sample at an optical density of 750nm. The assay has been developed to ensure compatibility with a number of detergents. The protein concentration was calculated as outlined in the manufacturer's guidelines. A BSA standard curve was generated each time the assay was performed. Standard curves were produced using Excel (Microsoft) and the straight line equation was used to calculate the concentration of the protein lysates.

2.2.3.8 Dialysis

Dialysis tubing (Sigma) was prepared by boiling the tubing for 10 minutes in 1mM EDTA / 2% (w:v) $NaHCO_3$, followed by boiling for 10 minutes in dH_2O. The tubing was then washed repeatedly in dH_2O and stored in 50% (v:v) ethanol at 4°C. Before use the tubing was washed in dH_2O.

Protein samples were dialysed in a 10 – 20 times excess of dialysis solution and were dialysed overnight at 4°C with constant stirring. The dialysis solution was changed at least once.

2.2.4 Antibody and related methods

2.2.4.1 Preparation of purified protein for antigen injection

To prepare the recombinant DISC1 protein for antigen injection, the purified protein was separated on a SDS-PAGE gel. Once the protein had migrated sufficiently through the gel, the gel was washed in dH_2O for 10 minutes. The wash step was repeated 2 times before staining the gel for 1 hour in an aqueous Coomassie blue solution. The gel was then destained using 1x Laemmli running buffer without SDS, until the appropriate band was visible. The band was cut out of the gel and ground to a fine powder under liquid nitrogen using a pestle and mortar. The powder was transferred to an eppendorf in PBS and sent on dry-ice to SAPU for antigen injection. Typically, 250µg of purified protein was loaded per gel and 1ml of PBS was used to resuspend the protein powder.

Aqueous Coomassie 0.1% (w:v) Brilliant Blue R250
in 1x Laemmli running buffer (without SDS)

2.2.4.2 Storage of antisera and purified antibodies

To avoid repeated freeze-thawing, crude antisera and purified antibodies (section 2.2.4.5) were aliquoted into appropriate volumes and stored at -20°C. To use, the antisera or antibodies were thawed and stored at 4°C for a maximum of 6 months.

2.2.4.3 Immunoglobin preparation by caprylic acid fractionation

The antiserum to be purified was thawed and 2 x volume of 60mM sodium acetate (pH4.0) was added. The solution was mixed vigorously using a magnetic stirrer before slowly adding an appropriate volume of caprylic acid (n-octanoic acid; Sigma) through a 19 gram needle. The volume of caprylic acid added depends on the animal the antiserum was raised in. For sheep and rabbits, 700µl or 750µl caprylic acid per 10ml of the original serum volume was added respectively. The solution was mixed for a further 30 minutes, after which it was subjected to centrifugation for 20 minutes at 3000xg, room temperature. The resulting

supernatant was filtered through 597½ filter paper (Schleicher & Schuell) and then the filtrate was dialysed (section 2.2.3.8) against 0.154M sodium chloride solution for 1 day. The caprylic acid purified antibodies were stored at 4°C until further use.

2.2.4.4 Preparation of SulfoLink column for antibody purification

For immunoaffinity purification of both the anti-peptide and anti-protein antibodies, columns were prepared with the DISC1 peptide and fusion protein bound to a sulfhydrl activated resin (SulfoLink® Coupling Gel; Pierce). The SulfoLink coupling gel was packed into a 5ml polypropylene column (Pierce) according to the manufacturer's guidelines. The DISC1 peptide and fusion protein were bound to the column as recommended in the manufacturer's guidelines: 1mg of DISC1 peptide and 10mg of purified DISC1 fusion protein was bound to the SulfoLink coupling gel. The coupling efficiency was determined by either measuring the optical density of the peptide solution at 250nm or SDS-PAGE analysis (section 2.2.3.1) of the fusion protein before and after passing through the column. All of the peptide and protein applied bound to the SulfoLink coupling gel. The columns were stored at 4°C with an overlay of 0.05% (w:v) sodium azide in PBS. The columns were stored for a maximum of one year.

2.2.4.5 Immunoaffinity purification of antibodies

Immunoaffinity purification of the antibodies was performed as described in Using Antibodies (Harlow and Lane, 1999c). The initial purifications were performed using both acid and base-sensitive elution conditions, however for both the anti-peptide and anti-protein antibodies, the acid elution conditions were found to be sufficient for elution of the majority of the antibodies, consequently the steps relating to the basic elution conditions were omitted. The DISC1 peptide or protein bound Sulfolink column (section 2.2.4.4) was washed with 10 bed-volumes of 10mM Tris pH 7.5 followed by 10 bed-volumes of 100mM glycine pH 2.5. Next the column was washed repeatedly in 10mM Tris pH 8.8 until the final pH reached 8.8. The column was then washed in 10 bed-volumes of 100mM triethylamine pH 11.5 followed by repeated washing in 10mM Tris pH 7.5 until the final pH reached 7.5.

The caprylic acid purified serum (section 2.2.4.3) was passed through the column 3 times. The remaining serum was stored at -20°C. A volume of the caprylic acid purified serum both before and after immunoaffinity purification was removed and stored at 4°C for subsequent analysis. The column was washed with 20 bed volumes of 10mM Tris pH 7.5 followed by 20 bed-volumes of 0.5M NaCl / 10mM Tris pH 7.5. The acid-sensitive antibodies were eluted by passing 850µl 100mM glycine pH 2.5 through the column and collecting the eluate in eppendorfs containing 150µl 1M Tris pH 8.0. This step was repeated 10 times and the eluates collected in individual eppendorfs. The column was then washed with 10mM Tris pH 8.8 until the final pH reached 8.8. The base-sensitive antibodies were eluted as described above, but 850µl 100mM triethylamine pH 11.5 was passed through the column 10 times and collected in 150µl 1M Tris pH 8.0. The column was finally washed in 10mM Tris pH 7.5 until a final pH of 7.5 was reached. The column was stored as usual with an overlay of 0.05% (w:v) sodium azide. To determine the elutions containing the antibodies, 5µl of each elution was analysed by SDS-PAGE (section 2.2.3.1). An aliquot of the caprylic acid purified antibodies before and after purification were also analysed. The elutions containing the antibodies were dialysed (section 2.2.3.8) in appropriate volumes against 0.02% (w:v) sodium azide in PBS. The concentration of the purified antibodies was determined by measuring the OD_{280} (section 2.2.3.6) of the antibodies. If the concentration of the antibodies was ≤1mg / ml, 1% (w:v) BSA was added before long-term storage at -20°C. Following immunoaffinity purification of DISC1-specific antibodies, any comparison between the pre-immune serum and the purified DISC1 antibodies was performed by diluting the pre-immune serum to the same starting concentration as the purified DISC1 antibodies, before diluting further as appropriate.

2.2.4.6 Peptide preabsorption of antibodies

Preabsorption of DISC1 anti-peptide antibodies was performed as described (Yamamoto *et al.*, 2000). The DISC1 anti-peptide antibody was diluted at the appropriate concentration (Table 2.4) in blocking buffer. DISC1 peptide (5mg / ml) was added to the antibody solution in increasing concentrations to determine the minimal concentration of peptide needed to completely abolish the antibody signal.

The solution was incubated overnight at 4°C with rotation. Before use the antibody solution was subjected to centrifugation at 800xg for 30 minutes. Control pre-absorptions were always set up without any peptide added.

2.2.4.7 Western blotting

Western blotting was performed using the BIORAD Trans-Blot Semi-Dry Electrophoretic Transfer Cell. The protein was transferred to PVDF membrane. Following electrophoretic transfer of proteins (section 2.2.3.1), the gel was equilibrated in transfer buffer for 3 washes of 10 minutes each. The membrane was pre-wetted in methanol before incubating in transfer buffer for 15 minutes. A transfer sandwich was assembled as described in the manufacturer's instructions. Optimal transfer conditions were determined for each protein as necessary, and typical transfer times were 30 – 45 minutes for an 8% and 1.5 hours for a 15% SDS-PAGE gel, at a constant voltage of 20V. Following transfer, the membrane was given 2 washes of 10 minutes each in dH_2O and then stained in Ponceau S for a few seconds before washing in dH_2O to allow visualization of the protein. The membrane was air-dried and stored at room-temperature. If necessary, the gel was stained in Coomassie (section 2.2.3.2) to determine the amount of protein remaining after transfer.

Bjerrum & Schafer-Nielson transfer buffer

48mM Tris
39mM glycine
0.04% (v:v) SDS
20% (v:v) MeOH
pH 9.0 – 9.4
stored at 4°C

Ponceau S

0.5% (w:v) Ponceau
in 2% (v:v) glacial acetic acid

2.2.4.8 Immunoblotting

Following protein transfer (section 2.2.4.7), the air-dried membrane was pre-wetted in methanol and the Ponceau S washed from the membrane by successive washes in dH_2O. The membrane was then incubated overnight in blocking buffer at 4°C. The next day, the membrane was rinsed twice in PBS-T (PBS with 0.1% (v:v) Tween 20) followed by 1 wash for 15 minutes and 2 washes for 5 minutes each in PBS-T. The primary antibody was diluted appropriately (Table 2.4) in blocking buffer and incubated with the membrane for a minimum of 1 hour. The membrane was washed again as above, before incubating in the appropriate HRP-conjugated secondary antibody. The secondary antibody was also diluted (Table 2.5) in blocking buffer but the incubation period was usually shorter than for the primary antibody, typically 40 minutes. Finally the membrane was rinsed twice in PBS-T followed by 1 wash for 15 minutes and 4 washes of 5 minutes each in PBS-T. The signal was detected using either Fast DAB (diaminobenzidine) tablets (Sigma) or ECL Plus (Amersham Biosciences). Both were applied according to the manufacturer's instructions. For ECL Plus, the membrane was exposed to autoradiography film. If necessary membranes were stored at 4°C until further use (section 2.2.4.9). DAB stained blots were never reused.

Blocking buffer	5% (w:v) nonfat milk (Marvel) in PBS-T

2.2.4.9 Stripping immunoblots

The membrane was pre-wetted in methanol and washed two times in dH_2O for 10 minutes each wash. The membrane was then incubated in stripping buffer for 30 minutes – 1 hour at 50°C with rotation, after which the blot was washed 2 times in PBS-T for 10 minutes each wash. Immunoblotting was performed as described (section 2.2.4.8), starting with the blocking step. Immunoblots were only stripped once to avoid removal of the protein from the membrane.

Stripping Buffer	50mM Tris-HCl (pH 6.8)
	1.6% (v:v) SDS
	80mM mercaptoethanol

2.2.4.10 Immunofluorescence

Coverslips (BDH) were sterilised by autoclaving and placed in individual wells of 12-well plates (Corning Incorporated). Cells were grown on the coverslips for a minimum of 24 hours. Before fixing the cells were washed once in PBS and fixed for 5 minutes in ice-cold methanol or 15 minutes in 4% (w:v) paraformaldehyde. Following fixation the cells were washed three times in PBS and paraformaldehyde fixed cells were permeabilised by incubating in 0.5% (v:v) Triton-X-100 for 20 minutes. The cells were then blocked for 30 minutes in blocking buffer. The primary antibody was diluted in blocking buffer (Table 2.4) and incubated on the cells for the appropriate time. The cells were washed 3 times for 2 minutes each wash in PBS-T (PBS with 0.2% (v:v) Tween 20). Next, the secondary antibody was diluted in blocking buffer (Table 2.5) and incubated on the cells for 40 minutes. The secondary antibody was subjected to centrifugation for 20 minutes at 16000xg to remove any protein aggregates that may have formed during storage. Following incubation with the secondary antibody, the cells were washed 3 times for 2 minutes each wash and the coverslips were mounted onto SuperFrost slides (BDH). Mowial mounting medium with DAPI was used to mount the coverslips. Slides were stored at 4°C protected from the light. Appropriate controls were set up: the cells were tested for autofluorescence by omitting both the primary and secondary antibodies, as well as determining the background fluorescence from the secondary antibody by omitting the primary antibody only. The slides were analysed with an Axioskop 2 MOT epifluorescence microscope (Zeiss) using 16x and 100x plan-NEOFLUAR oil objectives (Zeiss).

Blocking buffer	10% (v:v) serum (SAPU, Ellen's Glen Road, Edin EH17 7QT)
	1% (w:v) BSA
	in PBS-T

Mowial mounting medium

Mix 7.5g Mowial 40-88 (Aldrich) and 10ml glycerol then add 25ml dH_2O, cover and leave overnight at room temperature. The next day, add 50ml 0.2M Tris-HCl (pH 8.5) and mix. Heat the mixture in a boiling water bath for 20 minutes with periodic mixing and allow to cool. Add 1.75g Dabco™ (triethylenediamine; Sigma) and mix until dissolved. Finally add DAPI to a final concentration of 250ng / ml. Store at 4°C or at -20°C for long term storage.

2.2.4.10.1 Dual immunofluorescence

For dual immunofluorescence, the antibodies were diluted together in blocking buffer. In addition, the length of the washes was increased to 5 minutes each wash. To ensure the specificity of the secondary antibodies, controls were set up to test the secondary antibody on the wrong primary antibody, for example, a rabbit primary antibody with a mouse secondary antibody.

2.2.4.10.2 Dual immunofluorescence using primary antibodies derived from the same host animal

In some of the colocalisation studies (section 8.4), both of the primary antibodies were derived from rabbit. To enable dual immunofluorescence to be performed, the DISC1 anti-peptide antibody was directly conjugated to the fluorochrome Alexa-Fluor 488 (performed by K.Millar). The immunofluorescence protocol was performed as usual (section 2.2.4.10), applying the unconjugated primary antibody followed by the anti-rabbit secondary antibody. After the secondary antibody incubation, the cells were then blocked with rabbit serum for 30 minutes before applying the conjugated primary antibody.

TABLE 2.4: Primary antibody dilutions

ANTIBODY	COMPANY	DILUTION FOR IB	DILUTION FOR IF	FIXATIVE FOR IF
DISC1 anti-peptide	in-house*	1:1000	1:500	MeOH / PFA
DISC1 anti-peptide AF488 conjugated	in-house*	n.d.	1:50	MeOH†
DISC1anti-protein	in-house*	1:500	n.d.	
anti-DISC1-C2	A.Sawa*	1:200	1:100	MeOH / PFA
V5	Invitrogen	1:2000	1:200	MeOH / PFA
nucleoporin p62	BD Transduction	1:1000	n.d.	
VLA-2α	BD Transduction	1:250	n.d.	
GAPDH	Chemicon International	1:1000	n.d.	
α-tubulin (B-5-1-2)	Sigma	1:1000	1:3000	MeOH / PFA
β-actin (AC-15)	Sigma	n.d.	1:3000	MeOH†
γ-tubulin (GTU-88)	Sigma	n.d.	1:2000	MeOH
NF (2F11)	DAKO	n.d.	1:100	MeOH / PFA
GFAP	DAKO	n.d.	1:1000	MeOH / PFA
MAP2B	BD Transduction	n.d.	1:500	MeOH†
GM130	BD Transduction	n.d.	1:1000	MeOH†

IB immunoblotting; IF immunofluorescence; n.d. not determined;
MeOH methanol; PFA paraformaldehyde
† PFA not tested; * DISC1 antibodies generated in this project or independently by the Sawa lab

TABLE 2.5: Secondary antibody dilutions

ANTIBODY	COMPANY	DILUTION
anti-rabbit HRP conjugated	DAKO	1:3000
anti-goat HRP conjugated	DAKO	1:2000
anti-rabbit Alexa Fluor 594	Molecular Probes	1:1000
anti-mouse Alexa Fluor 488	Molecular Probes	1:1000

2.2.4.11 Fluorescent probes

For fluorescent detection of mitochondria and the endoplasmic reticulum, flurorescent probes (Molecular Probes) were obtained from Jianghui Hou (Molecular Endocrinology Section, MMC). MitoTracker® Deep Red 633 was used for detection of mitochondria and was applied as outlined in the manufacturer's instructions for the staining of fixed cells. However this procedure did not produce the expected mitochondrial staining pattern (section 8.4.3.3). Rhodamine B, hexyl ester, percholate (R6) was used for detection of the ER. The dye was applied to fixed cells at a final concentration of 0.5μg / ml for 1 minute. The cells were then washed 3 times for 5 minutes each wash and mounted as before (section 2.2.4.10).

2.2.4.12 Image analysis

Images were captured using SmartCapture 2 version 2.3.1 (Digital Scientific Ltd). Appropriate exposure times were set for the FITC and TxRed filters, typically 0.01 – 0.5s. No exposure time was set for the DAPI filter. The gain of the camera was set to 1.0 and 12-bit images were captured to enable direct comparisons between images. SmartCapture and Adobe PhotoShop 5.5 (Adobe Systems Incorporated) were used for adjustment of the final image. For images requiring direct comparisons, for example DISC1 anti-peptide antibody ± DISC1 peptide (Figure 4.8), all image capture and any subsequent steps were exactly the same.

2.2.5 Standard molecular biology methods

2.2.5.1 Agarose gel electrophoresis

Agarose gels were prepared by heating agarose MP (Invitrogen) in 1x TAE buffer. After dissolution of the agarose, ethidium bromide was added to the gel at a final concentration of 0.4 μg / ml. In general, 1.8% and 0.8% agarose gels were used for resolution of small and large DNA fragments respectively. DNA was loaded into the wells in 1x STOP loading buffer. The markers used were 1kb DNA ladder, λ DNA/ *Hind* III fragments or φX174 RF DNA/*Hae* III fragments (Invitrogen). Typically 500ng of DNA was loaded per marker lane. The gel was submerged in 1x TAE

buffer and a current of 50 - 100V was passed through the buffer to allow migration of the DNA through the gel. Following electrophoresis DNA was visualised by UV transillumination and images captured using a digital imager, UviTec (Thistle Scientific, Uddingston, Glasgow G71 6NZ).

TAE (20x)	0.8 M Tris-HCl (pH 8.0) 20 mM EDTA 0.4 M acetic acid autoclave
STOP loading buffer (10x)	10% (w:v) Ficoll 1mM EDTA Orange G to colour

2.2.5.2 Miniprep preparation of DNA

A single bacterial colony was used to innoculate 3ml of LB-Broth with the appropriate antibiotics added. The culture was grown overnight at 37°C with shaking and the next day DNA was prepared using QIAGEN buffers. 1.5ml of the culture was centrifuged for 2 minutes at 16000xg. The pellet was resuspended in 300µl Buffer P1 before adding 300µl Buffer P2 and incubating for 5 minutes at room temperature. Next, 300µl Buffer P3 was added and the lysate incubated for 30 minutes on ice before centrifugation for 2 minutes at 18000xg. The supernatant was removed for phenol-chloroform extraction (section 2.2.5.8) and an equal volume of isopropanol was added to the aqueous layer. The DNA was pelleted by centrifugation for 10 minutes at 16000xg and washed in 70% (v:v) ethanol followed by 100% ethanol. The pellet was then air-dried and the DNA resuspended in approximately 50µl dH_2O. DNA was stored at -20°C. The quality of the DNA was determined by agarose gel analysis (section 2.2.5.1) and an appropriate restriction digest (section 2.2.5.10) was performed to confirm the identity of the DNA.

Buffer P1	50mM Tris-HCl (pH8.0) 10mM EDTA 100µg / ml Rnase A	Buffer P2	200mM NaOH 1% SDS
Buffer P3	3M potassium acetate pH5.5		

2.2.5.3 Midiprep preparation of DNA

A single bacterial colony was used to innoculate 50ml of LB-Broth with the appropriate antibiotics added. The culture was grown overnight at 37°C with shaking and the next day DNA was prepared using the QIAGEN Plasmid Purification Midiprep Kit, as described by the manufacturer's. DNA was typically resuspended in 200µl dH_2O and stored at -20°C. The quality of the DNA was determined by agarose gel analysis (section 2.2.5.1) and an appropriate restriction digest (section 2.2.5.10) was performed to confirm the identity of the DNA.

2.2.5.4 Preparation of RNA

Preparation of RNA was performed in a designated Envair Class II Microbiological Safety Cabinet. RNA was prepared from cell lines and tissue using RNAzol B (Biogenesis), according to the manufacturer's instructions. RNA was resuspended in DEPC-treated dH_2O, aliquoted and stored at -70°C.

DEPC-treated dH_2O

50µl DEPC (diethyl polycarbonate) was added to 500ml dH_2O and allowed to evaporate overnight in a fume hood. The DEPC-treated dH_2O was autoclaved before use.

2.2.5.5 Preparation of cDNA

Preparation of cDNA was performed in a designated Envair Class II Microbiological Safety Cabinet. cDNA synthesis was carried out using the Roche™ 1st strand cDNA synthesis kit, as described by the manufacturer, using random hexameric primers.

Approximately 8µg of total RNA was DNase treated (section 2.2.5.11) prior to 1st strand synthesis. For every reaction, a control reaction was performed that lacked the reverse transcriptase (RT) enzyme, for use as a negative RT-PCR control. cDNA was stored at -20°C.

2.2.5.6 Quantification of DNA & RNA

Quantification of DNA and RNA was performed by measuring the optical density at 260nm. The following equations were used for determining the concentration:

DNA (µg / ml) = OD_{260} x 50 x dilution factor

RNA (µg / ml) = OD_{260} x 40 x dilution factor

In addition the purity of the nucleic acid was measured by determining OD_{260}/ OD_{280}. A value of ≤1.8 or 2.0 indicated the nucleic acid was contaminated with phenol or protein.

2.2.5.7 Dialysis of DNA

To adjust the salt content of DNA solutions, either before electroporation of plasmid DNA (section 2.2.1.2) or between a double restriction digest (section 2.2.5.10), an appropriate volume of DNA was placed on nitrocellulose filter discs of 0.025µm pore size (Millipore), which were floating on a pool of dH_2O. The DNA was left for 30 minutes to allow equilibration and the DNA recovered from the disc by pipetting.

2.2.5.8 Phenol-chloroform extraction of DNA

A 0.5 x volume of phenol and 0.5 x volume of chloroform was added to the nucleic acid solution. The solution was vortexed before centrifugation for 5 minutes at 16000xg. The upper aqueous layer containing the nucleic acids was removed and an equal volume of chloroform added. The solution was again vortexed and centrifugated for 5 minutes at 16000xg. The upper layer was removed and the nucleic acids precipitated (section 2.2.5.9)

2.2.5.9 Ethanol precipitation

DNA was precipitated from solution in a 2 x volume of 100% ethanol and 0.1 x volume of 3 M sodium acetate (pH5.0). The solution was incubated for a minimum of 30 minutes at -70°C and the DNA precipitated by centrifugation for 20 minutes at 16000xg. The DNA was washed in 70% (v:v) ethanol and air-dried before resuspending in dH_2O.

2.2.5.10 Restriction digest of DNA

An appropriate concentration or volume of DNA was digested: typically 5µg of plasmid DNA or an entire volume of amplified or ligated DNA. All restriction enzymes were from Roche, enabling double digests to be performed in one reaction. DNA was digested in 1x buffer with 2U enzyme per µg DNA and incubated for at least 4 hours at the optimal temperature for enzyme activity. Digested plasmid DNA was analysed by agarose gel analysis (section 2.2.5.1) to ensure complete digestion of the DNA.

2.2.5.11 DnaseI digestion of RNA

Typically 8µg RNA was treated to ensure enough RNA for both ±RT reactions during cDNA synthesis (section 2.2.5.5). The RNA was incubated with 20U of DNaseI (Roche) and 20U RNase inhibitor (Roche) in 1x DNaseI buffer (100mM sodium acetate (pH 5.0) / 5mM magnesium sulphate), for 30 minutes at 37°C. The DNaseI was removed by phenol-chloroform extraction (section 2.2.5.8) and the RNA ethanol precipitated in 3 x volume of 100% ethanol and 0.1 x volume of 7.5M ammonium acetate, followed by a 75% (v:v) ethanol wash. The RNA was resuspended in an appropriate volume of DEPC-treated dH_2O and stored at -70°C until cDNA synthesis.

2.2.5.12 Ligation of DNA

All ligations were performed in a 3:1 molar ratio of insert:vector. The digested DNA substrates (section 2.2.5.10) were incubated with 1U T4 DNA Ligase (Roche) in 1x ligase buffer (supplied by the manufacturer's). An overnight incubation at 16°C was

performed. The ligation reaction was dialysed (section 2.2.5.7) before digestion with *Sal*I (section 2.2.5.10). Both of the protein expression vectors contain *Sal*I cloning sites that are destroyed following correct ligation of the insert into the vector. Consequently only vector without the insert will digest, as linear plasmids are not as well transformed as circular plasmids, therefore background from recircularised plasmid will be reduced. The total ligation was electroporated (section 2.2.1.2) for selection of positive subclones (section 2.2.5.14).

2.2.5.13 Purification of DNA from agarose gel

DNA was purified from agarose gels using the QIAGEN QIAquick Gel Extraction kit which is suitable for the recovery of 70bp – 10kb DNA fragments. DNA was separated on a LMP agarose gel (section 2.2.5.1). The target band was illuminated by short-wave UV transillumination, excised and DNA extracted according to the manufacturer's instructions.

2.2.5.14 Bacterial colony lifts

Bacterial colonies were transferred from LB-agar plates to circular gridded nitrocellulose filters (Schleicher & Schuell) by placing the filters on the plates, leaving for 10 seconds and then carefully removing the filters. The filters were placed colony side up sequentially on 3MM (Whatman) filter paper soaked in 10% SDS (2 – 3 minutes), denaturation and renaturation solution (3 - 5 minutes each). The filters were rinsed in 2x SSC and air-dried before baking for 2 hours at 80°C. LB-agar plates were incubated at 37°C for 2 hours to allow regrowth of the colonies.

Denaturation solution 1.5M NaCl
0.5M NaOH

SSC (20x) 3M NaCl
0.3M trisodium citrate
pH7.0
autoclave

Renaturation solution 1.5M NaCl
0.5M Tris-HCl (pH7.5)

2.2.5.15 Radiolabelling of DNA

A gel slice containing the *DISC1* 980bp exon 2 was used as a probe for detection of subclones. The gel slice was melted by heating at 70°C and 13µl removed for labelling. The DNA was denatured by incubating at 100°C for 5 minutes. Next, 4µl of High Prime nucleic acid labelling system (Roche) and 3µl 10 µCi/ µl[α-^{32}P]-dCTP (Amersham Biosciences) was added to the denatured DNA and the reaction mix was incubated at 37°C for 15 minutes. Finally 80µl TE was added to the reaction mix and the DNA denatured again for 5 minutes at 100°C. The radiolabelled probe was kept on ice until use (section 2.2.5.16).

TE 10mM Tris-HCl (pH7.6)
1mM EDTA (pH8.0)

2.2.5.16 Hybridisation of radiolabelled probes to membrane bound DNA

Gridded filters (section 2.2.5.14) were layered between gauze, soaked in 2x SSC and transferred to a hybridisation tube (Hybaid). 20ml hybridisation mix was added and the filters incubated for 30 minutes at 68°C. Radiolabelled probe (section 2.2.5.15) was added to the hybridisation mix and incubated overnight at 68°C. The next day, the filters were washed in 10 minute batches, in pre-warmed (68°C) 0.1x SSC / 0.1% SDS. The filters were exposed overnight to autoradiography film at -70°C. Positive subclones were identified by aligning the autoradiography film with the gridded nitrocellulose filter.

Hybridisation mix
5x SSC
10% (w:v) dextran sulphate
0.5% (v:v) SDS
in 5x Denhardt's solution
filter

Denhardt's solution (5x)	0.1% (w:v) Ficoll
	0.1% (w:v) PVP (polyvinylpyrolidine)
	0.1% (w:v) BSA

2.2.5.17 Primer design

Oligonucleotide primers for PCR and RT-PCR (section 2.2.5.20) were selected manually. Typically oligonucleotides were 18 to 24 nucleotides long with approximately 50% G+C content and similar melting temperatures (Tm). Oligonucelotides were commercially synthesized (Sigma Genosys), at 0.3μM scale with standard purification. Oligonucleotides were resuspended in dH_2O, aliquoted and stored at -20°C.

2.2.5.18 Sequencing of plasmid DNA

Primers used for sequencing of the protein expression constructs are outlined in Table 2.6. Each sequencing reaction was performed in a 20μl volume, containing 5μl plasmid DNA (approx. 0.5 - 1μg), 4μl rhodamine sequencing mix (ABGene), 4μl half-term buffer (200mM Tris-HCl (pH 9.0) / 5mM $MgCl_2$), 1μl primer (10ng / μl) and 6μl dH_2O. Half-term buffer was added to maximise use of the rhodamine sequencing mix. Each sequencing reaction was set up in duplicate and was carried out on a MJ Research Peltier Thermal Cycler. The amplification cycle consisted of an initial denaturing step for 1 minute at 96°C, followed by 25 cycles of 30 seconds at 96°C and 4 minutes at 60°C or 66°C. Following amplification, the product was ethanol precipitated in 2μl 3M sodium acetate, 50μl ethanol (95% sequencing quality; Sigma) and 0.5μl pellet paint® coprecipitant (Novagen). The reaction was precipitated on ice for 10 minutes before centrifuging at 16000xg for 30 minutes at 4°C. The DNA was washed in 70% (v:v) ethanol and air dried. The use of pellet paint ensured the DNA pellet was visible. The pellets were sequenced using an in-house sequencing service and analysed (section 2.2.5.19).

TABLE 2.6: Primers for sequencing of protein expression vectors

Primer (5' → 3')	Position of first nucleotide(bp)†	Direction of primer
pET-32a(+) GACAAGGCCATGGCTGATATCG	224	reverse
pET-32a(+) ATCCCGTGGTATCCCGACTCTGCTG	476	reverse
pET-32a(+)* GGAATTGTGAGCGGATAACAATTC	761	reverse
pET-32a(+) ATCGGTGATGTCGGCGATATAGG	890	reverse
pGEX-5X-1 ATAATTCGTGTCGCTCAAGGC	90	forward
pGEX-5X-1 TCATCGGCTCGTATAATGTGTG	194	forward
pGEX-5X-1 AAGAGCGTGCAGAGATTTCAATGC	517	forward
pGEX-5X-1 TTGATAAGTACTTGAAATCCAGC	823	forward
DISC1 GCCAGACAGTGTGGCCTTGACTC	247	forward

† Nucleotide sequences were obtained from GenBank, pGEX-5X-1 (U13856) and DISC1 (AF222980), or the manufacturer, pET-32a(+) (http://www.novagen.com/SharedImages/TechnicalLiterature/7_pet32as.htm).

*As stated in the text (section 2.2.5.18), sequencing reactions were performed with 25 cycles of 30 seconds at 96°C and 4 minutes at 60°C, apart from this primer which was performed with 25 cycles of 30 seconds at 96°C and 4 minutes at 66°C.

2.2.5.19 Analysis of sequencing data

Sequencing files were imported into Consed (version 11.0), and assembled using the PhredPhrap script. The sequence was analysed and regions with poor quality sequence or with conflicting consensus sequence were re-sequenced. The consensus sequence was exported to HGMP-RC and aligned against DISC1 (GenBank AF222980) and the appropriate plasmid (pGEX-5X-1 GenBank U13856; pET-32a http://www.novagen.com/SharedImages/TechnicalLiterature/7_pet32as.htm) sequences using the FASTA2 (version 2.0) alignment package. FASTA2 was available within the GCG Sequence Analysis package. The sequence was manually checked to identify any mutations.

2.2.5.20 PCR & RT-PCR

Primers used for PCR (Table 2.7) and RT-PCR (Table 2.8) are shown. RT-PCRs were set up in a designated Envair Class II Microbiological Safety Cabinet. For PCR and RT-PCR from exon 1 to exon 2 of *DISC1*, the Advantage®-GC 2 PCR kit (BD Biosciences Clontech) was used due to the high GC content of this region. For all other RT-PCRs, ThermoStart Taq (ABGene) was used. 25µl reactions were set up containing 1µl plasmid DNA (diluted 1:100) or cDNA, 150ng each primer, 200µM dNTPs in a 1x buffer (supplied by the manufacturer's). For PCRs across GC rich regions, 1x GC polymerase and 1M GC-melt was also added. For all other PCRs, 1U ThermoStart Taq and a minimum of 1.5mM $MgCl_2$ was added. A negative control, containing dH_2O instead of DNA, was always set up and positive controls for the primers were used when available. PCRs were carried out in a MJ Research Peltier Thermal Cycler and involved an initial denaturation step at 94°C for 1 minute (GC) or 15 minutes (ThermoStart) followed by denaturation, annealing and extension cycles as indicated (Tables 2.7 & 2.8). Optimisation for each primer pair was performed by altering the magnesium concentration or the annealing temperature of the reaction. 5µl of each PCR was analysed on an agarose gel (section 2.2.5.1).

TABLE 2.7: Primers for amplification of *DISC1* inserts

Forward primer (5' →3')	**Position of first nucleotide (bp)***	**Amplification conditions**	**Product size (bp)**
exon1 AAAA**GAATTC**ATGCCAGGCGG GGGTCCTCAG	1		
Reverse primers (5' →3')			
exon2 AAAAA**GCGGCCGC**TCAACATC TTGCTGCCACCCAGCACTCC	427	94°C 1 min 67°C 1 min 68°C 1 min 30 cycles	426bp
exon2 AAAAA**GCGGCCGC**TCAACAAA GGCACTGTGAGAGCCAGGAG	607	94°C 1 min 67°C 1 min 68°C 1 min 30 cycles	606bp
exon2 AAAAA**GCGGCCGC**TCAACAAT GCATGTCACGCTCTGGCCTGG	876	94°C 1 min 68°C 2 min 30 cycles	875bp

For amplification of *DISC1* cDNA inserts for cloning of protein expression vectors (sections 3.3.2 & 3.3.3), the same forward primer was used in conjunction with one of three reverse primers. The primers have restriction enzyme sites (bold black nucleotides) incorporated into the sequence to enable digestion of the PCR product for subcloning. The enzymes incorporated are *Eco*RI and *Not*I for the forward and reverse primers respectively. In addition, the reverse primers also include a stop nucleotide (red nucleotides) and a cysteine residue (blue nucleotides). The cysteine residue is to aid in purification of the recombinant protein. * GenBank AF222980.

TABLE 2.8: Primers for detection of *DISC1* transcripts

Primer pair (5' → 3')	Transcript	Amplification conditions	Product size (bp)
DISC1			
forward (exon 1) GGAAGGAGCAGGAGGCAGCCCAG GCGGA **reverse (exon 2)** GCACGCTGCAGGTGGTAAGCAA	all	94°C 30 sec 68°C 2 min 35 cycles	152
forward (exon 11) GGAAGCTTGTCGATTGCTTATCC **reverse (exon 11*)** CAGAGAGGGGATGAGGTGAG	L	94°C 30 sec 58°C 1 min 72°C 1 min 35 cycles	196
forward (exon 11/12†) GACCCCTTTGAAGGAATCTTACAT **reverse (exon 12)** GGCCTGCAGAGTTTCCTTCACCATC	Lv	94°C 30 sec 63°C 1 min 72°C 1 min 35 cycles	178
forward (exon 9) GAATGCCGCCTTAGCCAAAGTG **reverse (exon9a[1])** TGTCCAGGACTCTGCATCACAG	S1	94°C 30 sec 63°C 1 min 72°C 1 min 35 cycles	210
forward (exon 9) TGTTGGTGTTGAGTTCCAGGAAT **reverse (intron 9[2])** GGAAGAGCACAGGAACACTTG	S2	94°C 30 sec 60°C 1 min 72°C 1 min 35 cycles	271
forward (exon 1 alt[3]) GCTCACCCAAGATGCCTCCAGAAG **reverse (exon 2)** GCACGCTGCAGGTGGTAAGCAA	Es	94°C 30 sec 68°C 1 min 72°C 1 min 35 cycles	214
GAPDH[4]			
forward GGGAGCCAAAAGGGTCATCA **reverse (exon 2)** GTGGCAGTGATGGCATGGAC		94°C 30 sec 55°C 1 min 72°C 1 min 35 cycles	210

All primers were designed from the full-length DISC1 cDNA sequence, GenBank AF222980, except [1]Incyte clone r2320731r6, [2]in-house cDNA plasmid FH1, [3]GenBank

AK025293 and [4]GenBank M33197. * was designed from within the alternatively spliced exon 11 sequence and † was designed to span the alternatively spliced exon 11 sequence. GAPDH primers were in use within the lab.

2.2.6 Bioinformatics

PubMed: http://www.ncbi.nlm.nih.gov/entrez/

GenBank: http://www.ncbi.nlm.nih.gov

UniGene: http://www.ncbi.nlm.nih.gov/UniGene

BLAST: http://www.ncbi.nlm.nih.gov/BLAST

PeptideStructure:

http://menu.hgmp.mrc.ac.uk/people/gcg/gcghelp/html/unix/peptidestructure.html

antigenic: http://www.hgmp.mrc.ac.uk/Software/EMBOSS/Apps/antigenic.html

PHDsec & PHDacc: http://cubic.bioc.columbia.edu/predictprotein

Compute pI/MW: http://us.expasy.org/tools/pi_tool.html

Translate: http://us.expasy.org/tools/dna.html

ClustalW: http://searchlauncher.bcm.tmc.edu/cgi-bin/multi-align/multi-align.html

BoxShade: http://www.ch.embnet.org/software/BOX_form.html

CHAPTER 3

THE GENERATION OF DISC1 ANTI-PEPTIDE AND ANTI-PROTEIN ANTISERA

3. The generation of DISC1 anti-peptide and anti-protein antisera

3.1 Introduction

Antibodies are an essential tool for determining the distribution of a protein and can be used in a variety of applications to glean insights into a protein of interest. For a protein of unknown function, such as DISC1, the use of antibodies is an obvious first step in unravelling its biological role. There are no commercially available antibodies to DISC1, so the generation of DISC1 antibodies was the initial aim of this project.

3.1.1 The advantages & disadvantages of polyclonal anti-peptide and anti-protein antibodies

Antibodies may be either polyclonal or monoclonal. Polyclonal antibodies contain a mixed population of antibody molecules whereas monoclonal antibodies contain only a single antibody molecule, thereby simplifying interpretation of the antibody signal. However the time and technical expertise required setting up a facility for monoclonal antibody production made the use of polyclonal antibodies the method of choice for the generation of DISC1 antibodies.

Polyclonal antibodies are commonly raised using either a short peptide sequence or purified protein as the antigen. The decision as to what should be used as the antigen usually involves two main considerations: the time constraints of the project, and cost (Harlow and Lane, 1988a). Anti-peptide antibodies have the advantage of being quick to produce, as the time taken to synthesize a peptide, immunize an animal and harvest the antibodies can be as little as 6 months. The resulting antibodies are highly specific and depending on the length of the peptide sequence will only bind to one or two epitopes in the native protein. In this respect anti-peptide antibodies are similar in specificity to monoclonal antibodies. The specificity of anti-peptide

antibodies for a single peptide sequence allows their use in the high-resolution identification of proteins, for example, differentiating between closely related proteins or identifying post-translational modifications of proteins. The main disadvantage of anti-peptide antibodies is the uncertainty that the chosen peptide sequence constitutes an antigenic epitope in the native protein. Consequently the cost involved in producing a usable antibody may prove to be very expensive, as numerous peptides can be tested before identifying one that will recognise the native protein. To avoid these problems, purified protein can be used as the antigen, as utilization of a larger proportion of the protein will increase the likelihood of producing a successful antibody. Anti-protein antibodies are often stronger in immunoassays due to the larger number of epitopes that are identified by the antibody population, and once immunoaffinity purified, can again be as specific as monoclonal antibodies. However the expression and purification of protein is a time consuming process and considerable optimisation is needed to produce enough antigen for an immunization program.

At the starting of this project, no antibodies to DISC1 were available, or being made. Therefore the aim was to produce both anti-peptide and anti-protein antibodies to maximise the chances of success. In addition, the generation of two independent DISC1 antibodies is likely to enable verification of the antibody signals and avoid erroneous conclusions being made, which is essential when characterising a novel protein.

3.1.2 Initial considerations in the generation of DISC1 antibodies

As described earlier (section 1.7.2), the DISC1 protein can be divided into two specific domains: an N-terminal head domain and a C-terminus of potentially varying size. For the production of DISC1 antibodies the N-terminus was considered a better choice for two reasons. First, the N-terminus shares no homologies to any known proteins and it was predicted that antibodies generated to this region would be less likely to cross-react with other proteins. This concern is less of a problem with

the anti-peptide antibodies as it is possible to design a DISC1-specific peptide from within the C-terminus. The second consideration in generating both antibodies to the N-terminus was to make sure the antibodies would be able to confirm one another in the immunoassays performed. The C-terminus was not considered such a good candidate for validation due to the potential for DISC1 protein isoforms with different C-termini. This is particularly an issue when determining the subcellular localisation of DISC1 as it is possible that the different isoforms have specific functions within the cell and will potentially show different subcellular localisation patterns. However as a consequence of selecting the N-terminus for antibody production, the DISC1 antibodies generated in this project are unable to discriminate between the potential DISC1 protein isoforms.

3.2 Considerations in choosing an antigenic peptide

The production of anti-peptide antibodies that are successfully able to recognise the native protein is dependent on being able to predict the regions of the protein that are most likely to be antigenic. A number of computer programs are available that predict the antigenicity of a protein from its primary and secondary structure (Stern, 1991). The algorithms that these programs use are based on the assumption that it is the surface exposed regions of a protein that are accessible to antibodies and consequently antigenic. Hydrophilic residues are generally surface exposed and deemed to be good antigenic sites whereas hydrophobic residues are usually buried within the interior of the protein and unlikely to be antigenic. In addition, the flexibility or mobility of the protein is also strongly correlated with antigenicity (Jameson and Wolf, 1988; Stern, 1991), as highly flexible turn or loop structures are more likely to be surface exposed. Therefore the hydrophilic residues found within turn or loop structures are more likely to be antigenic compared to the hydrophilic residues found within the more rigid β-sheet and α-helical structures.

Selecting a successful peptide sequence also depends on the size of the peptide and although an antigenic site can consist of only 6 amino acids, it is generally recommended that 10 – 15 amino acids should be used (Harlow and Lane, 1988b).

3.2.1 Determining antigenic peptides from DISC1 protein sequence

DISC1 protein sequence was analysed to determine which region of the protein would be most suitable for antibody production. The analysis was performed using two computer programs: PeptideStructure (performed by Colin Semple, Medical Genetics Section) and "antigenic" (performed by Martin Taylor, Medical Genetics Section). PeptideStructure is part of the GCG Sequence Analysis package and is based on the method of Jameson & Wolf (Jameson and Wolf, 1988). PeptideStructure uses the predicted hydophilicity, flexibility and surface probability of the protein, in conjunction with secondary structure predictions to calculate the antigenic index across the protein. The antigenic index is reported per amino acid and gives an indication of how antigenic that residue is within a specific sequence. Alternatively, "antigenic" uses a method developed by Kolaskar and Tongaonkar (Kolaskar and Tongaonkar, 1990) to predict the antigenic regions of a protein based on the physicochemical properties of amino acid residues and their frequency of occurrence in segmental epitopes. The predicted antigenic sequences are reported and a value is given for the antigenicity of the whole peptide sequence. "antigenic" is available as part of the Emboss package.

"antigenic" identified nine potential antigenic sequences from within the N-terminus of DISC1 (Figure 3.1). The antigenic index reported in PeptideStructure was obtained for each of the amino acids in the peptide sequences: the amino acids with a high antigenic index (≥ 1) are shown in blue whilst those unlikely to be antigenic (an antigenic index of ≤ 0) are shown in red. The antigenic index cut-off points were set arbitrarily, but analysis of the data from PeptideStructure ascertained that no well predicted turn structure occurred with an antigenic index of ≤ 0. Most of the amino acids with a negative antigenic index (highlighted in red) are predicted by the secondary structure prediction programs of PeptideStructure (Chou-Fasman and Garnier-Osguthorpe-Robson; (Jameson and Wolf, 1988) to be buried residues and therefore highly unlikely to be antigenic. This illustrates the importance of using

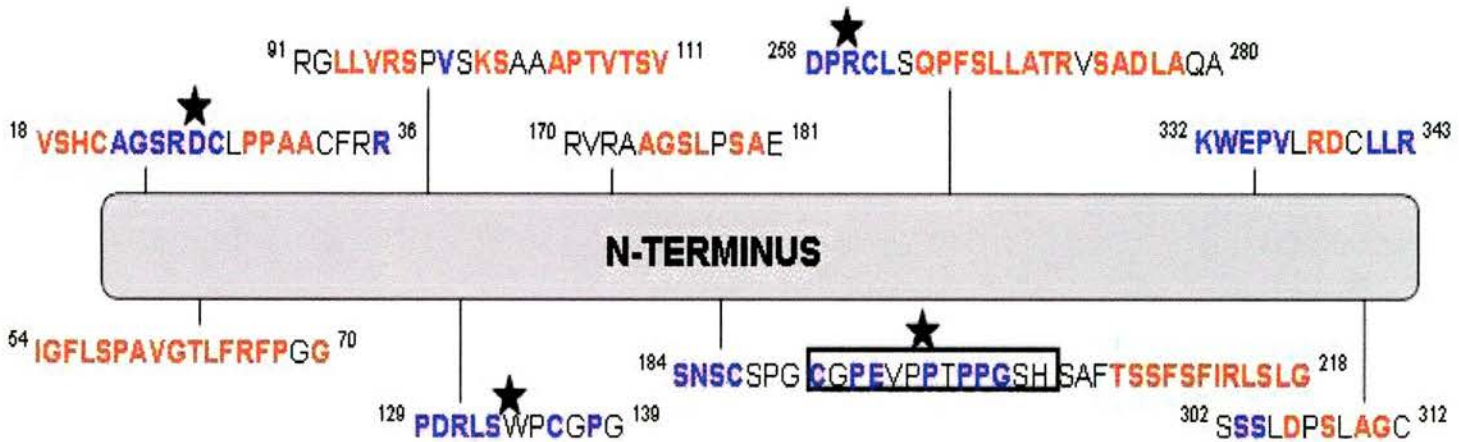

FIGURE 3.1: Identification of antigenic peptides within the N-terminus of DISC1

The nine peptide sequences identified by antigenic are shown on a representation of the N-terminus of DISC1. For each peptide sequence, the residues highlighted in red represent those with a low antigenic index (≤0), whilst the residues highlighted in blue are those with a high antigenic index (≥1), as determined by PeptideStructure. The peptide sequences predicted to be good antigenic sites by both antigenic and PeptideStructure as well as PHDsec & PHDacc are indicated by the black stars. The boxed amino acids represent the peptide sequence chosen for DISC1 antibody production.

more than one method to identify antigenic sites as a number of discrepancies between the two programs can be seen.

Next the putative antigenic peptide sequences were checked against the secondary structure of DISC1 as determined using the PHD secondary structure prediction programs, PHDsec and PHDacc. These programs are deemed to be the most reliable of the all the secondary structure prediction programs (C.Semple, personal communication) and ensured the chosen peptide sequences were comprised of residues predicted to be surface-exposed and in regions of looped structure. Four peptide sequences were identified which were predicted by all three methods to be good antigenic sites (Figure 3.1). Cross-reactivity of the peptides was determined using BLAST searches against the appropriate protein databases: SWISSPROT (blastp), PDB (blastp) and NR (tblastn). None of the selected peptides showed matches to any other proteins apart from DISC1.

A thirteen amino acid peptide sequence, CGPEVPPTPPGSH, was chosen. The peptide covers residues 191 – 203 of the DISC1 protein (Figure 3.1). The reasons for selecting this peptide are three-fold. Firstly the length of the antigenic site enabled a longer peptide to be selected than for the other regions. Secondly a naturally occurring cysteine residue was able to be incorporated into the peptide sequence. The cysteine residue was included to ensure the peptide would bind to the matrix to be used for immunoaffinity purification of the antibodies (section 4.2). Finally, the peptide sequence is not conserved in mouse, therefore the resulting antibodies should be human-specific.

It should be noted that as outlined above, BLAST searches were performed to ensure the peptide did not share any homologies to known proteins. At the time of peptide design, no matches, other than to DISC1, were found for the peptide sequence chosen. However a recent BLAST search using the parameters now available for searching for short nearly exact sequence matches revealed that the peptide does show a number of matches to many different proteins. Nevertheless, no match of greater than four consecutive amino acids was identified and the majority of matches

are due to the presence of the proline residues. Furthermore other than DISC1, none of these matches are reported to be of statistical significance (E=<0) and it is probable that these are chance observations expected with BLAST searching of any sequence. Thus as with any information gleaned from database searches, it is not clear how much emphasis can be placed on the findings.

3.2.2 Production of DISC1 anti-peptide antiserum

Small peptides are unlikely to be immunogenic on their own, and in order for the peptide to be recognised by the immune system of the host animal, the peptide is synthesized with a carrier protein attached. Carrier proteins are of high molecular weight and are usually from a species that is unrelated to the host animal in order to ensure an optimal immune response. Carrier proteins that are frequently used include bovine serum albumin (BSA) and the mollusc protein keyhole limphet hemocyanin (KLH) (Harlow and Lane, 1988c). KLH was chosen as a carrier protein for the DISC1 peptide and was conjugated to the peptide through the N-terminal cysteine residue.

The peptide was synthesized as a KLH-conjugate and the antibodies were raised in two New Zealand white rabbits. The whole process was carried out by Research Genetics, Inc (Huntsville, Alabama, USA). The immunization program involved an initial injection of 0.1mg peptide in complete Freund's adjuvant, followed by three boosters of 0.1mg peptide in incomplete Freund's adjuvant, at 2, 6 and 8 weeks. Freund's adjuvant, in complete (with addition of killed mycobacterium) or incomplete forms, is used to increase the magnitude and duration of the immune response to injected antigen. Complete Freund's adjuvant should only be used for the initial inoculation, to minimize animal discomfort. All inoculations were administered subcutaneously. A pre-immune test bleed was taken before the start of immunization, and production bleeds were taken at 4, 8 and 10 week intervals. After initial characterisation of the antisera, an additional booster of peptide was given and terminal bleeds were taken from both of the rabbits after 16 weeks.

3.3 Bacteria as a choice for recombinant protein expression

The main consideration when producing recombinant DISC1 protein for use as an antigen was to ensure a reproducibly high level of protein expression. In this regard, bacterial protein expression systems show several advantages over the more specialised insect or mammalian protein expression systems. Bacterial expression systems are in routine use and there are many commercially available vector systems which utilize tightly regulated promoters suitable for achieving high level protein expression. In addition, the number of fusion partners available offers a wide range of tools for improved protein folding, solubility and yield, as well as for the detection and purification of recombinant proteins (Makrides, 1996). However bacteria do not have the protein machinery for certain eukaryotic post-translational modifications and if these modifications are important to the function of the protein, the resulting recombinant protein may be functionally (and structurally) different to the native protein.

3.3.1 Two distinct purification tags to enable the production of DISC1-specific antibodies

For production and purification of the anti-protein antibodies, two recombinant DISC1 proteins were expressed, with each recombinant protein having a unique purification tag to ensure that the antibodies purified would be DISC1-specific (Figure 3.2). The vectors chosen for protein expression were the pGEX-5X-1 vector from Amersham Biosciences and the pET-32a(+) vector from Novagen. The pGEX-5X-1 vector encodes a GST (glutathione-S-transferase) tag at the N-terminus of the recombinant protein for purification purposes, while the pET-32a(+) vector encodes both a His-tag and an S-tag for purification of the recombinant protein. The His-tag is expressed at both the N and C-terminus of the recombinant protein whilst the S-tag is expressed only at the N-terminus. For purification of the recombinant DISC1 protein, the His-tag was used since the presence of two tags increases the chances of a successful purification. As well as fusion proteins to aid purification of the

recombinant protein, the pET-32a(+) vector contains a thioredoxin tag to increase the solubility of the recombinant protein (Makrides, 1996).

Both of the vectors chosen are chemically inducible using IPTG. The pGEX-5X-1 vector contains a *tac* promoter which is directly induced by IPTG to cause expression of the target gene. In contrast, the pET-32a(+) vector is indirectly induced by IPTG through the T7 promoter, when the vector is grown in a bacterial strain that contains the T7 RNA polymerase gene (λDE3 lysogen). The vectors were obtained as gifts from David Elliott (MRC Human Genetics Unit).

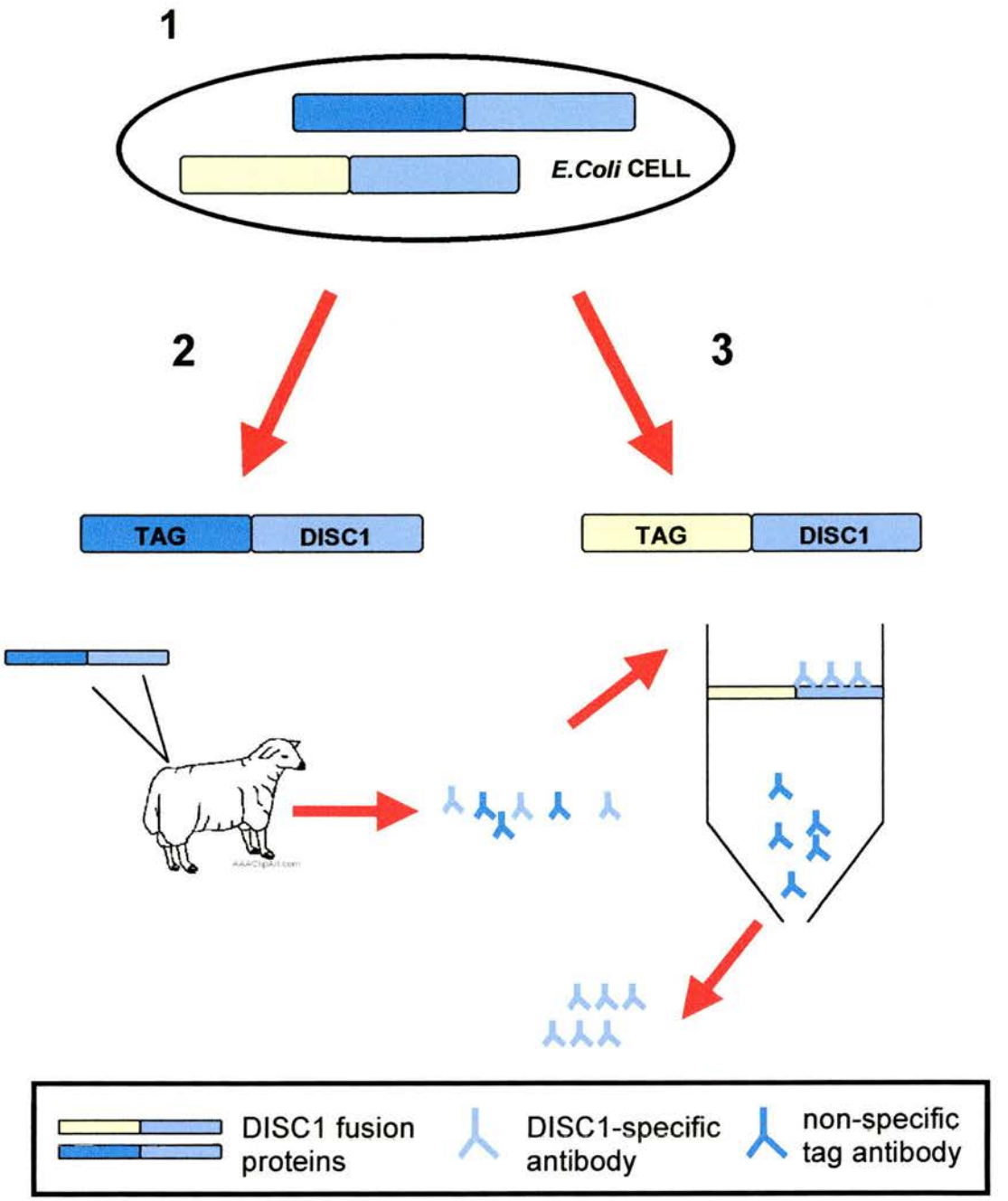

FIGURE 3.2: Production and purification of DISC1-specific anti-protein antibodies

The expression of two recombinant DISC1 proteins with unique purification tags (1), will enable one of the proteins to be used for antibody production (2) while the second fusion protein will be used for purification of the antibodies (3). The polyclonal antibodies generated to the first fusion protein will contain antibodies to both DISC1 and the tag protein. However as the tag protein on the second fusion protein is different, only the DISC1 antibodies should be purified ensuring a DISC1-specific pool of antibodies. It should be noted that a less complex strategy for the immunoaffinity purification of antibodies could have been adopted.

3.3.2 Protein expression using an 875bp DISC1 cDNA insert

As stated above (section 3.1.2), it had been decided that the DISC1 antibodies would be generated to the N-terminus of the human DISC1 protein. The N-terminus spans 1041bp of cDNA sequence equivalent to 347 amino acids (aa). At the distal portion of the N-terminus (293aa - 325aa), there is a serine rich region (Figure 3.3). This region was not included in the recombinant protein to be used for antibody production, as it was deemed more likely to generate non-specific antibodies. The first 875bp of cDNA sequence (292aa) was selected for protein expression.

The 875bp fragment was PCR amplified, using an in-house plasmid clone (FH1) containing the human DISC1 cDNA sequence as template. The primers were designed to incorporate *Eco*RI (forward primer) and *Not*I (reverse primer) restriction sites compatible with the cloning sites from both of the vectors (Table 2.7). In addition the reverse primer included the nucleotide sequence for a cysteine residue to enable binding of the recombinant protein to the matrix to be used for purification of the antibodies (section 4.2). The fragment was cloned into both of the vectors and positive subclones were fully sequenced to ensure no mutations had been introduced into either the *DISC1* coding sequence or the regulatory regions of the vectors.

Initial protein expression levels from each of the constructs were determined using BL21(DE3) cells. Small-scale cultures were induced as outlined in section 2.2.1.6, but using 5ml of LB-Broth instead of 100ml. A typical experiment involved the induction of >1 colony as it had been observed that the protein expression levels from individual colonies can differ greatly (D.Elliott, personal communication). A control using vector lacking the DISC1 insert was always performed to ensure that the induction had worked.

3.3.2.1 Expression of GST-tagged DISC1 protein

The typical expression levels of GST-tagged DISC1 protein following a three-hour induction at 37°C is shown in Figure 3.4. The DISC1 fusion protein is predicted to be 58kDa, consisting of a 29kDa GST tag protein fused to approximately 29kDa of

FIGURE 3.3: The regions of the N-terminus of DISC1 used for protein expression

The amino acid sequence of the N-terminus is shown with the boundary between the N- and C-termini indicated by the black arrowhead. The serine rich region at the distal portion of the N-terminus is shaded (with the serine residues in bold). For expression of recombinant DISC1 protein a total of three expression constructs per vector were made, containing either 426bp (first arrowhead), 606bp (second arrowhead) or 875bp (third arrowhead) of DISC1 cDNA sequence. The C-terminus of the protein expressed from these constructs is indicated by the blue arrowheads. Protein expression using the 875bp construct (section 3.3.2) and the 426 & 606bp constructs (section 3.3.3) is described in the appropriate section. For production of the anti-protein antibodies, the protein expressed from the 606bp construct (second arrowhead) was used. In addition, the peptide sequence used for generation of the DISC1 anti-peptide antibodies is highlighted in red.

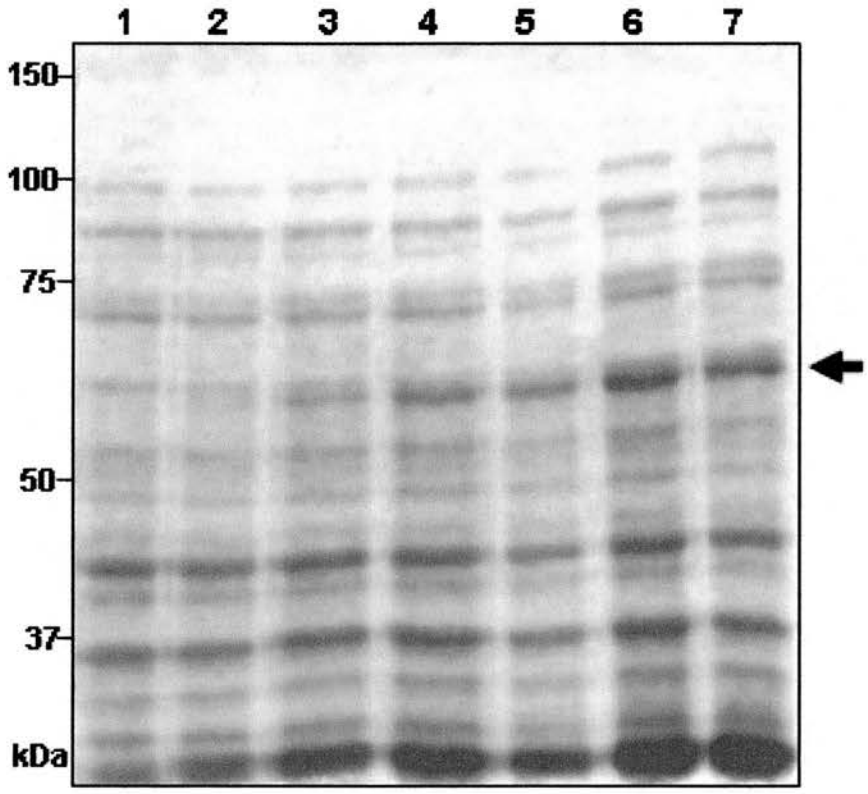

FIGURE 3.4: Expression of GST-tagged DISC1 protein using the 875bp construct

Equivalent volumes of bacterial cell lysates were analysed on an 8% SDS-PAGE gel. A sample of the cells was removed before IPTG addition (lane 1) and at 30 minutes intervals after IPTG addition (lanes 2 – 7). The GST-DISC1 fusion protein was successfully expressed (arrow).

DISC1 protein. Development of the fusion protein was monitored by removing a sample of cells at 30 minute intervals during the induction period. The level of expression shown is representative of all initial inductions performed and there was no enhancement of the protein expression levels from different colonies.

Before attempting to purify the DISC1 fusion protein, the solubility of the DISC1 fusion protein was ascertained. This was performed initially by resuspending the bacterial cell pellet in PBS and sonicating the cell lysate before centrifugation to pellet the insoluble bacterial proteins, leaving any soluble proteins in the supernatant. The DISC1 fusion protein was found to be in the insoluble protein fraction (data not shown). The purification process is made easier if the recombinant protein is in the soluble fraction, therefore attempts were made to solubilise the DISC1 fusion protein.

Increasing the solubility of a recombinant protein can be achieved by reducing the temperature at which the induction is performed, however induction of the DISC1 protein at 30°C had no effect on the solubility of the DISC1 fusion protein (data not shown). In addition a number of detergents (Sarkosyl, Triton-X-100 and SDS) were tested to determine if they aid solubilisation of the fusion protein. Resuspending the insoluble bacterial protein in a combination of all three detergents (2% Sarkosyl / 1% Triton-X-100 / 0.1% SDS) followed by heating at 95°C for 30 minutes resulted in the solubilisation of the DISC1 fusion protein (data not shown). However the level of solubilised protein was not very high and attempts to purify the soluble DISC1 protein via the GST tag were not successful (data not shown). Control purifications using the GST protein alone were successful and the inability to purify the recombinant DISC1 protein was most likely due to the low level of expressed protein.

To try and increase the expression levels of the recombinant protein various modifications of the induction stage were performed. Protein expression was carried out in JM109 cells, as the level of recombinant protein produced in different bacterial strains can vary (D.Elliott, personal communication). In addition, the effect of

altering the stage at which the IPTG was added, as well as the length of the induction times were examined. Altering the stage of bacterial growth at which the IPTG was added was to ensure the induction was being started during the exponential phase of growth, while changing the length of time the bacteria were induced for was to ensure optimal recombinant protein levels were being harvested. In practice, none of the above modifications had any effect on the overall protein expression levels (data not shown). The use of an alternative antibiotic, carbenicillin, was also tested, as ampicillin in the growth medium is destroyed over time, which allows the growth of non-transformed bacteria and can lead to the selection against plasmid transformed cells. Carbenicillin avoids this loss of plasmid effect (Novagen, 1992-2000). However as for the other modifications performed, the use of carbenicillin did not improve the expression levels of the recombinant DISC1 protein (data not shown) and the initial approach of expression at 37°C for three hours was deemed optimal.

3.3.2.2 Expression of His-tagged DISC1 protein

The expression level of His-tagged DISC1 protein following a three hour induction at 37°C was difficult to determine (Figure 3.5A). The predicted size of the DISC1 fusion protein is 49kDa, which is smaller than the GST-tagged protein due to the reduced size of the tag (predicted to be 20kDa). A strong band is seen in the induced sample at 55kDa, however a band of this size is also seen in the pre-induced sample. An independent means would be needed to verify this protein as the fusion protein.

3.3.2.3 Conclusions

Due to the lack of success in purifying the GST-tagged protein and also the doubt as to whether the His-tagged protein had even been induced, it was decided that further constructs would be made containing smaller DISC1 cDNA inserts. The use of shorter inserts and consequently smaller fusion proteins should maximise the chances of both a successful induction and subsequent purification as the size of the present recombinant proteins may be the limiting factor. This is because in general, more difficulties are encountered as the size of the fusion protein increases, particularly if the expressed proteins are >50kDa in size (Smith and Corcoran, 1994).

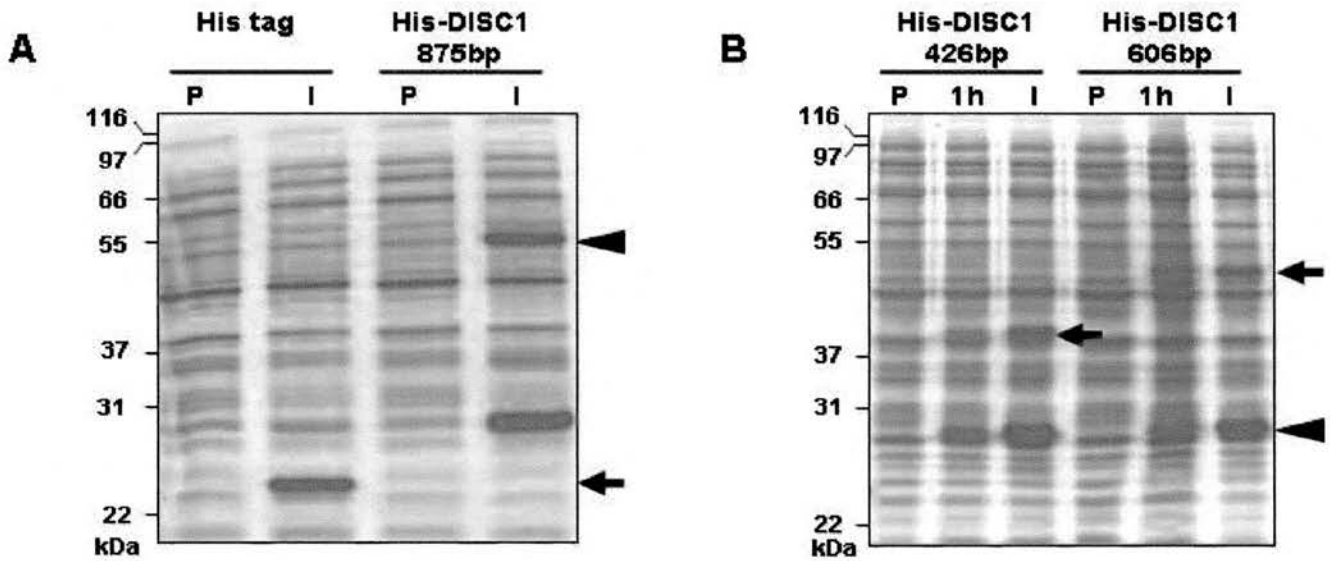

FIGURE 3.5: Expression of His-tagged DISC1 protein using expression constructs with varying sizes of DISC1 inserts

Equivalent volumes of bacterial cell lysates were analysed on 12% SDS-PAGE gels. Samples were removed before IPTG addition (P), at the end of the induction period (I) and where applicable, after 1 hour of induction (1h).

A: The control induction (lanes 1 & 2) using vector with no DISC1 insert, expressed tag protein at the approximate size (arrow). However induction of the His-tagged protein from the 875bp construct (lanes 3 & 4) was difficult to determine. A potential induced band is indicated at approximately 55kDa (arrowhead).

B: Induction of the His-tagged protein can be clearly seen with the 426 and 606bp constructs (arrows). A breakdown product of approximately 30kDa was always seen (arrowhead); also apparent in A.

3.3.3 The use of expression constructs with 426 / 606bp DISC1 cDNA inserts

In order to express smaller DISC1 fusion proteins, constructs were made containing either the first 426bp or 606bp of cDNA sequence from the N-terminus of DISC1 (Figure 3.3). These constructs were predicted to express GST-tagged proteins of 43kDa or 49kDa and His-tagged proteins of 34kDa or 40kDa respectively.

As for the original 875bp fragment (section 3.3.2), the DISC1 inserts were PCR amplified from plasmid clone FH1, using primers designed with the appropriate modifications (Table 2.7). Positive subclones for both the pET and pGEX vectors were again fully sequenced.

3.3.3.1 Expression of GST-tagged DISC1 protein

To determine the expression levels from each of the pGEX constructs, initial experiments were conducted using both constructs in four different cell types: BLR(DE3), BL21(DE3), BL21(DE3)pLySs and BL21. A sample of the cells was removed after one hour of IPTG induction to monitor the development of the DISC1 fusion proteins. Following a three hour induction at 37°C using BL21(DE3) and BLR(DE3) cells a low level of expression was obtained from all of the constructs (Figure 3.6). Similarly the expression levels were low for the other two cell types (data not shown). The DISC1 fusion proteins were expressed at approximately the size of the predicted fusion proteins: 43kDa (426bp) and 49kDa (606bp), but overall the use of shorter expression constructs did not greatly increase the protein expression levels. In addition a breakdown product of approximately 31kDa was always seen when recombinant DISC1 protein was expressed, implying that there is a site within the DISC1 fusion protein that is sensitive to cleavage by proteases.

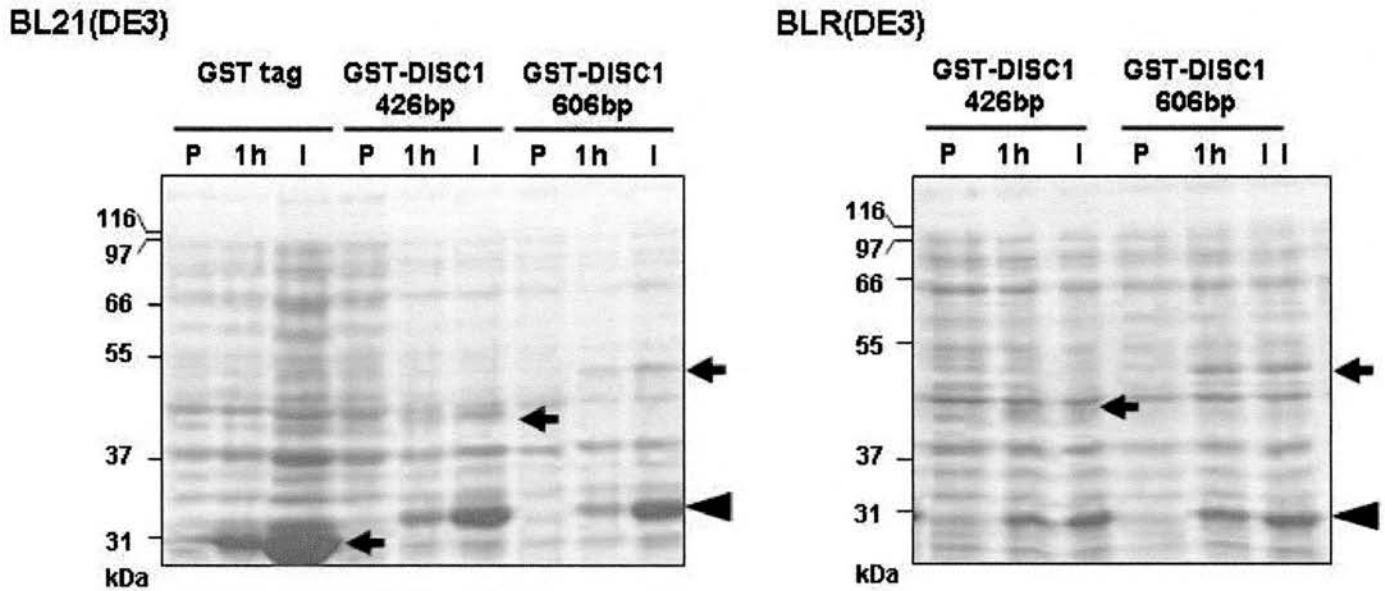

FIGURE 3.6: Expression of GST-tagged DISC1 protein using the 426 / 606bp constructs in BL21(DE3) and BLR(DE3) *E.coli* cells

Expression of the GST-tagged DISC1 protein was compared in a number of *E.coli* strains, including BL21(DE3) (left gel) and BLR(DE3) (right gel). Samples of cells were removed before IPTG addition (P), 1 hour after IPTG addition (1h) and at the end of the three hour induction (I). Equivalent volumes of bacterial cell lysates were analysed on 10% SDS-PAGE gels. The GST-DISC1 fusion proteins (arrows) are predicted to be approximately 43kDa (426bp) and 49kDa (606bp). A breakdown product of 31kDa (arrowhead) was always seen. The induction of GST protein was always performed as a control (shown for BL21(DE3) cells only).

No attempts were made to increase the protein expression levels from either the 426bp or 606bp constructs as optimisation using the 875bp construct had previously been unsuccessful (section 3.3.2.1). Despite the low expression levels, the solubility of the DISC1 fusion proteins was determined. The insoluble bacterial proteins were pelleted as outlined in section 3.3.2.1, but a different lysis buffer (section 2.2.1.8) was used. The recipe for this buffer was obtained from Xinsheng Nan (Medical Genetics Section). The DISC1 fusion proteins expressed from both the 426bp and 606bp constructs were partially solubilised using this lysis buffer (Figure 3.7A; data shown for 606bp construct only), as was the breakdown product.

For purification of the recombinant proteins, glutathione agarose (Sigma) was used to bind the GST-tagged proteins and then reduced glutathione was used to elute the bound proteins from the agarose. Several attempts were made before the fusion protein was successfully eluted and changes to the standard protocol (section 2.2.1.8) involved increasing the time the protein was allowed to bind to the beads and changing the elution conditions. As a result of the initial purification problems, a sample of the beads was taken before eluting the protein to ensure the GST-tagged DISC1 protein had bound to the beads. The use of 10mM reduced glutathione was sufficient to elute most of the DISC1 fusion protein expressed using the 606bp construct (Figure 3.7A). The breakdown product at 31kDa was also eluted.

3.3.3.2 Expression of His-tagged DISC1 protein

Expression levels were determined using BLR(DE3) cells, following a standard three hour induction at 37°C (Figure 3.5B). As for the GST-tagged proteins, the development of the fusion proteins was monitored by removing a sample of the cells after one hour of IPTG induction. The DISC1 fusion protein was successfully expressed from both constructs at approximately the predicted size: 34kDa (426bp) and 40kDa (606bp). The slight size discrepancy between the predicted sizes and the actual sizes seen on the gel is due to the slightly larger actual size of the tag protein (25kDa) compared to what was expected (20kDa).

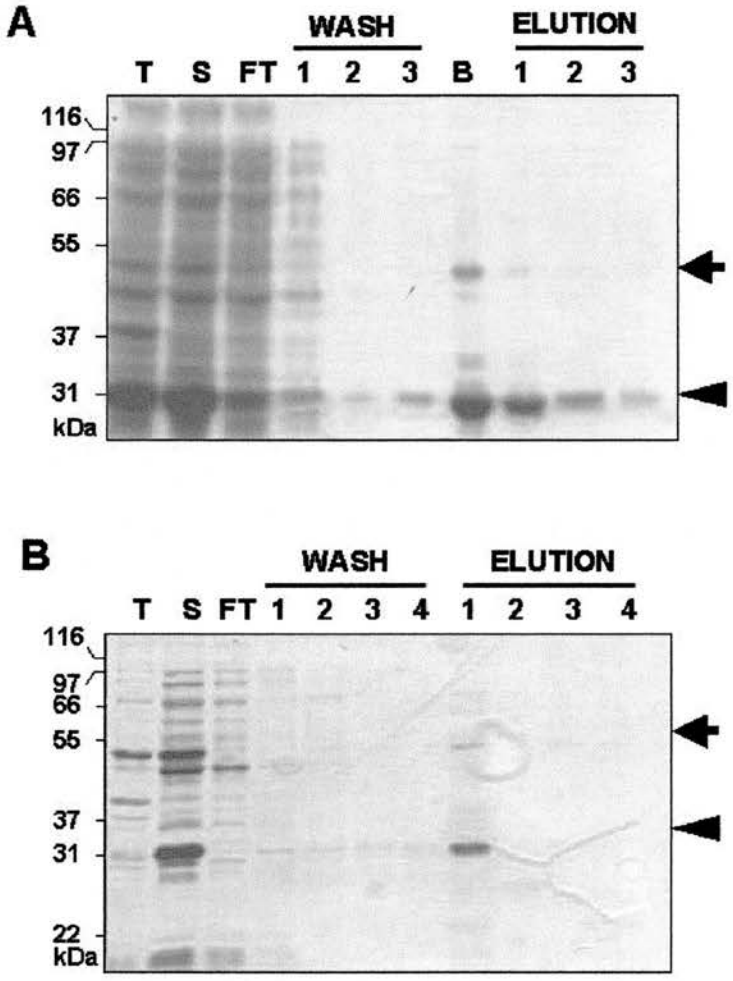

FIGURE 3.7: Purification of GST and His-tagged DISC1 protein

Purification of recombinant DISC1 protein expressed from the 606bp construct using either GST (A) or His (B) as the purification tag. The DISC1 fusion proteins were solubilised (S) from the total cell protein (T), and then bound to the appropriate matrix. The flow-through (FT) represents the protein that did not bind to the beads. The beads were washed, before eluting the DISC1 fusion protein using the appropriate solution. In addition, a sample of the beads (B) was analysed from the GST purification and ensured the fusion protein was bound to the beads. Equivalent volumes of each sample were analysed on 10% (A) or 12% (B) SDS-PAGE gels. The purified fusion proteins (arrows) were purified in conjunction with the breakdown products (arrowheads).

A breakdown product of approximately 30kDa was always present when the recombinant DISC1 protein was expressed, indicating that as for the GST-tagged proteins, there is a site within the recombinant DISC1 protein which is susceptible to cleavage by proteases. However, unlike the low levels of protein expression seen for all three GST-tagged fusion proteins, the expression levels of the His-tagged proteins from the 426bp and 606bp constructs appear slightly higher than the expression levels from the 875bp construct.

To determine if the His-tagged fusion proteins were soluble or insoluble, the procedure detailed previously was performed (section 3.3.2.1), but using a modified version (section 2.2.1.7) of the lysis buffer obtained from Xinsheng Nan. The use of imidazole, sodium dihydrogen phosphate and an altered sodium chloride concentration was necessary to ensure the components were compatible with the Ni-NTA matrix to be used for purification of the fusion protein (QIAGEN, 2000). The use of this lysis buffer solubilised the majority of the DISC1 fusion protein from both the 426bp and 606bp constructs (Figure 3.7B; data shown for 606bp construct only).

For purification purposes nickel-nitrilotriacetic acid (Ni-NTA), a metal-affinity chromatography matrix developed by QIAGEN, was used. The Ni-NTA matrix binds to His-tagged proteins with at least six consecutive His residues and imidazole can then be used to elute the bound protein. The use of 250mM imidazole was sufficient to elute the DISC1 fusion protein from both constructs (Figure 3.7B; data shown for 606bp construct only), as well as the breakdown product of 30kDa.

3.3.3.3 Conclusions

Due to the increased yield of purified protein obtained using the pET vector, it was decided that the His-tagged DISC1 protein would be used for the production of DISC1 antibodies whilst the GST-tagged DISC1 protein would be used for purification of the antibodies. In addition, the use of the 606bp construct was deemed more suitable as this construct contains the cDNA sequence that encompasses the peptide used for generation of the anti-peptide antibodies (Figure

3.3). Therefore it was appropriate to ensure the anti-protein antibodies included this region as well.

3.3.4 Production of DISC1 anti-protein antiserum

Before starting the immunization program, the identity of the His-tagged DISC1 protein was confirmed using the DISC1 anti-peptide antibodies now available (Figure 4.1).

The anti-protein antibodies were raised in a single sheep at the Scottish Antibody Production Unit (SAPU). The immunization program involved an initial injection of 250μg protein in complete Freund's adjuvant, followed by three boosters of 250μg protein in incomplete Freund's adjuvant, every 28 days. A total of 1mg of protein was required for the whole immunization program, and the first elution in the purification process (Figure 3.7A), typically yielded enough full-length DISC1 fusion protein for one injection. All injections were administered subcutaneously. A pre-immune test bleed was taken before the start of immunization, and production bleeds were taken 7 days after each booster injection.

3.4 Discussion

The generation of antibodies to the N-terminus of the human DISC1 protein was performed using both a chemically synthesized peptide and bacterially expressed recombinant protein as the antigen. To aid in the design of an antigenic peptide, two computer programs were used to predict antigenic regions within the N-terminus of DISC1. The programs have been designed using different parameters (Jameson and Wolf, 1988; Kolaskar and Tongaonkar, 1990) and consequently the regions of DISC1 that were predicted to be antigenic did not show much overlap between the two programs (Figure 3.1). Despite this, it was possible to select a thirteen amino acid peptide (^{191}CGPEVPPTPPGSH^{203}) predicted to be antigenic by both of the programs.

The expression of DISC1 protein for both antibody production and the subsequent purification of DISC1-specific anti-protein antibodies was dependent on the use of two DISC1 fusion proteins each with unique purification tags (Figure 3.2). Ultimately, three constructs were made for each of the vectors containing varying sizes of DISC1 cDNA sequence (Figure 3.3). The overall expression levels of the His-tagged proteins were higher than the expression levels obtained using the GST-tagged proteins. This may be due to the strength of the different promoters used by the vectors, although control inductions performed using empty vector alone show that both vectors are capable of inducing high levels of recombinant protein (Figures 3.5A & 3.6). To ensure no mutations had been introduced during subcloning of the DISC1 inserts, all of the expression constructs, including the promoter regions, were fully sequenced. No mutations were found and this ruled out the possibility that a mutation in the promoter region was responsible for the low levels of expression seen with the GST-tagged proteins. Attempts were made to increase the protein expression levels from the original 875bp construct but none of the modifications were successful. It is possible that if the development of the breakdown product at 31kDa could be minimised the overall yield of the full-length DISC1 fusion protein would be increased. The BL21 derived *E.coli* strains used for protein expression in this study (Table 2.1) are deficient in both *lon* and *ompT* proteases. The lack of these proteases should minimise the appearance of breakdown products, however alternative protease inhibitors could be tested to determine their use in reducing the appearance of the breakdown product.

The yield of the purified His-tagged protein was again greater than that achieved for the GST-tagged protein (Figure 3.7). This was probably due in part to the increased expression levels of the His-tagged proteins but also to the presence of the thioredoxin tag on the His-tagged DISC1 protein. The main determinant for successful purification of a recombinant protein is the solubility of the protein and in this regards, the thioredoxin tag has been engineered to increase the solubility of the protein (Makrides, 1996), thus aiding the purification process.

Expression of recombinant DISC1 protein from the expression vectors always resulted in the generation of a breakdown product. The size of the breakdown product was independent of the size of the DISC1 protein contribution but dependent on the size of the tag. Thus for all of the GST-tagged proteins a breakdown product of 31kDa was seen, whilst for all of the His-tagged proteins, a breakdown product of 30kDa was present. This would imply that within the DISC1 fusion proteins, there is a site (or sites) which are susceptible to protease cleavage. The site is unlikely to be within the tag portion of the protein as the size of the breakdown product was independent of the size of the DISC1 protein, remaining the same despite increasing contributions of the DISC1 protein. In addition both of the breakdown products were purified along with the appropriate fusion proteins which would only be possible with an intact tag. Therefore the susceptibility site (or sites) must lie within the DISC1 protein.

The use of both methods of antigen production has maximised the chances of producing a successful antibody to DISC1. Furthermore, the generation of both DISC1 anti-peptide and anti-protein antibodies will enable the specificity of the antibodies for the DISC1 protein to be determined.

CHAPTER 4

CHARACTERISATION OF DISC1 ANTI-PEPTIDE AND ANTI-PROTEIN ANTIBODIES

4. Characterisation of DISC1 anti-peptide and anti-protein antibodies

4.1 Introduction

Previous work on the DISC1 protein had been limited to *in-silico* data (section 1.7.2). This provided certain hints about the DISC1 protein but nothing about endogenous DISC1. As a result careful characterisation of the antibodies was paramount in order to ensure the resulting data generated could be interpreted with confidence. The characterisation of any antibody is aided by the use of more than one independent antibody to the same protein and in this respect, it was expected that the generation of two separate DISC1 antibodies would be useful. In addition, towards the end of the project DISC1 antibodies produced independently in another lab became available and were used to confirm the DISC1-specific signal. Cell lines expressing DISC1-tagged proteins were also useful in this respect. Finally, considerable time was spent sourcing a cell line that did not express DISC1, to use as a negative control to aid the characterisation process.

4.2 Purification of DISC1-specific antibodies

The DISC1 antisera obtained from both Research Genetics (section 3.2.2) and SAPU (section 3.3.4), were provided as crude serum preparations. Therefore in addition to the expected DISC1-specific antibodies, the serum contained many other antibody molecules as well as contaminating proteins. In order to obtain a DISC1-specific population of antibodies the serum was immunoaffinity purified, as the presence of non-specific antibodies and proteins would make interpretation of the DISC1-specific signal either problematic or impossible.

Both the anti-peptide and anti-protein antisera were initially caprylic acid purified (Steinbuch and Audran, 1969), to remove contaminating proteins and any non-immunoglobin G (IgG) antibody molecules. The purified populations of IgG antibody molecules were then immunoaffinity purified against either the DISC1

immunizing peptide (section 3.2.1) or the GST-tagged DISC1 fusion protein (section 3.3.3.3). Both the DISC1 peptide and the recombinant DISC1 protein were designed to incorporate a cysteine residue and this enabled the peptide and protein to be bound directly to the sulfhydrl activated resin (SulfoLink® Coupling Gel; Pierce) chosen for the purification of DISC1-specific antibodies.

Serum from each of the host animals used in the immunization programs was purified and the majority of the data presented within this thesis has been performed using the immunoaffinity purified antibodies. Crude DISC1 antisera were also tested in the initial characterisation of the antibodies (section 4.4) and at other times when necessary.

4.3 ELISA analysis of DISC1 anti-peptide antisera

ELISA's (Enzyme-Linked ImmunoSorbent Assay) were performed by Research Genetics on the crude anti-peptide antiserum to determine the success of the immunization program. The results received from Research Genetics are shown in Table 4.1. ELISA's were performed by binding the free peptide in solid phase (1μg per well), applying serial dilutions of the anti-peptide antiserum and then detecting the bound antiserum using biotinylated anti-rabbit IgG, HRP-SA conjugate, and ABTS. The antiserum was diluted in decreasing concentrations, 1:100, 200, 400, 800, 1600, 3200, 6400, 12800, 25600, 51200, 102400, 1:204800, and the titre values recorded are expressed as the reciprocal of the serum dilution that results in an OD_{405} of ≤0.2, an arbitrary cut-off point determined by Research Genetics. Thus a titre value of 50696 denotes that a serum dilution of 1:50696 results in an absorbance of ≤0.2, as calculated from a straight line curve of the data. A titre value of >204800 is the best value that can be reported with this particular assay.

TABLE 4.1: ELISA analysis of DISC1 anti-peptide antisera

Animal #	Pre-immune	4 week bleed	8 week bleed	10 week bleed
R99946	<50	50696	>204800	>204800
R99947	<50	39003	>204800	>204800

Both rabbits produced a strong immune response to the peptide and had reached the highest titre value by week 8. In contrast the pre-immune serum does not (as expected) contain any DISC1-specific antibodies, as evidenced by the low titre value.

The ELISA data presented indicates that the host animal responded to the immunizing peptide but it cannot provide any information regarding whether or not the antibodies will be able to detect native DISC1 protein.

4.4 Characterisation of DISC1 anti-peptide and anti-protein antibodies using bacterially expressed recombinant protein

The first step in characterising the DISC1 antibodies was to determine if they could detect recombinant DISC1 protein. For this purpose, bacterially expressed DISC1 protein (sections 3.3.2 & 3.3.3) was used. The bacterially expressed DISC1 fusion protein was clearly visible on a Coomassie stained gel, therefore it should be obvious whether or not the antibodies are capable of detecting the recombinant DISC1 protein.

4.4.1 Anti-peptide antibodies

Crude antisera from both of the rabbits were tested using the 8-week bleed. At this stage the sera contained a high titre of DISC1-specific antibodies as determined by the ELISA data (section 4.3). Antiserum from both of the rabbits strongly detects the His-tagged DISC1 fusion protein at approximately 45kDa (Figure 4.1A). The pre-immune serum was used as a negative control and did not detect the DISC1 fusion protein. The specificity of the anti-rabbit secondary antibody was also confirmed and it did not detect any bands in the absence of primary antibody (data not shown).

As expected from the use of crude antisera, a number of additional bands are detected along with the DISC1-specific band. Titrating the crude antisera had no effect on the appearance of these bands (Figure 4.1A). These potentially non-specific bands are particularly evident at approximately 40kDa (Figure 4.1A & B)

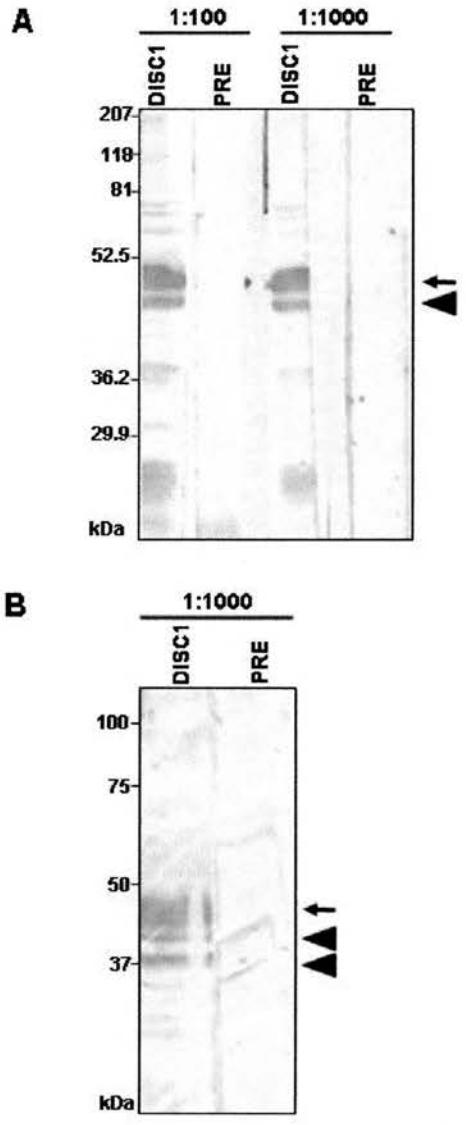

FIGURE 4.1: Specificity of DISC1 anti-peptide antisera for His-tagged recombinant DISC1 protein

Equivalent volumes of bacterial cell lysates were loaded in each lane. Crude DISC1 antiserum (DISC1) from each of the rabbits, R99946 (A) and R99947 (B), was tested at the indicated dilutions. The pre-immune serum (PRE) was used as a negative control. The antisera successfully detected the His-tagged recombinant DISC1 protein at approximately 45kDa (arrow). A number of non-specific bands were also detected (especially apparent in A), as were putative breakdown products of the full-length DISC1 protein (arrowheads; see Figure 4.2 also).

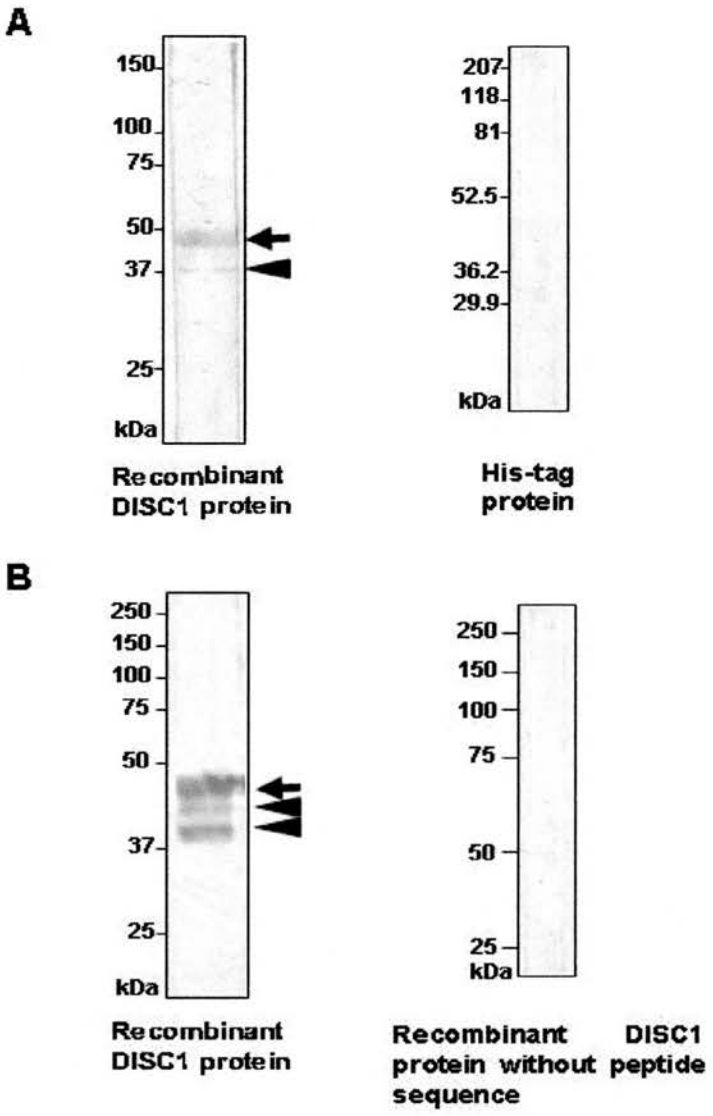

FIGURE 4.2: Specificity of DISC1 anti-peptide antibodies for His-tagged recombinant DISC1 protein

Equivalent volumes of bacterial cell lysates were loaded in each lane. For R99946 (A) the antibodies were diluted 1:100, while for R99947 (B) the antibodies were diluted 1:1000. The antibodies were tested against His-tagged recombinant DISC1 protein. Only the DISC1 fusion protein (arrow) and breakdown products were detected (arrowheads). To ensure the specificity of the antibodies, bacterial cell lysates containing the His-tag protein only (A) or recombinant DISC1 protein without the appropriate peptide sequence (B) were tested.

and 60 – 80kDa (Figure 4.1A). Following immunoaffinity purification, the DISC1 fusion protein and the 40kDa bands are still detected (Figure 4.2A & B). None of the 60 – 80kDa proteins are detected indicating these bands are unrelated to the DISC1 antibodies. The detection of the 40kDa bands by the purified DISC1 antibodies, as well as their close size to the DISC1 fusion protein, means these bands were assumed to represent breakdown products of the full-length DISC1 fusion protein. Interestingly, the 30kDa breakdown product that was always visible by Coomassie gel analysis of the His-tagged DISC1 fusion protein (section 3.3.3.2) was never detected by the antibodies. Caprylic acid purification alone did not reduce the number of non-specific bands compared to crude antisera (data not shown).

The purified anti-peptide antibodies also detect the GST-tagged DISC1 fusion protein (data not shown). In addition, further confirmation of the specificity of the antibodies was obtained by using either recombinant DISC1 protein that does not contain the appropriate peptide sequence (Figure 4.2B) or control bacterial cell extracts containing the His-tag protein only (Figure 4.2A). No bands were detected by either batch of the DISC1-specific antibodies. Furthermore the anti-peptide DISC1 signal is completely abolished by preabsorbing the antibodies (Yamamoto *et al.*, 2000) with increasing concentrations of the immunizing peptide (Figure 4.3). Preabsorbing the DISC1 antibodies with a minimum of 0.1μg of peptide per μl of primary antibody solution is enough to abolish the anti-peptide signal, even after prolonged exposure to autoradiography film (data not shown). The DISC1 antibody was used at a higher dilution than usual, because of the high localised concentration of DISC1 protein (3.5μg) in combination with the increased sensitivity of the detection method: the chemiluminescent detection reagent, ECL Plus (Amersham Biosciences) was used instead of DAB.

Both batches of the antibodies are comparable in their specificity for the recombinant DISC1 protein, as determined by the lack of background bands in the presence or absence of the appropriate recombinant DISC1 protein. The additional band detected

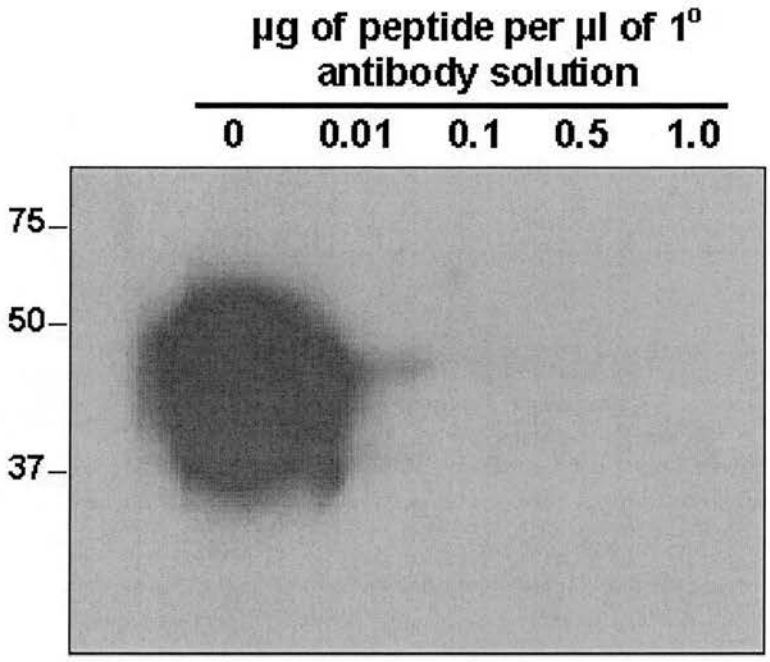

FIGURE 4.3: Pre-absorption of purified R99947 DISC1 anti-peptide antibodies using the immunizing peptide

3.5µg of purified recombinant DISC1 protein was loaded per lane. Immunodetection was performed using DISC1 antibodies (1:50000), which had been preabsorbed with increasing concentrations of the DISC1 peptide (0.01 – 1.0µg of peptide per µl of primary antibody solution). A control reaction containing DISC1 antibodies only was also performed. After a 5 minute exposure, the recombinant DISC1 protein was strongly detected in the absence of peptide, however in the presence of increasing concentrations of peptide this DISC1-specific signal is abolished. Due to the strength of the signal, it is not clear if the putative breakdown products identified in Figures 4.1 and 4.2 (arrowheads) are detected in the control lane with no peptide added (0µg of peptide). Nevertheless in previous immunoblots, these bands were detected, and subsequently removed following pre-absorption of the purified DISC1 antibodies with the immunizing peptide.

by the R99947 DISC1-specific antibodies (Figure 4.2B) was also detected using the R99946 DISC1-specific antibodies (data not shown), and the presence or absence of this band is most likely due to the quality of the bacterial protein extracts.

The reduced signal intensity seen with the purified R99946 antibodies is a reflection of the concentration of the purified antibodies. The R99947 antibodies were approximately four times more concentrated, as determined by calculating the antibody concentration at an optical density of 280nm (section 2.2.3.6). Due to the higher concentration of R99947 antibodies, most of the subsequent data presented in this thesis has been performed using the purified R99947 DISC1 anti-peptide antibodies (unless otherwise stated).

4.4.2 Anti-protein antibodies

The sheep serum from all three bleeds was tested to determine which of the bleeds would be most suitable for the purification of DISC1-specific antibodies (section 4.2). The crude DISC1 antisera were tested on GST-tagged DISC1 protein as the antisera had been raised against the His-tagged DISC1 fusion protein and may therefore contain antibodies to the His-tag protein. It can be seen that the crude serum from all three bleeds detects the DISC1 fusion protein at approximately 50kDa (Figure 4.4A). No signal was seen with either the pre-immune serum (Figure 4.4A) or by the anti-sheep secondary antibody alone (data not shown). There was no difference in the specificity of the bleeds, as determined by the number of additional bands detected, and likewise the strength of the signal from all three bleeds was comparable.

Due to the similarity of the three bleeds, no bleed appeared most suitable for purification of DISC1-specific antibodies, consequently serum from the third bleed was immunoaffinity purified (section 4.2). Following purification, the additional bands detected by the crude serum are still detected by the purified antibodies (Figure 4.4B), and are again likely to represent breakdown products of the full-length DISC1 fusion protein. The lower of the two bands is most likely the 31kDa

breakdown product visible by Coomassie gel analysis (section 3.3.3.1). Titrating the purified antibody reduced the background staining (data not shown).

The purified anti-protein antibodies also successfully detected the His-tagged DISC1 protein and did not detect any bands in bacterial cell extracts containing the His-tag protein alone (data not shown), providing further evidence for the specificity of the antibodies for the DISC1 protein.

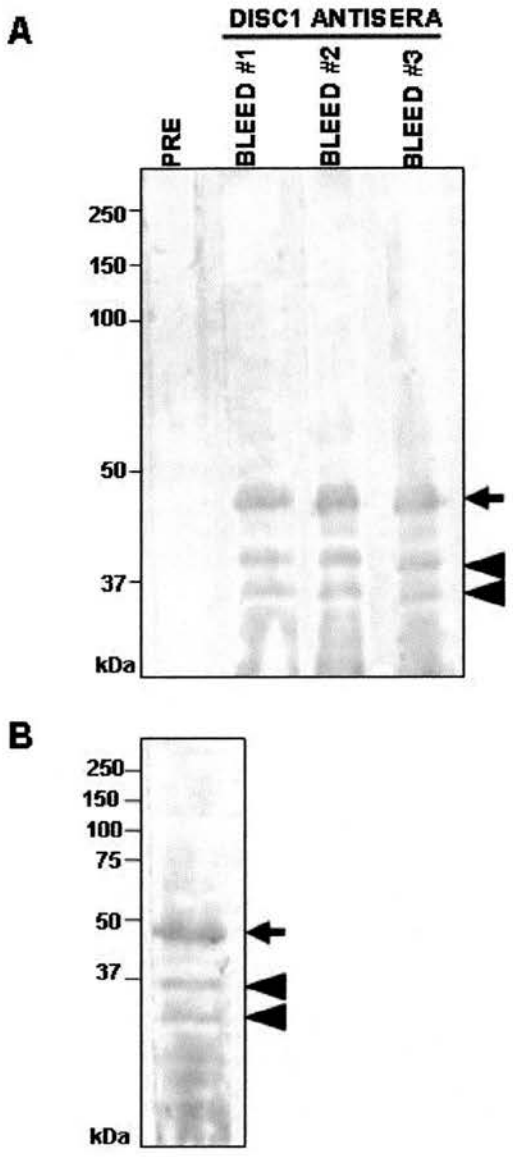

FIGURE 4.4: Specificity of DISC1 anti-protein antibodies for GST-tagged recombinant DISC1 protein

Equivalent volumes of bacterial cell lysates were loaded in each lane. Detection of the DISC1 recombinant protein was performed using crude antisera (A) and immunoaffinity purified antibodies (B); the pre-immune serum was used as a negative control (A). All dilutions were 1:500. Both the crude antisera (A) and the immunoaffinity purified antibodies (B) were able to detect the DISC1 fusion protein at approximately 50kDa (arrow), as well as two breakdown products of the full-length protein (arrowheads).

4.5 Characterisation of DISC1 anti-peptide and anti-protein antibodies using eukaryotically expressed recombinant DISC1 protein

A strong DISC1-specific signal on bacterially expressed DISC1 protein was encouraging (sections 4.4.1 & 4.4.2), but it was also necessary to determine whether the DISC1 antibodies could detect DISC1 protein that had been expressed in a mammalian expression system. Bacterially expressed recombinant protein may be structurally and functionally different to the native eukaryotic protein, as bacteria do not perform the correct post-translational modifications of eukaryotic proteins.

Stable transfected cell lines expressing exogenous human DISC1 protein were generated within the group (Kirsty Millar & Sheila Christie). The expression construct used for production of the stable cell lines contained the whole DISC1 open reading frame (2.6kb), and therefore these cells express the full-length DISC1 protein. In addition the recombinant protein is fused to a V5 peptide tag as an additional means to identify the expressed protein. The expression construct was transfected into a neuroblastoma cell line, SH-SY5Y, and stable cell lines identified that express the DISC1 protein.

Both the anti-peptide and anti-protein antibodies were able to detect recombinant DISC1 protein at the predicted size of approximately 110kDa (Figure 4.5). Endogenous DISC1 protein (section 4.6.1) was not detected, as in these instances, the 6% SDS-PAGE gels prepared did not resolve any proteins below what is shown. The pre-immune sera, used as a negative control, did not detect the DISC1 fusion protein; nonetheless the anti-peptide pre-immune serum did detect two bands, one of very similar size to the DISC1 fusion protein. This draws into question the suitability of pre-immune serum as a negative control for a purified antibody, as the specificity of an unknown population of antibodies and contaminating proteins is being compared to a highly specific antibody population, yet spurious cross-reactions are to be expected with use of a crude antibody population.

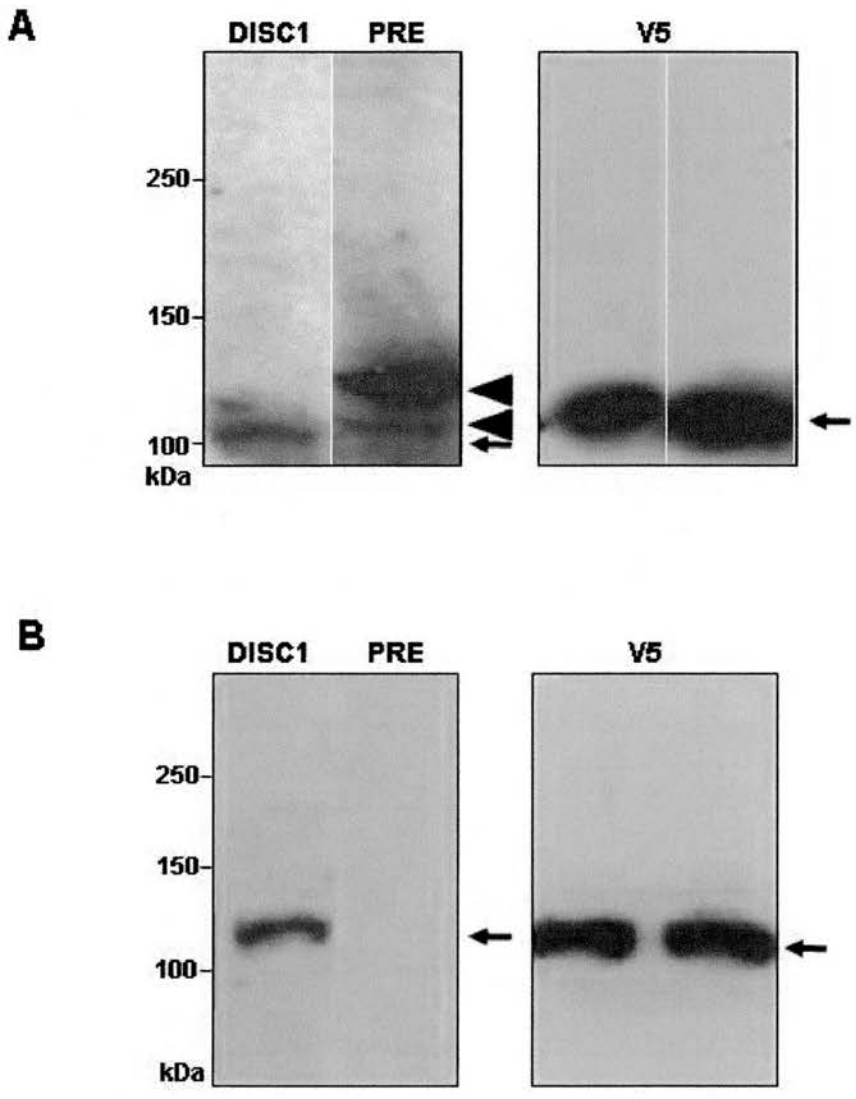

FIGURE 4.5: Both DISC1 antibodies detect V5-tagged recombinant DISC1 protein expressed in eukaryotic cells

Lysates from SH-SY5Y cells expressing V5-tagged DISC1 protein were loaded in each lane. Both the anti-peptide (A) and anti-protein (B) antibodies (DISC1) detect the 110kDa recombinant DISC1 protein (arrow). The pre-immune sera (PRE) were used as negative controls. The pre-immune serum for the anti-peptide antibody (A) detected two unrelated bands (arrowheads). The same blots were stripped and re-probed using a V5-specific antibody (V5). The V5 antibody detects recombinant DISC1 protein in all of the lanes (arrow).

To confirm the identity of the V5-tagged DISC1 protein, the blots were stripped and then re-probed using a V5-specific antibody (Invitrogen). The V5-tagged DISC1 fusion protein was strongly detected in all of the lanes, including those previously probed with the pre-immune serum.

4.6 Characterisation of DISC1 anti-peptide and anti-protein antibodies using endogenous DISC1 protein

Both the anti-peptide and anti-protein DISC1 antibodies were specific for recombinantly expressed DISC1 protein (sections 4.4.1, 4.4.2 & 4.5). To further characterise the antibodies their specificity for endogenous DISC1 protein was determined. For this purpose, a number of transformed human cell lines were used. These had been tested for expression of *DISC1* by RT-PCR (section 4.7.1). The cell lines were used firstly to ascertain by immunoblotting if the two antibodies confirmed one another with respect to the DISC1 protein isoforms detected. The second use of the cell lines was to determine if the subcellular localisation pattern from both of the antibodies was the same.

4.6.1 Immunoblotting

The DISC1 antibodies were tested on protein extracts prepared from a number of cell lines (Figure 4.6). As has already been discussed (section 1.7.1), a number of alternative *DISC1* transcripts were predicted to exist, therefore DISC1 protein isoforms of varying size were possible. Both of the DISC1 antibodies detected three bands in common (Figure 4.6), however the upper band at approximately 75kDa was detected by the anti-peptide antibodies only (the identity of the bands will be discussed in chapter 5).

Pre-absorption of the anti-peptide antibodies using the immunizing peptide abolished the antibody signal (Figure 4.6B), confirming that the additional band is without doubt due to the DISC1 anti-peptide antibodies. A control pre-absorption using a non-specific peptide directed against the Eef1a2 protein (obtained from H.Newbery, Medical Genetics Section) did not abolish the DISC1 anti-peptide signal. The

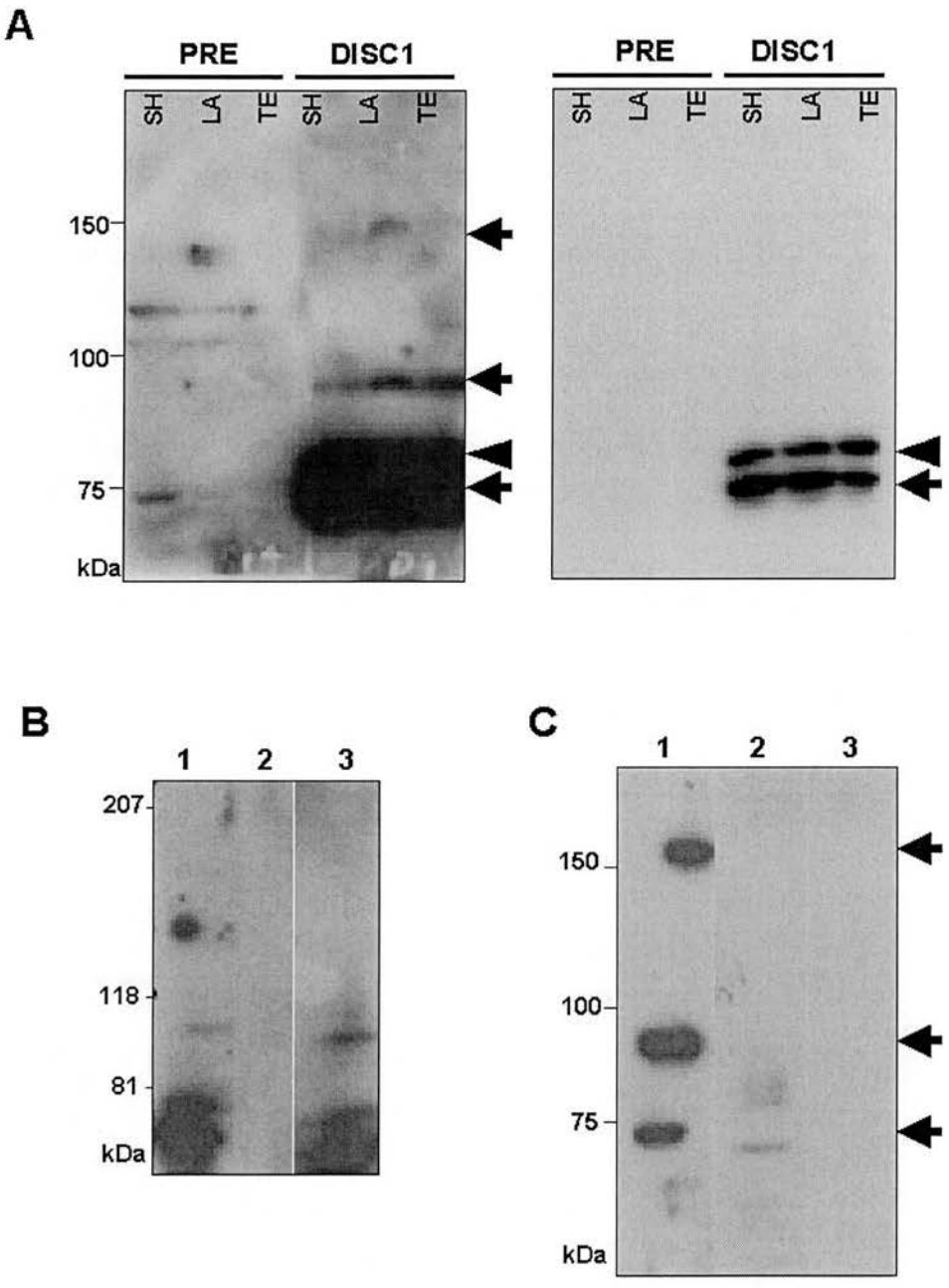

FIGURE 4.6: DISC1 anti-peptide and anti-protein antibodies detect endogenous DISC1 protein from transformed cell lines

Equivalent concentrations of protein were loaded in each lane. The DISC1 antibodies detected three bands in common (arrows). The DISC1 anti-peptide antibodies detected an additional band (arrowhead) which was not confirmed by the anti-protein antibodies.

A: DISC1 anti-peptide antibodies (1:400) were used to detect endogenous DISC1 protein in a number of transformed cell lines: SH-SY5Y (SH), LAN-5 (LA) and TE671 (Te). The pre-

immune serum was used as a negative control. Different exposures of the same blot are shown: 10 second (right) or 30 minute (left).

B: DISC1 anti-peptide antibodies (1:2000) were preabsorbed with the DISC1 immunizing peptide or a control peptide (Eef1a2). 0.01μg of peptide per μl of primary antibody solution was needed to abolish the signal from the DISC1 antibodies. Lane 1: no peptide; 2: DISC1 peptide; 3: Eef1a2 peptide.

C: DISC1 anti-protein antibodies (1:200) were used to detect endogenous DISC1 protein in the neuroblastoma cell line, SH-SY5Y. The pre-immune serum was used as a negative control and in addition the specificity of the anti-goat secondary antibody was tested by omitting the primary antibody. Lane 1: DISC antibody; 2: Pre-immune serum; 3: no primary antibody.

additional anti-peptide band is not seen in the rabbit pre-immune serum and titrating the anti-peptide antibody did not reduce the appearance of this band (data not shown). Neither of the secondary antibodies detected any bands (data shown for the anti-goat secondary antibody only).

4.6.2 Immunofluorescence

The cell staining pattern detected by both DISC1 antibodies was determined using the SH-SY5Y and U373 MG cell lines. Initial controls were performed to test for both autofluorescence and any background fluorescence from the secondary antibodies. The fluorescence seen was negligible (data not shown). For the anti-peptide antibody, a punctate peri-nuclear, cytoplasmic staining pattern was seen (to be discussed in chapter 8), after both methanol and paraformaldehyde fixation (Figure 4.7). No signal was seen with the use of the pre-immune serum (Figure 4.8). In addition the anti-peptide staining pattern was abolished following incubation of the DISC1 antibodies with the immunizing peptide. A control pre-absorption, incubating the pre-immune serum with the DISC1 peptide had no effect on the pre-immune signal (Figure 4.8).

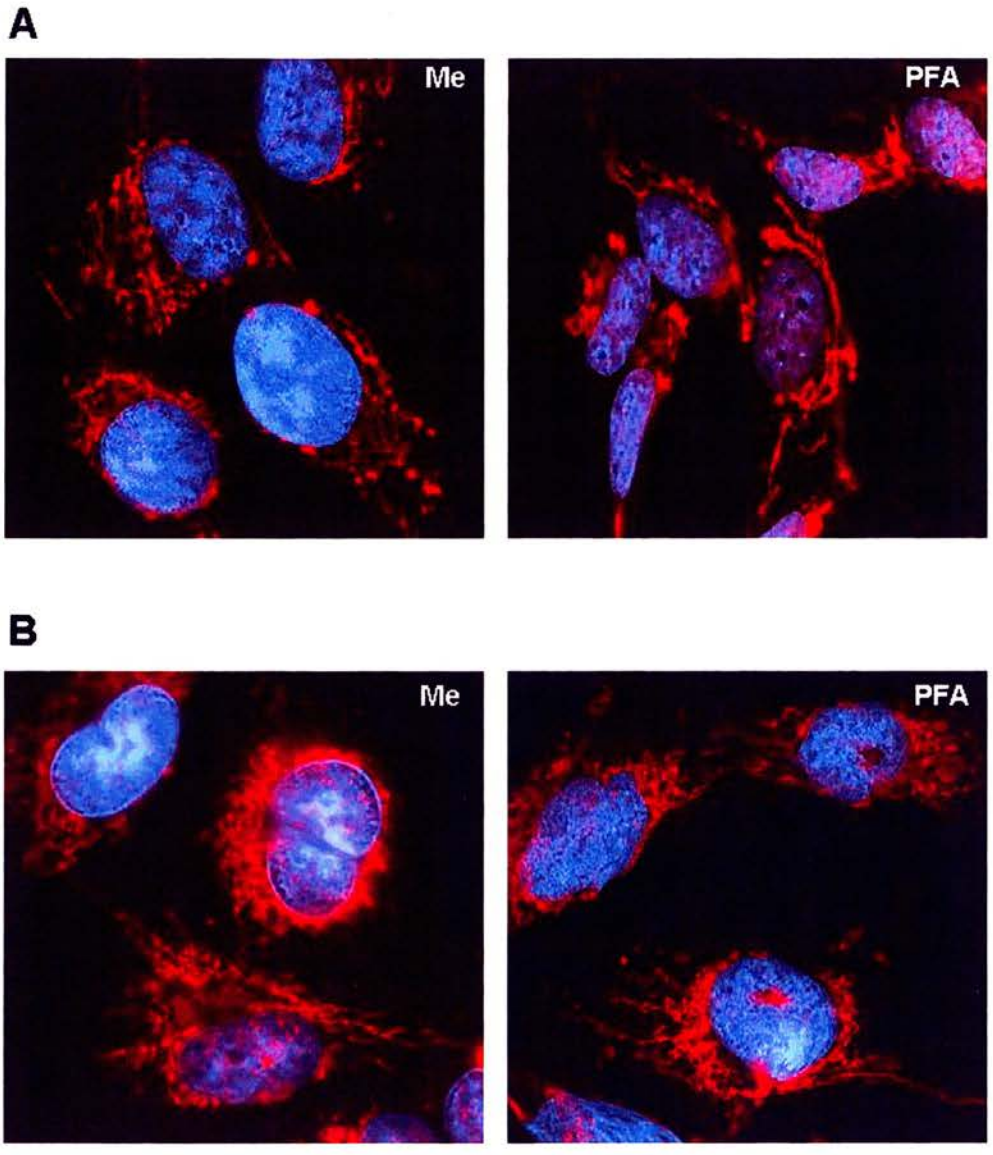

FIGURE 4.7: DISC1 anti-peptide antibodies detect a peri-nuclear, cytoplasmic staining pattern in cell lines

SH-SY5Y (A) and U373 MG (B) cells were fixed in either methanol (Me) or 4% paraformaldehyde (PFA). The DISC1 anti-peptide antibody was detected using an Alexa-Fluor 594 conjugated secondary antibody (red) and the nuclei were counterstained with DAPI (blue).

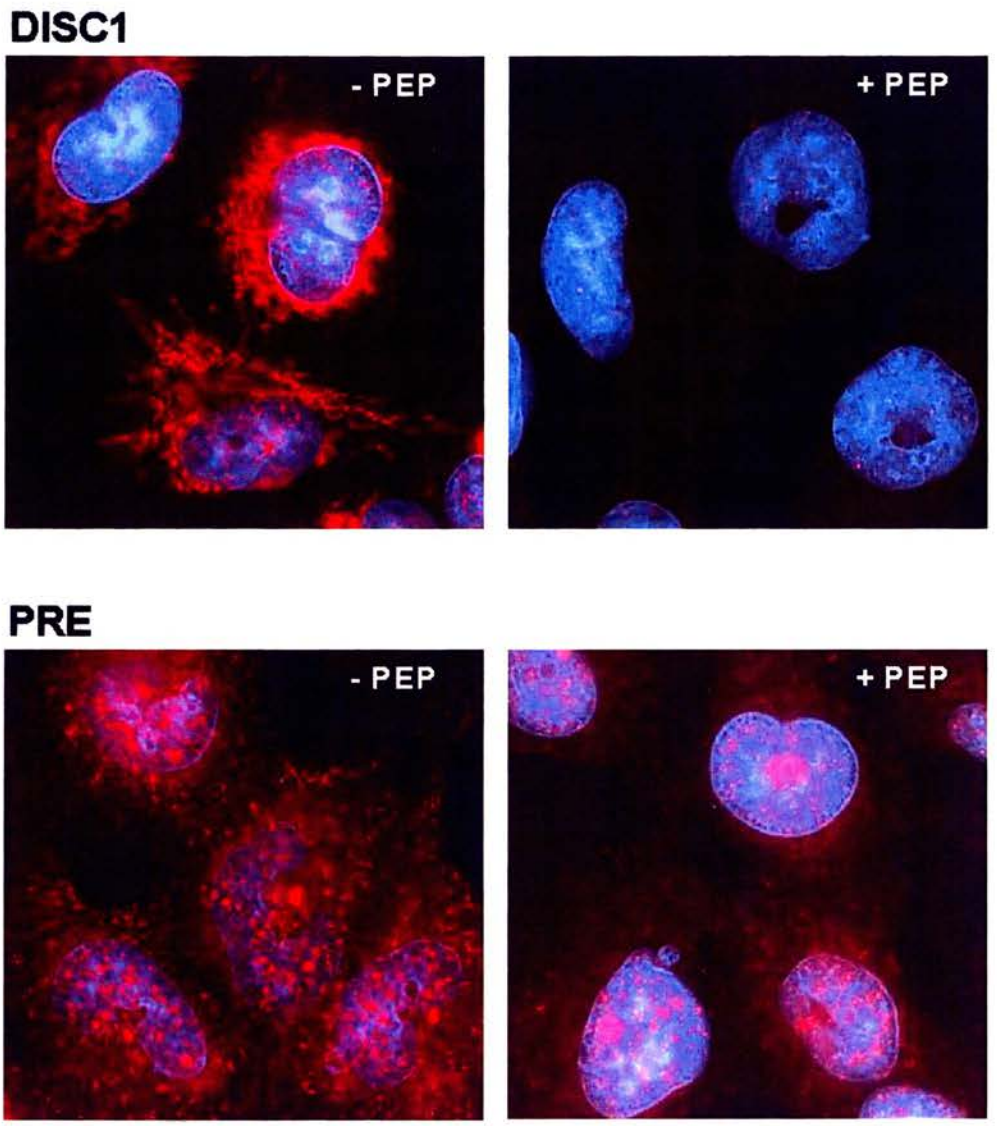

FIGURE 4.8: Specificity of the DISC1 anti-peptide antibodies for the subcellular localisation pattern seen in cell lines

Immunofluorescent detection of the DISC1 antibodies (DISC1) and pre-immune serum (PRE) was performed on methanol-fixed U373 MG cells. The antibodies were preabsorbed with (+ pep) or without (- pep) the immunizing peptide (0.05µg peptide per µl of primary antibody solution) and detected using an Alexa-Fluor 594 conjugated secondary antibody (red). The nuclei were counterstained with DAPI (blue).

For all of the subsequent data presented in this thesis, the anti-peptide antibodies were used after methanol fixation, as the use of paraformaldehyde fixation was found to increase the background signal especially within the nucleus (data not shown). To reduce paraformaldehyde induced fluorescence, fixed cells were incubated in sodium borohydride, but this had no effect on the background signal (data not shown). Other reagents, such as glycine, can also be used to reduce paraformaldehyde induced fluorescence.

In contrast, the DISC1 anti-protein antibody did not produce any signal above background (data not shown), despite considerable optimisation of the cell staining procedure (section 2.2.4.10). A number of fixatives were tested including paraformaldehyde (2 and 4%), methanol, methanol:acetone (1:1) and acid-alcohol (5% glacial acetic acid / 95% ethanol). In addition, following paraformaldehyde fixation, altering the length of the permeabilisation stage was examined. None of these modifications had any effect on the antibody signal. The primary antibody incubation step was increased from a one hour incubation to an overnight incubation but again no difference in the signal was seen. Finally, the crude DISC1 antiserum, caprylic acid purified serum and another batch of purified anti-protein antibodies were tested to determine if either the purification stage or the storage of the antibodies was affecting the specificity of the antibodies for the native DISC1 protein. Again these had no effect and it was concluded that the anti-protein antibodies were not going to be suitable for determining the subcellular localisation pattern of DISC1.

As the localisation of DISC1 within the cell is central to determining its function, it was important to confirm the anti-peptide subcellular localisation pattern. This was even more crucial because of the additional, potentially non-specific band detected on immunoblots by the anti-peptide antibodies (section 4.6.1).

4.7 A DISC1 negative cell line to aid characterisation of the antisera

The availability of a cell line not expressing DISC1, would aid and simplify characterisation of the DISC1 antibodies. A number of human cell lines were tested to determine if a DISC1 negative cell line could be found. Furthermore, the use of a rodent cell line enabled the specificity of the human specific anti-peptide antibodies to be determined.

4.7.1 Multiple cell lines tested for DISC1 expression by RT-PCR

A number of human cell lines were obtained from various sources (Table 2.3). H36PE2 RNA was obtained from Simon Cooper (Medical Genetics Section). The cell lines are all transformed cell lines and have been derived from different tissue sources. These were tested for expression of *DISC1* by RT-PCR (Table 4.2) using primers located within exon 1 and exon 2 of the *DISC1* gene (Table 2.8). This ensures that the majority of *DISC1* transcripts are identified.

None of the human cell lines tested were found to be DISC1 negative (Table 4.2), and the *DISC1* transcript is apparently ubiquitously expressed within human cell lines. This is analogous to the widespread expression pattern of the transcript within human tissue (section 1.7.1). The expression pattern of specific *DISC1* transcripts within the cell lines will be discussed in chapter 5.

TABLE 4.2: RT-PCR analysis of *DISC1* expression within human cell lines

CELL LINE	TISSUE (CELL TYPE) DERIVED FROM	RT-PCR
SH-SY5Y	brain (neuroblastoma)	+
LAN-5	brain (neuroblastoma)	+
TE671	brain (cerebellar medulloblastoma)	+
U373 MG	brain (glioblastoma)	+
MOG-G-CCM	brain (astrocytoma)	+
HepG2	liver (hepatocellular carcinoma)	+
MCF7	mammary gland (adenocarcinoma)	+
293	embryonic kidney	+
t(1;11) lymphoblast	lymphoblastoid	+
CACO-2	colon (colorectal carcinoma)	+
H36CE2	lens	+

A positive RT-PCR result was recorded if the expected product was seen in both the +RT reaction and positive control. A negative RT-PCR result would have been recorded if the expected product was seen only in the positive control. DISC1 cDNA clones were used for positive controls.

4.7.2 A rodent cell line as a negative cell line for a human-specific antibody

As no human cell line was found that was DISC1 negative, CHO (Chinese hamster ovary) cells were used as a negative cell line for the human-specific anti-peptide antibody.

CHO cells are derived from a Chinese hamster and consequently it was predicted that if the DISC1 anti-peptide staining pattern seen in human cell lines (Figure 4.7) was specific for the human DISC1 protein, the same staining pattern would not be seen in CHO cells. The DISC1 protein sequence of the Chinese hamster is not known, but it was assumed to be similar to the mouse DISC1 protein which does not contain the peptide used for immunization (section 3.2.1).

The DISC1 anti-peptide antibodies produced a completely non-specific pattern on CHO cells, which did not preabsorb after incubation of the antibodies with the peptide (Figure 4.9). A similar pattern was seen with the pre-immune serum and is

likely to represent a cross-reaction between the rabbit antibodies and the hamster cell line.

Use of the CHO cells confirmed that the subcellular localisation pattern seen with the DISC1 anti-peptide antibodies is human-specific.

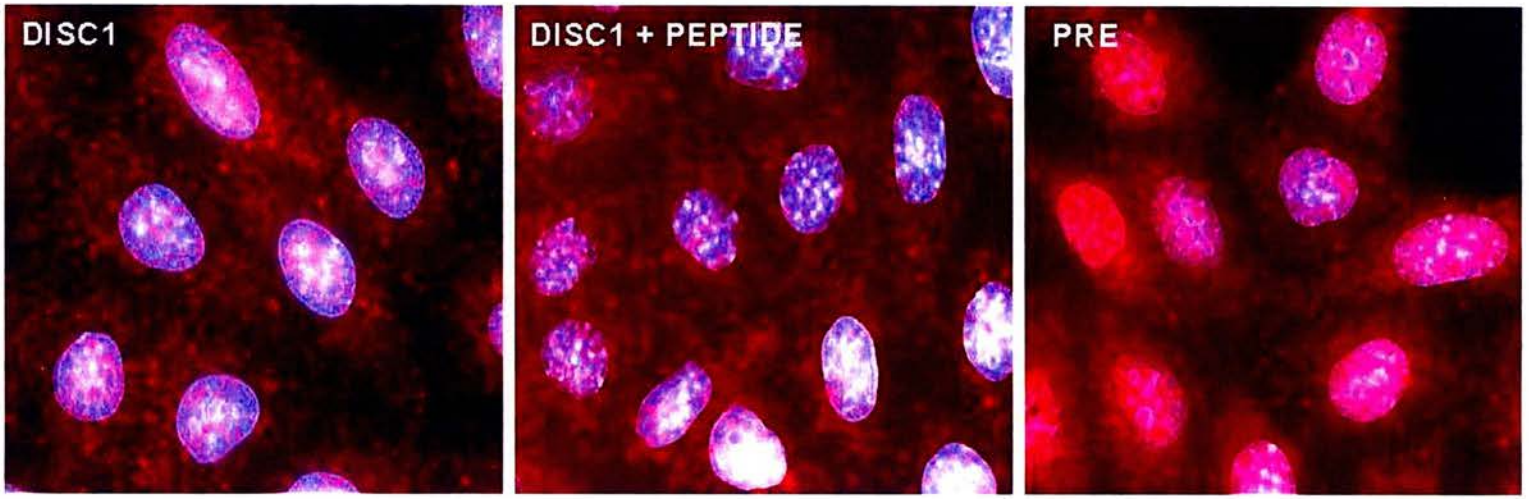

FIGURE 4.9: Use of CHO cells to determine the specificity of a human-specific antibody

Methanol fixed CHO cells were stained using either the DISC1 anti-peptide antibodies (DISC1) or the pre-immune serum (PRE). A non-specific staining pattern was seen which was not abolished by preabsorbing the DISC1 antibodies with the immunizing peptide (DISC1 + PEPTIDE). The antibodies were detected with an Alexa-Fluor 594 conjugated secondary antibody (red) and the nuclei counterstained using DAPI (blue).

4.8 The use of independent methods to determine the subcellular localisation pattern of the DISC1 protein

In addition to the use of protein specific antibodies, the subcellular localisation of a protein can be determined using recombinantly expressed protein that is partnered to an appropriate tag. The tag allows independent verification of the localisation of the protein, either directly by use of a fluorescent tag or indirectly using antibodies specific to the tag. As described earlier (section 4.5), DISC1 cell lines expressing V5-tagged DISC1 protein had been generated. In addition, transient transfected cell lines expressing DISC1 protein fused to GFP had also been generated within the group. These cell lines provided a potential alternative means of visualising DISC1 within the cell. Finally, towards the end of this project DISC1 antibodies generated independently by another group became available. These were also used to confirm the DISC1 subcellular localisation pattern.

4.8.1 Subcellular localisation of DISC1 cannot be confirmed by V5-tagged DISC1 protein

The SH-SY5Y cell line expressing V5-tagged DISC1 protein (section 4.5), was examined using the DISC1 anti-peptide antibody as well as the V5-specific antibody (Invitrogen) previously tested by immunoblotting (Figure 4.5).

The cell staining pattern, as determined by use of the DISC1 antibody, was the same in both V5-DISC1 expressing and control SH-SY5Y cell lines (Figure 4.10). However the signal from the V5 antibody was entirely non-specific and the same background speckles were seen in both V5-DISC1 expressing and control SH-SY5Y cells (Figure 4.10), even after various optimisations of the cell staining procedure (section 2.2.4.10). As described in section 4.6.2, different fixatives were tested as was the effect of increasing the primary antibody incubation step. Different blocking buffers were also tested (3% BSA plus 10% serum, 3% BSA alone, 10% serum alone, 1% casein and 5% Blotto), but these had no effect on the V5 antibody signal.

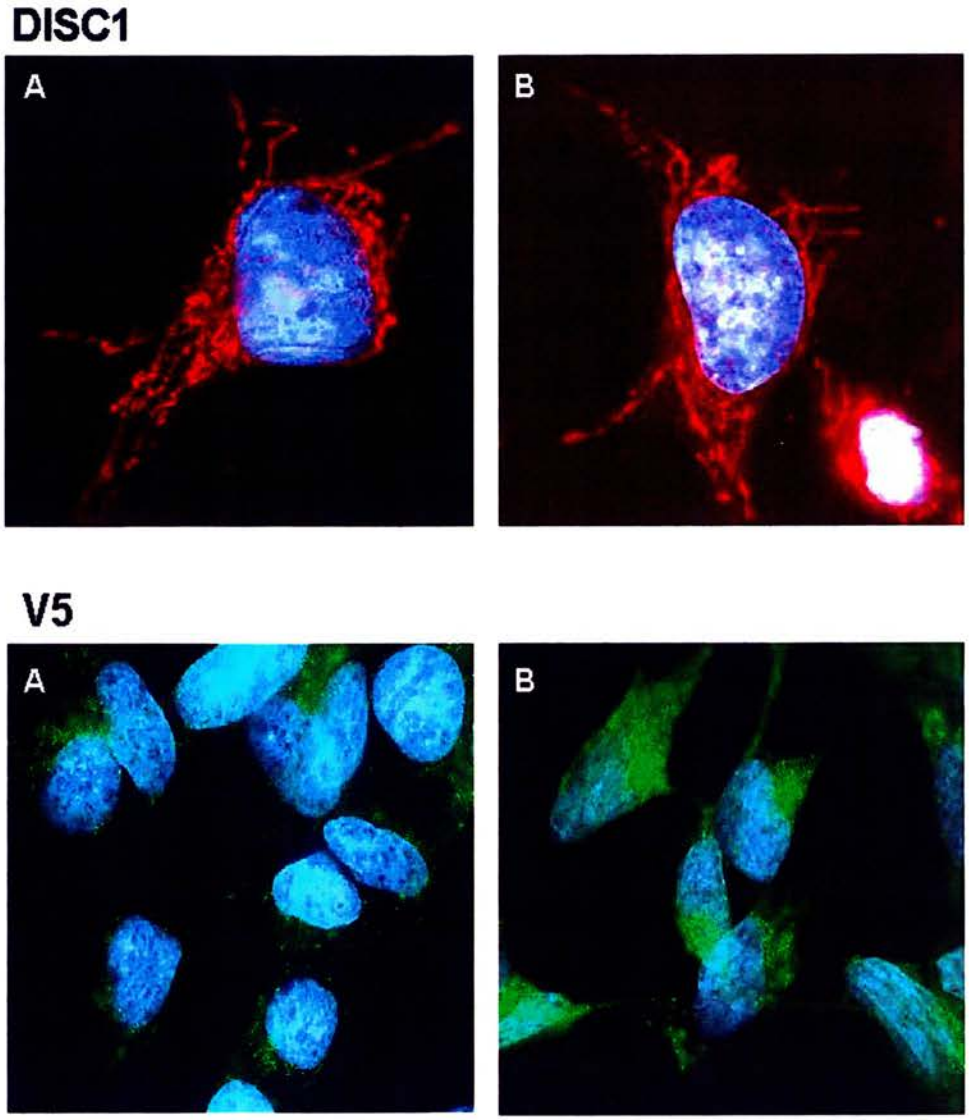

FIGURE 4.10: V5-tagged recombinant DISC1 as an independent method for the subcellular localisation of DISC1

V5.DISC1 expressing SH-SY5Y (B) and control SH-SY5Y (A) cells were stained using the DISC1 anti-peptide (upper panels; red) and V5 (lower panels; green) antibodies. The nuclei were counterstained with DAPI (blue). No difference in the staining pattern from either of the antibodies was seen when comparing control to overexpressing SH-SY5Y cells.

4.8.2 Subcellular localisation of DISC1 can be partially confirmed by GFP-tagged DISC1 protein

The following work with GFP-tagged DISC1 protein was performed by Kirsty Millar. Cells expressing GFP-tagged human DISC1 protein were generated using a number of cell lines, including U373 MG (human glioblastoma), HeLa (human adenocarcinoma), HT-1080 (human fibrosarcoma) and CHO (Chinese hamster ovary) cells.

GFP-tagged DISC1 protein expressed in human cell lines formed aggregate-like structures and did not produce the expected DISC1 subcellular localisation pattern. In contrast, expression of the GFP-DISC1 fusion protein in non-human cell lines produced a punctate pattern round the nucleus (Figure 4.11), similar to the pattern seen with the anti-peptide antibody. The absence of extensive cytoplasmic GFP expression may reflect the structure of the cell type rather than a difference in localisation.

As well as providing confirmation of the peri-nuclear localisation of DISC1, co-localisation of the DISC1 anti-peptide signal with the GFP signal, provided additional evidence for the specificity of the anti-peptide antibodies (data not shown).

The GFP-DISC1 fusion protein was not analysed by immunoblotting, as both the anti-peptide and anti-protein antibodies had successfully detected V5 tagged DISC1 protein (Figure 4.5), thus demonstrating the specificity of the antibodies for eukaryotically expressed DISC1 protein.

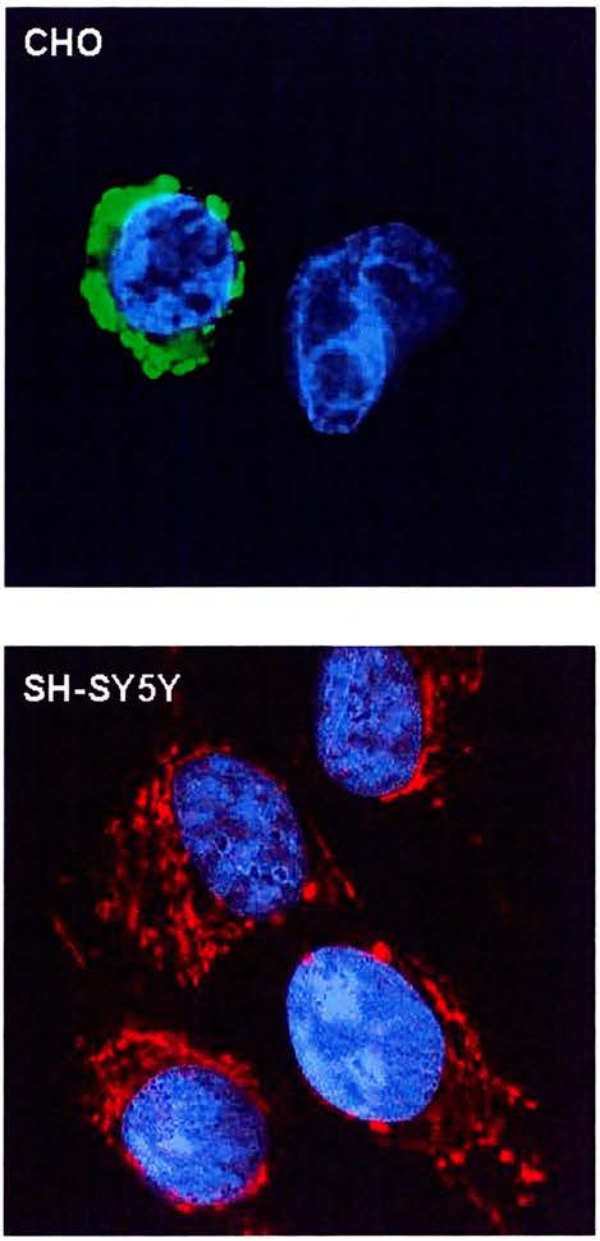

FIGURE 4.11: GFP-tagged recombinant DISC1 partially confirms the subcellular localisation pattern detected by the DISC1 anti-peptide antibody

GFP-tagged DISC1 protein expressed in CHO cells shows a peri-nuclear localisation similar to that observed in SH-SY5Y neuroblastoma cells.

4.8.3 An independent C-terminal DISC1 antibody confirms DISC1 subcellular localisation

A C-terminal antibody, rabbit anti-DISC1-C2, was obtained from Akira Sawa (Department of Psychiatry, John Hopkins University). The antibody had been generated against bacterially expressed GST-tagged rat DISC1 protein. The portion of the C-terminus selected for recombinant protein expression spans amino acids 601 – 854 of the C-terminus (Figure 4.12).

Anti-DISC1-C2 was tested using the SH-SY5Y and U373 MG cell lines after both methanol and paraformaldehyde fixation. The subcellular localisation pattern seen with this antibody was identical to the DISC1 anti-peptide staining pattern (Figure 4.13). As both of the antibodies had been raised in rabbits, co-localisation of the two antibodies was made possible by conjugating the DISC1 anti-peptide antibodies directly to a fluorescent tag (performed by Kirsty Millar) and then staining as described (section 2.2.4.10.2).

The merged images are expected to be yellow with the direct co-localisation of a green and red signal. However regions of the merged images, especially towards the periphery of the U373 MG cells, do not appear yellow. Nonetheless, examination of the signal-specific images does show that the pattern is identical but the green signal is fainter than the red signal. The signal from the anti-DISC1-C2 antibody is stronger despite increasing the incubation time for the conjugated anti-peptide antibody. This increased signal strength is due in part to amplification of the anti-DISC1-C2 signal from use of the secondary antibody, but probably also reflects the larger number of epitopes recognised by the anti-DISC1-C2 antibody: 253aa of recombinant protein was used as the antigen compared to only a 13aa peptide sequence for the DISC1 anti-peptide antibody.

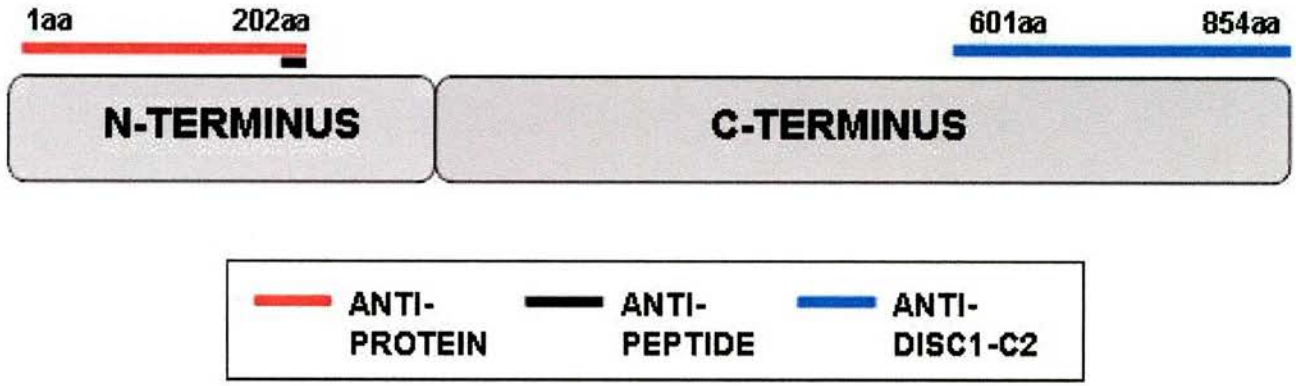

FIGURE 4.12: An independent C-terminal DISC1 antibody

The N-terminal regions of DISC1 selected for generation of the anti-peptide and anti-protein antibodies are shown on a representation of the protein. In addition, the C-terminal region selected for antibody production by Akira Sawa (anti-DISC1-C2) is highlighted.

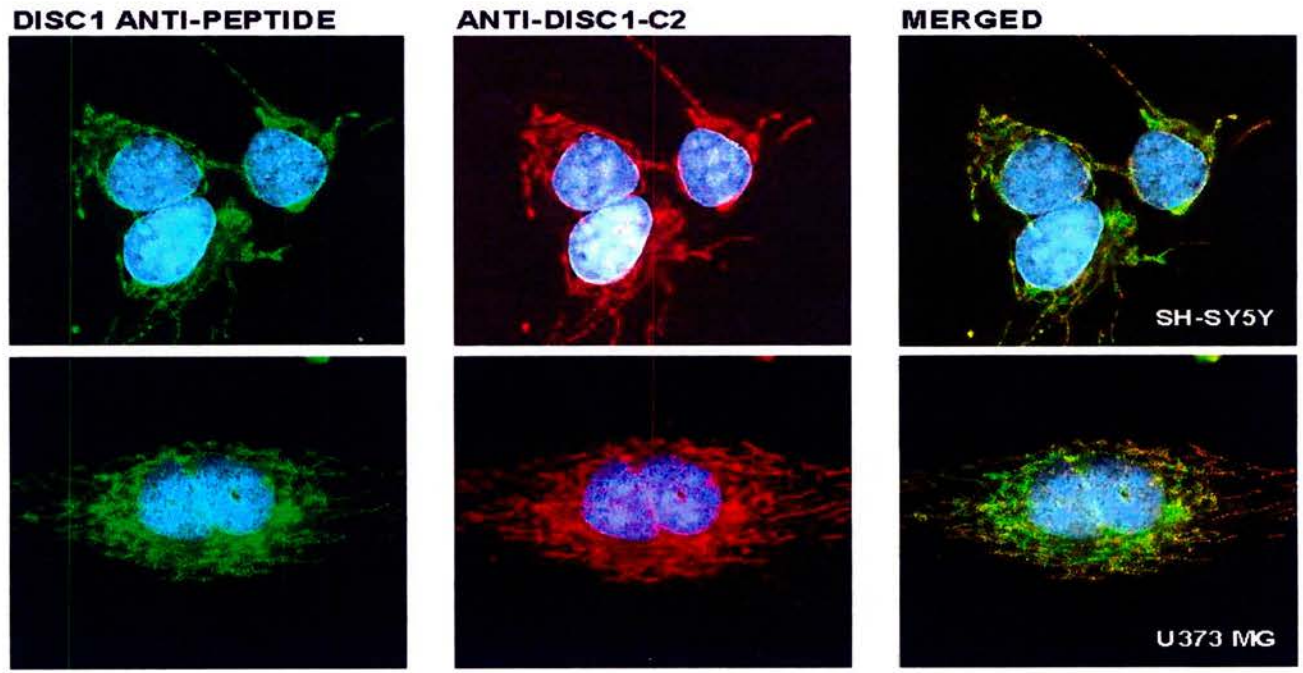

FIGURE 4.13: The use of an independent C-terminal DISC1 antibody confirms the subcellular localisation pattern of DISC1

Methanol fixed SH-SY5Y and U373 MG cells were double stained using the DISC1 anti-peptide (green) and anti-DISC1-C2 (red) antibodies. The nuclei were counterstained with DAPI (blue). Merged images are also shown. The staining pattern detected by both of the antibodies is identical, even in regions of the cell where no yellow signal is seen in the merged image.

4.9 Discussion

Nothing was known about endogenous DISC1 expression and consequently considerable time was spent characterising the signal from both of the DISC1 antibodies. To simplify interpretation of the antibody signal, DISC1-specific antibodies were immunoaffinity purified from the crude sera and used to detect recombinant and endogenous DISC1 protein. Both of the antibodies were specific for denatured recombinant DISC1 protein and were able to detect multiple isoforms of endogenous DISC1 protein (Figure 4.6), although the anti-peptide antibody also detected a band at >75kDa which was not confirmed by use of the anti-protein antibody. The presence of the additional band at >75kDa was also seen with the purified R99946 anti-peptide antibodies (data not shown). In contrast the specificity of the DISC1 antibodies for native DISC1 protein differed. A punctate peri-nuclear, cytoplasmic staining pattern was seen with use of the anti-peptide antibody (Figure 4.7), while no signal was obtained with the anti-protein antibody (section 4.6.2).

The lack of a DISC1-specific signal from the anti-protein antibody when tested against native DISC1 protein, may reflect the nature of the DISC1 protein used as an antigen: denatured DISC1 protein (section 2.2.4.1) was used as the antigen for the anti-protein antibodies, which may have resulted in the antibodies being unable to detect the native DISC1 protein (Watkins, 1989). If a fixation method or pre-treatment was used, that was more denaturing to the cells than those tested it may be possible to overcome this problem. Nonetheless it is common for antibodies to work in one technique and not another.

An additional detail regarding the use of the anti-protein antibody was that overall its performance on immunoblots was inconsistent. At times the signal was either absent or the background so high that no specific bands could be clearly seen. To address the source of this inconsistency a number of possibilities were examined. To determine if possible degradation of the DISC1 protein was affecting binding of the antibody, freshly prepared cell lysates were compared to older cell lysates. In addition storage of the antibodies was examined, by purifying a new batch of

antibodies. Neither improved the reliability of the signal (data not shown). The presence or absence of Tween in the blocking buffer and washes was also examined to ascertain if this was affecting binding of the antibody. Tween was found to be essential for the anti-protein antibody signal, but the reliability of the signal was not improved by Tween alone or even with increased Tween in the washes (data not shown). No explanation could be found for this inconsistency, especially as it appeared to be related only to the human DISC1 protein. As will be shown later, the anti-protein antibody was reliable when probing mouse and rat tissue (chapter 7).

Expression analysis of human cell lines by RT-PCR, revealed a ubiquitous distribution of the *DISC1* transcript. No cell lines were found to be DISC1 negative (Table 4.2), yet a DISC1 negative cell line would have greatly aided the characterisation of the DISC1 antibodies. It may be that the only way to generate a DISC1 negative cell line is by knocking out or knocking down the *DISC1* gene. Emerging technologies such as RNAi would be useful in this respect (Elbashir *et al.*, 2001; Hudson *et al.*, 2002). Indeed such a system would still be valuable in determining the identity of the putative non-specific anti-peptide band.

The use of cell lines expressing tagged DISC1 provided an additional opportunity for confirming the subcellular localisation of DISC1. Expression of the V5-tagged DISC1 protein was confirmed on immunoblots (Figure 4.5) but could not be verified in immunofluorescence studies by use of the same V5 antibody (Figure 4.10). The use of an alternative cell line (data not shown), demonstrated that the V5 antibody was suitable for cell staining studies. A possible explanation for the lack of a V5-specific signal on recombinant DISC1 protein is that the V5 epitope could be masked by folding of the DISC1 recombinant protein rendering the V5 epitope inaccessible to antibodies.

Confirmation of the punctate peri-nuclear DISC1 pattern was obtained using GFP-tagged protein expressed in non-human cell lines (Figure 4.11). Expression of GFP-tagged DISC1 protein in human cell lines formed aggregate-like structures rather than the peri-nuclear, cytoplasmic extensions expected. One reason may be that the

environment of the human cells was not conducive to the expression and correct localisation of the large GFP-tagged protein. The availability of DISC1 antibodies generated independently within another group successfully confirmed the DISC1 anti-peptide staining pattern (Figure 4.13), and the DISC1 subcellular localisation pattern.

Thorough characterisation of both the anti-peptide and anti-protein DISC1-specific antibodies enabled their specificity for the endogenous human DISC1 protein to be determined. In turn, data generated from use of the antibodies in their respective techniques can be viewed with confidence.

CHAPTER 5

DISC1-RELATED PROTEINS IN HUMAN

5. DISC1-related proteins in human

5.1 Introduction

The transcript data indicates that several alternative splice variants of *DISC1* are found in human (section 1.7.1). Therefore the protein expression pattern of DISC1 was examined in a number of human cell lines and foetal brain tissue to determine which of the alternative transcripts are likely to be translated into functional proteins. RT-PCR was then used to ascertain the relationship between the DISC1 protein expression pattern and the *DISC1* transcripts present in the cell lines and tissue.

5.2 Multiple DISC1-related bands identified in human cell lines and foetal brain tissue

The protein expression pattern of DISC1 was characterised in a number of human cell lines (Table 5.1). In addition foetal (11.1 weeks gestation) brain tissue was used to ensure the DISC1 proteins observed in the transformed cell lines were representative of the situation *in-vivo*. Foetal brain tissue was available within the group and had been obtained with the appropriate ethical permission from the MRC Tissue Bank.

5.2.1 DISC1 anti-peptide antibody

In all cell lines examined (Table 5.1), the anti-peptide antibody detected three major DISC1 bands of approximately 95kDa, 80kDa and 75kDa (Figures 5.1 & 4.6A). The 75kDa band is present as a doublet with the lower of the bands being less strongly detected. In addition a band of approximately 150kDa is frequently detected (Figure 4.6A). All of these bands are also observed in foetal brain tissue. The detection of these bands is prevented following pre-absorption of the antibody with the immunizing peptide (Figure 4.6B), suggesting that all the bands contain the DISC1 anti-peptide sequence.

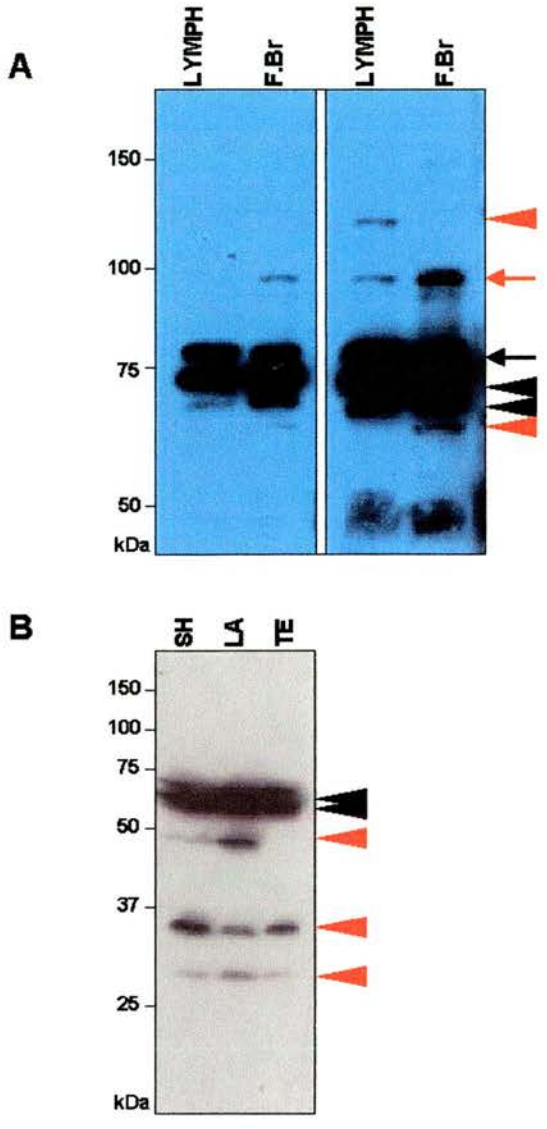

FIGURE 5.1: DISC1-related bands detected by the anti-peptide antibody in human cell lines and foetal brain tissue

A: Protein extracts from lymphoblastoid cells (LYMPH) and foetal brain tissue (F.Br) were analysed on an 8% SDS-PAGE gel. The anti-peptide antibody detects DISC1-related bands of 95kDa (red arrow), 80kDa (black arrow) and a 75kDa doublet (black arrowheads). Two putative breakdown products are also detected (red arrowheads). Short (left) and long (right) exposures of the same blot are shown.

B: Protein extracts from SH-SY5Y (SH), LAN-5 (LA) and TE671 (TE) were analysed on a 15% SDS-PAGE gel. The anti-peptide antibody detects the approximately 75kDa DISC1-related bands (black arrows), as well as a number of suspected breakdown products (black arrowheads).

No cell line showed evidence of up or down regulation of a specific band (data not shown) and the relative expression levels of the three major bands were unaltered across all samples examined: 75kDa > 80kDa > 95kDa. This relationship is also seen in foetal brain tissue.

TABLE 5.1: Detection of three major DISC1-related bands in human cell lines and foetal brain using different DISC1 antibodies

CELL LINE / TISSUE	75kDa			80kDa			95kDa		
	PEP	PRO	C2	PEP	PRO	C2	PEP	PRO	C2
SH-SY5Y	+	+	+	+	–	–	+	+	–
LAN-5	+	+	+	+	–	–	+	+	–
TE671	+	n.d.	+	+	n.d.	–	+	n.d.	–
U373 MG	+	n.d.	+	+	n.d.	–	+	n.d.	–
MOG-G-CCM	+	n.d.	+	+	n.d.	–	+	n.d.	–
293	+	n.d.	+	+	n.d.	–	+	n.d.	–
lymphoblast	+	n.d.	+	+	n.d.	–	+	n.d.	–
foetal brain	+	+	+	+	+	–	+	+	+

The presence of the three major DISC1-related bands was determined in a number of human cell lines and foetal brain tissue using three DISC1 antibodies: the N-terminal DISC1 anti-peptide (PEP) and anti-protein (PRO), and the C-terminal anti-DISC1-C2 (C2). + band detected – band not detected n.d. not determined.

5.2.2 Other DISC1 antibodies

The expected sizes of the DISC1 protein isoforms (Figure 5.2) indicate the 95kDa band is either the L or Lv isoform. Initially the bands at approximately 75kDa were expected to represent both the S1 and S2 isoforms, however no evidence for the existence of the S2 isoform was found by RT-PCR (section 5.3.2). Therefore these bands may represent other molecular forms of DISC1, possibly post-translationally modified products or alternatively may be non-specific cross-reactions between the anti-peptide antibody and an unrelated protein. To examine these possibilities, the protein expression patterns detected by the other available DISC1 antibodies were studied.

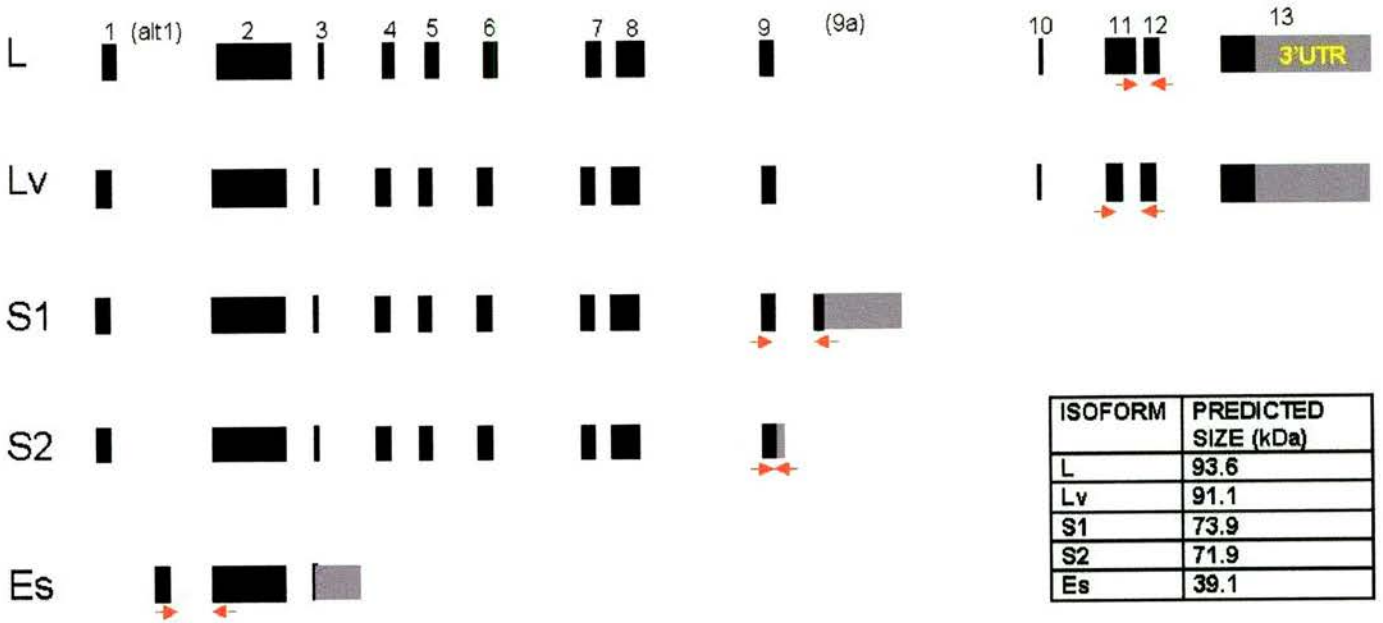

ISOFORM	PREDICTED SIZE (kDa)
L	93.6
Lv	91.1
S1	73.9
S2	71.9
Es	39.1

FIGURE 5.2: Primer location for detection of *DISC1* alternative transcripts

The exon structure of the five putative *DISC1* transcripts, L, Lv, S1, S2 and Es, are indicated. Black and grey boxes represent exons and the 3'UTR of each transcript, respectively. Red arrows indicate the locations of primers used for confirmation of the transcripts (section 5.3). The predicted molecular weight of the protein isoforms is indicated in the table.

In both the LAN-5 and SH-SY5Y cell line (Table 5.1), the DISC1 anti-protein antibody detected the 150kDa, 95kDa and 75kDa bands (Figure 4.6C). As described earlier (paragraph 3, section 4.9), the intensity of the bands shown is not representative of the anti-protein antibody. No evidence for the 80kDa band or a doublet of the 75kDa band was observed. In foetal brain the 80kDa band is also weakly detected (Figure 5.3A).

In all cell lines examined (Table 5.1), the anti-DISC1-C2 antibody (section 4.8.3) detected the 75kDa band (Figure 5.3B) but there was no evidence for a doublet of this band. Simultaneous identification of DISC1 using the anti-peptide and the anti-DISC1-C2 antibodies confirmed the identity of the band detected by the C-terminal antibody (Figure 5.3C). The 95kDa band is also weakly detected in foetal brain (data not shown). Table 5.2 summarises the results obtained using the different DISC1 antibodies for the three major DISC1-related proteins.

TABLE 5.2: Immunoblot intensity of the DISC1-related bands using different DISC1 antibodies

Antibodies	DISC1-related bands (kDa)									
	75		75 doublet		80*		95		150	
	C	B	C	B	C	B	C	B	C	B
anti-peptide (human; peptide aa191–203)	++++	++++	++	++	+ → +++	+ → +++	++	++	+	+
anti-protein (human; protein aa1–202)	+++	+++	-	-	-	+	+	+	+	+
C2 (rat; protein aa601–854)	+++	+++	-	-	-	-	-	+	-	-

C: human cell line; B: foetal brain tissue.

Symbols designate approximate band intensities: not detectable (-), faint (+), moderate (++), high (+++), very high (++++).

* The varied intensity of the 80kDa band, as detected by the anti-peptide antibody, reflects proteolytic degradation of this band (section 5.2.3).

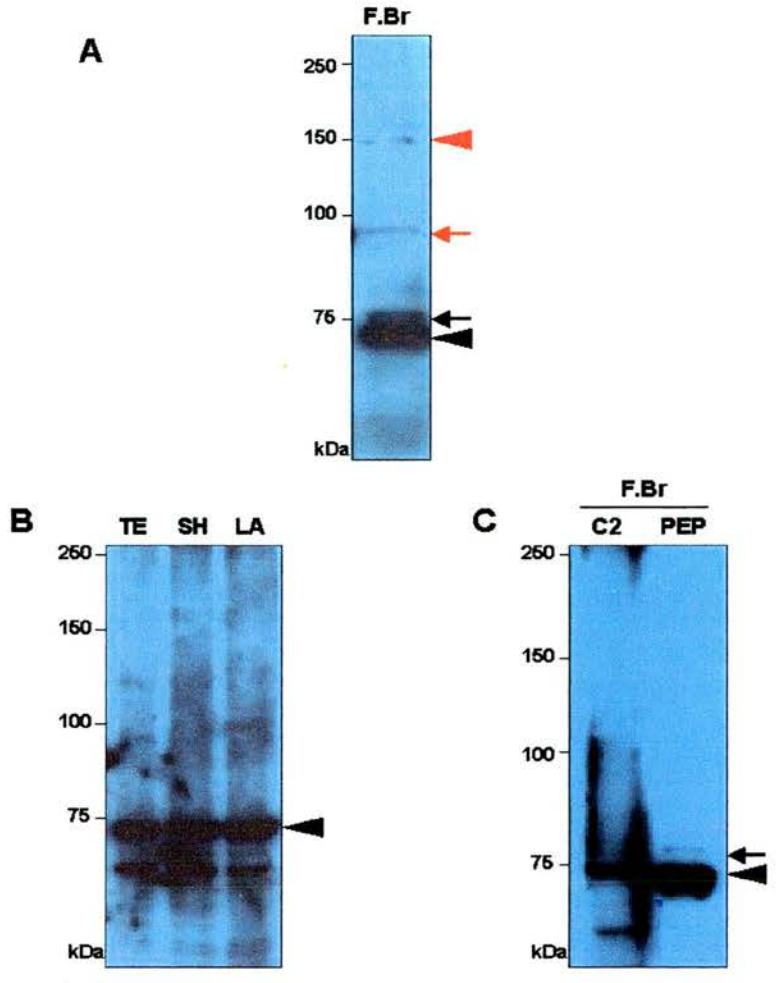

FIGURE 5.3: DISC1-related bands detected by additional DISC1 antibodies in human cell lines and foetal brain tissue

A: 30μg protein extract from foetal brain tissue was analysed on an 8% SDS-PAGE gel. The N-terminal DISC1 anti-protein antibody detects DISC1-related bands of 150kDa (red arrowhead), 95kDa (red arrow), 80kDa (black arrow) and 75kDa (black arrowhead).

B: 20μg protein extracts from TE671 (TE), SH-SY5Y (SH) and LAN-5 (LA) cell lines were analysed on an 8% SDS-PAGE gel. The C-terminal anti-DISC1-C2 antibody detects the 75kDa DISC1-related band (black arrowhead).

C: 20μg protein extract from foetal brain tissue (F.Br) was analysed on an 8% SDS-PAGE gel. Both the anti-DISC1-C2 (C2) and the DISC1 anti-peptide (PEP) antibody detect the 75kDa protein (black arrowhead). Only the anti-peptide antibody detects the 80kDa protein (black arrow).

5.2.3 Evidence of proteolytic degradation of DISC1 in protein extracts from transformed cell lines

Over the course of this project, additional bands detected by the DISC1 anti-peptide antibody were observed, despite preparing all lysates in the presence of protease inhibitors (sections 2.2.3.3 & 2.2.3.4). A band of approximately 110kDa is consistently detected in the lymphoblastoid cell lines and occasionally in other cell lines (Figure 5.1A). In addition, multiple bands below the 75kDa bands are commonly detected in a number of cell lines, but only a single additional band is seen in foetal brain tissue (Figures 5.1A). Multiple bands below the 95kDa band are detected rarely in the cell lines (data not shown) and bands of approximately 50kDa, 37kDa and 25kDa are occasionally detected in a number of cell lines and foetal brain tissue (Figure 5.1B). A number of observations were made regarding the appearance of these bands. The long-term storage of the samples is associated with the increased appearance of the bands, indicative of proteolytic degradation. The appearance of these bands is most frequently seen in the cell line extracts and only a single band below the 75kDa band was ever observed in the foetal brain sample despite prolonged storage of this sample: the same preparation of foetal brain was used throughout the project and had been stored for longer than the cell extracts. The appearance of multiple bands is also therefore related to either the lysis buffer used or another component in the preparation of the sample. In support of the first suggestion, storing the cell line extracts in sample buffer with DTT reduced the appearance of the multiple bands despite prolonged storage of the samples (data not shown). It was also observed that the intensity of the 80kDa band varied (Table 5.2), even with use of the same lysate (data not shown), and the presence of the additional multiple bands below the 75kDa bands is associated with a reduced intensity of this band, indicating these additional bands are breakdown products of the 80kDa protein (data not shown).

To summarise, five DISC1-related proteins are identified in human (Figure 5.4). Any additional bands detected represent proteolytic breakdown products of one or more of these proteins.

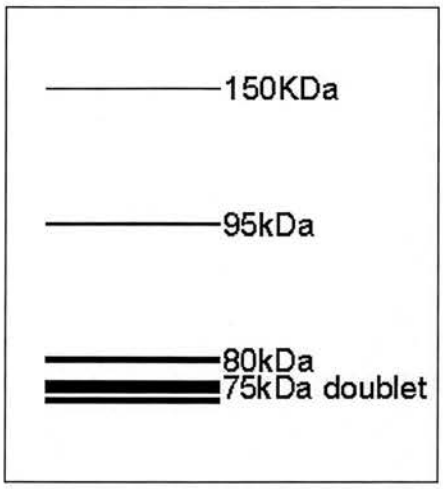

FIGURE 5.4: Five DISC1-related proteins are identified in human

A schematic of the DISC1 banding pattern in human. Five DISC1-related proteins are identified and although additional bands are detected (section 5.2.3), these are assumed to represent proteolytic breakdown products of one or more of these proteins.

5.3 Verification of the DISC1 protein isoforms identified in human

The immunoblot data suggests that both the L or Lv and S1 or S2 transcripts are translated into functional proteins. To aid in verification of the protein bands, RT-PCR was performed on the cell lines and human tissue samples using primers specific for each of the transcripts (Table 5.3; Figure 5.2). The primers were designed to span introns, with the exceptions of the L and S2 transcripts. cDNA clones were used to optimise the primers before testing on cell line and tissue cDNA.

TABLE 5.3: Primer location for RT-PCR verification of *DISC1* transcripts

TRANSCRIPT	LOCATION OF F PRIMER[1]	LOCATION OF R PRIMER[1]	cDNA CLONE (OBTAINED FROM)
L	exon 11	exon 11 spliced sequence	pBS.DISC1 / FH1 (in-house)
Lv	exon 11	exon 11 / 12	AB007926 (Kazuza DNA Research Institute)
S1	exon 9	alternative 3'UTR (exon 9a)	2320731r6 (Incyte)
S2	exon 9	alternative 3'UTR (intron 9)	FH1 (in-house)
Es[2]	alternative exon 1	exon 2	AK025293 (University of Tokyo)

[1] The sequences of the primers are given in Table 2.8.

[2] The exact composition of the Es transcript remains to be determined and in the present study the Es transcript was assumed to be comprised of an alternative exon 1 in conjunction with the alternative 3'UTR as suggested from the available cDNA clone EMBL: AK025293.

5.3.1 Cell lines

All the cell lines tested are found to express the L, Lv and S1 transcripts (Table 5.4). No evidence was found for the Es transcript in any of the cell lines (Table 5.4) and the presence of the S2 transcript was not tested in the cell lines as no evidence for its existence was found in tissue (section 5.3.2).

5.3.2 Tissue

The S1 transcript is detected in all tissues examined (Table 5.4), but no evidence was found for the existence of the S2 transcript in foetal brain, heart, liver or limb (Table 5.4). The Es transcript has a restricted pattern of expression and is detected in spleen only (Table 5.4).

TABLE 5.4: RT-PCR summary of the *DISC1* transcripts detected in cell lines and tissue

CELL LINE / TISSUE	L	Lv	S1	S2	Es
LAN-5	+	+	+	n.d.	–
SH-SY5Y	+	+	+	n.d	–
TE671	+	+	+	n.d	–
U373 MG	+	+	+	n.d	–
MOG-G-CCM	+	+	+	n.d	–
lymphoblast	+	+	+	n.d	–
H36CE2	+	+	+	n.d	–
brain	n.d	n.d	+	–	–
heart	n.d	n.d	+	–	–
liver	n.d	n.d	+	–	–
limb	n.d	n.d	+	–	–
spleen	n.d	n.d	+	–	+

n.d. not determined + positive RT-PCR – negative RT-PCR

A positive RT-PCR result was recorded if a product of the expected size was seen in both the +RT reaction and positive control, with no product observed in the negative controls. A negative RT-PCR result was recorded if a product of the expected size was seen in the positive control only. DISC1 cDNA clones (Table 5.3) were used as positive controls. To ensure the quality of the cDNA GAPDH RT-PCRs were performed.

5.4 Discussion

The DISC1 protein expression pattern in human suggests more than one potential isoform of DISC1 exists and the ubiquitous expression of three of the alternative *DISC1* transcripts in both cell lines and foetal tissue corroborates this. The 95kDa band is recognised by all three DISC1 antibodies, though the antibodies showed different affinities for the protein (Table 5.2). This band must represent the full-length DISC1 protein, however it is not clear if it is the L or Lv isoform as both transcripts are detected in all cell lines tested by RT-PCR (Table 5.4). The L and Lv isoforms are predicted to be 94kDa or 91kDa respectively (Figure 5.2), therefore the 95kDa band is more consistent in size with the L isoform though the predicted 3kDa difference between the two isoforms should be visible by immunoblotting. As the L isoform is not detected strongly by any of the antibodies (possibly reflecting the cellular concentration of the protein), it is reasonable to assume that if the Lv isoform

is present in reduced amounts it would not be visible unless increasing concentrations of protein are used. Alternatively the Lv isoform may have a short half-life or be particularly prone to proteolytic degradation. In support of the latter possibility, considerable degradation of the cell line extracts was observed (section 5.2.3). The development of isoform specific antibodies able to recognise either the L or Lv isoform will be useful in determining the exact identity of this protein, but for the subsequent data presented in this thesis this band will be referred to as the L isoform.

Of the major DISC1-related bands, the 75kDa band is most strongly detected by all three of the DISC1 antibodies and the affinity of the antibodies for this band is comparable (Tables 5.1 & 5.2). In contrast the 80kDa band is consistently detected by the anti-peptide antibody in all cell lines as well as in foetal brain, but is only weakly detected in foetal brain by the anti-protein antibody and not detected at all by the C-terminal antibody (Tables 5.1 & 5.2). Evidence that this band is undoubtedly DISC1-related was provided following comparison of lymphoblastoid cell lines derived from t(1;11) family members (chapter 6). The level of the 80kDa band is significantly reduced in cell lines derived from individuals with the translocation and is strong evidence that this band is DISC1-related. Several possibilities as to the identity of these proteins are feasible. Firstly, both of these bands are consistent in size with the 74kDa protein predicted to arise from translation of the S1 transcript. Secondly, these proteins may represent DISC1 protein translated from a downstream start site. The first ATG start codon of *DISC1* occurs in a weak context, CNNatgC, with the third ATG start codon in a stronger context, GNNatgG (Kozak, 1996). The translation of a protein from the third ATG start codon would result in a full-length DISC1 protein of either 76 or 78kDa depending on the isoform and is consistent with the sizes of the bands detected. Nonetheless a third explanation for these proteins is provided with recent evidence that DISC1 is a mitochondrial protein (section 8.4.3.3). Nuclearly encoded precursor proteins are translocated into mitochondria via specific mitochondrial targeting sequences. Cleavage of the precursor protein occurs in the mitochondrial matrix, and gives rise to the mature mitochondrial protein (Hartl and Neupert, 1990; Pfanner and Meijer, 1995). Thus it is probable that

the 95kDa DISC1 protein is the precursor protein with the 80kDa and 75kDa proteins representing the mature DISC1 proteins produced from the two protein isoforms, L and Lv. Further support for this notion is provided by the approximate size difference between these two proteins, which is consistent with the predicted 3kDa size difference between the two full-length protein isoforms. The use of nonactin, an ammonium ionophore which prevents the translocation of proteins into mitochondria (Mizzen *et al.*, 1989; Soltys and Gupta, 1996; Varma *et al.*, 1987), would enable this hypothesis to be tested. Throughout the rest of this thesis, these bands will be referred to as the 75kDa and 80kDa proteins.

In addition to the three major DISC1-related proteins, a 150kDa protein was often detected by both of the N-terminal antibodies, as well as the anti-DISC1-C2 antibody (A.Sawa, personal communication). A protein of this size was not predicted from any of the known *DISC1* transcripts yet the presence of intergenic transcripts between *DISC1* and the upstream *TRAX* gene were known to exist (section 1.6.3.2). A transcript extending from *TRAX* exon 2 through to *DISC1* exon 13 had been detected and if functional would generate a protein of 106kDa. To determine if the 150kDa protein was evidence of an intergenic protein, TRAX antibodies were tested on SH-SY5Y cell line extracts, but no proteins in addition to the 37kDa TRAX protein were detected (data not shown). Thus the most probable explanation for this large protein is that it represents a complex of DISC1 either with itself or another protein. Indeed it is known that DISC1 can homodimerize (K.Millar, personal communication; Ozeki *et al.*, 2002), therefore the complex may represent dimerization of the 75kDa or 80kDa proteins. Confirmation of this band as a DISC1 complex could be easily tested using denaturing and crosslinking reagents which would decrease or increase the appearance of this band respectively (Bradford *et al.*, 2001; Nadeau and Carlson, 2002).

The cell line protein extracts appeared to be susceptible to considerable proteolytic degradation (section 5.2.3). The storage of these lysates in sample buffer appears to be one way to avoid this. Due to this suspected degradation, it is not clear if the doublet at 75kDa (Figure 5.1) detected by the anti-peptide antibody represents a

potentially modified form of DISC1 or a breakdown product. The banding pattern is consistent with that commonly observed following phosphorylation (Sasaki *et al.*, 2000), and as this band was also detected in the foetal brain extract, which did not show the same level of degradation as the cell line extracts, it is possible that this band is a phosphorylated (or other modified) form of the 75kDa protein. The lack of detection of this band, and the putative breakdown products, by the other DISC1 antibodies may reflect the reduced affinity of these antibodies for the DISC1 protein. As described earlier (paragraph 3, section 4.9), the use of the anti-protein antibody on the cell lines was known to be limited and similarly the anti-DISC1-C2 antibody did not detect either the 80kDa or 95kDa bands (Table 5.1). Therefore the lack of corroboration from these antibodies may be due to the affinity of the antibody rather than evidence of a non-specific interaction, especially as all bands detected by the anti-peptide antibody are reduced in lymphoblastoid cell lines derived from translocation carriers (chapter 6).

The S2 transcript was not detected in any of the foetal tissues examined (Table 5.4). In addition to the lack of RT-PCR data, the current support for this transcript is poor, as the single EST (GenBank: HS833289) representing the transcript has been withdrawn. Therefore this putative transcript is unlikely to be real.

Utilization of the alternative exon 1 in spleen only (Table 5.4) implies the use of this exon is tissue-specific. Examination of adult tissue would ascertain if the use of this exon is also developmentally regulated. Furthermore the alternative exon 1 was not detected in any of the cell lines examined (Table 5.4), providing more evidence that the use of this exon is restricted. The presence of both tissue and cell lines that do not express the alternative exon 1 will be useful if a transcript utilizing this exon is identified.

Detection of the alternative exon 1 was used to determine the presence of the Es transcript, as the cDNA clone (GenBank: AK025293) containing this sequence indicates this exon occurs in conjunction with the alternative 3'UTR of the Es transcript. However this remains to be determined and additional RT-PCR will

ascertain if the alternative exon 1 and 3'UTR of the Es transcript are spliced into the same transcript. This would not rule out the possibility that the alternative exon 1 is also spliced into either of the longer transcripts in a tissue or developmentally restricted pattern. If the alternative exon 1 is indicative of the Es transcript, it would be interesting to examine the protein expression pattern of DISC1 in foetal spleen. The Es transcript is predicted to generate a protein of 39kDa, but no evidence for a protein of this size is seen in foetal brain or the cell lines examined (Figure 5.1B; but also U373 MG, data not shown). The appearance of the 37kDa protein in the foetal brain sample is indicative of proteolytic degradation (section 5.2.3). Thus if functional the Es transcript shows a restricted pattern of expression.

The protein expression pattern of DISC1 in humans is complex and the data generated in the present study is not able to conclusively determine the identity of all the bands detected. The most informative DISC1 antibody, the N-terminal anti-peptide antibody, was predicted (section 3.1.2) to detect all of the DISC1 protein isoforms, therefore the use of isoform specific antibodies or isoform negative cell lines and tissue will be one way of addressing the identity of the proteins. Furthermore it is unlikely that a protein as large as DISC1 is not subjected to post-translational modification and functional studies examining the potential modification of the DISC1 protein may provide further clues to the identity of the bands detected.

CHAPTER 6

DISC1 PROTEIN EXPRESSION LEVELS IN LYMPHOBLASTOID CELL LINES DERIVED FROM t(1;11) FAMILY MEMBERS

6. DISC1 protein expression levels in lymphoblastoid cell lines derived from t(1;11) family members

6.1 Introduction

Lymphoblastoid cell lines derived from the members of the t(1;11) family (section 1.6.1) were analysed to determine if a truncated DISC1 protein is produced from the translocated chromosome 1, and also to determine the effect of the translocation on the protein expression levels of DISC1.

6.1.1 Lymphoblastoid cell lines from members of the t(1;11) family

In the absence of any other tissue, lymphoblastoid cell lines derived from members of the t(1;11) family provide a valuable resource for determining the exact effect of the translocation on DISC1 expression, although it is not known if expression of DISC1 in lymphoblastoid cells reflects DISC1 expression within the brain. The cell lines were generated from members of the t(1;11) family (Fletcher *et al.*, 1993) and two cell lines from affected family members (translocation carriers with schizophrenia) and one cell line from a control family member (non-translocation carrier with no psychiatric diagnosis) were available.

6.1.2 Dominant-negative or haploinsufficiency?

The aim of this chapter was to determine the effect of the translocation on DISC1. It is assumed that the non-translocated DISC1 locus is functioning as normal but the effect of the translocation on the disrupted DISC1 locus may have many possible effects, of which the two most likely mechanisms are considered here. Firstly a truncated protein may be produced from the disrupted DISC1 locus which has the potential to exert a dominant-negative effect on the normal DISC1 protein, resulting in loss of DISC1 function. In addition, the truncated protein may have an abnormal function of its own. Secondly, haploinsufficiency may occur, whereby the intact

DISC1 locus does not produce enough protein for normal functioning of DISC1. In both models the prediction would be that the levels of normal DISC1 protein are reduced in translocation carriers compared to those without the translocation. The distinction between the two mechanisms will be the presence or absence of a truncated DISC1 protein.

6.2 No truncated DISC1 protein was found in translocation carriers

The truncated DISC1 protein produced from the translocation is predicted to be 64.5kDa. No evidence for a truncated protein is seen in either of the cell lines derived from the translocation carriers (Figure 6.1; data shown for one cell line only). In addition there is no evidence for any protein(s) of less than 65kDa which implies the lack of a truncated protein is not due to proteolytic degradation. GAPDH was used to ensure equivalent amounts of protein were analysed.

6.3 DISC1 protein expression levels are reduced in translocation carriers

In both of the cell lines derived from translocation carriers, there was a significant reduction in the levels of all DISC1-related proteins (Figure 6.2; data shown for one cell line only). Of note, the potentially peptide specific proteins of 80kDa and the lower 75kDa doublet (Table 5.2), as well as the putative 110kDa breakdown product (section 5.2.3) are all reduced, providing strong evidence that these bands are DISC1-related. An approximate estimate would be that the levels of DISC1 protein in the affected individuals are reduced two to three fold relative to the control. α-tubulin was used to ensure equivalent amounts of protein were analysed. The reduction in expression levels of all DISC1-related proteins was obtained consistently and with independent preparations of lymphoblastoid cell extracts.

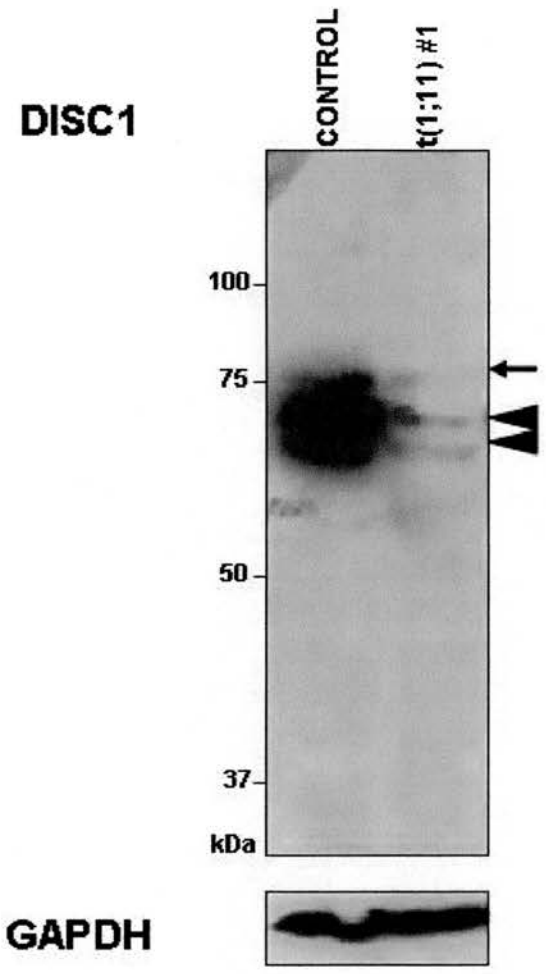

FIGURE 6.1: No evidence for a DISC1 truncated protein in lymphoblastoid cell lines derived from translocation carriers

30μg of protein was loaded per lane on a 10% SDS-PAGE gel. The anti-peptide antibody (upper) was used to detect DISC1. The DISC1-related bands detected are the 75kDa protein, present as a doublet (arrowheads), and the 80kDa protein (arrow). The blot was stripped and re-probed using GAPDH (lower).

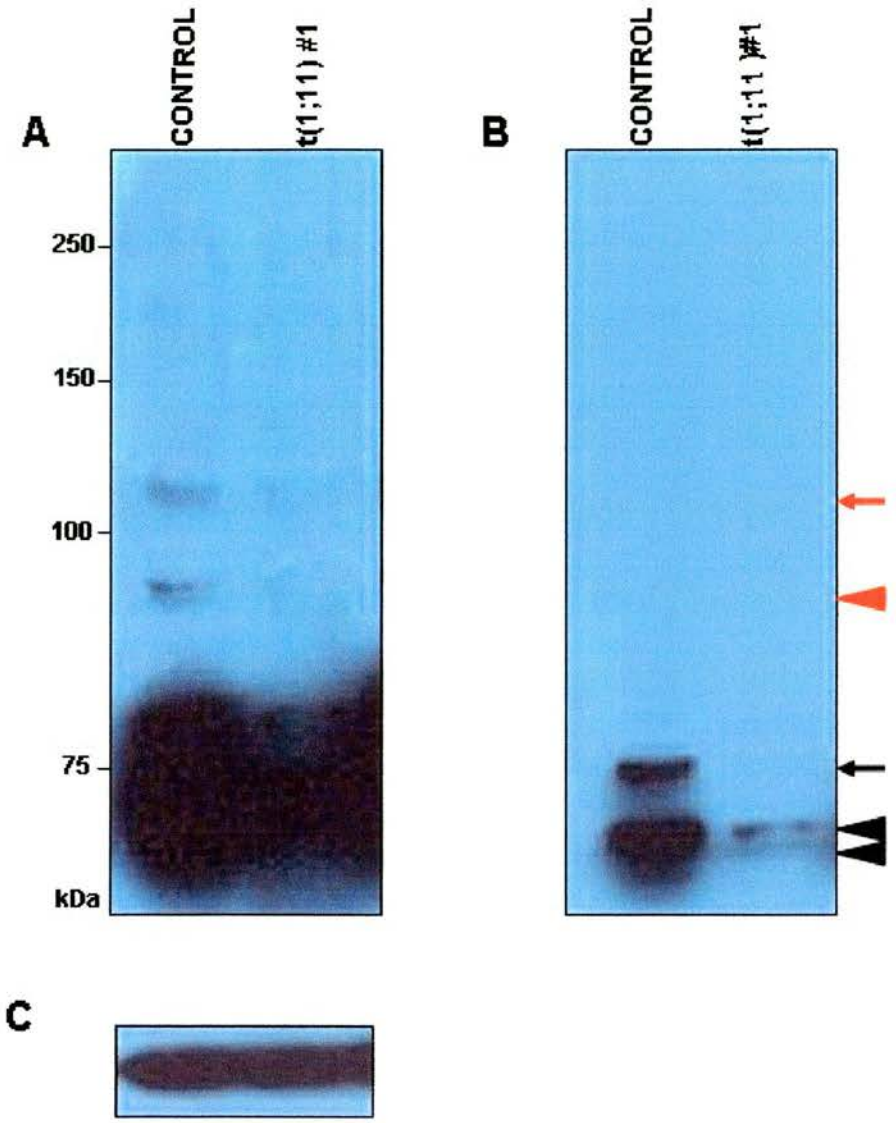

FIGURE 6.2: Expression levels of all DISC1-related bands are reduced in lymphoblastoid cell lines derived from translocation carriers

30μg of protein was loaded per lane on an 8% SDS-PAGE gel. The DISC1 anti-peptide antibody was used to detect DISC1 (A & B). The two images represent longer (A) and shorter (B) exposures of the same blot. The DISC1-related bands detected are the L isoform (red arrowhead), 75kDa protein, present as a doublet (black arrowheads), the 80kDa protein (black arrow) and the 110kDa putative breakdown product (red arrow). The blot was stripped and re-probed using α-tubulin (B).

6.4 Discussion

In the absence of a truncated DISC1 protein (Figure 6.1), the reduction in the levels of DISC1 is consistent with a haploinsufficiency model. All DISC1-related bands are reduced (Figure 6.2) including the potentially peptide specific proteins, providing support to the notion that these are DISC1-related proteins. Indeed examination of TRAX, a protein in close proximity to the translocation breakpoint (section 1.6.3.2), did not reveal any alteration in the protein levels between affected and control family members (K.Millar, personal communication), suggesting that only DISC1-related proteins are affected by the translocation.

The present data does not allow an accurate estimate of the reduction in the levels of the individual DISC1-related proteins and the use of densitometry would be useful in this regard. It remains to be determined if any of the DISC1 proteins are preferentially affected by the translocation. In the absence of isoform specific antibodies, the specificity afforded by quantitative RT-PCR methods such as the LightCycler™ or the TaqMan® assay (Freeman *et al.*, 1999; Bustin, 2000), would allow examination of the individual *DISC1* transcripts. Nonetheless, the data does indicate a >50% reduction in DISC1 expression in translocation carriers relative to controls. If as hypothesised (section 1.6.3.1), *DISC2* is involved in regulation of *DISC1*, it is possible that loss of *DISC2* from the disrupted locus leads to reduced *DISC1* expression from the normal locus.

Recent studies (Hayes *et al.*, 2002; Ozeki *et al.*, 2003) have focussed on the production of a mutant DISC1 protein as the disease causing mechanism. Though it is impossible to rule out the production of a truncated DISC1 protein within the brain, no evidence for a truncated DISC1 protein is found in translocation carriers and instead the disease causing mechanism is likely to be related to the reduction in DISC1 protein and haploinsufficiency. Recapitulating the effect of reduced DISC1 protein in cell lines or transgenic mice will enable the effect of the translocation on DISC1 to be examined.

CHAPTER 7

DISC1-RELATED PROTEINS IN MOUSE AND RAT

7. DISC1-related proteins in mouse and rat

7.1 Introduction

As described earlier (section 3.2.1), the DISC1 anti-peptide antibody was designed to be human-specific, whereas the anti-protein antibody was generated to the first 292 amino acids of the N-terminus, thereby increasing the chances of producing an antibody which will cross-react with DISC1 in other species. At the time the experiments for this chapter were performed, nothing was known about DISC1 protein expression in mouse or rat. Consequently the anti-protein antibody was used to examine the DISC1 expression pattern in mouse and rat, to determine if the multiple protein isoforms identified in human were also present in mouse and rat. The data presented in this chapter represents the first investigations into mouse and rat DISC1 by our group, and the data is discussed as such. However while writing my thesis, papers describing DISC1 in rodent were published by other groups (Ma *et al.*, 2002; Ozeki *et al.*, 2003).

7.2 DISC1 in mouse and rat

Recent data demonstrated the presence of two putative DISC1 protein isoforms in rat tissue (Ozeki *et al.*, 2003). In addition Northern blot analysis of mouse and rat tissue identified two transcripts (Ma *et al.*, 2002), and data generated within the group (Taylor *et al.*, 2003), suggested the involvement of three alternative *DISC1* transcripts in mouse. Therefore as in human, the *DISC1* gene in mouse and rat is alternatively spliced (Figure 7.1), though it is unclear at present exactly which transcripts are functional. To date the L, SV and Es transcripts have been identified in mouse (Ma *et al.*, 2002; Ozeki *et al.*, 2003; Taylor *et al.*, 2003), whilst in rat only the Lv transcript has been identified (Ozeki *et al.*, 2003). Nevertheless due to the high amino acid sequence conservation between mouse and rat DISC1 (Ozeki *et al.*, 2003), it is likely that all four transcripts are present in both species.

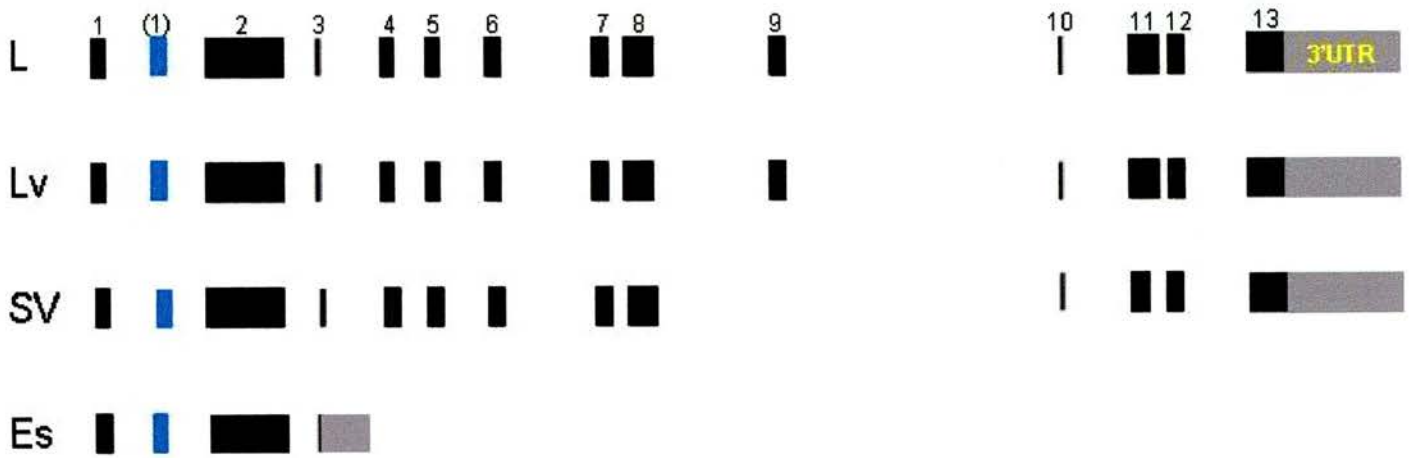

FIGURE 7.1: Alternative *DISC1* transcripts in mouse and rat

Black and grey boxes represent exons and the 3'UTR of each transcript, respectively. The alternative exon 1 is indicated by a blue box, although it is not known which transcript(s) this exon is spliced into. The L (long), Lv (long variant) and Es (extremely short) transcripts are orthologues of the human transcripts, while the SV (splice variant) transcript has no known human orthologue.

7.3 The DISC1 protein expression pattern in mouse and rat tissue does not confirm the presence of DISC1 splice variants

The tissues analysed are outlined in Table 7.1. Rat brain tissue was obtained from David Brown (Molecular Endocrinology Section, MMC) and multiple mouse tissues were obtained from Richard Moore (Medical Genetics Section).

TABLE 7.1: Mouse and rat tissue analysed for DISC1 expression

TISSUE	**MOUSE STRAIN**	**STAGE**
whole embryo	CD-1	embryo (14.5d)
whole embryo	CD-1	embryo (18.5d)
whole brain	CD-1	adult (8-12w)
kidney	pool	adult (8-12w)
spleen	CD-1	adult (8-12w)
heart	not recorded	adult (8-12w)
liver	not recorded	adult (8-12w)
TISSUE	**RAT STRAIN**	**STAGE**
whole brain	Wistar	embryo (18.5d)
cortex	Wistar	adult
cerebellum	Wistar	adult

In both mouse and rat, the anti-protein antibody revealed a restricted pattern of DISC1 expression (Figure 7.2A & B). A DISC1 band of approximately 95kDa is detected in mouse brain and the two brain regions from rat. The band detected in rat is 1 – 2 kDa smaller than the band detected in mouse, but both bands are consistent in size with the putative L isoform in human. Furthermore a DISC1 band of approximately 120kDa is detected in mouse heart only, while a 150kDa band, similar in size to the band observed in human, is detected in rat cortex and cerebellum as well as mouse heart and brain. In all tissues, except rat embryonic brain, additional bands are detected (black arrowheads in Figure 7.2A & B). However titration of the secondary antibody abolishes the appearance of these bands (data not shown), therefore they are likely to represent non-specific background bands. No convincing DISC1 bands are detected in any of the embryonic stages examined (lanes 1, 4 & 6;

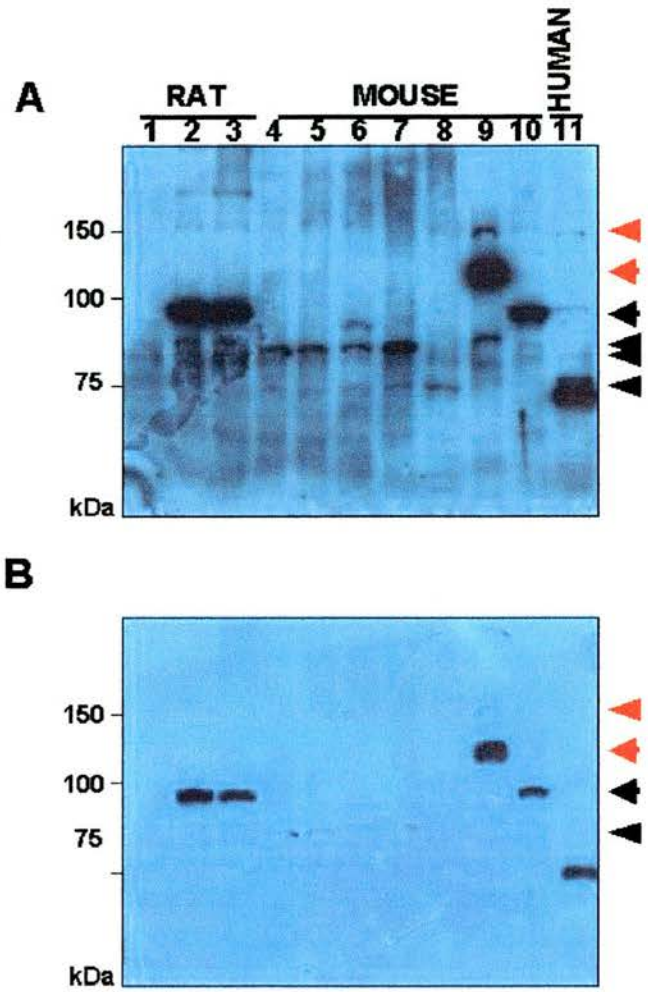

FIGURE 7.2: DISC1 protein in expression in multiple mouse tissues and rat brain

A & B: 30μg protein was loaded per lane on an 8% SDS-PAGE gel and the DISC1 anti-protein antibody was used to detect DISC1. The tissues analysed are: rat embryonic brain (1), adult cortex (2) & cerebellum (3), mouse whole embryo 14.5d (4), 18.5d (5), adult kidney (6), spleen (7), liver (8), heart (9) & brain (10). Human foetal brain tissue (11) was used as positive control. The images in A & B represent a longer exposure (A) & shorter (B) exposure of the same blot. The DISC1-related bands detected in mouse & rat are 95kDa (black arrow), 120kDa (red arrow) & 150kDa (red arrowhead) in size. A number of additional bands (black arrowheads) were also detected at this concentration of secondary antibody.

Figure 7.2A & B). Neither the pre-immune serum nor the secondary antibody detects any of the DISC1-related bands (data not shown).

The expected size of the protein generated from the Es transcript is 41.1kDa. No evidence for the presence of a DISC1-related protein of this size is detected (Figure 7.3). In addition no suspected breakdown products are observed and as for the human tissue protein extract, none of the rodent tissue extracts appear susceptible to the considerable proteolytic degradation observed in the cell line extracts (section 5.2.3).

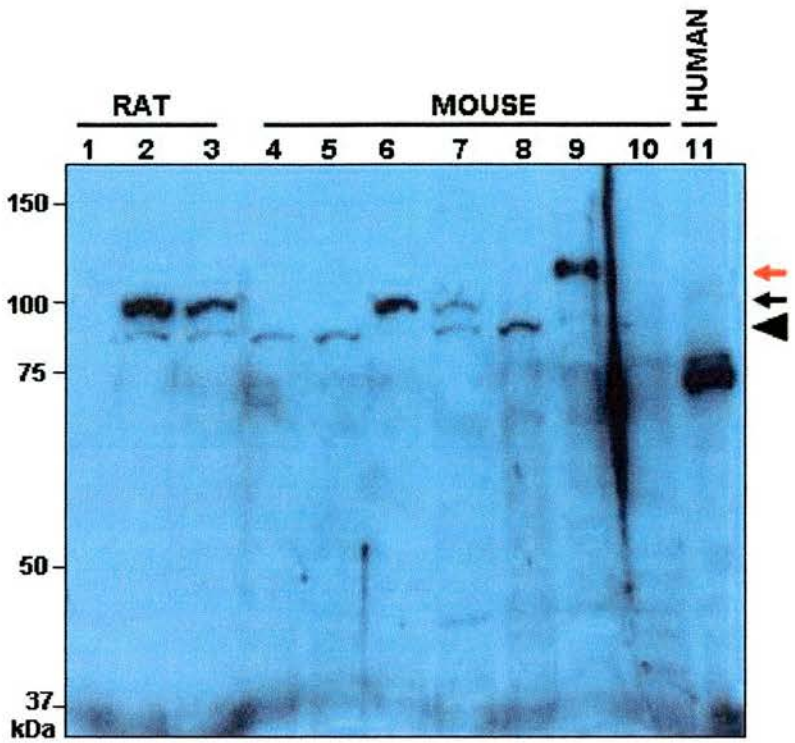

FIGURE 7.3: No evidence for a small DISC1 protein in multiple mouse tissues or rat brain

20µg protein was loaded per lane on a 10% SDS-PAGE gel and the DISC1 anti-protein antibody was used to detect DISC1. The tissues analysed are: rat embryonic brain (1), adult cortex (2) & cerebellum (3), mouse whole embryo 14.5d (4), 18.5d (5), adult brain (6), kidney (7), spleen (8), heart (9) & liver (10). Human foetal brain tissue (11) was used as positive control. The 95kDa (black arrow) & 120kDa (red arrow) DISC1-related mouse and rat bands are detected, as is the potentially non-specific band at 85kDa (black arrowhead).

7.4 Discussion

In contrast to the ubiquitous expression pattern of DISC1 in human cell lines, the results obtained with the DISC1 anti-protein antibody, indicate that in mouse tissue, DISC1 shows a restricted pattern of expression in both tissue specificity and developmental stage (Figure 7.2A & B). DISC1 is present in adult brain and heart only and the DISC1-related bands detected in the two tissues are not the same. The DISC1 band in brain is consistent in size with translation of the full-length splice variants, whilst the identity of the band detected in heart is unknown but could represent a post-translational modification of DISC1. The tissue specificity of DISC1 in rat was not determined due to the limited number of tissues available. Nevertheless, the data demonstrate that as in mouse, DISC1 exists as a single isoform in adult rat brain and is not detected in embryonic (E18.5) brain (Figure 7.2A & B). The examination of additional rat tissues will be needed to ascertain if the limited tissue expression and identification of a potentially novel DISC1 protein in mouse is also observed in rat. It was noted that the approximately 95kDa band detected in mouse and rat is not the same size. Prediction of the molecular weight of the mouse L and rat Lv DISC1 isoforms (GenBank: AY177673 & AY177674; section 7.2), is 92.6kDa and 90.4kDa respectively, consistent with the 1 – 2kDa size difference observed.

The data from the DISC1 anti-protein antibody indicates that the 75kDa and 80kDa proteins are human specific proteins. Nevertheless, the recent paper from the Sawa lab suggest otherwise, and in adult rat brain, heart, liver, kidney and thymus, two DISC1 bands of 75kDa and 100kDa were detected (Ozeki *et al.*, 2003), arguing against the restricted expression pattern of DISC1 in rodent. There are two possible explanations for this discrepancy. Firstly, as the two tested antibodies are raised against different termini of the DISC1 protein, it is possible that the 75kDa band could represent a transcript which does not utilize the known N-terminus. The *DISC1* transcript data at present is incomplete, and an alternative exon 1 has already been identified in mouse (K.Millar, personal communication; Ozeki *et al.*, 2003), as well as evidence for exon skipping (Ma *et al.*, 2002). The second possibility is the

75kDa protein does not contain any of the conserved epitopes between human and mouse or rat. The level of sequence homology between human and rat or mouse DISC1 is low, particularly within the N-terminus (Figure 7.4). If as suggested earlier (paragraph 2, section 5.4), the 75kDa protein represents a mitochondrially cleaved form of DISC1, the conserved epitopes between human and mouse or rat may have been removed, preventing detection of this protein by the human DISC1 anti-protein antibodies. Despite this anomaly, the current data does support the notion that there are human specific DISC1 proteins. Only a single protein of approximately 75kDa is detected in mouse and rat compared to three proteins between 75 – 80kDa in human. The use of cell lines or tissue derived from other species, and in particular primates would be useful to determine if these are indeed human specific DISC1 proteins.

The transcript data from adult mouse (Ma *et al.*, 2002) suggested *DISC1* is expressed in adult mouse heart, brain, kidney and testis. Two transcripts of 7.0 and 4.4kb are identified in heart, while only a 7.0kb transcript is found in brain and a 4.4kb transcript in kidney and testis. This study also reported the identification of a splice variant which skipped exon 9. The predicted size of this alternative isoform is 85kDa, which makes detection of one of the additional bands (middle black arrowhead in Figure 7.2A & B) in all of the mouse tissues except brain and liver intriguing, as this band is of the correct approximate size for this isoform. The identification of this band, and the other additional bands, as DISC1-related was excluded due to the disappearance of the bands following titration of the secondary antibody. Nonetheless the possibility that this band represents this alternative transcript cannot be ruled out until further mouse and rat specific antibodies have been developed. Alternatively pre-absorption of the anti-protein antibodies with recombinant DISC1 protein would determine if this band is DISC1-related or a non-specific interaction due to the secondary antibody.

The lack of a smaller protein (Figure 7.3) representing the Es isoform suggests that at least in the tissues examined it does not exist. The lack of an Es isoform in mouse is interesting, as initially this was the only *DISC1* transcript detected in mouse

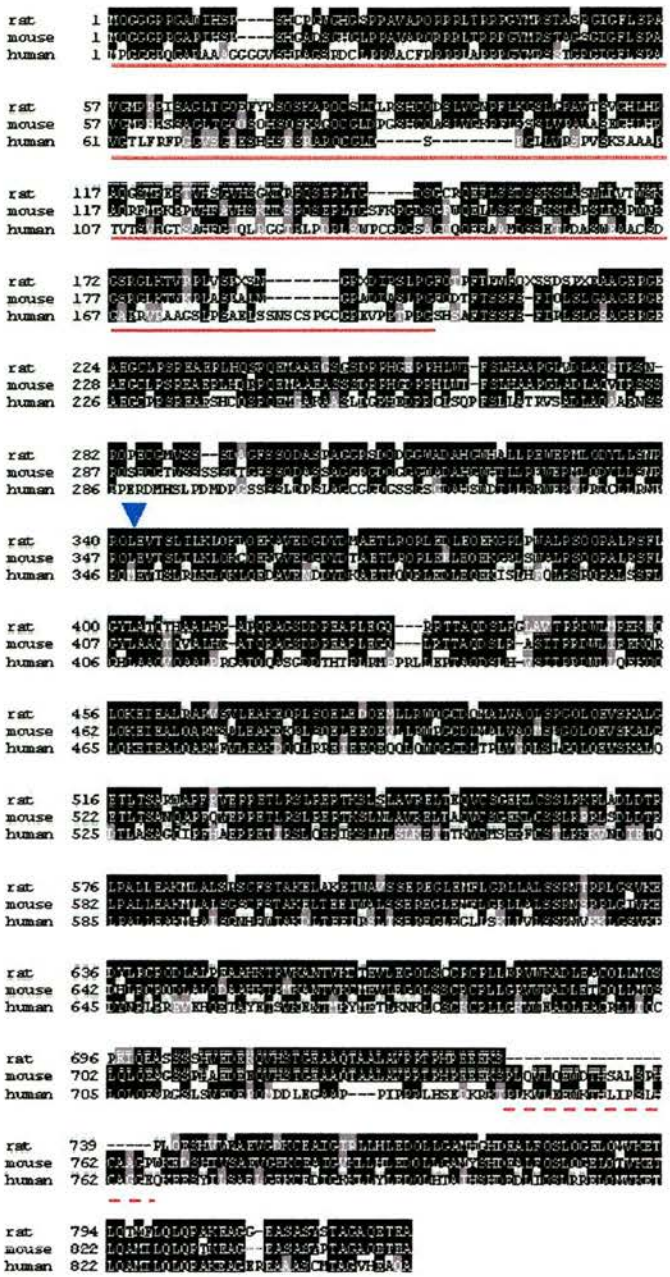

FIGURE 7.4: Sequence alignment of human, mouse and rat DISC1 protein

The human L (Genbank: AF222980), mouse L (Genbank: AY177673) and rat Lv (GenBank: AY177674) DISC1 amino acid sequences were aligned using ClustalW. BOXSHADE was used for a graphical output of the alignment. Residues conserved between all three species are highlighted in black, while similar residues are highlighted in grey. The boundary between the N- and C-termini is marked with a blue arrow. The region of the human DISC1 protein used for generation of the anti-protein antibodies is indicated with a solid red line. The alternatively spliced residues of the L and Lv isoforms are underlined with a dashed red line.

(M.Taylor, personal communication). If functional the Es isoform is highly restricted in either its developmental pattern of expression or tissue specificity, possibly even representing a cell-type specific isoform.

The 150kDa putative DISC1 complex identified in human was also detected in mouse and rat (Figure 7.2A & B). It was previously suggested (paragraph 4, section 5.4) that this protein represents a complex of DISC1 either with itself or another protein. If the complex represents an interaction between DISC1 and an unidentified protein, the similar size of the complex across all three species would imply this was an evolutionarily conserved interaction.

The expression pattern of DISC1 in mouse and rat shows similarities to that seen in human. However discrepancies between the N-terminal human DISC1 and the C-terminal rat DISC1 antibodies exist. The reason for this is not clear at present. Nonetheless, at least two proteins identified appear to show species specificity. The 120kDa protein identified in mouse heart was not seen in the human protein extracts examined. The analysis of human heart tissue or an appropriate cell line will ascertain if this is a species specific or tissue specific protein. Furthermore the 80kDa protein ubiquitously expressed in human is not found in either mouse or rat. Elucidation of the identity of this protein will determine if this is a human specific protein. Knowledge of the DISC1 expression pattern in non-human species is vital for the investigation of DISC1 function in mouse or rat model systems.

CHAPTER 8

SUBCELLULAR LOCALISATION OF DISC1

8. Subcellular localisation of DISC1

8.1 Introduction

The cellular compartment a protein operates within enables inferences to be made about its function within the cell. For this reason the subcellular localisation of DISC1 was studied in a number of transformed human cell lines and the relationship of DISC1 to specific cellular compartments was determined. In addition further investigation of the relationship of DISC1 to the cytoskeleton was examined using drugs that disrupt specific cytoskeletal proteins.

8.2 Morphology and chromosome 1q content of the neuroblastoma and glioblastoma cell lines

All human cell lines tested were found to express the *DISC1* transcript (section 4.7.1). Furthermore, the number of DISC1 protein isoforms detected within the cell lines did not vary (Table 5.1), and the relative expression levels of the isoforms also remained constant (section 5.2.1). To determine the subcellular localisation pattern of DISC1, neuroblastoma (SH-SY5Y and LAN-5) and glioblastoma (U373 MG) cell lines were studied predominantly as it was anticipated that these cell lines were most likely to be representative of the cells in the nervous system. Most of the subsequent data has been presented using the SH-SY5Y and U373 MG cell lines only.

8.2.1 Morphology

The LAN-5 and U373 MG cell lines contain a single population of cells which are either neuroblast or epithelial in morphology respectively. Conversely, the SH-SY5Y cell line contains at least two cell types which are described as being either N (neuroblastic) or S (substrate-adherent) cells (Encinas *et al.*, 2000). The N and S cells are readily distinguishable from one another by their morphology: N cells are neuroblast-like whereas S cells are epithelial in appearance (Ross *et al.*, 1983; Ciccarone *et al.*, 1989).

8.2.2 Chromosome 1q content

It was reported in the ATCC database that the SH-SY5Y cell line contains a trisomy of the chromosome 1q region. As this is the region of chromosome 1 where the *DISC1* gene is located (section 1.6), FISH analysis using a chromosome 1q paint and also a BAC from within the *DISC1* region was performed on both the original SH-SY5Y cell line obtained from Organon Laboratories NV and the cell line obtained latterly from the ECACC (performed and data provided by Jude Fantes & Pat Malloy, Medical Genetics Section). The SH-SY5Y cell line was found to have a duplication of the 1q region, including the *DISC1* locus, on one of the chromosomes (Figure 8.1A). To determine if a cell line could be found that did not contain an abnormal chromosome 1q content, additional cell lines were karyotyped (performed and data provided by Jude Fantes), namely the LAN-5, U373 MG and TE671 cell lines (Figure 8.1B-D). This revealed that the LAN-5 neuroblastoma cell line also contained the same duplicated chromosome 1 as the SH-SY5Y cell line. Furthermore, both the U373 MG and TE671 cell lines were found to contain at least three copies of the 1q region including the *DISC1* locus.

It was decided that the likelihood of finding a transformed cell line with a normal karyotype was minimal and as previously reported (section 5.2.1), the DISC1 protein expression levels from different cell lines appeared to be fairly comparable and therefore unaffected by the chromosome 1q karyotype.

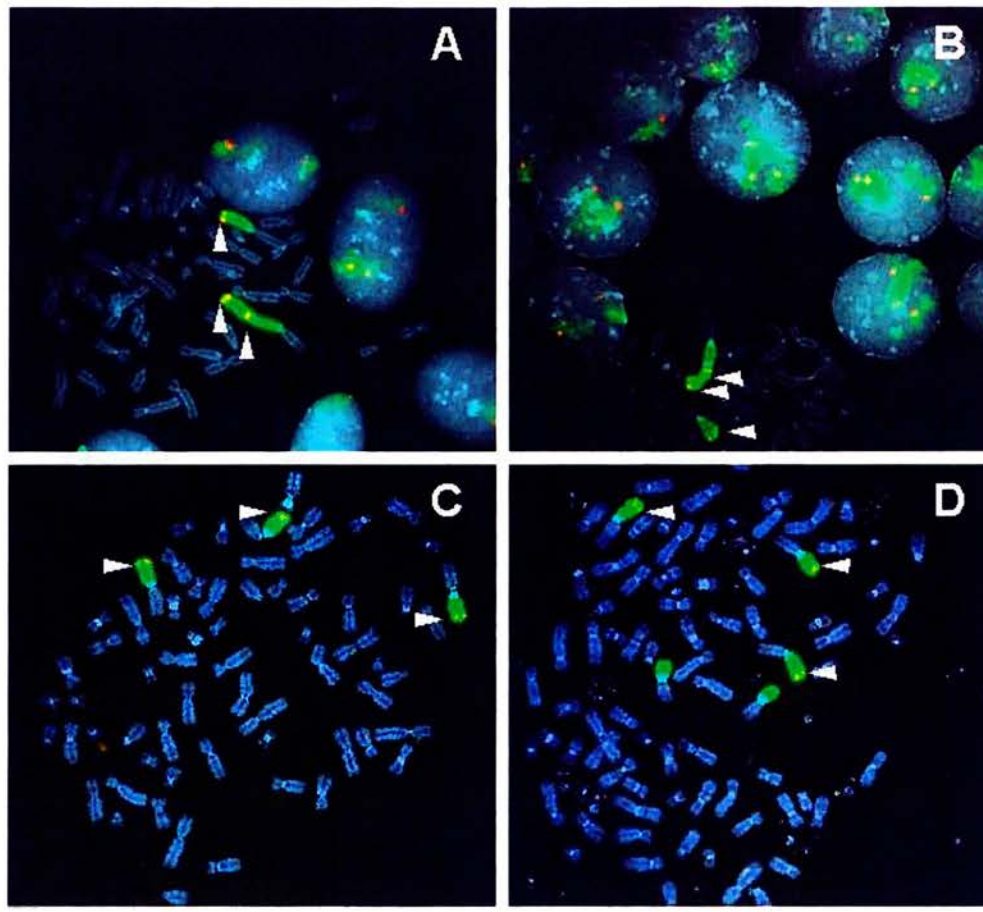

FIGURE 8.1: FISH analysis of chromosome 1q in four human transformed cell lines

The chromosome 1q karyotype of four human cell lines was determined using a chromosome 1q paint (green) and a BAC (135H6) from within the *DISC1* locus (red). The positions of the hybridised BAC are indicated in each cell type (arrowhead). The chromosomes are stained with DAPI (blue). In C & D only a metaphase spread is shown whilst in A & B interphase nuclei can also be seen.

The cell lines examined were: SH-SY5Y (A), LAN-5 (B), U373 MG (C) & TE671 (D).

8.3 The subcellular localisation of DISC1 within human cell lines

The *in-silico* data (section 1.7.2) did not reveal any strong indications as to the predicted cellular compartment that DISC1 would occupy. A putative nuclear localisation signal had been identified within the N-terminus of the protein, but it was not known if this was a functionally significant motif *in-vivo*.

In all the cell lines examined, DISC1 extends from a peri-nuclear location into the cytoplasm of the cells (Figure 8.2). DISC1 is organised within the cell in a potentially cytoskeletal associated pattern. The peri-nuclear structure of DISC1 is more evident in the neuroblastoma cell lines than in the glioblastoma cell line. The neuroblastoma cells display a clear peri-nuclear ring of DISC1 staining, which is either continuous or intermittent. Large puncta are commonly detected around the nucleus of the neuroblastoma cell lines and these large puncta often extend into the cytoplasm. The large cytoplasmic puncta are particularly evident within the epithelial-like cells of the SH-SY5Y cell line and it was noted that these puncta-like structures were not as common following paraformaldehyde fixation.

DISC1 is both filamentous and punctate in structure. The punctate pattern is particularly noticeable in the more flattened epithelial-like cells and in the extended processes of the neuroblast cells. These puncta are much smaller and dot-like compared to the large puncta observed in the neuroblastoma cells. The filamentous structures are of varied size and small filaments of DISC1 are seen over, but not within, the nuclear area. No evidence of a nuclear localisation of DISC1 was observed.

The exact distribution and structure of DISC1 within the cell is specific to the cell-type examined, most likely reflecting the cell shape and concomitant organisation of the cytoskeleton. Nonetheless, the overall organization of DISC1 within the different cell types is comparable.

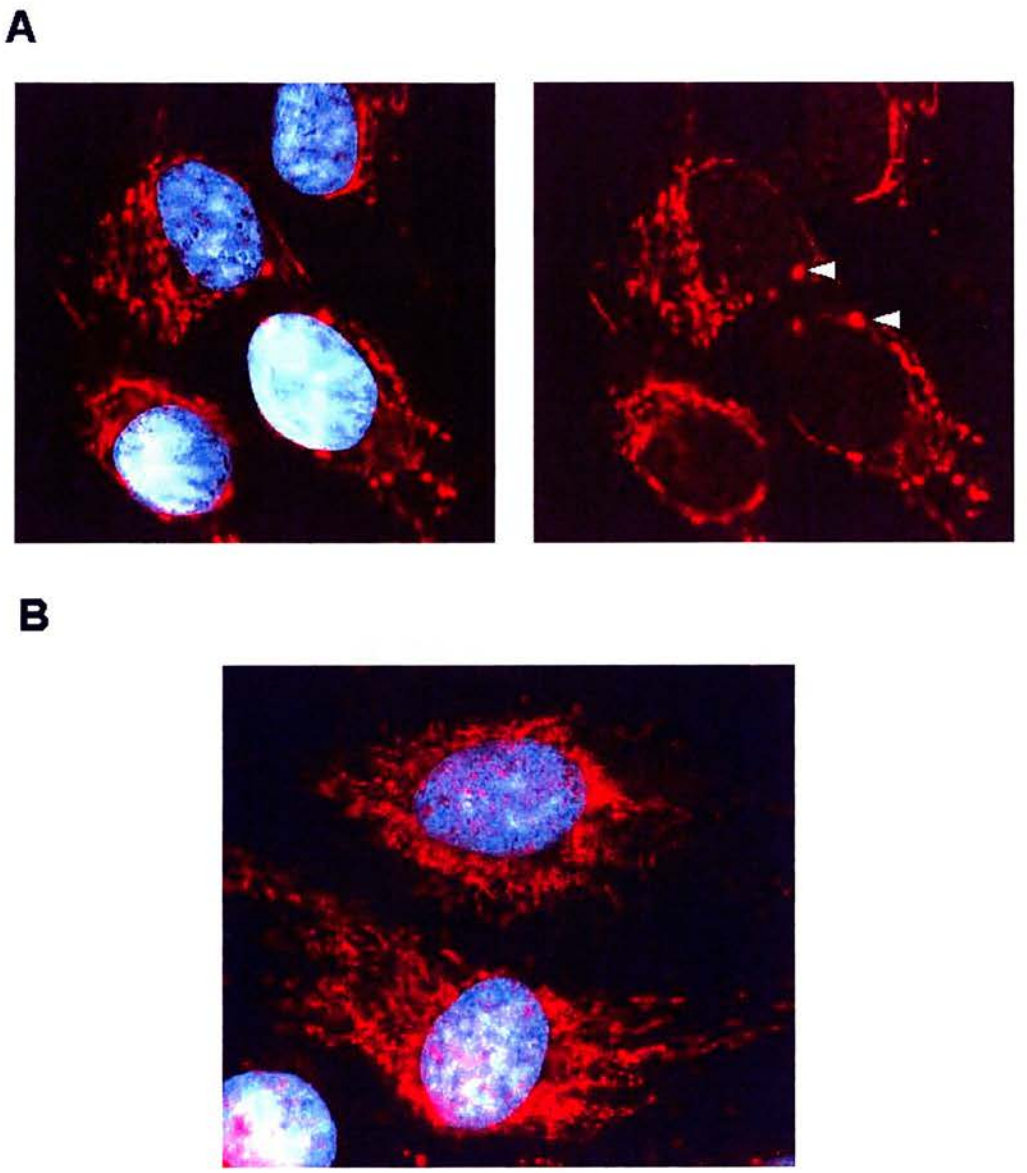

FIGURE 8.2: The subcellular localisation pattern of DISC1 within SH-SY5Y and U373 MG human cell lines

SH-SY5Y (A) and U373 MG (B) cells were fixed in methanol and DISC1 was detected using an Alexa-Fluor conjugated secondary antibody (red). The nuclei were counterstained with DAPI (blue). Punctate and fibrous DISC1 structures were observed within the cytoplasm of both cell types. In the SH-SY5Y cell line, large puncta (arrowhead) were also observed, and the peri-nuclear ring of DISC1 was clearly visible surrounding the nucleus (right).

8.4 The relationship of DISC1 to specific cellular compartments

To further examine the intracellular distribution of DISC1, colocalisation studies were performed using markers for specific cellular components.

8.4.1 The cytoskeleton

The initial focus was on the cytoskeleton as the organisation of DISC1 within the cytoplasm (Figure 8.2) appeared to be influenced by the cytoskeleton. The cytoskeleton is composed of three types of protein filaments, microtubules, microfilaments and intermediate filaments. All three filaments were examined using various antibodies: α-tubulin (microtubules), β-actin (microfilaments), GFAP and NF (glial fibrillary acidic protein & neurofilament respectively; both types of intermediate filaments).

8.4.1.1 Microtubules

There is no direct colocalisation between DISC1 and α-tubulin (Figure 8.3A), however the cytoplasmic structure of DISC1 is organised along the microtubules. This is particularly evident in the epithelial-like cells due to their more flattened appearance, and is most obvious towards the edges of the cells where there is increased resolution of individual microtubules.

8.4.1.2 Microfilaments

As for the microtubules, there is no direct colocalisation of DISC1 with β-actin (Figure 8.3B) but again there were regions of the cell where DISC1 is organised along the actin filaments. The association of DISC1 with actin is not as widespread as for tubulin.

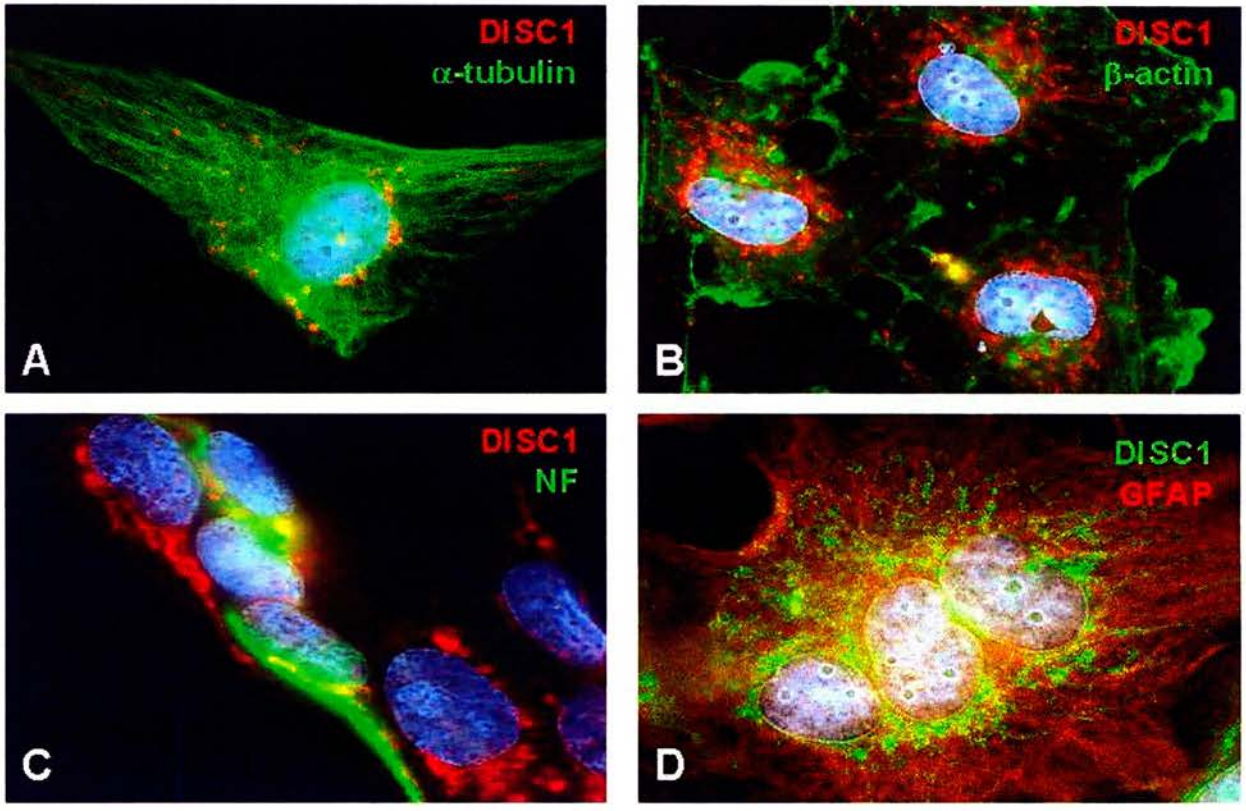

FIGURE 8.3: The relationship between DISC1 and the cytoskeleton

Cells were fixed and double-stained with antibodies for DISC1, α-tubulin (A), β-actin (B), NF (C) and GFAP (D). The respective colours of the antibodies are indicated on the images. The nuclei were counterstained with DAPI (blue). In all images except C, U373 MG cells are shown; SH-SY5Y cells are shown in C.

8.4.1.3 Intermediate filaments

In the SH-SY5Y and LAN-5 cell lines the relationship between DISC1 and NF is not clear (Figure 8.3C). Within the nuclear region of the cell the merged image of DISC1 and NF appeared yellow. However it is not clear if this is evidence of genuine colocalisation or a reflection of the proximity of the two proteins within this region. Furthermore there is no obvious relationship between the two proteins within the neurites of the neuroblast cells, though the reduced diameter of the neurites makes the determination of a relationship between DISC1 and specific components of the cytoskeleton problematic at the current resolution.

In the U373 MG cell line DISC1 is organised along the GFAP filaments (Figure 8.3D), as for the microtubules. In contrast to the microtubules (Figure 8.3A), this relationship is more obvious around the nucleus due to the better visualisation of the GFAP filaments in this region.

8.4.1.4 Conclusions

The organisation of DISC1 within the cytoplasm is shaped by the cytoskeleton, though the identification of a specific cytoskeletal component was not possible from the colocalisation data. DISC1 is most convincingly organised along microtubules but the involvement of microfilaments and intermediate filaments can not be excluded.

8.4.2 Proteins associated with microtubule function

To determine if a more specific relationship between DISC1 and the microtubules was evident, various other proteins related to microtubule function were examined using appropriate antibodies: γ-tubulin (centrosome), MAP2B (dendrite specific microtubule-associated protein) and cytoplasmic dynein intermediate chain (dynein motor).

8.4.2.1 γ-tubulin

DISC1 does not colocalise with γ-tubulin but is clustered around the centrosome (Figure 8.4A). In addition, DISC1 extends into the cytoplasm from the centrosome region. The γ-tubulin antibody produced a strong background signal which was not reduced despite optimisation of the antibody signal.

8.4.2.2 MAP2B

In undifferentiated SH-SY5Y and LAN-5 cells, there is no specific MAP2B signal (data not shown), indicating that neither of the cell types are representative of a mature neuronal phenotype. In differentiated SH-SY5Y and LAN-5 cells (section 9.2.1), a specific MAP2B signal is seen in some of the differentiated cells. However there is no colocalisation with DISC1 (Figure 8.4B). The yellow signal in the merged image is due to the proximity of the two proteins within this region as analysis of the individual signals revealed MAP2B surrounded the nucleus while DISC1 does not. As for the γ-tubulin antibody, the MAP2B antibody produced a high background signal that was not reduced by titrating the antibody.

8.4.2.3 Dynein

No specific signal was seen for this antibody on any of the cell types examined (data not shown) and the relationship of DISC1 to dynein could not be determined. Various modifications of the cell staining procedure were attempted (section 2.2.4.10), including altering the fixative and blocking buffer, increasing the incubation time and following a previously published protocol using the same antibody (Niethammer *et al.*, 2000). Nonetheless no signal above background was seen.

8.4.2.4 Conclusions

No colocalisation is observed between DISC1 and γ-tubulin or MAP2B. However a speculative relationship with γ-tubulin and the centrosome is observed. The relationship of DISC1 to dynein could not be determined with the antibody used.

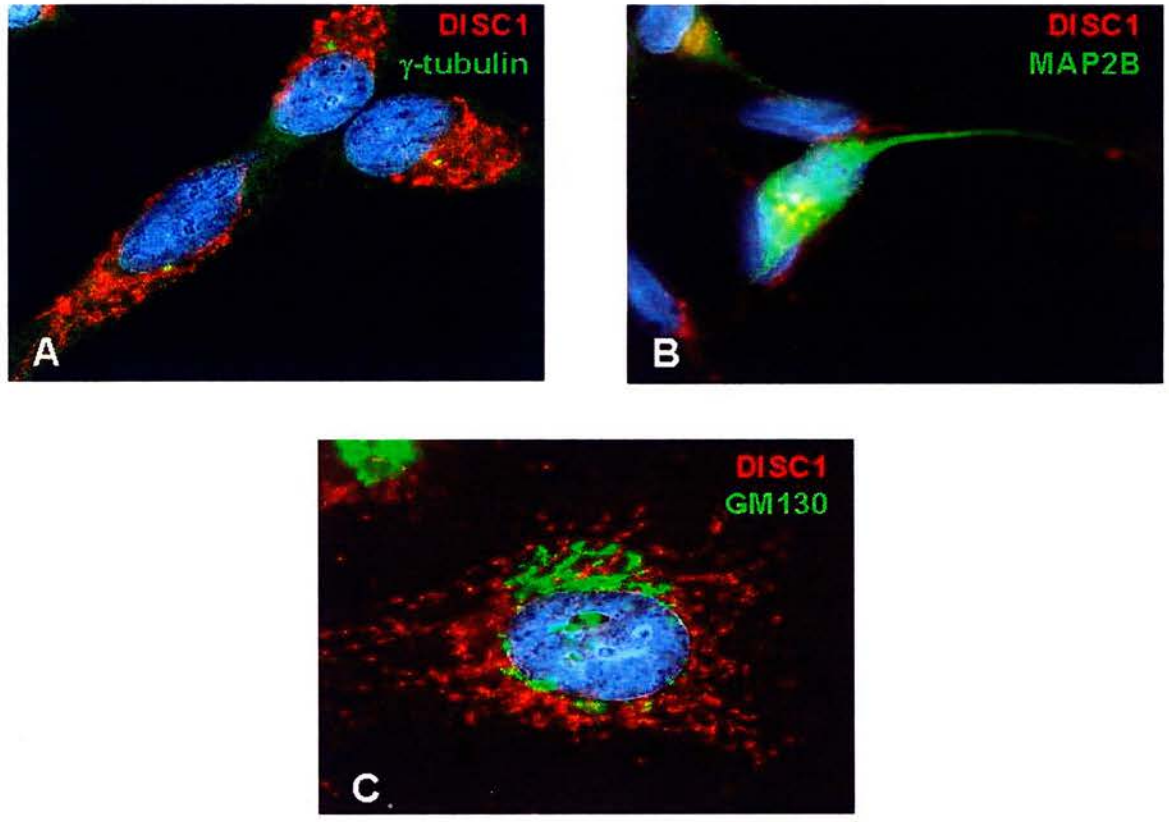

FIGURE 8.4: The relationship of DISC1 to γ-tubulin, MAP2B and the *cis*-golgi

SH-SY5Y cells were fixed and double-stained using antibodies for DISC1 (red) and γ-tubulin (A; green), MAP2B (B; green) and GM130 (C; green). The nuclei were counterstained with DAPI (blue). The poor resolution of the image in B was due to difficulties in co-visualisation of the fluorescent tags.

8.4.3 Organelles

The relationship of DISC1 to specific organelles was also investigated. The organelles were visualised using either antibodies, GM130 (*cis*-golgi) or fluorescent probes, rhodamine B (endoplasmic reticulum) and MitoTracker® Deep Red 633 (mitochondria).

8.4.3.1 cis-golgi

There is no colocalisation between DISC1 and GM130 (Figure 8.4C), but DISC1 and the *cis*-golgi are in close proximity to one another in the peri-nuclear region of the cell.

8.4.3.2 Endoplasmic reticulum

Direct colocalisation between DISC1 and rhodamine B is observed throughout the cytoplasm including the peri-nuclear region (Figure 8.5). However it cannot be concluded that DISC1 colocalises to the endoplasmic reticulum (ER) as rhodamine B also labels mitochondria, therefore an ER-specific marker would be needed to confirm this relationship. The structure labeled by rhodamine B is diffuse and representative of the ER (A Web Atlas of Cellular Structures; http://www.itg.uiuc.edu/technology/atlas/structures/reticulum/), but the correlation with DISC1 is less evident. Nonetheless regions of fibrous structure are observed in both the SH-SY5Y and U373 MG cell lines which show good structural correlation with DISC1 and the rhodamine B structure.

8.4.3.3 Mitochondria

Initial studies were performed using MitoTracker® (Molecular Probes), a mitochondrial specific fluorescent dye. No mitochondrial signal was obtained on fixed cells (data not shown), despite optimisation of the fixation method and also the incubation time and concentration of the MitoTracker dye. However the use of this dye on live cells revealed a direct colocalisation between DISC1 and mitochondria (data not shown; performed by Kirsty Millar & Sheila Christie). A mitochondrial

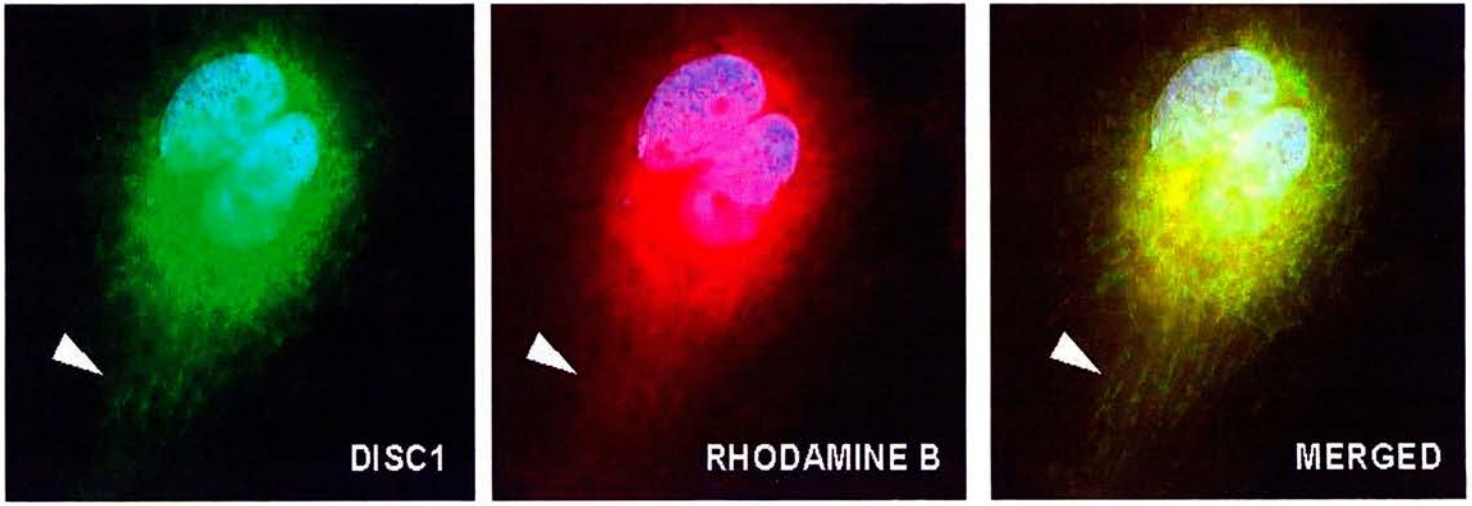

FIGURE 8.5: Colocalisation between DISC1 and rhodamine B

DISC1 (green) and rhodamine B (red) colocalised in both U373 MG (above) and SH-SY5Y (not shown) cells. The nuclei were counterstained with DAPI (blue). Merged images are also shown. Fibrous structure showing good correlation between DISC1 and rhodamine B is indicated (arrowhead).

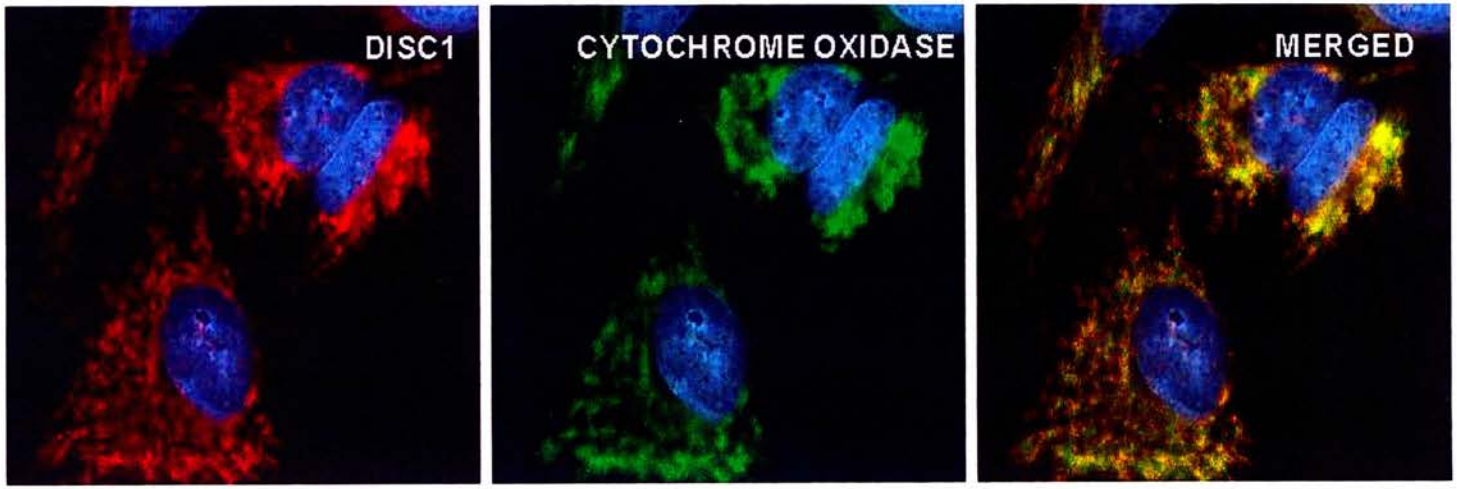

FIGURE 8.6: Colocalisation of DISC1 to the mitochondria

DISC1 (red) colocalises with cytochrome oxidase (green), a mitochondrial specific marker, in U373 MG cells (above) and SH-SY5Y (not shown) cells. The nuclei were counterstained with DAPI (blue). Merged images are also shown.

specific antibody, cytochrome oxidase subunit VIc (COX6c), confirmed this result (Figure 8.6; performed by Kirsty Millar & Sheila Christie). The nature of DISC1 and COX6c immunostaining is not identical. COX6c appears diffuse compared to the predominantly punctate DISC1. Nonetheless the pattern of the two proteins within the cell shows good correlation and the proteins are clearly localised to the same structure.

8.4.3.4 Conclusions

The use of two mitochondrial-specific reagents reveals that DISC1 colocalises to mitochondria. A tentative colocalisation to the ER is also observed but confirmation of this result is needed. No colocalisation with the *cis*-golgi is observed.

8.5 Examination of the effect on DISC1 following disruption of the cytoskeleton

The localisation of DISC1 to the mitochondria and possibly also the endoplasmic reticulum (section 8.4.3.4), only became known towards the end of this project, therefore the initial conclusion from the colocalisation experiments was that DISC1 is associated with the cytoskeleton (section 8.4.1.4). However it is not apparent from the colocalisation studies which component, or components, of the cytoskeleton are more important to the function of DISC1. To further investigate the relationship between DISC1 and the cytoskeleton, drugs that disrupt microtubules and microfilaments were employed to determine if this had any effect on the localisation of DISC1. The lack of specific drugs to disrupt either GFAP or NF prevented the relationship between DISC1 and these intermediate filaments from being studied further. In addition, the relationship of DISC1 to cold-stable microtubules was examined and experiments were undertaken to evaluate the effect on DISC1 following disruption and subsequent reformation of the tubulin network. These experiments were performed using the SH-SY5Y and U373 MG cell lines.

8.5.1 Microtubule disruption using nocodazole and taxol

Nocodazole completely disrupts the microtubules and no filament structure is seen (Figure 8.7A & C). This is accompanied by a reduction in α-tubulin fluorescence. On the other hand, taxol results in disorganisation of the microtubules, with no clear radiation from the centrosome and fragmentation of the microtubules at the edges of the cell (Figure 8.8A). After administration of both drugs, no neurites extend from the neuroblast SH-SY5Y cells (data not shown).

Following nocodazole treatment, the organisation of DISC1 within the cell is disrupted (Figure 8.7B & D), but the overall structure of DISC1 is maintained. At higher concentrations of nocodazole (>5μgml^{-1}), complete dissociation of DISC1 from the nucleus is seen in some cells (Figure 8.7D). The peri-nuclear ring is still present and is visible in the U373 MG cells (Figure 8.7B), possibly due to dissociation of DISC1 from the nucleus. Control cells treated with DMSO alone show none of these changes in DISC1 organisation (data not shown).

Treatment of the cells with taxol results in the complete loss of the normal organisation of DISC1 within the cytoplasm (Figure 8.8B). The effect of taxol is more pronounced than nocodazole. DISC1 is present as small puncta only and the filamentous DISC1 structure is lost. In addition none of the large puncta are observed in the SH-SY5Y cells. The punctate pattern of DISC1 is scattered throughout the cytoplasm but at higher concentrations of taxol (>50μM), DISC1 clusters around the nucleus. Again the control cells treated with DMSO alone show none of these effects (data not shown).

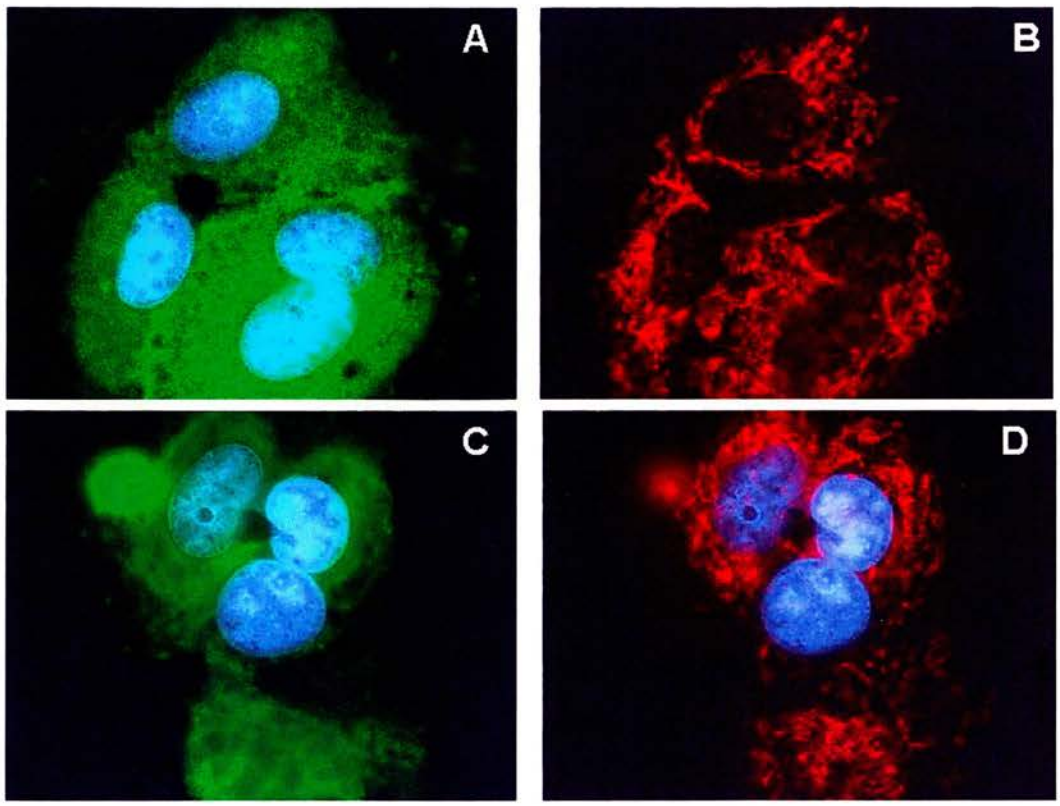

FIGURE 8.7: The organisation of DISC1 is disrupted following nocodazole treatment

U373 MG cells were treated with 2μgml^{-1} (upper) or 10μgml^{-1} (lower) nocodazole, before fixing the cells and double-staining using antibodies for α-tubulin (A & C; green) and DISC1 (B & D; red). The nuclei were counterstained with DAPI (blue). DAPI staining is not shown in B to reveal the presence of the peri-nuclear ring, not usually visible with this cell type. The effect of nocodazole on SH-SY5Y cells was the same (data not shown).

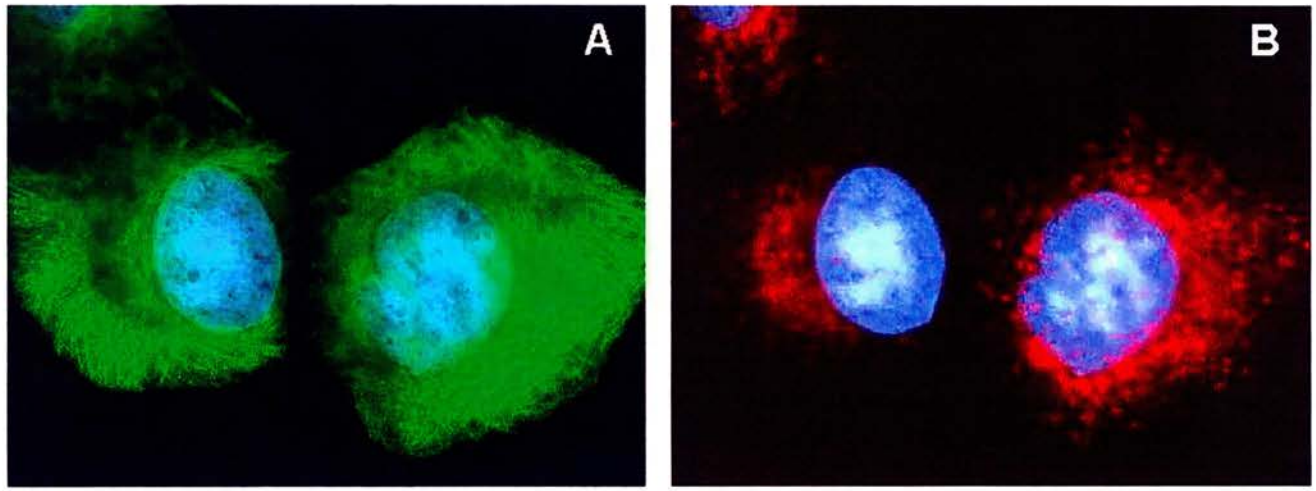

FIGURE 8.8: Taxol treatment results in complete loss of the organisation of DISC1

U373 MG cells were treated with 10μM taxol before fixing the cells and double staining using antibodies for α-tubulin (A; green) and DISC1 (B; red). The nuclei were counterstained with DAPI (blue). The effect of taxol on SH-SY5Y cells was the same (data not shown).

8.5.2 Microfilament disruption using cytochalasin B

Cytochalasin B treatment results in an abnormal distribution of the microfilaments (Figure 8.9A & C). There is an overall reduction in β-actin fluorescence accompanied by intermittent regions of bright fluorescence. In contrast to microtubule disruption (section 8.5.1), neurites are still visible in the SH-SY5Y neuroblast cells.

Following cytochalasin B treatment, there is an intense clustering of DISC1 around the nucleus (Figure 8.9B & D), which was difficult to image, and in the SH-SY5Y cells the peri-nuclear ring is not seen. DISC1 is still organised within the cytoplasm in a cytoskeletal associated pattern, however there is a loss of the filamentous structure and only small DISC1 puncta are visible, similar to what was observed following taxol treatment (Figure 8.8B). Within the U373 MG cells a rearrangement of the cytoplasmic distribution of DISC1 is observed. DISC1 is arranged in a star-like orientation (Figure 8.9D), especially at higher concentrations of cytochalasin B (>50μM). These star-like structures are never seen in untreated cells or in those treated with DMSO alone. Examination of the microtubules following cytochalasin B treatment reveals the microtubules are also arranged into star-like structures, along which DISC1 is distributed (data not shown). The effect of cytochalasin B is more pronounced in the SH-SY5Y cells and at higher concentrations of cytochalsin B (>50μM), there is loss of the organisation of DISC1 (Figure 8.9B), and the effect is similar to taxol disruption of microtubules (Figure 8.8). The control cells treated with DMSO alone show none of these effects (data not shown).

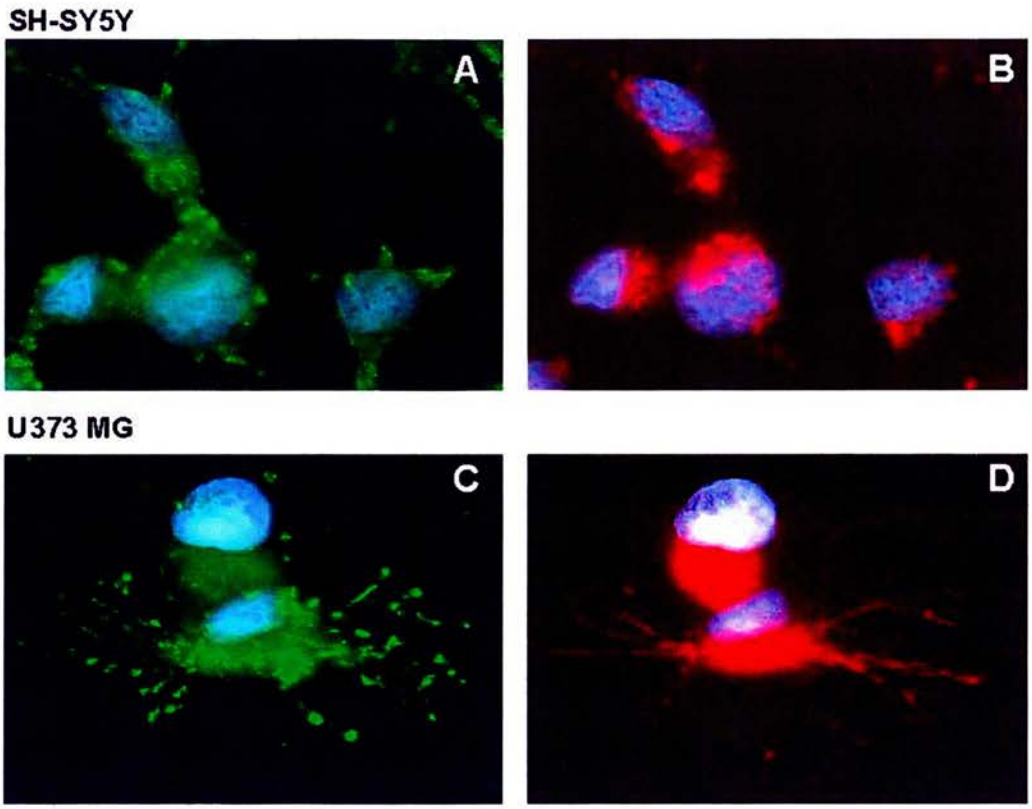

FIGURE 8.9: The structure of DISC1 is predominantly disrupted following cytochalasin B treatment

SH-SY5Y (upper) or U373 MG (lower) cells were treated with 50μM cytochalasin B before fixing the cells and double-staining using antibodies for β-actin (A & C; green) and DISC1 (B & D; red). The nuclei were counterstained with DAPI (blue). The poor resolution of DISC1, particularly around the nucleus, was due to difficulties in visualisation of the fluorescent tag.

8.5.3 Exposure of cold-stable microtubules

In certain cell types, including neurons and fibroblasts, there are subpopulations of microtubules that resist depolymerizing conditions including exposure to the cold (Denarier *et al.*, 1998; Andrieux *et al.*, 2002). These cold-stable microtubules are believed to be important to the morphology and function of the cell. The relationship of DISC1 to cold-stable microtubules was examined in SH-SY5Y cells.

The initial protocols followed (Denarier *et al.*, 1998; Bosc *et al.*, 2001) used a permeabilisation buffer before fixing the cells. However the permeabilisation buffer was found to completely destroy the cells, therefore immediately after exposing the cells to ice (section 2.2.2.7), the cells were fixed and processed as usual.

Following exposure to the cold, no microtubules are visible (Figure 8.10A) and the α-tubulin signal is similar to that observed after nocodazole treatment (Figure 8.7A & C). DISC1 is still present (Figure 8.10B) but there is only a partial maintenance of the organisation of DISC1, again similar to the disruption of DISC1 following nocodazole treatment (Figure 8.7B & D).

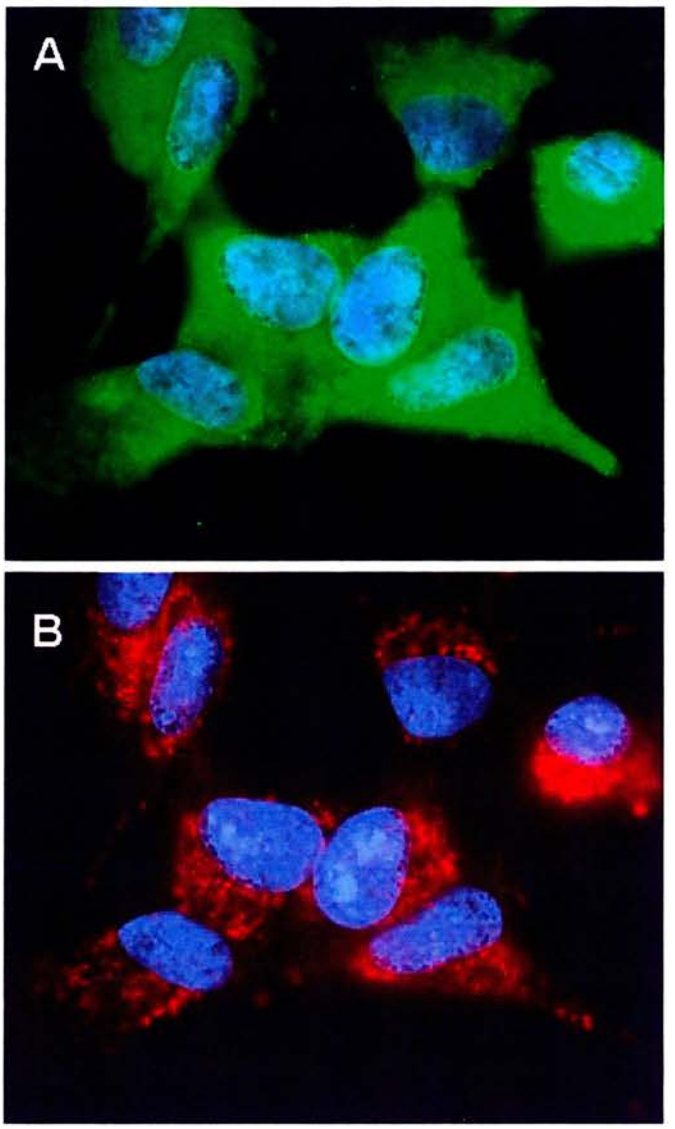

FIGURE 8.10: Disorganisation of DISC1 is observed following exposure to the cold

SH-SY5Y cells were exposed to the cold for 30 minutes before fixing the cells and double-staining for α-tubulin (A; green) and DISC1 (B; red). The nuclei were counterstained using DAPI (blue).

8.6 The effect on DISC1 following reformation of the tubulin network

The organisation of DISC1 within the cell is clearly dependent upon the microtubules (section 8.5.1), therefore an experiment was undertaken to determine the effect on DISC1 following the disruption and subsequent reformation of the tubulin network. The published protocol (Zmuda and Rivas, 1998) was used to determine the location of the centrosome: nocodazole induced depolymerization of microtubules, which were removed in an extraction buffer allowing visualization of repolymerizing microtubules from the centrosome. In the present study the protocol was used to examine reformation of the tubulin network by allowing the cells to recover in drug-free medium for longer than the published incubation times (section 2.2.2.8). SH-SY5Y cells were used for the following experiment.

After a 3 – 5 minute recovery period, the developing tubulin network was visible in some cells, clearly emanating from the centrosome (Figure 8.11A). After a 15 minute recovery period, the tubulin network appeared fully mature in all of the cells (Figure 8.11B). However the effect of DISC1 could not be studied as it was found that the use of the extraction buffer in the absence of any other treatment, completely removed DISC1 from the cell (Figure 8.11C). Incubation in the extraction buffer for only 10 seconds was enough to completely remove DISC1. The fibrous structures visible were also seen in the absence of the DISC1 antibody (data not shown) and must represent a non-specific cellular structure. It was not possible to alter the stage at which the extraction buffer was used, as it is unlikely that the cells would survive exposure to gluteraldehyde. In addition this step was necessary to remove depolymerized microtubules present after nocodazole treatment alone (compare α-tubulin staining in Figure 8.7A & C with Figure 8.11A). The microtubules were not affected by the use of extraction buffer alone (Figure 811C).

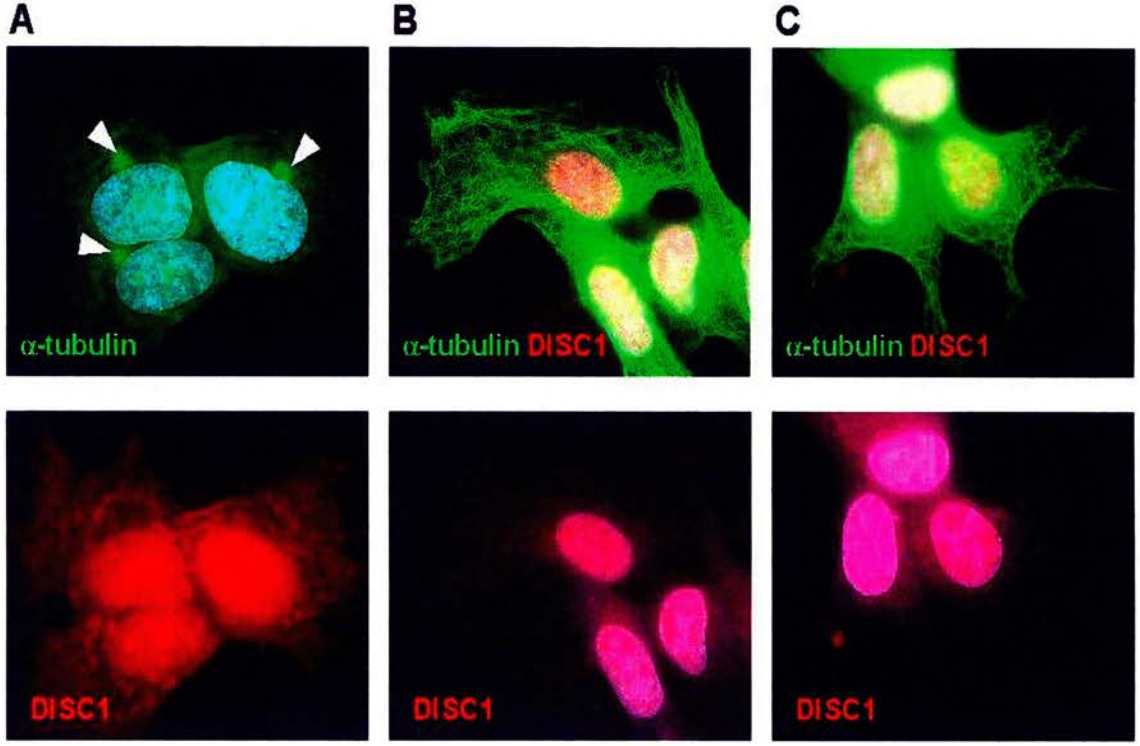

FIGURE 8.11: The effect on DISC1 following reformation of the tubulin network cannot be studied

SH-SY5Y cells were treated with nocodazole and allowed to recover in drug-free medium for 5 (A) or 15 (B) minutes. The cells were then incubated in an extraction buffer to remove depolymerized microtubules before fixing and double staining with antibodies for α-tubulin (green) and DISC1 (red). The nuclei were counterstained with DAPI (blue). The development of the tubulin network from the centrosome (arrowhead) is clearly visible after 5 minutes recovery. Control cells were not treated with nocodazole but incubated in extraction buffer alone (C).

8.8 Discussion

DISC1 was found to colocalise with mitochondria within the cell (Figure 8.6; Ozeki *et al.*, 2003). Mitochondria have been found to adopt many structures within the cell, dependent not only on the cell type but also on the condition of the cells, state of the cell cycle and also the fixation method (Bereiter-Hahn, 1990). In line with the latter point, the presence of the large puncta observed in the neuroblastoma cell lines was dependent on the fixative used and the puncta were only observed following methanol fixation. Nevertheless these puncta, as with all structures observed, are mitochondrial, as evidenced by complete colocalisation of DISC1 with mitochondrial markers. Although DISC1 adopted a characteristic cytoskeletal associated organisation within the cell, the exact structure and distribution of DISC1 was dependent on the cell type examined. DISC1 within the 293 cell line was present as large peri-nuclear puncta only (data not shown), similar to the puncta observed in the neuroblastoma cell lines but dissimilar to the pattern of DISC1 within the glioblastoma cell line.

In addition to the mitochondria, potential colocalisation was observed between DISC1 and the ER (Figure 8.5). Rhodamine B, the fluorescent dye used to stain the ER, is marketed as a mitochondrial probe (Molecular Probes), however at the concentrations used (section 2.2.4.11), rhodamine B has been reported as exclusively staining the ER (Yang *et al.*, 1997). In addition colocalisation of rhodamine B with known ER-specific markers has been reported (Terasaki and Reese, 1992; Yang *et al.*, 1997) and rhodamine B has been used as a direct ER marker in other studies (Arregui *et al.*, 1998; Northwood *et al.*, 1999). Therefore it is possible that the colocalisation of DISC1 to the ER is real but confirmation with an independent ER-specific marker, such as the antibody BiP would be useful in this respect. In support of a genuine relationship between DISC1 and the ER, there is considerable overlap in the distribution of the ER and mitochondria, and in *Xenopus* endothelial cells mitochondria were only found in areas where the ER was present (Bereiter-Hahn, 1990).

The original observation from the subcellular localisation pattern of DISC1 (section 8.3) was that the distribution of DISC1 within the cytoplasm was being influenced by the cytoskeleton. However the colocalisation studies using antibodies for specific components of the cytoskeleton did not enable a more specific conclusion to be made regarding which, if any, of the filaments was more important to the function of DISC1. More direct evidence for the involvement of DISC1 with both the microtubules and microfilaments was provided by the use of drugs that disrupt either microtubules or microfilaments. Nocodazole and taxol both disrupt microtubules but do so by different mechanisms, nocodazole causes depolymerization of the existing tubulin network by blocking assembly of microtubules from tubulin (Baas *et al.*, 1994), while taxol stimulates polymerization of tubulin into microtubules, thereby stabilizing existing microtubules (Carson *et al.*, 1997). The third drug tested, cytochalasin B, disrupts microfilaments by blocking actin polymerization and causing depolymerization of microfilaments (Carson *et al.*, 1997). All of these drugs had an effect on the normal distribution pattern of DISC1 (Figures 8.7 - 8.9). Nocodazole and taxol resulted in disorganisation of DISC1 within the cell. The level of disorganisation seen after nocodazole treatment was related to the concentration of nocodazole used, while the effect of taxol on the organisation of DISC1 was more pronounced and a complete loss of the normal distribution of DISC1 was seen using low concentrations of taxol (10μM). The effect seen following cytochalasin B treatment was more complex and was predominantly characterised by loss of normal DISC1 structure. There was maintenance of the distribution of DISC1 within the cytoplasm, although in the case of the U373 MG cells, the morphology of the cells had been altered into star-shaped structures (Figure 8.9). However at higher concentrations (>50μM) of cytochalasin B the distribution of DISC1 was lost and the pattern was similar to that seen following taxol treatment. This effect was most pronounced in the SH-SY5Y cell line and may reflect a greater interdependence of microtubules and microfilaments in this cell line.

Further support for the association of DISC1 with microtubules was provided following disruption of cold-labile microtubules. In SH-SY5Y cells exposure to cold resulted in the complete loss of microtubules (Figure 8.10) and as for the nocodazole

induced loss of microtubules, a concomitant disorganisation of DISC1 was observed. The lack of cold-stable microtubules has been reported for HeLa cells (Denarier *et al.*, 1998) and could therefore also be a feature of SH-SY5Y cells. Alternatively the absence of microtubules following depolymerizing treatments may reflect the detection reagent used: the association of acetylated α-tubulin with cold-stable microtubules has been reported (Cambray-Deakin *et al.*, 1988), while other groups have used β-tubulin to detect cold-stable microtubules (Denarier *et al.*, 1998; Andrieux *et al.*, 2002). The use of another tubulin antibody would be necessary before conclusively determining the presence or absence of cold-stable microtubules in this cell line.

Disruption of the cytoskeleton provides direct evidence that both the structure and organisation of DISC1 is closely associated with microtubules. In particular stabilization of microtubules seen after taxol treatment appears to be crucial for the normal pattern of DISC1 within the cell. Association with the cytoskeleton is known to be important for the distribution of mitochondria within the cell. Mitochondria have long been linked with microtubules (Bereiter-Hahn, 1990) but there is also evidence indicating microfilaments (Morris and Hollenbeck, 1995; Hollenbeck, 1996) and neurofilaments (Straube-West *et al.*, 1996) may also be involved.

The effect on DISC1 following depolymerization and reformation of the tubulin network could not be examined due to the complete removal of DISC1 following incubation in the extraction buffer (Figure 8.11). This result, though not informative towards the initial aim of the experiment, may be important in determining the strength of the interaction between DISC1 and microtubules. Other proteins would need to be studied before any conclusion could be made. Examination of both mitochondria directly and other microtubule-associated proteins would be useful in this regards.

Identification of the subcellular localisation of DISC1 has begun to offer the opportunity to unravel its function. Mitochondria have been extensively studied and consequently much is known about their function within the cell. The next challenge

will be to determine where DISC1 fits into the role of the mitochondria and how this relates to both the function and subsequent dysfunction of the nervous system.

CHAPTER 9

DISC1 LOCALISATION DURING DIFFERENTIATION OF NEUROBLASTOMA CELL LINES

9. DISC1 localisation during differentiation of neuroblastoma cell lines

9.1 Introduction

DISC1 colocalises with mitochondria in transformed cell lines (section 8.4.3.3), but the function of this association is not known. In order to investigate DISC1 in a more neuronal-like cell, human neuroblastoma cell lines were differentiated according to published protocols, to determine which strategy produces the most neuronal-like cells. Subsequently, the subcellular localisation and protein expression pattern of DISC1 was examined during differentiation.

9.1.1 The suitability of cell culture systems for the study of endogenous human proteins

Cell lines, such as those used in the present study (Table 2.3) are a useful resource for examining the function of a protein. However as cell lines are usually karyotypically abnormal, primary cell cultures are often utilized in order to confirm the data generated using cell lines, as they are deemed to be more representative of the biological context. Nonetheless, the use of primary cell cultures is limited by both the heterogeneity of the cultures and difficulties in obtaining sufficient amounts of cells (Whittemore and Snyder, 1996). In particular, the study of endogenous human proteins, such as DISC1, is restricted and more often than not prevented by the lack of availability of appropriate tissue. In the study of the nervous system one approach to overcome the lack of tissue availability, has been to differentiate neuroblastoma derived cell lines to a neuronal phenotype, with the rationale being that the closer a cell line mimics the behaviour of a primary neuron, the more valid are the conclusions.

9.1.2 Differentiation of human neuroblastoma cell lines

The SH-SY5Y and LAN-5 neuroblastoma cell lines have both been studied as a model system for neuronal differentiation. The SH-SY5Y cell line can be differentiated to a neuronal phenotype using a number of inducing reagents, of which retinoic acid (RA) and the phorbol ester, 12-O-tetradecanoyl-13-phorbol-acetate (TPA), are the most common. The phenotype of the differentiated SH-SY5Y cell differs depending upon the inducing agent (Pahlman *et al.*, 1995). RA treatment drives SH-SY5Y cells to differentiate along a sympathetic chromaffin lineage, whereas TPA induces differentiation along a sympathetic adrenergic lineage. In addition, the morphology of the differentiated SH-SY5Y cells differs. RA treated cells appear more spread out and polar with longer neurites compared to TPA treated cells (Feng and Porter, 1999; Guarneri *et al.*, 2000). However, as described earlier (section 8.2.1), one drawback to the use of the SH-SY5Y cell line is that it contains at least two starting populations of cell types thus complicating interpretation of neuronal differentiation. To overcome this problem, Encinas *et al* (Encinas *et al.*, 2000) described the differentiation of SH-SY5Y cells using a combination of RA and brain-derived neurotrophic factor (BDNF), to produce a homogenous population of differentiated cells.

The differentiation of the LAN-5 neuroblastoma cell line has not been studied as extensively as the SH-SY5Y cell line, but differentiation to a mature neuronal phenotype has been reported following both RA (Lanciotti *et al.*, 1992; Hill and Robertson, 1997; Hill and Robertson, 1998) and TPA treatment (Lanciotti *et al.*, 1992). Phenotypic analysis of RA treated LAN-5 cells suggest they differentiate along a sympathetic cholinergic lineage, while morphologically they extend long axonal-like processes (Hill and Robertson, 1997).

In the present study RA induced differentiation of both cell lines was performed, as well as BDNF treatment of the SH-SY5Y cells.

9.2 Defining a neuronal-like cell

In order to determine the success of the differentiation strategy, it was necessary to define features of a neuronal-like cell. The neuron is a highly polarized cell and extends elongated cellular processes, termed axons and dendrites. The establishment of this polarity begins very soon after the initiation of neurite outgrowth (Mattson, 1999), although the mechanisms responsible for neuronal polarization are largely unknown. A typical vertebrate neuron extends a single axon and many dendrites (Baas, 1999), the structure and function of which differ in many aspects. Morphologically, axons are long thin processes with few branches, whereas dendrites are short thick processes with a tapered appearance and numerous branches (Crino and Eberwine, 1996; Zmuda and Rivas, 1998). Axons and dendrites contain domain specific proteins, such as GAP43 and MAP2, which can be used to selectively label axons and dendrites respectively.

Therefore in order to determine if the differentiated neuroblastoma cells adopted neuronal characteristics, the neuronal specific marker, neurofilament (NF) and the dendrite specific marker, MAP2B were examined. The morphology of the differentiated cells was also determined.

9.2.1 Neurofilament

NF had previously identified (section 8.4.1.3) a subset of NF positive cells in both the SH-SY5Y and LAN-5 cell lines, with more NF positive cells observed in the LAN-5 cell line (Table 9.1). Following RA induced differentiation, the number of NF positive cells is reduced in both the SH-SY5Y and LAN-5 cell lines (Table 9.1) with increasing days in culture. In contrast, addition of BDNF to RA treated SH-SY5Y cells results in an increase in the number of NF positive cells (Table 9.1).

TABLE 9.1: Neurofilament expression during differentiation

DIFFERENTIATION STRATEGY	NF +VE CELLS 0	NF +VE CELLS 1	NF +VE CELLS 2
SH-SY5Y / RA*	24%	26%	9%
SH-SY5Y / RA + BDNF†	24%	20%	39%
LAN-5 / RA†	38%	32%	20%

The approximate % of NF positive cells was determined by selecting random fields of view for counting. The % above represents the average of 3. Stage 0: before differentiation; Stage 1: 2 days differentiation; Stage 2: 6 days* or 7 days† days differentiation. For the SH-SY5Y cells sequentially treated with RA and BDNF, the number of NF positive cells at stages 1 & 2 was determined during BDNF differentiation.

In undifferentiated cells, NF is confined to the cell body, whereas in differentiated cells NF extends throughout the processes (Figure 9.1; data shown for SH-SY5Y cells only), reflecting the mature neuronal-like phenotype of these cells.

9.2.1 MAP2B

Overall the use of the present MAP2B antibody (BD Transduction) was problematic due to the considerable background seen with the antibody. Utilization of this antibody on U373 MG cells enabled the background signal to be identified (data not shown), as glioblastoma cells do not express MAP2B.

On the assumption that the low intensity speckled signal is background, no MAP2B staining is seen in undifferentiated or RA treated SH-SY5Y cells (data not shown). However BDNF treatment clearly resulted in the expression of MAP2B around the cell body and within the neurites of some cells (Figure 9.2). Likewise no MAP2B staining is seen in undifferentiated LAN-5 cells (data not shown), but expression of MAP2B is seen in RA treated LAN-5 cells (Figure 9.2). The unlabelled cells show the considerable background signal from the MAP2B antibody.

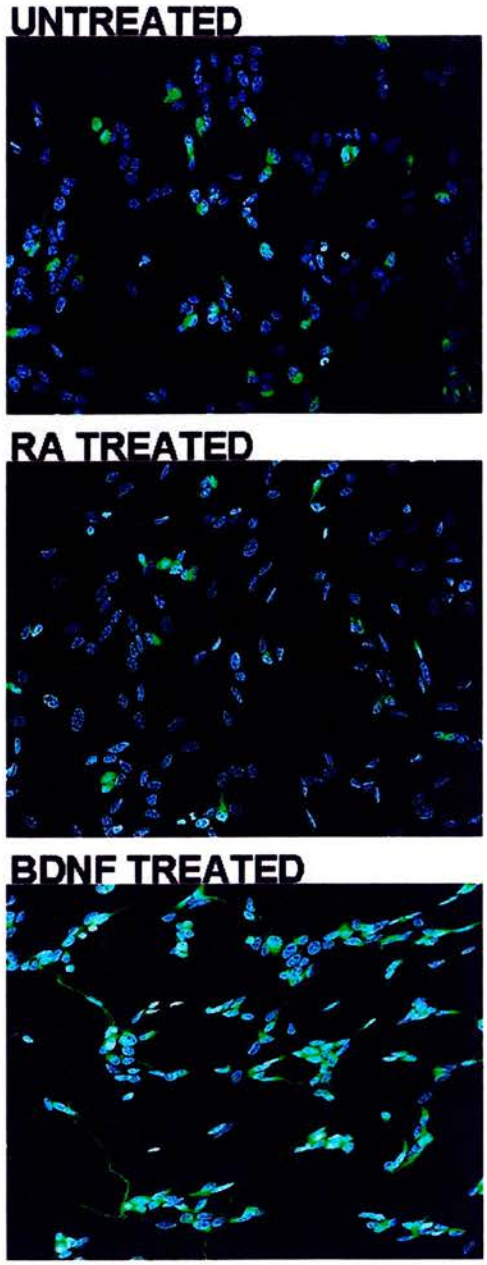

FIGURE 9.1: Neurofilament distribution in SH-SY5Y cells

SH-SY5Y cells were fixed in methanol and stained for NF (green). The nuclei were counterstained with DAPI (blue). In untreated and 6d RA treated cells, NF is predominantly localised to the cell body. However in 7d BDNF treated cells NF extends into the processes, consistent with the development of a neuronal-like phenotype in these cells.

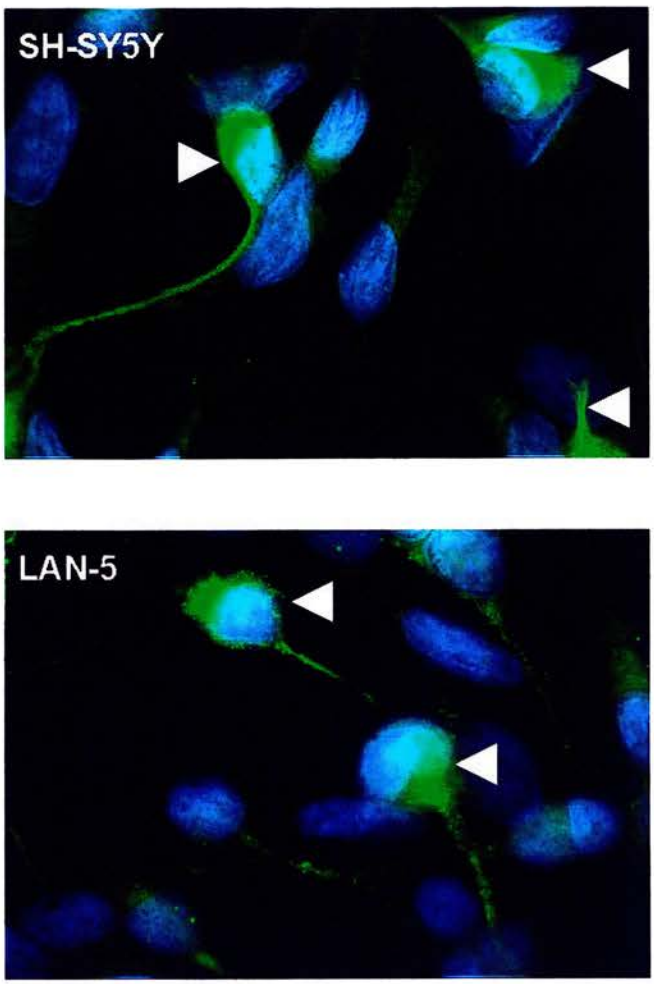

FIGURE 9.2: MAP2B expression in differentiated SH-SY5Y and LAN-5 cells

After 7d differentiation in BDNF (SH-SY5Y) or RA (LAN-5), the cells were fixed in methanol and stained using the dendrite specific marker, MAP2B (green). The nuclei were counterstained with DAPI (blue). MAP2B positive cells (arrowhead) extend a single dendritic process. The background signal is evident in the unlabelled cells.

9.2.3 The morphology of differentiated neuroblastoma cells

The majority of differentiated SH-SY5Y and LAN-5 cells are small rounded bipolar cells (Figure 9.3; upper panels). Multipolar pyramidal shaped cells (Figure 9.5B) are observed in earlier stages of differentiation and are possibly indicative of an early developmental stage, with retraction of one or more of the processes providing the mature bipolar morphology. Fully differentiated RA treated LAN-5 and BDNF treated SH-SY5Y cultures form an extensive network of cells with well connected neurites (Figure 9.3; upper panels).

9.2.4 Overgrowth of RA treated SH-SY5Y cultures

RA induced differentiation of the SH-SY5Y cell line, is known to result in overgrowth of the culture with non-differentiating epithelial S cells (Encinas *et al.*, 2000). This overgrowth can be prevented by sequential treatment of the cells with RA followed by BDNF in a serum-free medium. The absence of serum prevents survival of non-differentiating S cells, while BDNF ensures survival of differentiated neuronal-like cells. Therefore, approximate cell numbers were determined during treatment of the SH-SY5Y cell line with RA and BDNF to ensure the cells were not proliferating in the presence of BDNF.

Overgrowth of the RA treated SH-SY5Y culture by the epithelial S cells is observed (Figure 9.4). At day 5, approximately the same number of cells is seen in control and differentiated cell cultures. After addition of BDNF to the cultures, the number of cells does not increase while the number of control cells increases linearly. This provides further support that addition of BDNF to these cultures is supporting their differentiation along a neuronal lineage.

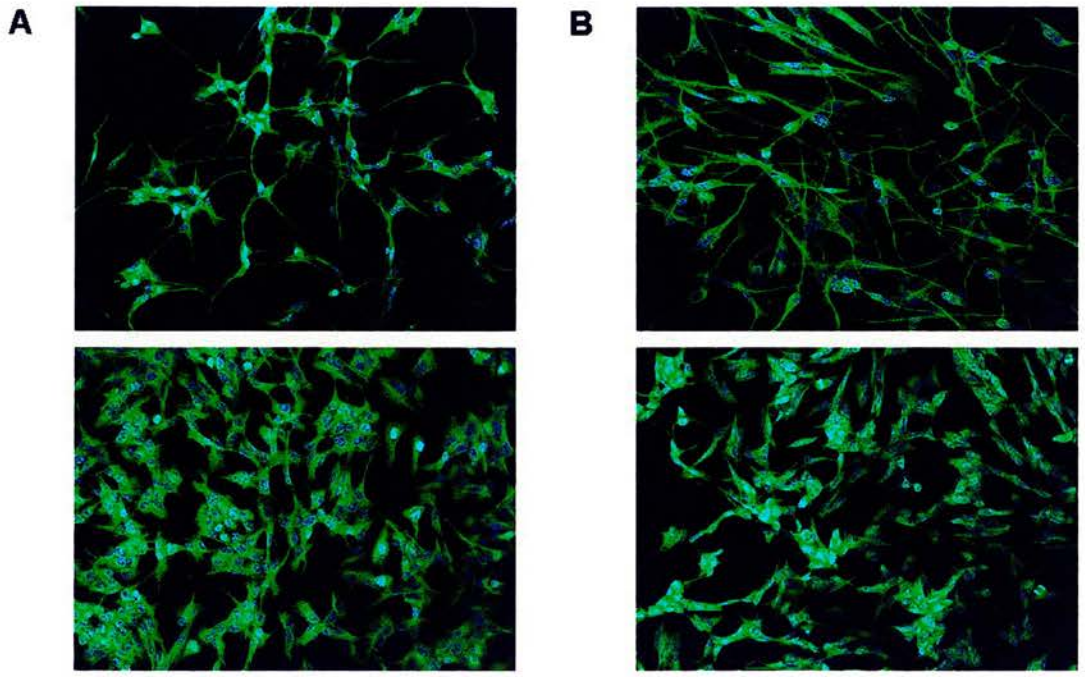

FIGURE 9.3: A network of neuronal-like cells is observed in fully differentiated neuroblastoma cells

SH-SY5Y and LAN-5 cells were fixed in methanol and microtubules detected using α-tubulin (green). The nuclei were counterstained with DAPI (blue).

A: SH-SY5Y cells treated with (upper) or without (lower) RA + BDNF and cultured for 12 days.

B: LAN-5 cells treated with (upper) or without (lower) RA and cultured for 7 days.

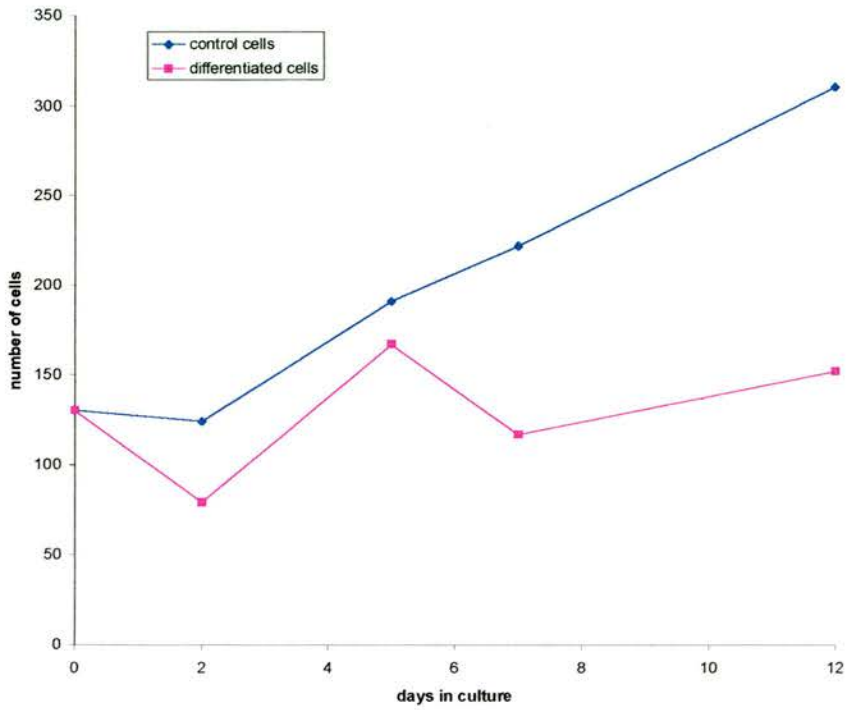

FIGURE 9.4: Growth of SH-SY5Y cells treated sequentially with RA and BDNF

The number of cells after growth in the absence (control cells) or presence (differentiated cells) of the differentiation reagents was determined. Random fields of view were selected for counting and the numbers above represent the average of 3. The cells were treated with RA from days 1 – 5 and BDNF (in serum-free medium) from days 5 – 12: the arrow represents the change from RA to BDNF.

9.3 DISC1 localisation during neurite outgrowth

A neurite is defined as being a cytoplasmic extension with a growth cone at the distal tip that lacks clear characteristics of an axon or dendrite (da Silva and Dotti, 2002). Neuronal growth cones are the structures responsible for guiding the neurite towards the appropriate targets, thus ensuring the development of the correct neuronal pathways. Once the target has been reached growth cones are important in synapse formation. Growth cones are characterised by a microtubule core surrounded by an actin based microfilament network. The actin network is comprised of a lamellipodium domain with filopodia protrusions. Larger elaborate growth cones are associated with growth of the neurite whilst small growth cones with little protrusive activity are associated with non-growing neurites (Ruthel and Hollenbeck, 2000). Furthermore the microtubule network adopts a characteristic configuration, either looped or splayed, depending on if the growth cone is paused or advancing respectively (Dent *et al.*, 1999). Splaying of the microtubule bundle along the neurite shaft is also associated with the development of interstitial branches (Dent *et al.*, 1999).

In the present study, the subcellular localisation of DISC1 was examined during neurite outgrowth to determine if the characteristic peri-nuclear localisation pattern in undifferentiated neuroblastoma cells (section 8.3) was altered in differentiated cells. In addition, the association of DISC1 with features of the growth cone, as described above, was also examined by double staining with α-tubulin (microtubules), β-actin (lamellipodium and filopodia) and synaptotagmin (synapse formation).

9.3.1 DISC1 extends into the neurites of differentiating neuroblastoma cells

In a typical culture, a number of SH-SY5Y and LAN-5 cells spontaneously exhibit short neurites. Following differentiation, the number of cells exhibiting this

phenotype increases and the overall length of the neurites also increases (Figure 9.3), which is apparent after 2 days in RA.

Upon differentiation DISC1 extends into the neurites and appears as punctate structures within the neurite shaft (Figures 9.6 & 9.7). DISC1 is often present at the base of a developing neurite and there is a frequent absence of the peri-nuclear ring (Figure 9.5A). In cells with multiple neurites (Figure 9.5B), DISC1 is usually detected in all the neurites but varied amounts of DISC1 are seen within each neurite, possibly representative of the energy demand of the neurite.

9.3.2 DISC1 localises to the growth cones of differentiating neuroblastoma cells

Growth cone-like structures are visible after 2 days RA treatment in both SH-SY5Y and LAN-5 cultures. Detection of microtubules reveals the presence of both looped and splayed growth cones (Figures 9.5A & 9.6A respectively), while the actin network shows extensive filopodia protrusions from the lamellipodium (Figure 9.7B). Growth cone-like structures are visible throughout RA induced differentiation of SH-SY5Y cells but are diminished in appearance in later stages (7 days) of RA treated LAN-5 and early stages (2 days) of BDNF treated SH-SY5Y cultures, when extensive neurite networks (Figure 9.3) are visible.

DISC1 is localised to the tips of neurites and is present in all growth cone-like structures (Figures 9.6 & 9.7), but is not found within the filopodia-like protrusions of differentiated cells (Figure 9.7B). Within the large flattened tubulin growth cone-like structures, DISC1 is distributed around the periphery of the growth cone (Figure 9.7B). The localisation of DISC1 within the differentiating cells is more closely associated with tubulin than actin.

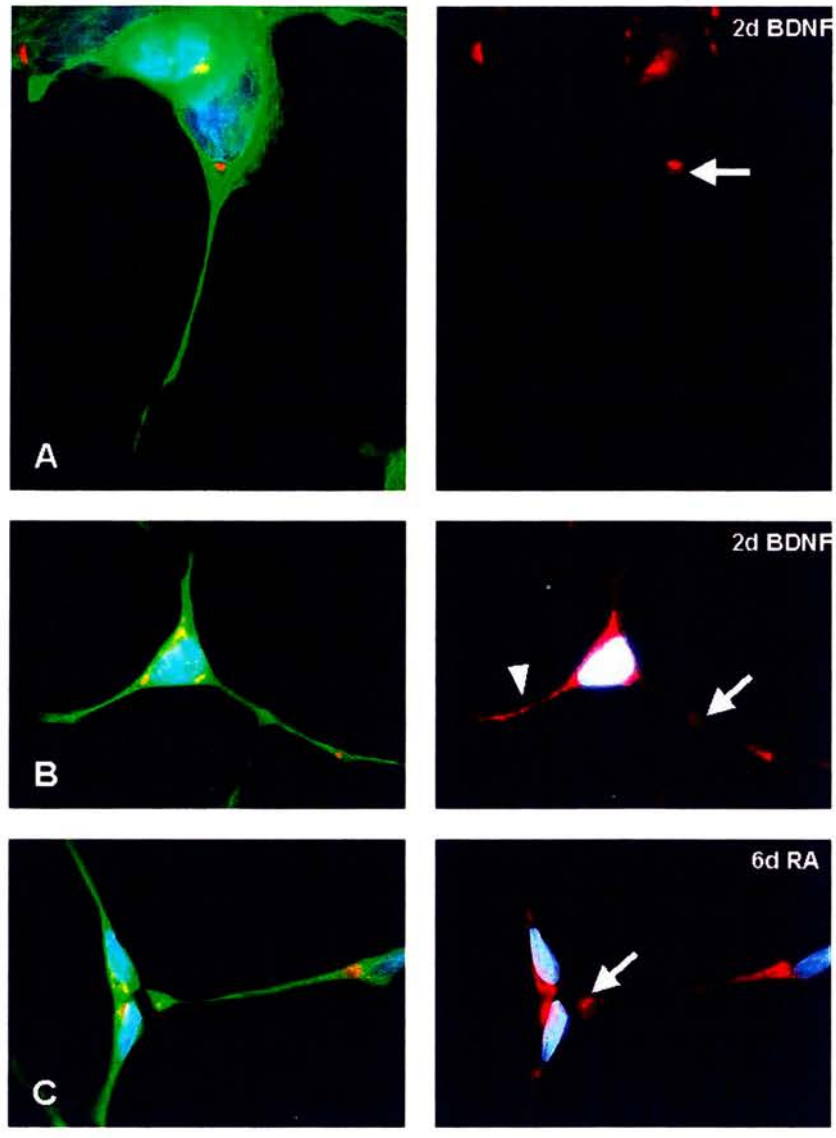

FIGURE 9.5: DISC1 localisation during differentiation of SH-SY5Y cells

Differentiated SH-SY5Y cells were fixed in methanol and double-stained using antibodies for α-tubulin (green) and DISC1 (red). The nuclei were counterstained with DAPI (blue). Merged (left) and DISC1 only (right) images are shown.

A: DISC1 is present at the base of developing neurites (arrow), with frequent absence of the peri-nuclear ring also observed.

B: DISC1 is present in all the neurites but is seen at increased levels in one of the neurites (arrowhead). In addition, DISC1 clusters at branch points (arrow).

C: DISC1 is present at the putative connection sites (arrow) between cells.

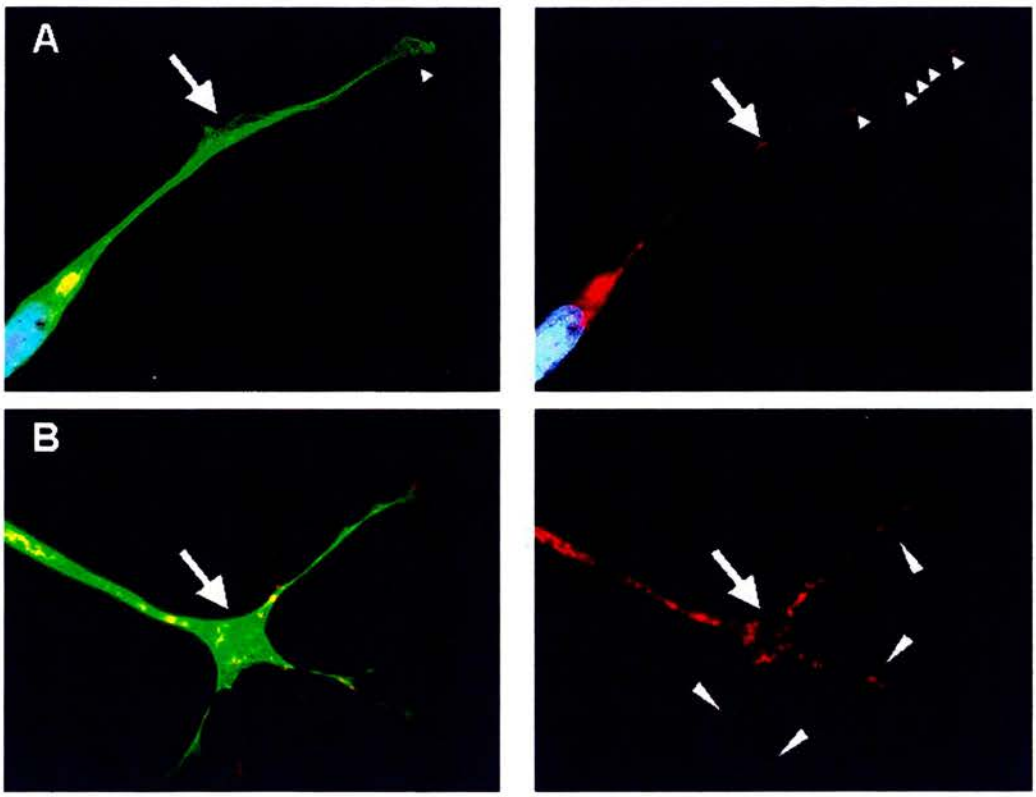

FIGURE 9.6: DISC1 is present at microtubule growth-cone like structures

After 2 days differentiation in RA, SH-SY5Y cells were fixed in methanol and double-stained using antibodies for α-tubulin (green) and DISC1 (red). The nuclei were counterstained with DAPI (blue). Merged (left) and DISC1 only (right) images are shown.

A: DISC1 is present within neurites in a punctate pattern and is localised to splaying growth-cone like structures (arrowheads). DISC1 is also clustered at points within the neurite shaft which show microtubule splaying (arrow).

B: DISC1 is present within flattened growth-cone like structures (arrow) and is distributed at the periphery of the growth cone as well as within the branches (arrowheads).

9.3.3 DISC1 is associated with the branch points of differentiating neuroblastoma cells

Branching is a feature of the differentiated cells and is not observed in undifferentiated cells. Branching of microtubules and microfilaments is observed both along the neurite shaft (Figure 9.5B) and at growth cone-like structures (Figures 9.6B & 9.7B). Splaying of the microtubules along the neurite shaft is also observed (Figure 9.6A).

DISC1 is commonly observed to cluster at both the branch points within neurite shafts (Figure 9.5B), and at points where splaying of the microtubules is evident (Figure 9.6A). DISC1 is distributed along the branches of tubulin growth cone-like structures (Figure 9.6B), but as described above (section 9.3.2), is not seen in filopodia-like branches.

9.3.4 The association between DISC1 and sites of synapse formation could not be studied

In both RA treated LAN-5 and SH-SY5Y cells, connections between cells were formed after 4 – 7 days in culture (Figure 9.5C). Furthermore in RA treated LAN-5 and BDNF treated SH-SY5Y cultures, networks of cells are formed with extensive connections between cells (Figure 9.3).

DISC1 is often present at the putative connections sites between cells (Figure 9.5C). To determine if DISC1 is localised to areas of the neurite involved in synapse formation, colocalisation with synaptotagmin (BD Transduction), a synaptic vesicle protein, was attempted. Both methanol and paraformaldehyde fixation were tested along with titration of the antibody. However, no synaptotagmin positive signal was observed in SH-SY5Y cells after 4 days of RA induced differentiation.

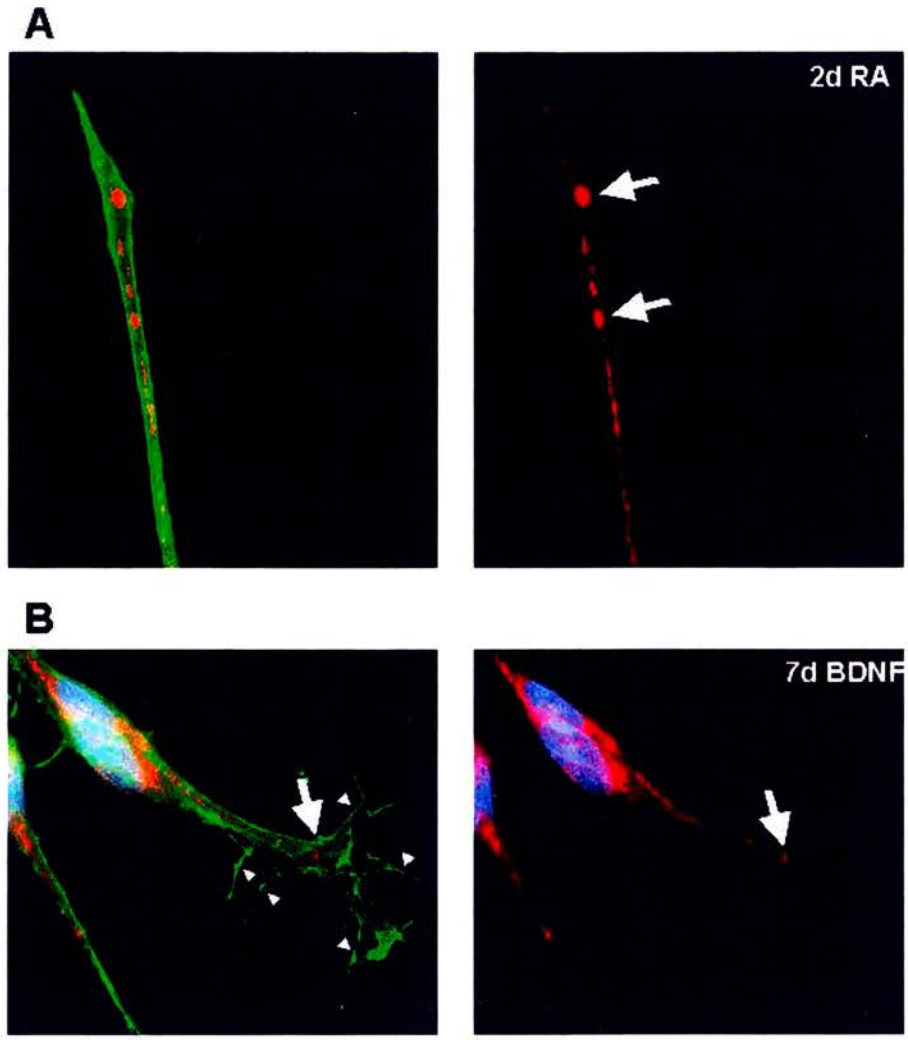

FIGURE 9.7: DISC1 relationship to microfilaments during SH-SY5Y differentiation

Differentiated SH-SY5Y cells were fixed in methanol and double-stained using antibodies for β-actin (green) and DISC1 (red). The nuclei were counterstained with DAPI (blue). Merged (left) and DISC1 only (right) images are shown.

A: DISC1 is present at the tips of developing neurites in a punctate pattern. Large puncta (arrow) possibly reflects increased energy demands of the cell within these regions.

B: DISC1 is restricted to the lamellipodium (arrow) and does not localise to filopodia (arrowheads).

9.4 DISC1 protein expression pattern during differentiation

A number of DISC1-related proteins were identified in human (chapter 5). It is likely that these proteins have different, yet unknown functions, therefore to determine if one of the DISC1-related proteins is preferentially involved in differentiation of the neuroblastoma cell lines, the DISC1 expression pattern was examined during differentiation. Protein analysis of the transformed cell lines and foetal brain tissue had shown that the levels of the DISC1-related bands were fairly uniform: the approximately 75kDa bands are most strongly detected with the 95kDa band being less strongly detected (Table 5.2).

A single well of a 6 well plate was removed every day during RA induced differentiation of LAN-5 cell lines (section 2.2.2.5). The cells were pelleted, protein lysates prepared in 10µl RIPA buffer (section 2.2.3.3), and the entire 10µl analysed by immunoblotting. The DISC1 anti-peptide antibody was incubated overnight as the resulting protein yield was expected to be low.

Neither the 95kDa or 80kDa and 75kDa DISC1-related bands are detected at any of the days examined (Figure 9.8), but replication is needed to determine if this is a genuine feature of the cells. During differentiation (days 2 – 7; Figure 9.8A), the predominant DISC1 protein detected is a potentially novel band of approximately 65kDa. The multiple bands detected (day 1; Figure 9.8A) at <75kDa are similar to the putative proteolytic products detected previously (section 5.2.3). However, it would be unwise to place too much emphasis on the findings, as the protein content of the samples, as determined by α-tubulin, is dramatically varied. This variation in tubulin content is likely to reflect lower than expected yield of protein, although the reason for this is not known. No DISC1 or α-tubulin signal is seen in the cells harvested before differentiation (day 0; Figure 9.8), though the DISC1 expression pattern is expected to be the same as that detected previously (Figure 4.6A). The day 1 sample does not show the novel DISC1 band but contains a high tubulin content, while in the day 7 sample, tubulin is virtually undetectable despite the presence of DISC1.

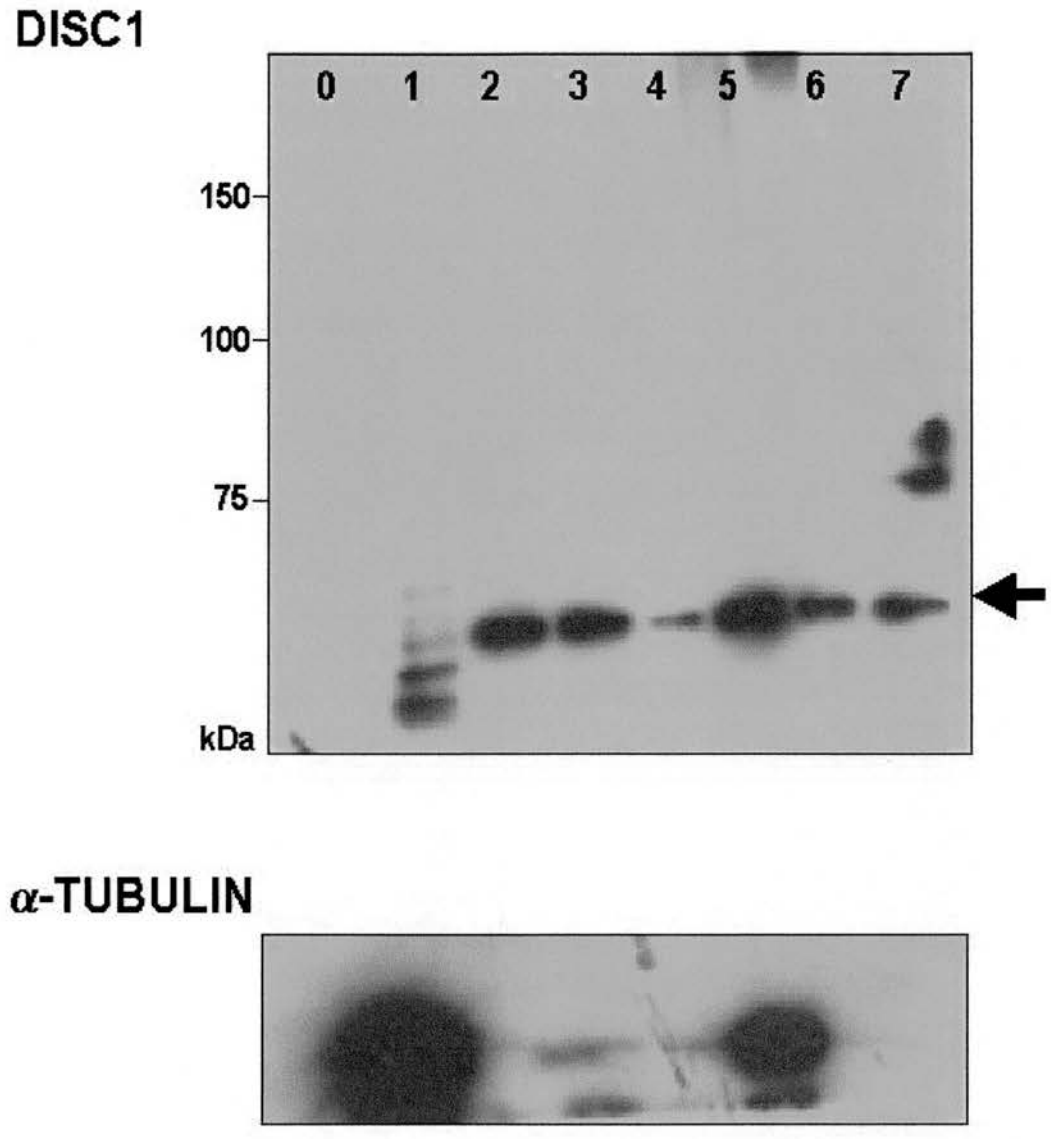

FIGURE 9.8: Identification of a novel DISC1-related band during RA induced differentiation of LAN-5 cells

Equivalent volumes of protein were loaded per lane and the blot probed consecutively using DISC1 anti-peptide (upper) and α-tubulin (lower) antibodies. 0: day 0, before addition of RA; 1 - 7: days 1 - 7 of RA differentiation. A potentially novel DISC1-related band of 65kDa (arrow) was detected from 2 – 7 days of differentiation.

9.5 Discussion

The differentiation of neuroblastoma cell lines provided an opportunity to examine DISC1 in a neuronal-like cell, therefore the initial aim of this study was to determine which differentiation strategy produced the most neuronal-like cell population. Sequential treatment of the SH-SY5Y cell line with RA and BDNF resulted in the most neuronal-like population of cells. The culture had the highest proportion of NF positive cells (39%; Table 9.1) with MAP2B expression in a subset of cells (Figure 9.2), suggesting there is neuronal differentiation towards a polarized cell type. Use of an axonal specific marker would allow the extent of polarization to be determined. In addition, the extensive network of cells formed in the SH-SY5Y BDNF treated cultures (Figure 9.3A) is consistent with the adoption of neuronal characteristics. However not all of the cells differentiated neuronally, as evidenced by NF expression, and prolonged culture (>12 days) may be needed to produce a fully homogenous neuronal cell population.

RA treatment of the SH-SY5Y cell line produced the least neuronal-like cultures, with few NF positive cells (9%; Table 9.1), no MAP2B staining (section 9.2.1) and no extensive network of cells forming (data not shown). There was a reduction in the number of NF positive cells as differentiation progressed (Table 9.1), likely due to the overgrowth of the culture with the epithelial-like cells (Figure 9.4). The absence of MAP2B staining may reflect the phenotype of the cells: as described earlier (section 9.1.2), RA treated SH-SY5Y cells differentiate along a sympathetic chromaffin lineage. Chromaffin cells are neuroendocrine cells and share features in common with neurons but do not polarize into dendritic and axonal compartments. MAP2 staining was observed in TPA treated SH-SY5Y cells (Meyerson *et al.*, 1994) and though not tested in the present study, utilization of this differentiating reagent may generate a more neuronal-like SH-SY5Y cell population than RA alone.

RA treatment of the LAN-5 cell line produced a differentiated cell population that was comparable in morphology to the BDNF treated SH-SY5Y culture. The cells formed an extensive network (Figure 9.3B), and a subset of the cells are MAP2B

positive (Figure 9.2). However as for the RA treated SH-SY5Y cell line, the number of cells expressing NF was reduced in the 7 day differentiated cell population, compared to the undifferentiated cell population (Table 9.1). The reason for this is unclear but unlike the RA treated SH-SY5Y cell line, the NF in the differentiated cell line is expressed in the neurites (data not shown), analogous to the BDNF treated SH-SY5Y cell line (Figure 9.1), suggesting there is differentiation to a more neuronal cell type with addition of RA. A possible explanation for the overall reduction in NF expression in the RA treated LAN-5 cell line may be related to the NF antibody, as the NF antibody detects the NF-H and NF-L forms of NF. It was previously reported (Encinas *et al.*, 2000) in the SH-SY5Y cell line that NF triplet expression changed during acquisition of a neuronal phenotype. It may be that the reduction in NF expression reflects the acquisition of NF-M in the cells. Alternatively it may suggest that RA treated LAN-5 cells do not differentiate to a homogenous neuronal cell population. Utilization of a more stable neuronal marker, such as neuron-specific enolase, may be better for determination of a neuronal cell.

As described (section 9.1.2), the RA treated LAN-5 cells are known to differentiate to a sympathetic cholinergic phenotype. The phenotype of the BDNF treated SH-SY5Y cell line has not been examined, though it would be expected to be of a sympathetic lineage. Examination of a neuronal cell type derived from the central rather than the peripheral nervous system may provide a better model system within which to study DISC1 function, due to the predicted dysfunction of CNS (central nervous system) cell types in psychiatric illness. Utilization of a CNS derived cell culture would require DISC1 to be examined in other species, such as rat or mouse, where cortical and hippocampal primary neurons are routinely cultured.

The redistribution of DISC1 from a predominantly peri-nuclear location to the shafts and tips of developing neurites (sections 9.3.1 – 9.3.3) is consistent with the localisation of DISC1 to mitochondria and provides further support for this relationship. The clustering of mitochondria at the base of the axon has been described (Mattson, 1999), and is consistent with the presence of DISC1 at the base of developing neurites (Figure 9.5A). Furthermore movement of mitochondria along

axons and dendrites is well studied (Hollenbeck, 1996; Overly *et al.*, 1996), as is their presence at growth cones (Morris and Hollenbeck, 1993; Dent *et al.*, 1999). DISC1 is definitely localised to tubulin growth cone-like structures (Figure 9.6) including both putative looped, pausing growth cones and flattened, active growth cones. The observed preferential association of DISC1 to tubulin, rather than actin associated structures (section 9.3.2), is consistent with a study (Morris and Hollenbeck, 1995) which found mitochondria do not move into neurites containing microfilaments only, but will move into neurites containing microtubules only. Direct colocalisation of DISC1 and mitochondria in differentiated SH-SY5Y cells was confirmed (K.Millar, personal communication).

The localisation of DISC1 to sites of synapse formation could not be studied (section 9.3.4), but this may reflect the phenotype of the differentiated cells (RA treated SH-SY5Y cell line), rather than the antibody. Examination of synaptotagmin expression in the definitely neuronal-like BDNF treated SH-SY5Y cell line would be more suitable as it is not clear how neuronal the RA treated SH-SY5Y cells are. Nevertheless, synaptotagmin has previously been detected in undifferentiated SH-SY5Y cells (Goodall *et al.*, 1997). Localisation of DISC1 to the synapse is important, as schizophrenia at least, is believed to be a disorder related to synaptic defects (section 1.3.3.2).

The identification of a potentially novel DISC1-related protein during RA induced differentiation of the LAN-5 cell line (Figure 9.8) is intriguing, though the experiment would need to be replicated, to ensure the validity of the result. The translation of a specific protein during neuronal differentiation would imply a role for this unidentified DISC1 protein in neurite outgrowth, though no such protein was reported in differentiated rat PC12 cells (Ozeki *et al.*, 2003). As for the protein identification of the other DISC1-related bands (section 5.4), possibilities for the production of an alternative protein include translation of an unidentified DISC1 transcript, or modification and processing of the translated DISC1 protein.

The use of differentiated neuroblastoma cells provides the opportunity to study the function of DISC1, and its relationship to the mitochondria, in an easily manipulated neuronal-like cell. As development of the nervous system is believed to be important to the subsequent dysfunction associated with schizophrenia, investigation of DISC1 in processes such as neurite outgrowth and synapse formation will be of value.

CHAPTER 10

CONCLUDING REMARKS AND FUTURE WORK

10. Concluding remarks & future work

10.1 Summary

At the time of starting this project, *DISC1* had been identified from a translocation breakpoint associated with psychiatric illness in a large Scottish family, and was thus being investigated within the group as a candidate gene for psychiatric illness. *In-silico* studies had been performed on DISC1, but had shed few clues to the function of DISC1 *in-vivo*. Therefore the main aim of this thesis was to generate DISC1 antibodies and to begin investigations into the function of DISC1.

To this end, an anti-peptide antibody was produced (chapter 3) which has been shown to be highly specific for endogenous and exogenous DISC1 (chapter 4). A number of protein species of DISC1 were identified in human (chapter 5), explained in part but not completely by current knowledge about *DISC1* transcripts. Preliminary investigations into the consequence of the translocation on *DISC1* suggest the disease causing mechanism is due to haploinsufficiency (chapter 6). In addition, the relationship between DISC1 and a number of cellular compartments was determined (chapter 8). The subcellular localisation of DISC1 was also examined during differentiation of neuroblastoma cells (chapter 9).

In addition, an anti-protein antibody was also generated (chapter 3), though there are concerns about the reliability of this antibody (chapter 4). In comparison to the DISC1 expression pattern in human, only a single DISC1 isoform was identified in mouse and rat (chapter 7). Thus the development of DISC1 antibodies and the data presented within this thesis has begun to provide insights into endogenous DISC1.

10.2 Generation of DISC1 specific antibodies

10.2.1 Concluding remarks

Anti-peptide and anti-protein antibodies were generated to the N-terminus of DISC1 to ensure detection of all known DISC1 proteins. The generation of two antibodies was to maximize the chance of an informative antibody and to enable validation of the antibody signals. As nothing was known about endogenous DISC1, characterisation of the antibodies was paramount. Consequently, the anti-peptide antibody has proved to be the most informative and reliable in all techniques tested, including immunohistochemistry (data not shown).

Although the development of each and every antibody involves an element of chance, with unknown variables being involved at every stage of production, from the work performed for this thesis, I see no advantage in adopting the more time consuming approach of generating recombinant protein for use as the antigen. The increased cost of producing several anti-peptide antibodies was a disadvantage to the generation of multiple anti-peptide antibodies, yet the cost can be minimized by immunization of more than one peptide at once into the same animal.

The development of a specific antibody is hindered by the possibility of cross-reactions between the antibody and unknown proteins. With anti-peptide antibodies this risk is increased due to the reduced size of the immunizing agent. Cross-reactions identified on immunoblots pose considerable interpretation problems for immunocytochemistry, especially as in the case of DISC1, when there is no prior knowledge about the cellular location of the protein. Indeed this was a concern for a long time with the anti-peptide antibody, and highlights the advantage of a negative control. The t(1;11) derived lymphoblastoid cell lines were useful in this respect, but were not available until the end of this project.

10.2.2 Future work

The generation of more DISC1 antibodies is needed and is being performed within the group. The need for selective isoform specific antibodies, rather than a generic antibody is now the focus. Consequently the selection of appropriate peptides will be simplified as the choice is limited to regions of the isoforms which differ (Figure 1.5). The need for extensive characterisation of these antibodies is not as necessary due to knowledge of the anticipated DISC1 expression pattern.

10.3 DISC1-related proteins in human

10.3.1. Concluding Remarks

Immunoblotting coupled to RT-PCR was used to determine the potential DISC1 isoforms detected in human. Human cell lines were used predominantly but a foetal brain sample was used as an reference for endogenous expression. The anti-peptide antibody generated in this project was the most informative antibody, although additional anti-protein antibodies were used to confirm (or not) the proteins detected. Three major DISC1-related proteins of 95kDa, 80kDa and 75kDa were identified, with a doublet of the 75kDa protein also reported. Furthermore RT-PCR detected the L, Lv and S1 transcripts in all cell lines. Due to the detection of three bands of similar size at approximately 75kDa, it was not possible to absolutely identify the S1 isoform.

Although all DISC1-related proteins detected by the anti-peptide antibody are likely to be real (chapter 6), only the 75kDa and 100kDa proteins were ever confirmed by either of the other two antibodies. With no knowledge regarding the epitopes these antibodies detect, it is difficult to ascertain if this is due to the composition of the proteins, and is therefore an informative result, or if this is due to the affinity of the antibodies. Furthermore the proteolytic degradation observed in the cell line protein extracts, hampered interpretation of genuine DISC1 proteins. Subsequent work within the group has found the lower band of the 75kDa doublet to be the predominant DISC1 isoform in mitochondria (K.Millar, personal communication),

yet the possibility this protein was a breakdown product could not be excluded from the present study.

10.3.2 Future Work

Determining the identity of the human DISC1 proteins is a priority. The development of isoform specific antibodies for the L, Lv and S1 proteins is underway. Nonetheless, current transcription data cannot account for two of the approximately 75kDa proteins, therefore at present it seems likely these proteins represent alternative forms of the full-length isoforms. Two likely suggestions include use of alternative translation initiation sites and protein cleavage. The development of full-length constructs with the downstream translation initiation sites mutated would address the first suggestion. The use of downstream translation initiation sites was reported to be unlikely (Kozak, 1996), yet alternative translation initiation sites have contributed to the protein diversity of the WT1 protein (Scharnhorst *et al.*, 1999), and post-transcriptional modification of *WT1* produces at least 24 different protein isoforms (Wagner *et al.*, 2003). Furthermore two DISC1 promoters were predicted from *in-silico* data, and the use of alternative promoters has been reported as a possible mechanism to utilize alternative downstream translation initiation sites (Ayoubi and Van De Ven, 1996). The second suggestion is related to cleavage of the full-length DISC1 protein. Numerous protease cleavage sites are identified within DISC1, therefore the inhibition of potential proteases may not be a simple task to investigate.

Complementary techniques for determining the proteins detected by immunoblotting include immunoprecipitation coupled to mass spectrometry and cell culture experiments examining the effect of knocking out or knocking down the transcripts. The latter would be a time consuming process by conventional gene targeting strategies, and the reduced time scale afforded by RNAi may be a more suitable approach (Hudson *et al.*, 2002).

10.4 DISC1 protein expression levels in lymphoblastoid cell lines derived from t(1;11) family members

10.4.1 Concluding Remarks

Lymphoblastoid cell lines derived from t(1;11) family members offered an opportunity to examine the effect of the translocation on DISC1. The reduction in DISC1 expression levels and lack of truncated protein suggest the development of illness is associated with reduced levels of DISC1. Though there are some concerns about relating DISC1 expression in lymphoblastoid cell lines to the brain, no difference in DISC1 expression has been detected in a wide range of cell lines. Furthermore platelets, another component of peripheral blood, are well studied for their involvement in determining biochemical changes within the brain (Camacho and Dimsdale, 2000).

10.4.2 Future Work

The lack of a truncated protein in t(1;11) carriers will focus subsequent animal models of DISC1. The best approach would be either to knock-down DISC1 to similar levels found in t(1;11) carriers or alternatively model the translocation using *Cre-loxP* gene targeting strategies (Smith *et al.*, 1995). The *Cre-loxP* site-specific recombination system provides a powerful means for exactly recapitulating human chromosomal rearrangements in the mouse (Yu and Bradley, 2001). The P300 amplitude and latency is reduced in all translocation carriers including those with no evidence of a psychiatric disturbance (Blackwood *et al.*, 2001), therefore the functional suitability of a DISC1 transgenic mouse could be determined by measurement of the P300 ERP (Ehlers and Somes, 2002). Replication for the involvement of DISC1 in independent psychiatric populations is a must, and from the protein level, will include examining DISC1 expression levels in brain tissue from collections such as the Stanley Foundation.

10.5 DISC1-related proteins in mouse and rat

10.5.1 Concluding Remarks

Generation of the anti-protein antibody provided a means to investigate DISC1 in other species, due to the potential for cross-reactivity of this antibody with DISC1 orthologues. In various mouse tissue and rat brain, a full-length DISC1 isoform of approximately 100kDa was detected in adult brain only. A protein of 120kDa was also detected in mouse heart.

The data generated in this project shows considerable differences to data already published (Ozeki *et al.*, 2003), and work subsequently performed in this group (data not shown). There are a number of caveats to the suitability of the strategy adopted. Firstly, considerable characterisation of both DISC1 antibodies for human DISC1 was performed, whereas no such characterisation was performed to determine the specificity of the anti-protein antibody for mouse or rat DISC1. Secondly the anti-protein antibody has been found to be unreliable for interpretation of human DISC1. Though due to some unknown factor, it appeared to be reliable for detection of mouse and rat DISC1, the results should be viewed with some caution until there is independent confirmation. Thirdly, the considerable lack of DISC1 protein conservation between human and mouse or rat poses problems, again especially as the epitopes recognised by the anti-protein antibody are not known. Despite this the predicted size difference between rat and mouse DISC1 was detected by the anti-protein antibody suggesting at least this protein is definitely DISC1. Therefore it is a mystery why this full-length protein has not been detected in the other tissue samples, as has been found with use of a mouse specific anti-peptide antibody (data not shown).

10.5.2 Future work

The examination of DISC1 in mouse and rat is a must due to the limitations of work in humans. The development of species specific antibodies is underway. The use of a model system offers many opportunities for determining the function of DISC1.

The development of transgenic mice will be invaluable in determining the function of DISC1, with reduction (section 10.4.2) and overexpression of DISC1 allowing complementary phenotypes to be examined. The use of promoters with restricted or inducible expression would allow DISC1 function to be examined in a temporally and spatially controlled manner. The promoter of the *Camk2a* gene would be one suitable promoter, with restricted expression in the postnatal mouse forebrain (Dragatsis *et al.*, 2000), a region likely to be important in the pathogenesis of schziophrenia (section 1.3.2).

Moreover, cell culture studies in human are limited and necessitate the move to primary and organotypic cultures. Although the use of human primary and organotypic cultures is reported (Bakhiet *et al.*, 2001; Letinic and Rakic, 2001), the regulations surrounding this type of work make it very prohibitive. The differentiation of human neuroblastoma cell lines, suggest the end phenotype may not be particularly representative of CNS-derived neurons, therefore the need to examine DISC1 in a more functionally relevant cell type, such as hippocampal or cortical primary cultures, is necessary.

10.6 Subcellular localisation of DISC1

10.6.1 Concluding Remarks

The subcellular location of DISC1 was determined by systematic examination of the relationship between DISC1 and various cellular organelles or compartments. In addition the intracellular distribution of DISC1 in differentiated neuroblastoma cell lines was examined. Use of differentiated neuroblastoma cell lines enabled DISC1 to be examined in a more functionally relevant cell type. DISC1 was found to adopt a predominantly mitochondrial location, supported directly by colocalisation with mitochondrial markers and also indirectly by its relationship with the cytoskeleton and intracellular distribution during neuroblastoma differentiation.

The initial conclusion from these studies had been that DISC1 was cytoskeletal. Though correct in light of the known interaction between mitochondria and the

cytoskeleton, the mitochondrial localisation of DISC1 only became known at the end of this project and thereby prevented this relationship from being examined further.

10.6.2 Future work

The mitochondrial localisation of DISC1 is confirmed by two DISC1 antibodies generated to opposite ends of the protein: the N-terminal anti-peptide antibody and the C-terminal anti-protein antibody, suggesting this is the predominant cellular location (discussed below). Subcellular fractionation would be an obvious next step to confirm the mitochondrial location of DISC1. Specific elucidation of DISC1 function in mitochondria will require knowledge of interacting proteins, a task which is being undertaken concurrently within the group, and a move into more amenable and functionally relevant culture systems (section 10.5.2).

Nonetheless, the most important prerequisite for determining the function of DISC1 appears to be teasing out the identification and function of the DISC1 protein isoforms, as initial data from the lab suggests DISC1 is not wholly mitochondrial (K.Millar, personal communication). Development of tagged constructs for the full-length L, Lv and S1 isoforms would enable the independent locations of these proteins to be studied in complementation to the development of antibodies (section 10.2.2).

It will also be of interest to determine how similar yet distinct proteins are targeted to different cellular regions. It is intriguing in this respect that the C-termini show the most pronounced differences between the isoforms. The presence or absence of certain protein-protein interaction domains may alter the interaction between DISC1 and proteins important for cellular targeting such as transport and anchoring proteins. Furthermore the 3'UTR of a transcript is known to be important for subcellular targeting (Conne *et al.*, 2000), and as two of the *DISC1* transcripts utilize alternative 3'UTRs, such a role may prove to be of relevance. Finally the only functionally conserved motif identified in DISC1 was an N-terminal NLS. Although no evidence for DISC1 nuclear localisation was observed, the nuclear targeting of adenomatous

polyposis coli (APC), another multi-compartmentalized protein, was found to be dependent on the phosphorylation status of the NLS (Bienz, 2002). Thus the subcellular targeting of a protein is complex and likely to be mediated by many factors. To begin to investigate subcellular targeting of DISC1, the easiest strategy may be to develop a panel of DISC1 constructs with different N- and C- terminal contributions, although multiple lines of investigation could be pursued.

In conclusion, the generation of DISC1 antibodies and the preliminary investigations of DISC1 presented within this thesis have provided the initial stepping stones for further investigations into the function of DISC1, and its involvement in the aetiology of psychiatric illness.

REFERENCES

References

Andreasen, N. C. (1995). Symptoms, signs, and diagnosis of schizophrenia. Lancet *346*, 477-481.

Andreasen, N. C., O'Leary, D. S., Cizadlo, T., Arndt, S., Rezai, K., Ponto, L. L., Watkins, G. L., and Hichwa, R. D. (1996). Schizophrenia and cognitive dysmetria: a positron-emission tomography study of dysfunctional prefrontal-thalamic-cerebellar circuitry. Proc Natl Acad Sci U S A *93*, 9985-9990.

Andrieux, A., Salin, P. A., Vernet, M., Kujala, P., Baratier, J., Gory-Faure, S., Bosc, C., Pointu, H., Proietto, D., Schweitzer, A., Denarier, E., Klumperman, J., and Job, D. (2002). The suppression of brain cold-stable microtubules in mice induces synaptic defects associated with neuroleptic-sensitive behavioral disorders. Genes Dev *16*, 2350-2364.

Aoki, K., Ishida, R., and Kasai, M. (1997). Isolation and characterization of a cDNA encoding a Translin-like protein, TRAX. FEBS Lett *401*, 109-112.

Arregui, C. O., Balsamo, J., and Lilien, J. (1998). Impaired integrin-mediated adhesion and signaling in fibroblasts expressing a dominant-negative mutant PTP1B. J Cell Biol *143*, 861-873.

Ayoubi, T. A., and Van De Ven, W. J. (1996). Regulation of gene expression by alternative promoters. Faseb J *10*, 453-460.

Baas, P. W., Pienkowski, T. P., Cimbalnik, K. A., Toyama, K., Bakalis, S., Ahmad, F. J., and Kosik, K. S. (1994). Tau confers drug stability but not cold stability to microtubules in living cells. J Cell Sci *107*, 135-143.

Baas, P. W. (1999). Microtubules and neuronal polarity: lessons from mitosis. Neuron *22*, 23-31.

Badner, J. A., and Gershon, E. S. (2002). Meta-analysis of whole-genome linkage scans of bipolar disorder and schizophrenia. Mol Psychiatry *7*, 405-411.

Bakhiet, M., Tjernlund, A., Mousa, A., Gad, A., Stromblad, S., Kuziel, W. A., Seiger, A., and Andersson, J. (2001). RANTES promotes growth and survival of human first-trimester forebrain astrocytes. Nat Cell Biol *3*, 150-157.

Bassett, A. S. (1992). Chromosomal aberrations and schizophrenia. Autosomes. Br J Psychiatry *161*, 323-334.

Baumann, B., and Bogerts, B. (1999). The pathomorphology of schizophrenia and mood disorders: similarities and differences. Schizophr Res *39*, 141-148.

Ben-Shachar, D. (2002). Mitochondrial dysfunction in schizophrenia: a possible linkage to dopamine. J Neurochem *83*, 1241-1251.

Bereiter-Hahn, J. (1990). Behavior of mitochondria in the living cell. Int Rev Cytol *122*, 1-63.

Berrettini, W. H. (2000). Are schizophrenic and bipolar disorders related? A review of family and molecular studies. Biol Psychiatry *48*, 531-538.

Bienz, M. (2002). The subcellular destinations of APC proteins. Nat Rev Mol Cell Biol *3*, 328-338.

Blackwood, D. (2000). P300, a state and a trait marker in schizophrenia. Lancet *355*, 771-772.

Blackwood, D. H., Fordyce, A., Walker, M. T., St Clair, D. M., Porteous, D. J., and Muir, W. J. (2001). Schizophrenia and affective disorders--cosegregation with a translocation at chromosome 1q42 that directly disrupts brain-expressed genes: clinical and P300 findings in a family. Am J Hum Genet *69*, 428-433.

Bosc, C., Frank, R., Denarier, E., Ronjat, M., Schweitzer, A., Wehland, J., and Job, D. (2001). Identification of novel bifunctional calmodulin-binding and microtubule- stabilizing motifs in STOP proteins. J Biol Chem *276*, 30904-30913.

Bradford, A. D., Terris, J. M., Ecelbarger, C. A., Klein, J. D., Sands, J. M., Chou, C. L., and Knepper, M. A. (2001). 97- and 117-kDa forms of collecting duct urea transporter UT-A1 are due to different states of glycosylation. Am J Physiol Renal Physiol *281*, F133-143.

Brown, R. G., and Pluck, G. (2000). Negative symptoms: the 'pathology' of motivation and goal-directed behaviour. Trends Neurosci *23*, 412-417.

Bustin, S. A. (2000). Absolute quantification of mRNA using real-time reverse transcription polymerase chain reaction assays. J Mol Endocrinol *25*, 169-193.

Camacho, A., and Dimsdale, J. E. (2000). Platelets and psychiatry: lessons learned from old and new studies. Psychosom Med *62*, 326-336.

Cambray-Deakin, M. A., Robson, S. J., and Burgoyne, R. D. (1988). Colocalisation of acetylated microtubules, glial filaments, and mitochondria in astrocytes in vitro. Cell Motil Cytoskeleton *10*, 438-449.

Cannon, T. D. (1996). Abnormalities of brain structure and function in schizophrenia: implications for aetiology and pathophysiology. Ann Med *28*, 533-539.

Carlsson, A., Waters, N., Holm-Waters, S., Tedroff, J., Nilsson, M., and Carlsson, M. L. (2001). Interactions between monoamines, glutamate, and GABA in schizophrenia: new evidence. Annu Rev Pharmacol Toxicol *41*, 237-260.

Carson, J. H., Worboys, K., Ainger, K., and Barbarese, E. (1997). Translocation of myelin basic protein mRNA in oligodendrocytes requires microtubules and kinesin. Cell Motil Cytoskeleton *38*, 318-328.

Chua, S. E., and Murray, R. M. (1996). The neurodevelopmental theory of schizophrenia: evidence concerning structure and neuropsychology. Ann Med *28*, 547-555.

Ciccarone, V., Spengler, B. A., Meyers, M. B., Biedler, J. L., and Ross, R. A. (1989). Phenotypic diversification in human neuroblastoma cells: expression of distinct neural crest lineages. Cancer Res *49*, 219-225.

Conne, B., Stutz, A., and Vassalli, J. D. (2000). The 3' untranslated region of messenger RNA: A molecular 'hotspot' for pathology? Nat Med *6*, 637-641.

Crino, P. B., and Eberwine, J. (1996). Molecular characterization of the dendritic growth cone: regulated mRNA transport and local protein synthesis. Neuron *17*, 1173-1187.

da Silva, J. S., and Dotti, C. G. (2002). Breaking the neuronal sphere: regulation of the actin cytoskeleton in neuritogenesis. Nat Rev Neurosci *3*, 694-704.

Denarier, E., Fourest-Lieuvin, A., Bosc, C., Pirollet, F., Chapel, A., Margolis, R. L., and Job, D. (1998). Nonneuronal isoforms of STOP protein are responsible for microtubule cold stability in mammalian fibroblasts. Proc Natl Acad Sci USA *95*, 6055-6060.

Dent, E. W., Callaway, J. L., Szebenyi, G., Baas, P. W., and Kalil, K. (1999). Reorganization and movement of microtubules in axonal growth cones and developing interstitial branches. J Neurosci *19*, 8894-8908.

Devon, R. S., Evans, K. L., Maule, J. C., Christie, S., Anderson, S., Brown, J., Shibasaki, Y., Porteous, D. J., and Brookes, A. J. (1997). Novel transcribed sequences neighbouring a translocation breakpoint associated with schizophrenia. Am J Med Genet *74*, 82-90.

Devon, R. S., Anderson, S., Teague, P. W., Muir, W. J., Murray, V., Pelosi, A. J., Blackwood, D. H., and Porteous, D. J. (2001). The genomic organisation of the metabotropic glutamate receptor subtype 5 gene, and its association with schizophrenia. Mol Psychiatry *6*, 311-314.

Dragatsis, I., Levine, M. S., and Zeitlin, S. (2000). Inactivation of Hdh in the brain and testis results in progressive neurodegeneration and sterility in mice. Nat Genet *26*, 300-306.

Ehlers, C. L., and Somes, C. (2002). Long latency event-related potentials in mice: effects of stimulus characteristics and strain. Brain Res *957*, 117-128.

Ekelund, J., Hovatta, I., Parker, A., Paunio, T., Varilo, T., Martin, R., Suhonen, J., Ellonen, P., Chan, G., Sinsheimer, J. S., *et al.* (2001). Chromosome 1 loci in Finnish schizophrenia families. Hum Mol Genet *10*, 1611-1617.

Ekelund, J. (2002). Talk presented at Xth World Congress on Psychiatric Genetics (Brussels).

Elbashir, S. M., Harborth, J., Lendeckel, W., Yalcin, A., Weber, K., and Tuschl, T. (2001). Duplexes of 21-nucleotide RNAs mediate RNA interference in cultured mammalian cells. Nature *411*, 494-498.

Elseth, G. D., and Baumgardner (1995). Principles of modern genetics (St.Paul, Minneapolis, West Publishing Company), Chromosome mutations pp.266-267 Cellular & molecular approaches to mapping pp.343-344.

Encinas, M., Iglesias, M., Liu, Y., Wang, H., Muhaisen, A., Cena, V., Gallego, C., and Comella, J. X. (2000). Sequential treatment of SH-SY5Y cells with retinoic acid and brain-derived neurotrophic factor gives rise to fully differentiated, neurotrophic factor-dependent, human neuron-like cells. J Neurochem *75*, 991-1003.

Feng, Z., and Porter, A. G. (1999). NF-kappaB/Rel proteins are required for neuronal differentiation of SH- SY5Y neuroblastoma cells. J Biol Chem *274*, 30341-30344.

Fiez, J. A. (1996). Cerebellar contributions to cognition. Neuron *16*, 13-15.

Finkenstadt, P. M., Kang, W. S., Jeon, M., Taira, E., Tang, W., and Baraban, J. M. (2000). Somatodendritic localization of Translin, a component of the Translin/Trax RNA binding complex. J Neurochem *75*, 1754-1762.

Finkenstadt, P. M., Jeon, M., and Baraban, J. M. (2002). Trax is a component of the Translin-containing RNA binding complex. J Neurochem *83*, 202-210.

Fletcher, J. M., Evans, K., Baillie, D., Byrd, P., Hanratty, D., Leach, S., Julier, C., Gosden, J. R., Muir, W., Porteous, D. J., St.Clair, D., and van Heyningen, V. (1993). Schizophrenia-associated chromosome 11q21 translocation: identification of flanking markers and development of chromosome 11q fragment hybrids as cloning and mapping resources. Am J Hum Genet *52*, 478-490.

Ford, J. M. (1999). Schizophrenia: the broken P300 and beyond. Psychophysiology *36*, 667-682.

Freedman, R., Coon, H., Myles-Worsley, M., Orr-Urtreger, A., Olincy, A., Davis, A., Polymeropoulos, M., Holik, J., Hopkins, J., Hoff, M., *et al.* (1997). Linkage of a neurophysiological deficit in schizophrenia to a chromosome 15 locus. Proc Natl Acad Sci U S A *94*, 587-592.

Freeman, W. M., Walker, S. J., and Vrana, K. E. (1999). Quantitative RT-PCR: pitfalls and potential. Biotechniques *26*, 112-122, 124-115.

Friel, D. D. (2000). Mitochondria as regulators of stimulus-evoked calcium signals in neurons. Cell Calcium *28*, 307-316.

Frith, C. (1995). Functional imaging and cognitive abnormalities. Lancet *346*, 615-620.

Fuster, J. M. (2001). The prefrontal cortex-an update. time is of the essence. Neuron *30*, 319-333.

Gainetdinov, R. R., Mohn, A. R., and Caron, M. G. (2001). Genetic animal models: focus on schizophrenia. Trends Neurosci *24*, 527-533.

Glatt, C. E., and Freimer, N. B. (2002). Association analysis of candidate genes for neuropsychiatric disease: the perpetual campaign. Trends Genet *18*, 307-312.

Goodall, A. R., Dank, K., Walker, J. H., Ball, S. G., and Vaughan, P. F. T. (1997). Occurrence of two types of secretory vesicles in the human neuroblastoma SH-SY5Y. J Neurochem *68*, 1542-1552.

Guarneri, P., Cascio, C., Piccoli, T., Piccoli, F., and Guarneri, R. (2000). Human neuroblastoma SH-SY5Y cell line: neurosteroid-producing cell line relying on cytoskeletal organization. J Neurosci Res *60*, 656-665.

Hakak, Y., Walker, J. R., Li, C., Wong, W. H., Davis, K. L., Buxbaum, J. D., Haroutunian, V., and Fienberg, A. A. (2001). Genome-wide expression analysis reveals dysregulation of

myelination-related genes in chronic schizophrenia. Proc Natl Acad Sci U S A *98*, 4746-4751.

Harlow, E., and Lane, D. (1988). Antibodies: a laboratory manual. (CSHL Press, Cold Spring Harbor, New York). Immunizations (a) pp.72-73 (b) p.76 (c) p.77.

Harlow, E., and Lane, D. (1999). Using antibodies: a laboratory manual. (CSHL Press, Cold Spring Harbor, New York). (a) Electrophoresis pp.410-411 (b) Protein techniques p.451 (c) Handling antibodies pp.77-80.

Harrison, P. J. (1999). The neuropathology of schizophrenia. A critical review of the data and their interpretation. Brain *122*, 593-624.

Hartl, F. U., and Neupert, W. (1990). Protein sorting to mitochondria: evolutionary conservations of folding and assembly. Science *247*, 930-938.

Hayes, C., Cothliff, R., Heavens, R., Smith, D., Camargo, L. M., Ma, L., Myers, J., Buchanan, K., Morris, J. A., Siranthsinghji, D. S. S., Rosahl, T. W., and Whiting, P.W. (2002). Dose-dependent embryonic lethality associated with over expression of a truncated *Disrupted In Schizophrenia* (*DISC1*) transgene in mice. Paper presented at Mouse Molecular Genetics 2002 (Cold Spring Harbor, New York).

Heyman, I., and Murray, R. M. (1992). Schizophrenia and neurodevelopment. J R Coll Physicians Lond *26*, 143-146.

Hill, D. P., and Robertson, K. A. (1997). Characterization of the cholinergic neuronal differentiation of the human neuroblastoma cell line LA-N-5 after treatment with retinoic acid. Brain Res Dev Brain Res *102*, 53-67.

Hill, D. P., and Robertson, K. A. (1998). Differentiation of LA-N-5 neuroblastoma cells into cholinergic neurons: methods for differentiation, immunohistochemistry and reporter gene introduction. Brain Res Brain Res Protoc *2*, 183-190.

Hollenbeck, P. J. (1996). The pattern and mechanism of mitochondrial transport in axons. Front Biosci *1*, d91-d102.

Hudson, D. F., Morrison, C., Ruchaud, S., and Earnshaw, W. C. (2002). Reverse genetics of essential genes in tissue-culture cells: 'dead cells talking'. Trends Cell Biol *12*, 281-287.

Hyman, S. (2000). Mental illness: genetically complex disorders of neural circuitry and neural communication. Neuron *28*, 321-323.

Jameson, B. A., and Wolf, H. (1988). The antigenic index: a novel algorithm for predicting antigenic determinants. Comput Appl Biosci *4*, 181-186.

Jurewicz, I., Owen, R. J., O'Donovan, M. C., and Owen, M. J. (2001). Searching for susceptibility genes in schizophrenia. Eur Neuropsychopharmacol *11*, 395-398.

Kane, J. M., and McGlashan, T. H. (1995). Treatment of schizophrenia. Lancet *346*, 820-825.

Karayiorgou, M., and Gogos, J. A. (1997). A turning point in schizophrenia genetics. Neuron *19*, 967-979.

Katsetos, C. D., Hyde, T. M., and Herman, M. M. (1997). Neuropathology of the cerebellum in schizophrenia--an update: 1996 and future directions. Biol Psychiatry *42*, 213-224.

Knable, M. B. (1999). Schizophrenia and bipolar disorder: findings from studies of the Stanley Foundation Brain Collection. Schizophr Res *39*, 149-152.

Knable, M. B., Torrey, E. F., Webster, M. J., and Bartko, J. J. (2001). Multivariate analysis of prefrontal cortical data from the Stanley Foundation Neuropathology Consortium. Brain Res Bull *55*, 651-659.

Kobayashi, S., Takashima, A., and Anzai, K. (1998). The dendritic translocation of translin protein in the form of BC1 RNA protein particles in developing rat hippocampal neurons in primary culture. Biochem Biophys Res Commun *253*, 448-453.

Kolaskar, A. S., and Tongaonkar, P. C. (1990). A semi-empirical method for prediction of antigenic determinants on protein antigens. FEBS Lett *276*, 172-174.

Kostyuk, P. G., Shmigol, A. V., Voitenko, N. V., Svichar, N. V., and Kostyuk, E. P. (2000). The endoplasmic reticulum and mitochondria as elements of the mechanism of intracellular signaling in the nerve cell. Neurosci Behav Physiol *30*, 15-18.

Kozak, M. (1996). Interpreting cDNA sequences: some insights from studies on translation. Mamm Genome *7*, 563-574.

Lanciotti, M., Montaldo, P. G., Folghera, S., Lucarelli, E., Cornaglia-Ferraris, P., and Ponzoni, M. (1992). A combined evaluation of biochemical and morphological changes during human neuroblastoma cell differentiation. Cell Mol Neurobiol *12*, 225-240.

Lander, E. S., and Schork, N. J. (1994). Genetic dissection of complex traits. Science *265*, 2037-2048.

Lander, E., and Kruglyak, L. (1995). Genetic dissection of complex traits: guidelines for interpreting and reporting linkage results. Nat Genet *11*, 241-247.

Lawrie, S. M., Whalley, H., Kestelman, J. N., Abukmeil, S. S., Byrne, M., Hodges, A., Rimmington, J. E., Best, J. J., Owens, D. G., and Johnstone, E. C. (1999). Magnetic resonance imaging of brain in people at high risk of developing schizophrenia. Lancet *353*, 30-33.

Leboyer, M., Bellivier, F., Nosten-Bertrand, M., Jouvent, R., Pauls, D., and Mallet, J. (1998). Psychiatric genetics: search for phenotypes. Trends Neurosci *21*, 102-105.

Letinic, K., and Rakic, P. (2001). Telencephalic origin of human thalamic GABAergic neurons. Nat Neurosci *4*, 931-936.

Lewis, D. A. (2000). Is there a neuropathology of schizophrenia? Recent findings converge on altered thalamic-prefrontal cortical connectivity. The Neuroscientist *6*, 208-218.

Lewis, D. A., and Lieberman, J. A. (2000). Catching up on schizophrenia: natural history and neurobiology. Neuron *28*, 325-334.

Ma, L., Liu, Y., Ky, B., Shughrue, P. J., Austin, C. P., and Morris, J. A. (2002). Cloning and Characterization of *Disc1*, the Mouse Ortholog of DISC1 (Disrupted-in-Schizophrenia 1). Genomics *80*, 662-672.

MacIntyre, D. J., Blackwood, D. H., Porteous, D. J., Pickard, B. S., and Muir, W. J. (2003). Chromosomal abnormalities and mental illness. Mol Psychiatry *8*, 275-287.

Magni, P., Beretta, E., Scaccianoce, E., and Motta, M. (2000). Retinoic acid negatively regulates neuropeptide Y expression in human neuroblastoma cells. Neuropharmacology *39*, 1628-1636.

Makrides, S. C. (1996). Strategies for achieving high-level expression of genes in Escherichia coli. Microbiol Rev *60*, 512-538.

Marchbanks, R. M., Mulcrone, J., and Whatley, S. A. (1995). Aspects of oxidative metabolism in schizophrenia. Br J Psychiatry *167*, 293-298.

Mattson, M. P. (1999). Establishment and plasticity of neuronal polarity. J Neurosci Res *57*, 577-589.

Mattson, M. P., LaFerla, F. M., Chan, S. L., Leissring, M. A., Shepel, P. N., and Geiger, J. D. (2000). Calcium signaling in the ER: its role in neuronal plasticity and neurodegenerative disorders. Trends Neurosci *23*, 222-229.

McCarley, R. W., Wible, C. G., Frumin, M., Hirayasu, Y., Levitt, J. J., Fischer, I. A., and Shenton, M. E. (1999). MRI anatomy of schizophrenia. Biol Psychiatry *45*, 1099-1119.

McGinnis, R. E., Fox, H., Yates, P., Cameron, L. A., Barnes, M. R., Gray, I. C., Spurr, N. K., Hurko, O., and St Clair, D. (2001). Failure to confirm NOTCH4 association with schizophrenia in a large population-based sample from Scotland. Nat Genet *28*, 128-129.

McGuffin, P., Owen, M. J., and Farmer, A. E. (1995). Genetic basis of schizophrenia. Lancet *346*, 678-682.

McLean, P. J., Kawamata, H., and Hyman, B. T. (2001). α-synuclein-enhanced green fluorescent protein fusion proteins form proteasome sensitive inclusions in primary neurons. Neuroscience *104*, 901-912.

Meyerson, G., Parrow, V., Gestblom, C., Johansson, I., and Pahlman, S. (1994). Protein synthesis and mRNA in isolated growth cones from differentiating SH-SY5Y neuroblastoma cells. J Neurosci Res *37*, 303-312.

Millar, J. K., Brown, J., Maule, J. C., Shibasaki, Y., Christie, S., Lawson, D., Anderson, S., Wilson-Annan, J. C., Devon, R. S., St Clair, D. M., Blackwood, D. H. R., Muir, W. J., and Porteous, D. J. (1998). A long-range restriction map across 3 Mb of the chromosome 11 breakpoint region of a translocation linked to schizophrenia: localization of the breakpoint and the search for neighbouring genes. Psychiatr Genet *8*, 175-181.

Millar, J. K., Christie, S., Semple, C. A., and Porteous, D. J. (2000a). Chromosomal location and genomic structure of the human translin-associated factor X gene (TRAX; TSNAX) revealed by intergenic splicing to DISC1, a gene disrupted by a translocation segregating with schizophrenia. Genomics *67*, 69-77.

Millar, J. K., Wilson-Annan, J. C., Anderson, S., Christie, S., Taylor, M. S., Semple, C. A., Devon, R. S., Clair, D. M., Muir, W. J., Blackwood, D. H., and Porteous, D. J. (2000b). Disruption of two novel genes by a translocation co-segregating with schizophrenia. Hum Mol Genet *9*, 1415-1423.

Millar, J. K., Christie, S., Anderson, S., Lawson, D., Hsiao-Wei Loh, D., Devon, R. S., Arveiler, B., Muir, W. J., Blackwood, D. H., and Porteous, D. J. (2001). Genomic structure and localisation within a linkage hotspot of Disrupted In Schizophrenia 1, a gene disrupted by a translocation segregating with schizophrenia. Mol Psychiatry *6*, 173-178.

Mimmack, M. L., Ryan, M., Baba, H., Navarro-Ruiz, J., Iritani, S., Faull, R. L., McKenna, P. J., Jones, P. B., Arai, H., Starkey, M., Emson, P. C., and Bahn, S. (2002). Gene expression analysis in schizophrenia: reproducible up-regulation of several members of the apolipoprotein L family located in a high-susceptibility locus for schizophrenia on chromosome 22. Proc Natl Acad Sci U S A *99*, 4680-4685.

Mirnics, K., Middleton, F. A., Marquez, A., Lewis, D. A., and Levitt, P. (2000). Molecular characterization of schizophrenia viewed by microarray analysis of gene expression in prefrontal cortex. Neuron *28*, 53-67.

Miyamoto, Y., Yamada, K., Noda, Y., Mori, H., Mishina, M., and Nabeshima, T. (2001). Hyperfunction of dopaminergic and serotonergic neuronal systems in mice lacking the NMDA receptor epsilon1 subunit. J Neurosci *21*, 750-757.

Mizzen, L. A., Chang, C., Garrels, J. I., and Welch, W. J. (1989). Identification, characterization, and purification of two mammalian stress proteins present in mitochondria, grp 75, a member of the hsp 70 family and hsp 58, a homolog of the bacterial groEL protein. J Biol Chem *264*, 20664-20675.

Mohn, A. R., Gainetdinov, R. R., Caron, M. G., and Koller, B. H. (1999). Mice with reduced NMDA receptor expression display behaviors related to schizophrenia. Cell *98*, 427-436.

Moldin, S. O. (1997). The maddening hunt for madness genes. Nat Genet *17*, 127-129.

Morris, R. L., and Hollenbeck, P. J. (1993). The regulation of bidirectional mitochondrial transport is coordinated with axonal outgrowth. J Cell Sci *104*, 917-927.

Morris, R. L., and Hollenbeck, P. J. (1995). Axonal transport of mitochondria along microtubules and F-actin in living vertebrate neurons. J Cell Biol *131*, 1315-1326.

Muir, W. J., Gosden, C. M., Brookes, A. J., Fantes, J., Evans, K. L., Maguire, S. M., Stevenson, B., Boyle, S., Blackwood, D. H., St Clair, D. M., *et al.* (1995). Direct microdissection and microcloning of a translocation breakpoint region, t(1;11)(q42.2;q21), associated with schizophrenia. Cytogenet Cell Genet *70*, 35-40.

Nadeau, O. W., and Carlson, G. M. (2002). Chemical cross-linking in studying protein-protein interactions. In *Protein-protein interactions*, Golemis E. (Ed.) (CSHL Press, Cold Spring Harbor, New York). pp 75 - 91.

Niethammer, M., Smith, D. S., Ayala, R., Peng, J., Ko, J., Lee, M. S., Morabito, M., and Tsai, L. H. (2000). NUDEL is a novel Cdk5 substrate that associates with LIS1 and cytoplasmic dynein. Neuron *28*, 697-711.

Northwood, I. C., Tong, A. H., Crawford, B., Drobnies, A. E., and Cornell, R. B. (1999). Shuttling of CTP:Phosphocholine cytidylyltransferase between the nucleus and endoplasmic reticulum accompanies the wave of phosphatidylcholine synthesis during the G(0) --> G(1) transition. J Biol Chem *274*, 26240-26248.

Novagen. pET system manual. Edition 9 (1992-2000). p.33.

O'Donovan, M. C., and Owen, M. J. (1996). The molecular genetics of schizophrenia. Ann Med *28*, 541-546.

O'Donovan, M. C., and Owen, M. J. (1999). Candidate-gene association studies of schizophrenia. Am J Hum Genet *65*, 587-592.

Overly, C. C., Rieff, H. I., and Hollenbeck, P. J. (1996). Organelle motility and metabolism in axons vs dendrites of cultured hippocampal neurons. J Cell Sci *109*, 971-980.

Owen, M. J., and Cardno, A. G. (1999). Psychiatric genetics: progress, problems, and potential. Lancet *354 Suppl 1*, SI11-14.

Ozeki, Y., Fujii, K., Kleiderlein, J., Park, U., Luo, X., Kamiya, A., Yamada, N., Okawa, M., Snyder, S. H., Ross, C. A., and Sawa, A. (2002). DISC-1: Its function and possible implication for mental illness. Poster presented at Xth World Congress on Psychiatric Genetics (Brussels).

Ozeki, Y., Tomoda, T., Kleiderlein, J., Kamiya, A., Bord, L., Fujii, K., Okawa, M., Yamada, N., Hatten, M. E., Snyder, S. H., Ross, C., and Sawa, A. (2003). Disrupted-in-Schizophrenia-1 (DISC-1): Mutant truncation prevents binding to NudE-like (NUDEL) and inhibits neurite outgrowth. Proc Natl Acad Sci USA *27*, 289-294.

Pahlman, S., Hoehner, J. C., Nanberg, E., Hedborg, F., Fagerstrom, S., Gestblom, C., Johansson, I., Larsson, U., Lavenius, E., Ortoft, E., and Soderholm, H. (1995). Differentiation and survival influences of growth factors in human neuroblastoma. Eur J Cancer *4*, 453-458.

Pfanner, N., and Meijer, M. (1995). Protein sorting. Pulling in the proteins. Curr Biol *5*, 132-135.

Prescott, C. A., and Gottesman, I. I. (1993). Genetically mediated vulnerability to schizophrenia. Psychiatr Clin North Am *16*, 245-267.

Pulver, A. E. (2000). Search for schizophrenia susceptibility genes. Biol Psychiatry *47*, 221-230.

QIAGEN. The QIAexpressionist™. Edition 4 (2000). pp.61-62.

Raedler, T. J., Knable, M. B., and Weinberger, D. R. (1998). Schizophrenia as a developmental disorder of the cerebral cortex. Curr Opin Neurobiol *8*, 157-161.

Rang, H. P., and Dale, M. M. (1991). Neuroleptic Drugs. In *Pharmacology* (2nd edn) (Edinburgh, Churchill Livingstone). p.647.

Ross, R. A., Spengler, B. A., and Biedler, J. L. (1983). Coordinate morphological and biochemical interconversion of human neuroblastoma cells. J Natl Cancer Inst *71*, 741-747.

Ruthel, G., and Hollenbeck, P. J. (2000). Growth cones are not required for initial establishment of polarity or differential axon branch growth in cultured hippocampal neurons. J Neurosci *20*, 2266-2274.

Sasaki, S., Shionoya, A., Ishida, M., Gambello, M. J., Yingling, J., Wynshaw-Boris, A., and Hirotsune, S. (2000). A LIS1/NUDEL/cytoplasmic dynein heavy chain complex in the developing and adult nervous system. Neuron *28*, 681-696.

Sawa, A., and Snyder, S. H. (2002). Schizophrenia: diverse approaches to a complex disease. Science *296*, 692-695.

Scharnhorst, V., Dekker, P., van der Eb, A. J., and Jochemsen, A. G. (1999). Internal translation initiation generates novel WT1 protein isoforms with distinct biological properties. J Biol Chem *274*, 23456-23462.

Sealfon, S. C., and Olanow, C. W. (2000). Dopamine receptors: from structure to behavior. Trends Neurosci *23*, S34-40.

Sedvall, G., and Farde, L. (1995). Chemical brain anatomy in schizophrenia. Lancet *346*, 743-749.

Selemon, L. D., and Goldman-Rakic, P. S. (1999). The reduced neuropil hypothesis: a circuit based model of schizophrenia. Biol Psychiatry *45*, 17-25.

Semple, C. A., Devon, R. S., Le Hellard, S., and Porteous, D. J. (2001). Identification of genes from a schizophrenia-linked translocation breakpoint region. Genomics *73*, 123-126.

Sharp, F. R., Tomitaka, M., Bernaudin, M., and Tomitaka, S. (2001). Psychosis: pathological activation of limbic thalamocortical circuits by psychomimetics and schizophrenia? Trends Neurosci *24*, 330-334.

Silbersweig, D. A., Stern, E., Frith, C., Cahill, C., Holmes, A., Grootoonk, S., Seaward, J., McKenna, P., Chua, S. E., Schnorr, L., Jones, T., and Frackowiak, R., S., J. (1995). A functional neuroanatomy of hallucinations in schizophrenia. Nature *378*, 176-179.

Simpson, P. B. (2000). The local control of cytosolic Ca2+ as a propagator of CNS communication--integration of mitochondrial transport mechanisms and cellular responses. J Bioenerg Biomembr *32*, 5-13.

Sklar, P., Schwab, S. G., Williams, N. M., Daly, M., Schaffner, S., Maier, W., Albus, M., Trixler, M., Eichhammer, P., Lerer, B., Hallmayer, J., Norton, N., Williams, H., Zammit, S., Cardno, A. G., Jones, S., McCarthy, G., Milanova, V., Kirov, G., O'Donovan, M. C., Lander, E. S., Owen, M. J., and Wildenauer, D. B. (2001). Association analysis of NOTCH4 loci in schizophrenia using family and population-based controls. Nat Genet *28*, 126-128.

Smith, A. J., De Sousa, M. A., Kwabi-Addo, B., Heppell-Parton, A., Impey, H., and Rabbitts, P. (1995). A site-directed chromosomal translocation induced in embryonic stem cells by Cre-loxP recombination. Nat Genet *9*, 376-385.

Smith, D. B., and Corcoran, L. M. (1994). Expression and purification of glutathione-*S*-transferase fusion proteins In *Current Protocols in Molecular Biology*, Ausubel, F. M., Brent

R., Kingston R. E., Moore D. D., Seidman J. G., Smith J. A., and Struhl K. (Eds.) (Wiley, USA). p.16.7.6.

Soltys, B. J., and Gupta, R. S. (1996). Immunoelectron microscopic localization of the 60-kDa heat shock chaperonin protein (Hsp60) in mammalian cells. Exp Cell Res *222*, 16-27.

St Clair, D., Blackwood, D., Muir, W., Carothers, A., Walker, M., Spowart, G., Gosden, C., and Evans, H. J. (1990). Association within a family of a balanced autosomal translocation with major mental illness. Lancet *336*, 13-16.

Steinbuch, M., and Audran, R. (1969). The isolation of IgG from mammalian sera with the aid of caprylic acid. Arch Biochem Biophys *134*, 279-284.

Stern, P. S. (1991). Predicting antigenic sites on proteins. Trends Biotechnol *9*, 163-169.

Stone, T. W. (1995). Psychotic disorders: neuroleptic drugs. In *Neuropharmacology* (Oxford University Press, Oxford). pp.76, 79 & 80.

Straube-West, K., Loomis, P. A., Opal, P., and Goldman, R. D. (1996). Alterations in neural intermediate filament organization: functional implications and the induction of pathological changes related to motor neuron disease. J Cell Sci *109*, 2319-2329.

Tamminga, C. A. (1998). Schizophrenia and glutamatergic transmission. Crit Rev Neurobiol *12*, 21-36.

Tandon, K., and McGuffin, P. (2002). The genetic basis for psychiatric illness in man. Eur J Neurosci *16*, 403-407.

Taylor, M. S. (2002). Comparative and molecular characterisation of a schizophrenia susceptibility locus. (PhD thesis). University of Edinburgh. p84.

Taylor, M. S., Devon, R. S., Millar, J. K., and Porteous, D. J. (2003). Evolutionary constraints on the Disrupted in Schizophrenia locus. Genomics *81*, 67-77.

Terasaki, M., and Reese, T. S. (1992). Characterization of endoplasmic reticulum by co-localization of BiP and dicarbocyanine dyes. J Cell Sci *101*, 315-322.

Tsai, G., Passani, L. A., Slusher, B. S., Carter, R., Baer, L., Kleinman, J. E., and Coyle, J. T. (1995). Abnormal excitatory neurotransmitter metabolism in schizophrenic brains. Arch Gen Psychiatry *52*, 829-836.

Tsuang, M. (2000). Schizophrenia: genes and environment. Biol Psychiatry *47*, 210-220.

Tucholski, J., Lesort, M., and Johnson, G. V. (2001). Tissue transglutaminase is essential for neurite outgrowth in human neuroblastoma SH-SY5Y cells. Neuroscience *102*, 481-491.

Usiello, A., Baik, J. H., Rouge-Pont, F., Picetti, R., Dierich, A., LeMeur, M., Piazza, P. V., and Borrelli, E. (2000). Distinct functions of the two isoforms of dopamine D2 receptors. Nature *408*, 199-203.

Varma, M., Aebi, U., Fleming, J., and Leavitt, J. (1987). A 60-kDa polypeptide in mammalian cells with epitopes related to actin. Exp Cell Res *173*, 163-173.

Vawter, M. P., Barrett, T., Cheadle, C., Sokolov, B. P., Wood, W. H., III, Donovan, D. M., Webster, M., Freed, W. J., and Becker, K. G. (2001). Application of cDNA microarrays to examine gene expression differences in schizophrenia. Brain Res Bull *55*, 641-650.

Wagner, K. D., Wagner, N., and Schedl, A. (2003). The complex life of WT1. J Cell Sci *116*, 1653-1658.

Waterwort, D. M., Bassett, A. S., and Brzustowicz, L. M. (2002). Recent advances in the genetics of schizophrenia. Cell Mol Life Sci *59*, 331-348.

Watkins, S. (1989). Immunohistochemistry In *Current Protocols in Molecular Biology*, Ausubel, F. M., Brent R., Kingston R. E., Moore D. D., Seidman J. G., Smith J. A., and Struhl K. (Eds.) (Wiley, USA). p.14.6.12.

Wei, J., and Hemmings, G. P. (2000). The NOTCH4 locus is associated with susceptibility to schizophrenia. Nat Genet *25*, 376-377.

Weinberger, D. R. (1995). From neuropathology to neurodevelopment. Lancet *346*, 552-557.

Weinberger, D. R. (1999). Cell biology of the hippocampal formation in schizophrenia. Biol Psychiatry *45*, 395-402.

Whatley, S. A., Curti, D., and Marchbanks, R. M. (1996). Mitochondrial involvement in schizophrenia and other functional psychoses. Neurochem Res *21*, 995-1004.

Whittemore, S. R., and Snyder, E. Y. (1996). Physiological relevance and functional potential of central nervous system-derived cell lines. Mol Neurobiol *12*, 13-38.

Yamamoto, M., Gotz, M. E., Ozawa, H., Luckhaus, C., Saito, T., Rosler, M., and Riederer, P. (2000). Hippocampal level of neural specific adenylyl cyclase type I is decreased in Alzheimer's disease. Biochim Biophys Acta *1535*, 60-68.

Yang, L., Guan, T., and Gerace, L. (1997). Integral membrane proteins of the nuclear envelope are dispersed throughout the endoplasmic reticulum during mitosis. J Cell Biol *137*, 1199-1210.

Yu, Y., and Bradley, A. (2001). Engineering chromosomal rearrangements in mice. Nat Rev Genet *2*, 780-790.

Zmuda, J. F., and Rivas, R. J. (1998). The Golgi apparatus and the centrosome are localized to the sites of newly emerging axons in cerebellar granule neurons in vitro. Cell Motil Cytoskeleton *41*, 18-38.